



University  
of Glasgow

Zilmer Johansen, Anne Katrine (2014) *Estrogen metabolism in pulmonary arterial hypertension*. PhD thesis.

<http://theses.gla.ac.uk/5199/>

Copyright and moral rights for this thesis are retained by the author

A copy can be downloaded for personal non-commercial research or study, without prior permission or charge

This thesis cannot be reproduced or quoted extensively from without first obtaining permission in writing from the Author

The content must not be changed in any way or sold commercially in any format or medium without the formal permission of the Author

When referring to this work, full bibliographic details including the author, title, awarding institution and date of the thesis must be given

# **Estrogen Metabolism in Pulmonary Arterial Hypertension**

**Anne Katrine Zilmer Johansen  
BSc (Hons)**

Submitted in fulfilment of the requirements of the degree of Doctors of Philosophy  
in the Institute of Cardiovascular and Medical Sciences,  
University of Glasgow

Institute of Cardiovascular and Medical Sciences  
College of Medical, Veterinary and Life Sciences  
University of Glasgow

©A.K.Z. Johansen 2014

## **Author's Declaration**

I declare that this thesis has been written entirely by myself and is a record of the work performed by myself, except where acknowledgement has been made. This thesis has not been previously submitted for a higher degree. The research was carried out principally in the Institute of Cardiovascular and Medical Sciences, College of Medical, Veterinary and Life Sciences at the University of Glasgow under the supervision of Professor Mandy MacLean. All HPLC experiments were carried out in the Queens Medical Research Institute, College of Medicine and Veterinary Medicine at the University of Edinburgh under the supervision of Dr. Ruth Andrew.

# Acknowledgement

My PhD has been a wonderful experience and for that I would especially like to thank my supervisor Professor Mandy MacLean. Her extensive support, guidance and the opportunities that she has provided me with have no doubt made this a very fruitful three years. Four years ago I wandered into her office with no idea of what I wanted to do in the future. Today it is very clear and I would not have got here without Mandy. You have been a wonderful supervisor and an inspiration to me. In my final year, we started a fantastic collaboration with Dr. Ruth Andrew from the University of Edinburgh. This was a key part in the success of my research in my final year. Ruth, thank you so much for the knowledge, skills and fantastic supervision that I have received from you. I would also especially like to thank the British Heart Foundation and their sponsors for providing me with the financial support for this research.

The MacLean research group have certainly also made this a very positive experience for me on both a professional and personal level. I would especially like to thank my mentor Dr. Kevin White for absolutely everything (including all the pain). You have been an inspiration to me, the best mentor that I could have asked for and I have learnt so much from you. I would also like to give special thanks to Dr. Ian Morecroft, Dr. Kirsty Mair, Ms. Margaret Nilsen and Dr. Yvonne Dempsie for all their support around the lab. Ian and Kirsty, I would especially like to thank you both for your patience and all the time that you devoted to help me with my work. Ian, I miss the weekend singing sessions. And Mags, thanks so much for all your help with immunohistochemistry, your comedian nature and Tuesday olives.

Lynn Loughlin has been a lab/cardboard mum, an amazing friend and a colleague. This has been invaluable to me over the past three years. I would also like to thank all my wonderful friends, especially my fellow scientists Emma Wallace, Fiona Greig and Afshan Dean. Emma, you have been the most amazing friend (and colleague) over the years and I have so many good and fun memories with you. Like your mum said, we are so lucky to have found each other. Never forget the Mexicans. Fiona, it didn't take long for us to realize that we had a lot in common and the need for a wine on a Friday. You are one of my best friends and thank you for always being there for me. And I can only thank Afshan for the many wonderful and disastrous nights at the Corinthian (and beyond). We have certainly had some good times. It has been so amazing to have you here in my final year and I look forward to the many good times ahead. And an especially big thank you goes to Katie

Stewart, Line Mohr, Denice Albek, Joe Ferguson and Alan Rae for always believing in me and for being such amazing friends. And a big thank you to the girls from 144 - Alex Morris, Morgan Reres, Anna Terje and Kirsteen Bressendorff.

And finally, my biggest thank you goes to my wonderful family who have always been so extremely supportive of everything that I do although we are Worlds apart. Mum and Dad, you are just amazing. Thank you so much for all the opportunities that you have given me that has got me where I am today. You have always inspired me and encouraged me to do anything that I wanted to. You are always here for me. And as you would say Dad Insha'Allah. Both the Zilmer and the Johansen have helped me in many ways. Definitely the ying and the yang. My beautiful siblings, Jonas, Sofie, Ida and Jessica you are all my best friends and I just love you. I wish we could all spend more time together. And thanks so much to my amazing acquired family, Jørgen, Ruth and Ted for being the best addition to the family and for truly being family. Og tusind tak til min Danske familie, specielt famse, farfar, Wally, Anne, enkefrue Zilmer og søstre Lene. I har alle spillet en kæmpe rolle i mit liv og har hjulpet mig at nå hertil. Jeg savner jer.

Man kan hvad man vil.

Anne Katrine Zilmer Johansen

# Table of Contents

Author's Declaration.....	ii
Acknowledgement.....	iii
List of Tables.....	xi
List of Figures .....	xii
List of Publications .....	xvi
List of Abbreviations and Definitions.....	xvii
Abstract .....	xxiii
Chapter 1 .....	1
Introduction .....	1
1.1    The pulmonary circulation .....	2
1.1.1    Pulmonary vascular structure and function.....	2
1.1.1.1    Pulmonary arteries, veins and capillaries .....	3
1.1.2    The function of the pulmonary circulation.....	4
1.1.3    Regulation of blood flow in the pulmonary circulation .....	4
1.1.4    Regulation of vascular tone: the endothelium.....	5
1.1.5    Excitation-contraction coupling .....	5
1.1.6    Effect of hypoxia on pulmonary vasoconstriction and remodeling .....	6
1.2    Pulmonary hypertension.....	7
1.2.1    Classification of pulmonary hypertension .....	7
1.2.2    Pulmonary arterial hypertension .....	9
1.2.2.1    Idiopathic and heritable pulmonary arterial hypertension .....	9
1.2.2.2    Drug and toxin-induced pulmonary arterial hypertension.....	9
1.2.2.3    Associated pulmonary arterial hypertension.....	10
1.2.3    The diagnosis, prognosis and epidemiology of pulmonary arterial hypertension .....	10
1.2.4    Pulmonary arterial hypertension arteriopathy .....	11
1.2.5    The right heart .....	15
1.2.6    Inflammation and pulmonary arterial hypertension.....	15
1.2.7    Treatments.....	16
1.2.7.1    Ca <sup>2+</sup> channel blockers .....	17
1.2.7.2    Endothelin receptor antagonists.....	17
1.2.7.3    Prostanoids.....	19
1.2.7.4    Phosphodiesterase 5 inhibitors.....	19
1.2.7.5    Adempas® approved to treat pulmonary arterial hypertension .....	20
1.2.8    Emerging therapies.....	20
1.3    Genetic basis of pulmonary arterial hypertension .....	21

1.3.1	Bone morphogenic protein receptor type II .....	21
1.3.1.1	BMPR-2 signaling in the pulmonary vasculature.....	22
1.3.2	Genetic modifiers .....	24
1.3.2.1	The serotonin transporter .....	24
1.3.2.2	Cytochrome P450 1B1 .....	24
1.3.3	Newly identified genetic mutations .....	25
1.3.3.1	Potassium channel, subfamily K, member 3 (Ma et al., 2013).....	25
1.4	Animal models of pulmonary arterial hypertension .....	25
1.4.1	Hypoxic-induced pulmonary hypertension .....	25
1.4.2	Monocrotaline-induced pulmonary hypertension .....	26
1.4.3	Development of pulmonary hypertension in animal models that display heightened serotonin activity .....	27
1.4.3.1	Serotonin transporter overexpressing mice.....	27
1.4.3.2	S100 Ca <sup>2+</sup> binding protein A4 overexpressing mice .....	27
1.4.3.3	The SUGEN-Hypoxic Model of pulmonary arterial hypertension.....	27
1.4.3.4	Dexfenfluramine-induced pulmonary hypertension .....	28
1.5	Serotonin signaling.....	28
1.5.1.1	The serotonin transporter and pulmonary arterial hypertension.....	28
1.6	Steroidogenesis.....	30
1.6.1	Aromatase .....	33
1.6.2	Estrogens .....	35
1.6.3	Tissue regulation of estrogens.....	36
1.6.4	Estrogen receptors .....	37
1.6.4.1	Ligand-mediated regulation of estrogen receptor signaling .....	38
1.6.4.2	Ligand-independent regulation of estrogen receptor signaling .....	38
1.6.4.3	Non-genomic signaling effects of estrogen receptors.....	39
1.6.4.4	Estrogen receptor variants and their signaling.....	40
1.6.4.5	Estrogen and the cardiovascular system .....	41
1.7	Cytochrome P450 Enzymes .....	42
1.7.1	Catalytic cycle of cytochrome P450 enzymes .....	43
1.7.2	Oxidative metabolism of estrogens: 17β-estradiol and estrone .....	45
1.7.2.1	The oxidative metabolism of 17β-estradiol .....	47
1.7.2.2	The oxidative metabolism of estrone.....	47
1.7.3	CYP1B1 .....	49
1.7.3.1	Regulation of CYP1B1 .....	49
1.7.3.2	CYP1B1 and cancer.....	51
1.7.3.3	CYP1B1 and cardiovascular diseases.....	53

1.7.3.4	Physiological role for CYP1B1 .....	54
1.7.4	Phase 2 metabolism of hydroxylated estrogens .....	54
1.8	Gender and pulmonary arterial hypertension .....	54
1.8.1	Estrogens and experimental pulmonary hypertension .....	56
1.8.1.1	Estrogens and monocrotaline-induced pulmonary hypertension.....	56
1.8.1.2	Estrogens and hypoxic-induced pulmonary hypertension.....	57
1.8.1.3	Estrogens in genetically-susceptible and drug-induced pulmonary hypertension .....	58
1.8.1.4	Estrogens in SU-hypoxic-induced pulmonary arterial hypertension.....	59
1.8.1.5	Estrogens and dexfenfluramine-induced pulmonary hypertension .....	59
1.8.1.6	Estrogen effects in vitro.....	60
1.8.2	Progesterone and pulmonary hypertension .....	61
1.8.3	Androgens and pulmonary hypertension .....	61
1.8.4	CYP1B1 and pulmonary hypertension .....	64
1.9	Aims .....	65
Chapter 2	.....	66
Methods	.....	66
2.1	Chemicals reagents and equipment .....	67
2.2	Animals .....	67
2.2.1	General experimental design.....	67
2.2.2	Cytochrome P450 1B1 knockout mice .....	67
2.2.3	Serotonin transporter overexpressing mice .....	68
2.3	Models of pulmonary hypertension.....	68
2.3.1	Monocrotaline-induced pulmonary hypertension .....	68
2.3.1.1	2,3',4,5'-Tetramethoxystilbene study .....	69
2.3.2	Chronic hypobaric hypoxia.....	69
2.3.2.1	2,3',4,5'-Tetramethoxystilbene study in hypoxic pulmonary hypertension.....	69
2.3.2.2	2,3',4,5'-Tetramethoxystilbene study in SERT+ pulmonary hypertension.....	70
2.3.2.3	Effect of CYP1B1 metabolites in pulmonary hypertension .....	70
2.4	Assessment of pulmonary hypertension.....	70
2.4.1	Anaesthesia .....	70
2.4.2	Systemic arterial pressure .....	71
2.4.3	Right ventricular pressure .....	72
2.4.3.1	In mice .....	72
2.4.3.2	In rats .....	72
2.4.4	Tissue harvest.....	74

2.4.5	16 $\alpha$ -hydroxyestrone urinary analysis .....	74
2.4.6	Right ventricular hypertrophy .....	74
2.5	Small vessel wire myography.....	75
2.5.1.1	Isolation of the intra-pulmonary artery.....	75
2.5.1.2	Vessel mounting onto a myograph .....	75
2.5.1.3	Pressure Standardization.....	75
2.6	Immunohistochemistry .....	77
2.6.1	Tissue Fixation and Paraffin Embedding .....	77
2.6.2	Immunohistochemistry.....	79
2.6.2.1	Haematoxylin and eosin counter-staining.....	80
2.6.2.2	Quantitative Analysis of CYP1B1 Immunoreactivity .....	82
2.6.3	Pulmonary vascular remodeling.....	82
2.6.3.1	Elastic picro-sirius red staining.....	82
2.7	Sodium dodecyl sulphate – polyacrylamide gel electrophoresis.....	83
2.7.1	Protein solubilization .....	83
2.7.2	Bicinchoninic acid protein assay.....	83
2.7.3	Western blotting .....	85
2.8	RNA analysis.....	88
2.8.1	RNA extraction .....	88
2.8.2	Reverse transcription.....	89
2.8.3	Quantitative real time-polymerase chain reactions .....	89
2.9	Cell culture .....	89
2.9.1	Human pulmonary arterial smooth muscle cells.....	89
2.9.1.1	Sub-culturing of human pulmonary arterial smooth muscle cells .....	90
2.9.2	Charcoal-stripped fetal bovine serum .....	92
2.10	Thymidine incorporation assay.....	93
2.11	CellTiter-Glo® luminescent cell viability assay.....	93
2.12	17 $\beta$ -estradiol immunoassay .....	94
2.12.1	17 $\beta$ -estradiol levels in extracellular medium .....	96
2.13	High performance liquid chromatography.....	96
2.13.1	Optimisation of separation of estrogen metabolites by high performance liquid chromatography .....	96
2.13.2	Optimization of estrogen metabolite extraction.....	97
2.13.2.1	Solvent Extractions .....	97
2.13.2.2	Oasis SPE Extraction .....	98
2.13.2.3	High performance liquid chromatography.....	99
2.13.2.4	Extraction of radiolabelled <sup>14</sup> C-17 $\beta$ -estradiol and optimisation of concentration required for optimum detection.....	99

2.13.3	Estrogen metabolism in cells .....	100
2.13.3.1	High performance liquid chromatography.....	100
2.14	Statistical analysis and data handling .....	101
Chapter 3	.....	102
The Estrogen Metabolizing Enzyme Cytochrome P450 1B1 Influences the Development of Pulmonary Arterial Hypertension .....		102
3.1	Introduction .....	103
3.2	Results .....	105
3.2.1	Hypoxia alters the estrogen metabolic axis in human pulmonary arterial smooth muscle cells .....	105
3.2.2	Pulmonary CYP1B1 expression is increased in experimental and clinical PAH.....	105
3.2.3	Effect of chronic hypoxia in CYP1B1 deficient mice .....	112
3.2.4	Intra-pulmonary arterial vasoconstriction in CYP1B1 <sup>-/-</sup> Mice .....	117
3.2.5	Effect of CYP1B1 on uterine + ovary weights .....	117
3.2.6	Inhibition of CYP1B1 is protective on the development of hypoxia-induced PAH.....	121
3.2.7	Monocrotaline-induced PH is moderately altered by TMS treatment in male but not female rats.....	127
3.2.8	Survival is improved in rats treated with TMS .....	134
3.2.9	Estrogen synthesis and metabolism is dysregulated in female SERT <sup>+</sup> mice.....	135
3.2.10	Inhibition of CYP1B1 regresses pulmonary hypertension in female SERT <sup>+</sup> mice.....	138
3.3	Discussion .....	145
Chapter 4	.....	152
Dynamic Alterations in the Estrogen Metabolic Axis in Pulmonary Hypertension .....		152
4.1	Introduction .....	153
4.2	Results .....	157
4.2.1	The CYP1B1 metabolite 16 $\alpha$ -hydroxyestrone is increased by hypoxia .....	157
4.2.2	16 $\alpha$ -hydroxyestrone inflicts a pulmonary hypertensive phenotype in female mice only.....	157
4.2.3	16 $\alpha$ -hydroxyestrone-induced proliferation is inhibited by a reactive oxygen species scavenger and an inhibitor of extracellular regulated kinase 1/2 .....	164
4.2.4	4-hydroxyestradiol attenuates serotonin-induced vasoconstriction in the pulmonary arteries.....	165
4.2.5	Effect of estrogen metabolism by CYP1B1 on cellular function.....	170
4.2.6	17 $\beta$ -estradiol intracellular levels in human pulmonary arterial smooth muscle cells.....	174
4.2.7	Depletion of 17 $\beta$ -estradiol from the extracellular medium in human pulmonary arterial smooth muscle cells.....	174
4.2.8	Patient characteristics.....	174

4.2.9	Absorption profiles of estrogen metabolites by high performance liquid chromatography.....	178
4.2.10	Combined chromatogram of estrogen metabolites .....	183
4.2.11	Extraction of estrogen metabolites-method development.....	186
4.2.12	Extraction and recovery of <sup>14</sup> C-17β-estradiol .....	186
4.2.13	Estrogen metabolism over time in human pulmonary arterial smooth muscle cells.....	192
4.2.14	Evidence for an altered estrogen metabolic profile in pulmonary arterial hypertension .....	198
4.3	Discussion .....	207
Chapter 5	.....	218
General Discussion	.....	218
5.1	General Discussion.....	219
5.1.1	The therapeutic potential of CYP1B1 inhibition in the management of PAH.....	225
5.1.2	Targeting estrogen metabolism in the management of PAH.....	227
5.1.3	Concluding remarks .....	228
5.2	Future Perspective .....	231
6.1	References .....	232
7.1	Appendices .....	263
8.1	Supplemental data .....	264
8.1.1	Western blots corresponding to figure 3-1.....	264
8.1.2	Western blots corresponding to figure 3-22 and 3-23.....	265
8.1.3	Effect of tempol and UO126 on cell proliferation to complement figure 4-7.....	266

## List of Tables

Table 1-1 WHO classification of pulmonary hypertension .....	8
Table 2-1 Process for paraffin-embedding small animal tissues .....	78
Table 2-2 Antibody manufacturers and optimal concentrations for immunohistochemistry .....	81
Table 2-3 Experimental details for antibodies used for protein analysis by western blotting .....	87
Table 2-4 Oasis® HLB extraction of Estrogen metabolites .....	99
Table 3-1 Patient characteristics of human lung sections .....	106
Table 3-2 Phenotypic data from wild-type and CYP1B1 <sup>-/-</sup> mice .....	119
Table 3-3 Effect of CYP1B1 inhibitor 2,3',4,5'-tetramethoxystilbene (TMS) in normoxic and hypoxic C57BL/6 mice on haemodynamics and phenotypes .....	126
Table 3-4 Phenotypic data from monocrotaline wister rats treated with vehicle or the CYP1B1 inhibitor 2,3',4,5'-tetramethoxystilbene (TMS) .....	132
Table 3-5 Effect of SERT overexpression, hypoxia and TMS on mean systemic arterial pressures and heart rate .....	144
Table 4-1 Phenotypic data from 16 $\alpha$ -hydroxyestrone treated mice .....	163
Table 4-2 Phenotypic data from 4-hydroxyestradiol treated mice .....	169
Table 4-3 Patient characteristics of control human pulmonary arterial smooth muscle cells .....	175
Table 4-4 Patient characteristics of pulmonary arterial hypertension human pulmonary arterial smooth muscle cells .....	175
Table 4-5 Estrogen compound retention times on the Sunfire C18 Column .....	185
Table 4-6 Summary of metabolite formation in human pulmonary arterial smooth muscle cells .....	206

## List of Figures

Figure 1-1 Pulmonary arterial hypertension arteriopathy .....	14
Figure 1-2 Synthesis of estrogens from cholesterol.....	32
Figure 1-3 Aromatisation of testosterone to 17 $\beta$ -estradiol .....	35
Figure 1-4 Chemical structure of estrone and 17 $\beta$ -estradiol.....	36
Figure 1-5 Catalytic cycle of cytochrome P450 enzymes.....	44
Figure 1-6 Metabolism of estrone and 17 $\beta$ -estradiol and the effects of downstream metabolites .....	46
Figure 1-7 Cytochrome P450 mediated metabolism of estrone and 17 $\beta$ -estradiol.....	48
Figure 1-8 Transcriptional activation of cytochrome P450 enzymes by the aryl hydrocarbon receptor .....	50
Figure 2-1 Representative mean systemic arterial pressures .....	71
Figure 2-2 Representative right ventricular pressure .....	73
Figure 2-3 A representative bicinchoninic acid protein assay standard curve.....	84
Figure 2-4 Distal human pulmonary arterial smooth muscle cell morphology .....	91
Figure 2-5 Removal of 17 $\beta$ -estradiol from foetal bovine serum .....	92
Figure 2-6 Schematic of the 17 $\beta$ -estradiol immunoassay.....	95
Figure 3-1 Effect of hypoxia on protein expression of CYP1B1, COMT and 17 $\beta$ -HSD1 in human pulmonary arterial smooth muscle cells (hPASMCs).....	107
Figure 3-2 Immunolocalisation of CYP1B1 in normoxic and hypoxic murine pulmonary arteries .....	108
Figure 3-3 Immunolocalisation of CYP1B1 in SU-hypoxic murine pulmonary hypertension .....	109
Figure 3-4 Immunolocalisation of CYP1B1 in pulmonary arteries from patients with PAH .....	110
Figure 3-5 Cellular localisation of CYP1B1 in human vascular lesions .....	111
Figure 3-6 Right ventricular hypertrophy in chronically hypoxic CYP1B1 <sup>-/-</sup> mice .....	113
Figure 3-7 Right ventricular systolic pressures in chronically hypoxic CYP1B1 <sup>-/-</sup> mice.....	114
Figure 3-8 Representative expression of $\alpha$ -smooth muscle actin positive cells in response to hypoxia in wild-type and CYP1B1 <sup>-/-</sup> mice.....	115
Figure 3-9 Pulmonary vascular remodeling in chronically hypoxic CYP1B1 <sup>-/-</sup> mice.....	116
Figure 3-10 Vasoreactivity of the intrapulmonary arteries in chronically hypoxic CYP1B1 <sup>-/-</sup> mice.....	118
Figure 3-11 The dry weights of the uterus and ovaries in chronically hypoxic female CYP1B1 <sup>-/-</sup> mice.....	120
Figure 3-12 The CYP1B1 inhibitor 2,3',4,5'-tetramethoxystilbene (TMS) attenuates the development of chronic hypoxia-induced right ventricular hypertrophy in mice.....	122
Figure 3-13 The CYP1B1 inhibitor 2,3',4,5'-tetramethoxystilbene (TMS) attenuates the development of chronic hypoxia-induced right ventricular systolic pressures in mice .....	123
Figure 3-14 Representative $\alpha$ -smooth muscle actin-stained pulmonary arteries in normoxic and chronic hypoxic C57BL/6 mice dosed with vehicle- or the CYP1B1 inhibitor 2,3',4,5'-tetramethoxystilbene (TMS) .....	124
Figure 3-15 The CYP1B1 inhibitor 2,3',4,5'-tetramethoxystilbene (TMS) attenuates the development of chronic hypoxia-induced pulmonary vascular remodeling .....	125
Figure 3-16 Monocrotaline induces right ventricular hypertrophy and this is unaffected by the CYP1B1 inhibitor 2,3',4,5'-tetramethoxystilbene (TMS) .....	128
Figure 3-17 Monocrotaline induces increases in right ventricular pressures and this is unaffected by unaffected by the CYP1B1 inhibitor 2,3',4,5'-tetramethoxystilbene (TMS) .....	129

Figure 3-18 Representative $\alpha$ -smooth muscle actin–stained pulmonary arteries in monocrotaline (MCT) rats treated with vehicle- or the CYP1B1 inhibitor 2,3',4,5'-tetramethoxystilbene (TMS) .....	130
Figure 3-19 Monocrotaline increases pulmonary vascular remodeling and this is unaffected by unaffected by the CYP1B1 inhibitor 2,3',4,5'-tetramethoxystilbene (TMS) .....	131
Figure 3-20 Monocrotaline and CYP1B1 inhibition with 2,3',4,5'-tetramethoxystilbene (TMS) on uterus+ovary weights/body weights.....	133
Figure 3-21 CYP1B1 inhibition with 2,3',4,5'-tetramethoxystilbene (TMS) improves survival in monocrotaline treated rats as assessed by Kaplan-Meier survival analysis .....	134
Figure 3-22 Overexpression of SERT+ on aromatase expression and 17 $\beta$ -estradiol concentrations in whole lung homogenates .....	136
Figure 3-23 Lung CYP1B1 expression is increased in female SERT+ mice .....	137
Figure 3-24 SERT mice have increased right ventricular systolic pressures which are exacerbated by hypoxia and reversed by CYP1B1 inhibition with 2,3',4,5'-tetramethoxystilbene (TMS) .....	139
Figure 3-25 Representative right ventricular pressure traces from wild-type, SERT+ and SERT+ mice treated with the CYP1B1 inhibitor 2,3',4,5'-tetramethoxystilbene (TMS)...	140
Figure 3-26 Right ventricular hypertrophy in female SERT+ mice in normoxic and hypoxic conditions and the effect of CYP1B1 inhibition with 2,3',4,5'-tetramethoxystilbene (TMS).....	141
Figure 3-27 Representative $\alpha$ -smooth muscle actin–and von-Willebrand stained pulmonary arteries in wild-type and SERT+ mice treated with vehicle- or the CYP1B1 inhibitor 2,3',4,5'-tetramethoxystilbene (TMS) .....	142
Figure 3-28 SERT mice have increased pulmonary vascular remodeling and this is reversed by CYP1B1 inhibition with 2,3',4,5'-tetramethoxystilbene (TMS).....	143
Figure 4-1 Summary of the hydroxylation of estrone and 17 $\beta$ -estradiol by human cytochrome P450 isoforms.....	154
Figure 4-2 Urinary levels of the 16 $\alpha$ -hydroxyestrone is increased by chronic hypoxia in male and female mice.....	158
Figure 4-3 16 $\alpha$ -hydroxyestrone (16 $\alpha$ -OHE1) induces right ventricular hypertrophy in female mice only .....	159
Figure 4-4 16 $\alpha$ -hydroxyestrone (16 $\alpha$ -OHE1) increases right ventricular systolic pressures in female mice only .....	160
Figure 4-5 Representative $\alpha$ -smooth muscle actin–stained pulmonary arteries in 16 $\alpha$ -hydroxyestrone (16 $\alpha$ -OHE1) or vehicle treated C57BL/6 male and female mice.....	161
Figure 4-6 16 $\alpha$ -hydroxyestrone (16 $\alpha$ OHE1) increases pulmonary arterial remodeling in female mice only .....	162
Figure 4-7 16 $\alpha$ -hydroxyestrone (16 $\alpha$ -OHE1)-induced proliferation in human pulmonary arterial smooth muscle cells (hPASMCs) is mediated by the formation of reactive oxygen species (ROS).....	164
Figure 4-8 4-hydroxyestradiol (4-OHE2) has no effects on right ventricular hypertrophy or right ventricular systolic pressures.....	166
Figure 4-9 4-hydroxyestradiol had no effects on pulmonary vascular remodeling .....	167
Figure 4-10 4-hydroxyestradiol reduces serotonin-induced vasoconstriction .....	168
Figure 4-11 Effect of 4-hydroxyestradiol on uterus + ovary weights.....	169
Figure 4-12 Effect of 4-hydroxyestrone (4-OHE1) and 2-methoxyestradiol (2-MeOHE2) on human pulmonary arterial smooth muscle cell (hPASMC) viability and proliferation for 3 days .....	171
Figure 4-13 Effect of 4-hydroxyestrone (4-OHE1) and 2-methoxyestradiol (2-MeOHE2) on human pulmonary arterial smooth muscle cell (hPASMC) viability and proliferation for 3 days .....	172

Figure 4-14 Representative microphotographs of human pulmonary arterial smooth muscle cells (hPASMCs) following incubations with 4-hydroxyestrone (4-OHE1) and 2-methoxyestradiol (2-MeOHE2) for 3 days .....	173
Figure 4-15 Representative microphotographs of human pulmonary arterial smooth muscle cells (hPASMCs) following incubations with 4-hydroxyestrone (4-OHE1) and 2-methoxyestradiol (2-MeOHE2) for 5 days .....	173
Figure 4-16 Intracellular 17 $\beta$ -estradiol (17 $\beta$ -E2) concentrations in pulmonary arterial smooth muscle cells (hPASMCs): effect of serotonin .....	176
Figure 4-17 Depletion of 17 $\beta$ -estradiol from the extracellular medium in human pulmonary arterial smooth muscle cells (hPASMCs) .....	177
Figure 4-18 Chromatograms of 17 $\beta$ -estradiol, estrone and 17 $\alpha$ -estradiol .....	179
Figure 4-19 Chromatograms of 16 $\alpha$ -hydroxyestrone, 16 $\alpha$ -hydroxyestradiol, 16 epiestrinol and 17 epiestrinol .....	180
Figure 4-20 Chromatograms of 2-hydroxyestrone, 2-hydroxyestradiol, 4-hydroxyestrone and 4-hydroxyestradiol.....	181
Figure 4-21 Chromatograms of 2-methoxyestrone, 2-methoxyestradiol, 4-methoxyestrone and 4-methoxyestradiol.....	182
Figure 4-22 Ultraviolet absorption profiles of the 15 estrogen metabolites with the Sunfire C18 column .....	184
Figure 4-23 Extraction recoveries of estrogen metabolites with a ethyl acetate solvent extraction.....	187
Figure 4-24 Extraction recoveries of estrogen metabolites with a dichloromethane solvent extraction.....	188
Figure 4-25 Extraction recoveries of estrogen metabolites with a diethyl ether solvent extraction.....	189
Figure 4-26 Extraction recovery of estrogen metabolites using Oasis® HLB columns....	190
Figure 4-27 Percentage extraction recovery of radiolabelled 17 $\beta$ -estradiol .....	191
Figure 4-28 Metabolism of 17 $\beta$ -estradiol over time in control female human pulmonary arterial smooth muscle cells (PASMCs) .....	194
Figure 4-29 Metabolism of 17 $\beta$ -estradiol over time in control male human pulmonary arterial smooth muscle cells (PASMCs) .....	195
Figure 4-30 Metabolism of 17 $\beta$ -estradiol over time in PAH female human pulmonary arterial smooth muscle cells (PASMCs) .....	196
Figure 4-31 Metabolism of 17 $\beta$ -estradiol over time in PAH male human pulmonary arterial smooth muscle cells (PASMCs).....	197
Figure 4-32 Estrogen metabolic profile in control- and pulmonary arterial hypertension-pulmonary arterial smooth muscle (PASMCs) cells after 10 minutes.....	199
Figure 4-33 Estrogen metabolic profile in control- and pulmonary arterial hypertension-pulmonary arterial smooth muscle cells (PASMCs) after 30 minutes.....	200
Figure 4-34 Estrogen metabolic profile in control- and pulmonary arterial hypertension-pulmonary arterial smooth muscle cells (PASMCs) after 1 hour .....	201
Figure 4-35 Estrogen metabolic profile in control- and pulmonary arterial hypertension-pulmonary arterial smooth muscle cells (PASMCs) after 2 hours.....	202
Figure 4-36 Estrogen metabolic profile in control- and pulmonary arterial hypertension-pulmonary arterial smooth muscle cells (PASMCs) after 4 hours.....	203
Figure 4-37 Estrogen metabolic profile in control- and pulmonary arterial hypertension-pulmonary arterial smooth muscle cells (PASMCs) after 24 hours.....	204
Figure 4-38 Estrogen metabolic profile in control- and pulmonary arterial hypertension-pulmonary arterial smooth muscle cells (PASMCs) after 48 hours.....	205
Figure 5-1 Summary diagram .....	230
Figure 8-1 Full western blots for effect of hypoxia on protein expression of CYP1B1, COMT and 17 $\beta$ -HSD1 .....	264

Figure 8-2 Full western blots of aromatase and CYP1B1 expression in normoxic, hypoxic and SERT+ mice .....	265
Figure 8-3 The effect of tempol and UO126 on thymidine incorporation.....	266

## List of Publications

Mair, KM, **Johansen, AKZ**, Wright, AF, Wallace, E & Maclean, MR. (2013). Pulmonary arterial hypertension: basis of sex differences in incidence and treatment response. *Br J Pharmacol*, 171, 567-579. [Appendix 1]

Austin, ED, Lahm, T, West, J, Tofovic, SP, **Johansen, AK**, MacLean, MR, Alzoubi, A & Oka, M. (2013). Gender, sex hormones and pulmonary hypertension. *Pulm Circ*, 3, 294-314. (All authors contributed equally to this article) [Appendix 2]

White, K, **Johansen, AK (co-first)**, Nilsen, M, Ciuculan, L, Wallace, E, Paton, L, Campbell, A, Morecroft, I, Loughlin, L, McClure, JD, Thomas, M, Mair, KM & MacLean, MR. (2012). Activity of the estrogen-metabolizing enzyme cytochrome P450 1B1 influences the development of pulmonary arterial hypertension / clinical perspective. *Circulation*, 126, 1087-1098. [Appendix 3]

Published abstracts:

MacLean, M.R., White, K. & **Johansen, A.K.** The estrogen-metabolizing enzyme, cytochrome P450 1B1 influences the development of exaggerated hypoxia-induced pulmonary arterial hypertension in female mice over-expressing the serotonin transporter. Oral Presentation at the American Thoracic Society Conference published in the *American Journal of Respiratory and Critical Care Medicine* 185; 2012:A6520

MacLean, M.R., Morecroft, I., Mair, K.M., White, K., Nilsen, M., & **Johansen, A.K.** (2011) Cytochrome P450 1B1 promotes the development of pulmonary arterial hypertension. Poster presentation at the American Heart Association Conference published in *Circulation*, 124: A10227

## List of Abbreviations and Definitions

AA	Ascorbic acid
ABT	1-aminobenzotriazole
AF-1	Activation function-1
AF-2	Activation function-2
AHR	Aryl hydrocarbon receptor
AIP	Aryl hydrocarbon receptor-interacting protein
ALK1	Activin receptor-like kinase
Ang II	Angiotensin II
AP-1	Activator protein-1
ARNT	Aryl hydrocarbon receptor nuclear translocator
ATP	Adenosine triphosphate
BCA	Bicinchoninic acid
BMPs	Bone morphogenic proteins
BMPR-2	Bone morphogenic protein receptor type II
Ca <sup>2+</sup>	Calcium
CaCl <sub>2</sub>	Calcium chloride
cAMP	Cyclic adenosine monophosphate
CAV1	Caveolin 1
cGMP	Cyclic guanosine monophosphate
CO	Cardiac output
COMT	Catechol-O-methyl transferase
CS-PRF-DMEM	Charcoal stripped-phenol red-free Dulbecco's modified eagle medium
CYP	Cytochrome P450
CYP1A1	Cytochrome P450 1A1
CYP1A2	Cytochrome P450 1A2
CYP2A6	Cytochrome P450 2A6
CYP3A4	Cytochrome P450 3A4
CYP3A5	Cytochrome P450 3A5
CYP19A1	Cytochrome P450 19A1/aromatase
CYP1B1	Cytochrome P450 1B1
CYP1B1 <sup>-/-</sup>	CYP1B1 knockout mice
CYP2B6	Cytochrome P450 2B6
CYP2C8	Cytochrome P450 2C8

CYP2C9	Cytochrome P450 2C9
CYP2C11	Cytochrome P450 2C11
CYP2C19	Cytochrome P450 2C19
DAB	3, 3'-diaminobenzidine
DHEA	Dehydroepiandrostenedione
DHEA-S	Dehydroepiandrostenedione-sulfate
DHT	Dihydrotestosterone
DMEM	Dulbecco's modified eagle medium
DMSO	Dimethyl sulfoxide
DNA	Deoxyribonucleic acid
dNTPs	Deoxynucleotide triphosphates
DOCA	Deoxycorticosterone acetate
DPBS	Dulbecco's phosphate buffered saline
DRE	Dioxin response element
E1	Estrone
17 $\beta$ -E2	17 $\beta$ -estradiol
E3	Estriol/16 $\alpha$ -hydroxyestradiol
ECL	Electrochemiluminescence
EET	Epoxyeicosatrienoic acid
ENG	Endoglin
eNOS	Endothelial nitric oxide synthase
16-epi-E3	16-epiestriol
17-epi-E3	17-epiestriol
ER $\alpha$	Estrogen receptor $\alpha$
ER $\beta$	Estrogen receptor $\beta$
ERE	Estrogen response element
ERK1/2	Extracellular regulated kinase 1/2
E1-S	Estrone sulfate
ESR1	Estrogen receptor 1
ESR2	Estrogen receptor 2
ET-1	Endothelin-1
ETB	Endothelin receptor A
ETB	Endothelin receptor B
FBS	Foetal bovine serum
FDA	Food and drug administration
GABA	Gamma-aminobutyric acid

GAPDH	Glyceraldehyde 3-phosphate dehydrogenase
GC-MS	Gas chromatography-mass spectrometry
GDF	Growth differentiation factors
GP-1	G-protein coupled estrogen receptor-1
HCl	Hydrogen chloride
HDL	High density lipoprotein
HETE	Hydroxyeicosatetraenoic acid
5-HETE	5-hydroxyeicosatetraenoic acid
15-HETE	15-hydroxyeicosatetraenoic acid
HIF	Hypoxia inducible factor
HIF-1 $\alpha$	Hypoxia inducible factor-1 $\alpha$
HIV	Human immunodeficiency virus
HLB	Hydrophilic-lipophilic-balanced
HPAH	Heritable pulmonary arterial hypertension
hPASMCs	Human pulmonary arterial smooth muscle cells
HPLC	High performance liquid chromatography
HRP	Horse radish peroxidase
3 $\beta$ -HSD	3 $\beta$ -hydroxysteroid dehydrogenase
17 $\beta$ -HSD1	17 $\beta$ -hydroxysteroid dehydrogenase 1
17 $\beta$ -HSD2	17 $\beta$ -hydroxysteroid dehydrogenase 2
17 $\beta$ -HSD3	17 $\beta$ -hydroxysteroid dehydrogenase 3
Hsp90	Heat shock protein 90
IPAH	Idiopathic pulmonary arterial hypertension
ID-1	Inhibitor of DNA binding-1
IL-6	Interleukin-6
IV	Intravenous
JNK	c-Jun N terminal kinase
KCl	Potassium chloride
KCNK3	Potassium channel subfamily K member 3
KH <sub>2</sub> PO <sub>4</sub>	Monopotassium phosphate
KLF-4	Kruppel-like factor 4
KMNO <sub>4</sub>	Potassium permanganate
LC-MS	Liquid chromatography-mass spectrometry
LDL	Low density lipoprotein
LH	Luteinizing hormone
LM	Lauryl maltoside

MAPK	Mitogen activated protein kinase
mAu	Milli absorbance units
$\alpha$ -MHC	$\alpha$ -myosin heavy chain
$\beta$ -MHC	$\beta$ -myosin heavy chain
MgCl	Magnesium chloride
MCT	Monocrotaline
MFO	Mixed-function oxidase
MLC	Myosin light chain
MLCK	Myosin light chain kinase
MLCP	Myosin light chain phosphatase
2-MeOHE1	2-methoxyestrone
2-MeOHE2	2-ethoxyestradiol
4-MeOHE1	4-methoxyestrone
4-MeOHE2	4-methoxyestradiol
mSAP	mean systemic arterial pressure
MnSOD	Manganese superoxide dismutase
NADPH	Nicotinamide adenine dinucleotide phosphate
NBF	Neutral buffered formalin
NaCl	Sodium chloride
NaHCO <sub>3</sub>	Sodium bicarbonate
NaH <sub>2</sub> PO <sub>4</sub>	Monosodium phosphate
Na <sub>2</sub> HPO <sub>4</sub>	Sodium phosphate
NIH	National institutes of health
NO	Nitric oxide
NaOH	Sodium hydroxide
NSCLC	Non-small cell lung cancer
2-OHE1	2-hydroxyestrone
2-OHE2	2-hydroxyestradiol
4-OHE1	4-hydroxyestrone
4-OHE2	4-hydroxyestradiol
6 $\alpha$ -OHE2	6 $\alpha$ -hydroxyestradiol
7 $\alpha$ -OHE2	7 $\alpha$ -hydroxyestradiol
15 $\alpha$ -OHE2	15 $\alpha$ -hydroxyestradiol
16 $\alpha$ -OHE1	16 $\alpha$ -hydroxyestrone
16 $\alpha$ -OHE2	16 $\alpha$ -hydroxyestradiol/estriol
16 $\beta$ -OHE2	16 $\beta$ -hydroxyestradiol

PAH	Pulmonary arterial hypertension
PAP	Pulmonary arterial pressure
PASMCs	Pulmonary arterial smooth muscle cells
PBS	Phosphate buffered saline
PCR	Polymerase chain reaction
PDE	Phosphodiesterase
PDE5	Phosphodiesterase 5
PGE2	Prostaglandin E2
PH	Pulmonary hypertension
PI3K	Phosphoinositide 3-kinase
PKG	Protein kinase G
p38MAPK	p38 mitogen activated kinase
PPHTN	Portopulmonary hypertension
PRF-DMEM	Phenol red-free Dulbecco's modified eagle medium
PVDF	Polyvinylidene fluoride
PVR	Pulmonary vascular remodeling
PVSMC	Pulmonary vascular smooth muscle cell
RAGE	Receptor for advanced glycation end products
REVEAL	Registry to evaluate early and long-term pulmonary arterial hypertension disease management
ROMs	Reactive oxygen intermediates
ROS	Reactive oxygen species
RVH	Right ventricular hypertrophy
RVP	Right ventricular pressure
RVSP	Right ventricular systolic pressure
S100A4/mts1	S100 calcium binding protein
Smad	Sma and Mad (mothers against decapetaplegic)-related proteins
SAP	Systemic arterial pressure
SERT	Serotonin transporter
SERT+	Serotonin transporter overexpressing mice
SLC6A4	Soluble carrier family 6, member 4
$\alpha$ -SMA	$\alpha$ -smooth muscle actin
SNPs	Single nucleotide polymorphisms
StAR	Steroidogenic acute regulatory protein
SU	SU5416; Vascular endothelial growth factor receptor inhibitor
TBS	Tris buffered saline

TBST	Tris buffered saline-tween
TCDD	2,3,7,8-tetrachlorodibenzodioxin
TGF- $\beta$	Transforming growth factor- $\beta$
TMS	2,3',4,5'-tetramethoxystilbene
TNF $\alpha$	Tumour necrosis factor $\alpha$
TPH1	Tryptophan hydroxylase 1
TXA <sub>2</sub>	Thromboxane A <sub>2</sub>
UV	Ultraviolet
VEGF	Vascular endothelial growth factor
VEGF-R	Vascular endothelial growth factor receptor
VSMC	Vascular smooth muscle cell
WHO	World health organisation
WSPH	World symposium on pulmonary hypertension

## Abstract

Pulmonary arterial hypertension (PAH) is a devastating and progressive vasculopathy of the pulmonary arteries for which there is no cure. There is an urgent need for more effective therapies. PAH is characterised by elevated pulmonary arterial pressures and obstructive vascular lesions in the distal vasculature by excessive cellular proliferation. As a result, the right ventricle is placed under excessive strain resulting in adaptive hypertrophy which progresses to maladaptive hypertrophy and failure. PAH is more common in women than in men suggesting that estrogens may be integral to disease pathogenesis. Understanding the biological basis for this sex difference would offer a new treatment paradigm in this devastating cardiovascular disease. Here, we challenged the concept that the estrogen metabolic axis is dysregulated in PAH.

New insights have revealed a potential contribution of the estrogen metabolizing enzyme, cytochrome P450 1B1 (CYP1B1) in the development of PAH.  $17\beta$ -estradiol ( $17\beta$ -E2) and estrone (E1) are metabolized by the activity of CYP1B1 to the 2-, 4- and 16-hydroxylated estrogens. Here, we defined the role of CYP1B1 in the pathogenesis of PAH. CYP1B1 expression was increased in both experimental (hypoxia and SU5416+hypoxia) and in heritable and idiopathic PAH (HPAH and IPAH, respectively). Both male and female CYP1B1 knockout mice (CYP1B1<sup>-/-</sup>) were challenged with chronic hypoxia to induce PAH as assessed by right ventricular systolic pressures (RVSP), right ventricular hypertrophy (RVH) and pulmonary vascular remodeling. CYP1B1<sup>-/-</sup> mice were protected against hypoxia-induced pulmonary hypertension (PH). CYP1B1 inhibition with the highly potent and selective inhibitor 2,3',4,5'-tetramethoxystilbene (TMS; 3 mg/kg/day by intra-peritoneal injection) attenuated the development of hypoxia-induced PH. Only moderate effects were observed with CYP1B1 inhibition in monocrotaline-induced PH, despite improving survival rates. Female mice that over-express the human serotonin transporter gene (SERT<sup>+</sup> mice) develop a spontaneous PAH phenotype at 5 months of age which is dependent on circulating levels of  $17\beta$ -E2. Here, we provide evidence that the estrogen metabolic axis is dysregulated in these mice and this may underlie their PAH phenotype. The estrogen synthesizing enzyme aromatase and CYP1B1 was increased in whole lung homogenates of female SERT<sup>+</sup> mice compared to wild-type mice. Despite increased expression of aromatase,  $17\beta$ -E2 concentrations were unchanged. CYP1B1 inhibition with TMS (1.5mg/kg/day by intra-peritoneal injection) attenuated the PAH phenotype in female SERT<sup>+</sup> mice as assessed by RVSP and pulmonary vascular remodeling.

Other studies have identified that the 16-hydroxylated metabolites of estrogens (17 $\beta$ -E2 and E1) are the only CYP1B1 metabolites to induce cellular proliferation, with the most profound effects observed with 16 $\alpha$ -hydroxyestrone (16 $\alpha$ -OHE1). In mice exposed to chronic hypoxia, urinary concentrations of 16 $\alpha$ -OHE1 were increased. Chronic dosing of 16 $\alpha$ -OHE1 in mice (1.5mg/kg/day by intra-peritoneal injection for 28 days) resulted in the development of a PAH phenotype in female mice only. 16 $\alpha$ -OHE1 induced cellular proliferation in human pulmonary arterial smooth muscle cells (hPASMCs) and this was inhibited by a scavenger of reactive oxygen species (ROS) and an inhibitor of extracellular regulated kinase 1/2 (ERK 1/2). 4-hydroxylation is the predominant metabolic pathway activated by CYP1B1 activity and we therefore investigated the effects of the 4-hydroxylated metabolite of 17 $\beta$ -E2 *in vivo*. 4-hydroxyestradiol (4-OHE2) had no effects on PAH parameters in mice (1.5mg/kg/day by intra-peritoneal injection for 28 days). However, serotonin-induced vasoconstriction of the intra-pulmonary arteries was dramatically reduced in arteries harvested from mice dosed with 4-OHE2. More recent studies have identified that 4-hydroxyestrone (4-OHE1) is the predominant CYP1B1 metabolite in the lungs of mice. Interestingly, despite evidence for a pathogenic function of CYP1B1 activity *in vivo*, 4-OHE1 inhibited cellular proliferation in hPASMCs as assessed by thymidine incorporation whilst no effects were reported on cell viability.

We provide evidence for an altered estrogen metabolic axis in PAH, by in part, overexpression of the putatively pathological CYP1B1. Yet, the dynamic estrogen metabolic profile in pulmonary vascular cells remains undetermined. To address this, we developed a high fidelity HPLC method to quantitatively fate map estrogen metabolism in hPASMCs to determine the dynamic regulation of estrogen metabolism in PAH. We provide the first direct evidence that hPASMCs metabolize 17 $\beta$ -E2 and that estrogen metabolism is pathologically altered in PAH. Our metabolic screen revealed a prominent role for 17 $\beta$ -hydroxysteroid dehydrogenase enzymes in hPASMCs by rapid formation of E1 in all groups studied, increasing with time, with the highest activity in male control hPASMCs and the lowest activity in female control hPASMCs. In female control hPASMCs there was no evidence of CYP activity, whilst numerous metabolites were formed in the other groups studied. The formation of the pathogenic 16 $\alpha$ -hydroxylated estrogens was only evident in PASMCs from both male and female PAH patients at 24 and 48 hours. Globally, this study introduces a platform to elucidate effects of PAH insults and potential therapies on the estrogen-metabolic profile in pulmonary vascular cells.

Overall, we provide eminent evidence that the estrogen metabolic axis is pathologically altered in PAH and is influenced by gender. This provides a strong rationale for the application of estrogen-sensitive therapies in the management of this highly female discriminating disease.

# **Chapter 1**

## **Introduction**

## 1.1 The pulmonary circulation

At birth we are primed to take our first breath. Instantly there is a dramatic reduction in pulmonary vascular resistance (PVR) accompanied by closure of the ductus arteriosus, which is used in foetal life to bypass the pulmonary circulation. Subsequently the pulmonary arterial pressures (PAPs) rise and the lungs assume their prime function of gaseous exchange.

### 1.1.1 Pulmonary vascular structure and function

Deoxygenated blood drains into the right atrium of the heart from the superior and inferior vena cava returning blood from the upper and lower extremities. During the diastolic contraction of the heart, the tricuspid valves open allowing blood to flow into the right ventricle. During systole of the heart, the tricuspid valves close and blood is pushed through the semi-lunar valves into the main pulmonary artery which bifurcates into the left and the right pulmonary arteries. Each artery then enters its respective lung at the hilum through the parenchyma and is thereafter referred to as the intra-lobar pulmonary artery. This runs parallel to the respiratory tree alongside the bronchus to the alveoli where it becomes a mesh-like network of millions of capillaries from which gas exchange can occur. Only a very thin barrier exists between the pulmonary capillaries and alveoli allowing for passive diffusion of carbon dioxide and oxygen. There are approximately 480 million alveoli in the lungs with the prime purpose of increasing the surface area for gas exchange (Ochs *et al.*, 2004). The pulmonary arteries and veins each have 15 orders of branching between the main pulmonary artery and the capillaries and between the capillaries and left atrium, respectively (Huang *et al.*, 1996).

The lungs are unique in that they are the only organ that receives the entire cardiac output (CO) resulting in a high flow system of about 5 litres of blood per minute, which increases to about 25 litres during exercise. The primary function of the pulmonary circulation is gas exchange. Hence the pulmonary arteries have thin walls with a minimal smooth muscle cell layer resulting in a low-pressure, low-resistance system. The pulmonary artery is the only artery in the entire body that carries deoxygenated blood and similarly, the pulmonary vein is the only vein that carries oxygenated blood. The normal mean PAP is between 14mmHg and 20mmHg (Badesch *et al.*, 2009), which allows for adequate oxygen replenishment and unloading of carbon dioxide. In contrast, in the systemic circulation, mean pressures are of the order of 100mmHg. PAP is a result of CO and PVR and thus

$PAP = CO \times PVR$ . PVR is related to the intraluminal vessel wall diameter - the smaller the diameter, the greater the PVR. For this reason, arteries in the pulmonary circulation are normally fully dilated. Distension and recruitment of closed arteries are important mechanisms that are employed to reduce PVR when the cardiac output is increased, for example during exercise.

The lungs also contain a functionally distinct second circulation known as the bronchial circulation. The bronchial circulation arises from the systemic circulation and serves as the supplier of oxygen and nutrients to the conducting portions within the lung.

#### *1.1.1.1 Pulmonary arteries, veins and capillaries*

Mesenchymal cells differentiate into the heterogeneous population of vascular cells that comprise the vessel walls within the pulmonary circulation. The pulmonary arteries and veins have three distinct vascular layers. The tunica intima is the innermost layer of the vessel and is composed of a homogenous population of endothelial cells. The medial layer, the tunica media, is comprised of smooth muscle cells. The tunica externa is the outermost layer that consists primarily of collagen and fibroblasts. Each respective layer is separated by an extracellular matrix known as the basement membrane. Within the distal component of the lung, an extensive capillary network separates arteries from veins.

The structural composition of pulmonary arteries is functionally altered as it extends down the length of the vessel towards the base of the lung. Pulmonary arteries can be defined according to their structural composition as elastic, muscular or partially muscular pulmonary arteries. Elastic vessels contain numerous elastic laminae bound by external and internal elastic laminae and extend peripherally into transitional vessels which contain fewer elastic laminae. Once only an internal and external elastic lamina exists around the smooth muscle cell layer, these vessels are termed muscular. As the artery extends into the more distal portions of the lungs, the smooth muscle cell layer becomes sparse (partially-muscular) or absent (non-muscular) prior to extension into the capillary bed (deMello & Reid, 1991; Jones & Capen, 2011). Pre-acinar arteries (including the main pulmonary artery) are associated with bronchi, bronchioles or terminal bronchioles and contain numerous elastic laminae between smooth muscle layers and are more than 3200 $\mu$ m in diameter. As it extends beyond the ninth airway generation, the vessels become muscular and are generally more than 150 $\mu$ m in diameter (Elliot & Reid, 1964; Jones & Capen, 2011). Partially muscular pulmonary arteries are typically 75 $\mu$ m to 90 $\mu$ m in diameter

(Jones & Capen, 2011). Pulmonary arteries are much less muscular than systemic arteries as the pressure and resistance is much lower within these arteries.

Pulmonary arteries follow a branching pattern closely associated with the branching pattern of the bronchial tree, although there are many more pulmonary arterial branches than there are bronchial branches and these increase within the periphery (Elliot & Reid, 1964). The pulmonary artery will eventually extend into the alveolar capillaries, which form a dense anastomosing hexagonal network for which gas exchange can occur (Weibel, 1963). Oxygenated blood is then drained into the pulmonary vein, which carries the blood to the left atria where it is retained until diastole, allowing it to enter the left ventricle for subsequent pumping around the body.

### **1.1.2 The function of the pulmonary circulation**

The primary function of the pulmonary circulation is to facilitate gas exchange - unloading of carbon dioxide and loading of oxygen. Oxygen is obtained from inspired air and binds with haemoglobin within red blood cells and is essential to sustain metabolic processes throughout the entire body. Re-oxygenation is exquisitely facilitated by the gas-blood interface between the alveoli and the extensive alveolar capillary network.

In addition to facilitating gas exchange, the pulmonary circulation functions as a filtration system to remove fine particles and potentially lethal thromboemboli from the mixed venous blood before it returns to the systemic circulation (Comroe, 1966). This process is chiefly regulated by the pulmonary endothelium which releases mediators that promotes fibrinolysis. The location of the lungs together with the vast surface area of the pulmonary vasculature allows for this unique filtration function. Additionally the pulmonary circulation also serves as a blood reservoir for the left ventricle (Comroe, 1966).

### **1.1.3 Regulation of blood flow in the pulmonary circulation**

Pulmonary blood flow is most profoundly regulated by gravity and increases about 9 fold from the apex to the base of the lung (West *et al.*, 1964). Arterial, venous and alveolar pressures affect the distribution of blood flow within the lungs (West *et al.*, 1964). Blood flow and ventilation is regulated by ventilation-perfusion matching (West & Dollery, 1960). In 1946, Von Euler and Liljestrand characterised a vital difference in response to hypoxia between the systemic and pulmonary circulations (Euler & Liljestrand, 1946). In the systemic circulation hypoxia caused vasodilatation. In contrast, they observed that the

pulmonary arteries uniquely constricted in response to hypoxia (described in more detail below). This is perhaps not surprising considering the functional role of the two separate systems. In the pulmonary circulation the vasoconstrictor response to hypoxia aids in moving the passage of blood to well aerated areas mediating ventilation-perfusion matching. In the systemic circulation, hypoxia results in vasodilation in order to increase perfusion to meet the energy requirements of tissues and organs. In the lungs, ventilation-perfusion matching is also achieved by airway constriction in response to pulmonary arterial occlusion. This serves to direct inspired air towards alveoli with a denser blood flow. The matching of blood to a sufficient oxygen supply is therefore a critical regulator of blood flow in the lungs.

#### **1.1.4 Regulation of vascular tone: the endothelium**

Endothelial cells form the innermost lining of the vasculature and act as a mediator of physiological and injurious stimuli. Under normal physiological conditions there is an exquisite control of the production and secretion of vasoactive mediators. The predominant vasoconstrictors include endothelin-1 (ET-1) and thromboxane A<sub>2</sub> (TXA<sub>2</sub>) and the vasodilators include nitric oxide (NO) and prostacyclin, which can act in a paracrine fashion on the vascular endothelium and in an autocrine fashion on the underlying vascular smooth muscle cell layer. The endothelium is innervated by adrenergic and cholinergic nerve fibres that regulate vascular tone. Activation of adrenergic fibres causes vasoconstriction via the release of noradrenaline. In contrast, activation of cholinergic fibres causes release of acetylcholine resulting in vasodilation. The pulmonary endothelium is also an active participator in the metabolism of circulating mediators such as angiotensinogen, serotonin and noradrenaline, which are all regulators of vascular tone. The endothelium is sensitive to alterations in blood flow and this can have dramatic consequences for the endothelial cell fate and it is therefore an extremely important regulator of vascular tone. The balance of vasodilators and vasoconstrictors is therefore critical in important in maintaining the normal function of the endothelium.

#### **1.1.5 Excitation-contraction coupling**

Pulmonary vascular smooth muscle cell (PVSMC) tone is regulated by excitation-contraction coupling whereby a generated action potential drives depolarisation of the cell membrane resulting in PVSMC contraction. This process is driven by the interactions between actin and myosin. During cross-bridge cycling, myosin (an ATPase) interacts with actin resulting in vascular smooth muscle cell contraction, which is exquisitely mediated

via calcium ( $\text{Ca}^{2+}$ ) (Ward & Knock, 2011). This process is mediated by phosphorylation of myosin light chain (MLC) and the  $\text{Ca}^{2+}$ -calmodulin activated myosin light chain kinase (MLCK). Thereby, vasoconstriction is predominantly mediated by  $\text{Ca}^{2+}$  mobilization. PVSVC contraction is terminated by dephosphorylation of MLC by myosin light chain phosphatase (MLCP).

### **1.1.6 Effect of hypoxia on pulmonary vasoconstriction and remodeling**

In the pulmonary vasculature, exposure to acute hypoxia induces vasoconstriction and exposure to chronic hypoxia results in vascular remodeling. The most profound hypoxia-induced vasoconstriction occurs in the small pulmonary arteries (Weir & Archer, 1995). Potassium ( $\text{K}^+$ ) and  $\text{Ca}^{2+}$  are key regulators of pulmonary vascular tone in response to hypoxia. PSMCs have a resting membrane potential equivalent to the estimated equilibrium of  $\text{K}^+$  ions (Weir & Olschewski, 2006). Hypoxia inhibits  $\text{K}^+$  conductance in PSMCs resulting in cell depolarisation and the opening of L-type  $\text{Ca}^{2+}$  channels causing entry of  $\text{Ca}^{2+}$  ions and subsequent vasoconstriction (Post *et al.*, 1992).  $\text{Ca}^{2+}$  entry in to the smooth muscle cells is a key regulator of hypoxia-induced vasoconstriction. This is evident from studies showing that hypoxic pulmonary vasoconstriction in the rat lungs is inhibited with  $\text{Ca}^{2+}$  antagonists (McMurtry *et al.*, 1976). In chronic hypoxia, endothelial prostacyclin production is decreased in both proximal and distal pulmonary arteries together with a decreased formation of the vasoconstrictor prostaglandin E2 (PGE2) (Badesch *et al.*, 1989). Furthermore, chronic hypoxia results in an increased production of vasoconstrictors such as ET-1 and serotonin (Eddahibi *et al.*, 2000; Li *et al.*, 1994). This creates an imbalanced environment that favours pulmonary vasoconstriction.

Chronic hypoxia causes medial thickening of the pulmonary artery by smooth muscle cell hypertrophy and an increase in extracellular connective tissue, microfibrils, collagen fibres and elastin (Meyrick & Reid, 1980). In particular, hypoxia results in the muscularisation of previously non-muscular pulmonary arteries. Additionally, in the large elastic pulmonary arteries, structural changes including thickening of the media and adventitia contribute to altered flow dynamics that may influence both the right ventricle and the distal vasculature (Stenmark *et al.*, 2006). Interestingly, despite dramatic alterations in vascular morphology, the increases in medial and adventitial thickness of the pulmonary arteries and the corresponding right ventricular hypertrophy (RVH) recover to normal once returned to normoxic conditions (Meyrick & Reid, 1980). However, the structural effects induced by

hypoxia are irreversible and are associated with increases in extracellular collagen fibres, a reduced distensibility and lumen narrowing (Meyrick & Reid, 1980).

## 1.2 Pulmonary hypertension

Pulmonary hypertension (PH) is a complex, insidious and devastating vascular disease characterised by persistent elevations in PAPs and remodeling of the pulmonary vascular network. This includes obliterative remodeling of the pulmonary vasculature by excessive endothelial and smooth muscle cell proliferation and loss of the distal pulmonary circulation. The increased pulmonary pressures and vascular resistance challenges the right heart causing excessive strain that instigates adaptive hypertrophy that will eventually lead to maladaptive hypertrophy resulting in dilatation and right ventricular heart failure. PH can manifest itself through a plethora of aetiologies and it has therefore been necessary to group PH into subcategories to assist medical practitioners in providing the most suitable treatment options.

### 1.2.1 Classification of pulmonary hypertension

Since 1973 the World Symposium on Pulmonary Hypertension (WSPH) has brought together experts within pulmonary vascular diseases together to discuss and collate the latest scientific contributions within the field. From this, the World Health Organisation (WHO) classification of PH is derived, which is categorised according to shared histologies and vascular pathologies. Identification of PH WHO category is essential to direct the correct treatment regimen and to predict the potential outcome. The most recent WSPH was held in Nice in February 2013 from which the table below is derived (Table 1-1) (Simonneau *et al.*, 2013). The WHO classification is subcategorised into five groups of disorders that are known to cause PH: PAH (group 1); PH owing to left heart disease (group 2); PH owing to lung diseases and/or hypoxia (Group 3); chronic thromboembolic PH (Group 4); and PH with unclear multifactorial mechanisms (Group 5).

**Table 1-1 WHO classification of pulmonary hypertension****Group 1** Pulmonary arterial hypertension (PAH)

1.1 Idiopathic (IPAH)

1.2 Heritable (HPAH)

1.2.1 BMPR-2

1.2.2 ALK1, ENG, SMAD9, CAV1, KCNK3

1.2.3 Unknown

1.3 Drug- and toxin-induced

1.4 Associated PAH

1.4.1 Connective tissue diseases

1.4.2 HIV infection

1.4.3 Portal hypertension

1.4.4 Congenital heart diseases

1.4.5 Schistosomiasis

1.4.6 Chronic haemolytic anemia

1' Pulmonary veno-occlusive disease and/or pulmonary hemangiomatosis

1'' Persistent pulmonary hypertension of the newborn

**Group 2** Pulmonary hypertension owing to left heart disease

2.1 Systolic dysfunction

2.2 Diastolic dysfunction

2.3 Valvular disease

2.4 Congenital/acquired left heart inflow/outflow tract obstruction and congenital cardiomyopathies

**Group 3** Pulmonary hypertension owing to lung diseases and/or hypoxia

3.1 Chronic obstructive pulmonary disease

3.2 Interstitial lung disease

3.3 Other pulmonary diseases with mixed restrictive and obstructive pattern

3.4 Sleep-disordered breathing

3.5 Alveolar hypoventilation disorders

3.6 Chronic exposure to high altitude

3.7 Developmental abnormalities

**Group 4** Chronic thromboembolic pulmonary hypertension (CTEPH)**Group 5** Pulmonary hypertension with unclear multifactorial mechanisms

5.1 Hematologic disorders: chronic haemolytic anemia, myoproliferative disorders, splenectomy

5.2 Systemic disorders: sarcoidosis, pulmonary Langerhans cell histiocytosis:  
lymphangioliomyomatosis, neurofibromatosis, vasculitis

5.3 Metabolic disorders: glycogen storage disease, Gaucher disease, thyroid disorders

5.4 Others: tumoral obstruction, fibrosing mediastinitis, chronic renal failure on dialysis, segmental  
PH

BMPR-2 = bone morphogenic protein receptor 2; ALK1 = activin receptor-like kinase; CAV1 = caveolin 1; KCNK3 = potassium channel subfamily K member 3

## 1.2.2 Pulmonary arterial hypertension

PH is characterised as PAPs exceeding 25mmHg at rest (Badesch *et al.*, 2009). The diagnosis of group 1 PH, PAH, requires the additional diagnosis of pulmonary wedge pressures equal or greater than 15mmHg (Badesch *et al.*, 2009). PAH is the most fatal subtype of PH and is a progressive and devastating vasculopathy of the pulmonary arteries characterised by dysregulated endothelial cell proliferation and apoptosis paired with exuberant proliferation of apoptotic-resistant smooth muscle cells (Schermyly *et al.*, 2011). Previously non-muscular pulmonary arteries develop a smooth muscle layer eventually leading to obliteration and loss of the small distal arteries and the formation of complex vascular lesions (Cool *et al.*, 1999). There is currently no cure for the treatment of PAH and newer, more effective therapies are urgently required. The WHO have subcategorised PAH as is shown in Table 1-1: idiopathic PAH (IPAH), heritable PAH (HPAH), and drug and toxin-induced and PAH secondary to other diseases.

### 1.2.2.1 Idiopathic and heritable pulmonary arterial hypertension

In IPAH, the cause is neither inherited nor does it carry any identified risk factor. Germline mutations in the bone morphogenic receptor 2 gene (BMPR-2), a member of the transforming growth factor- $\beta$  signaling (TGF- $\beta$ ) family, are accountable for at least 70% of HPAH and 10% to 40% of apparently sporadic cases of IPAH (Lane *et al.*, 2000; Machado *et al.*, 2001; Thomson *et al.*, 2000). In a few cases, mutations in other genes belonging to the TGF- $\beta$  super family have been reported: activin receptor-like kinase type 1 (ALK1), endoglin (ENG) and Sma and Mad (mothers against decapetaplegic)-related proteins (SMAD) 9. Additionally novel gene mutations in caveolin-1 (CAV1) (Austin *et al.*, 2012a) and the gene encoding the potassium channel super family K member-3 (KCNK3) (Ma *et al.*, 2013) have been identified.

### 1.2.2.2 Drug and toxin-induced pulmonary arterial hypertension

Anorectic drugs have been associated with the development of PAH. In the 1960s there was an epidemic of PAH amongst obese patients taking the anorectic drug aminorex. These findings were later confirmed by the observation that patients taking the pharmacologically related drug dexfenfluramine for more than 3 months were at a high risk of developing PAH (Abenhaim *et al.*, 1996; Kramer & Lane, 1998). To date, there are now several drugs and toxins that have been associated with the development of PAH and these have been classified on the strength of evidence for their association with PAH into

definite, possible, likely and unlikely (Simonneau *et al.*, 2013). Definite associations according to the updated clinical classification of PAH (Simonneau *et al.*, 2013) include aminorex, fenfluramines, dexfenfluramines, toxic rapeseed oil, benfluorex and selective serotonin reuptake inhibitors. Possible associations include cocaine, phenylpropanolamine, St. John's wort, chemotherapeutic agents, interferon  $\alpha$  and  $\beta$  and amphetamine-like drugs. Likely risk factors include amphetamines, tryptophan, methamphetamines and dasatinib. Unlikely risk factors include estrogen, oral contraceptives and cigarette smoke (Simonneau *et al.*, 2013).

### 1.2.2.3 Associated pulmonary arterial hypertension

The development of PAH is also recognised to occur secondary to other diseases. These include connective tissue diseases, such as scleroderma, human immunodeficiency virus (HIV), portal hypertension, congenital heart disease in adults, schistosomiasis and chronic haemolytic anaemia (Simonneau *et al.*, 2013).

## 1.2.3 The diagnosis, prognosis and epidemiology of pulmonary arterial hypertension

The symptoms of PAH are non-specific and include breathlessness, fatigue and syncope (Rich *et al.*, 1987) making a prompt diagnosis challenging. Electrocardiograms provide valuable information on right ventricular function by measuring RVH. Chest radiographs, pulmonary functional tests and echocardiography amongst other tests are all useful indicators of lung and heart functions. However, right heart catheterisation is essential for the diagnosis of PAH and to test the vasoreactivity of the pulmonary circulation (Galie *et al.*, 2004).

The epidemiology of PAH has been outlined by three major registries (Badesch *et al.*, 2010; Humbert *et al.*, 2006; Ling *et al.*, 2012). In the UK/Ireland (Ling *et al.*, 2012) and France (Humbert *et al.*, 2006) the estimated incidence of PAH is 6.6 cases per million and 15 cases per million, respectively. In all three registries, the median age at diagnosis was 50 years old and IPAH was the most common form of PAH diagnosed. A higher proportion of patients were female with a reported 70% in the UK and Ireland (Ling *et al.*, 2012), 65.3% in France (Humbert *et al.*, 2006) and 80% in the USA (Badesch *et al.*, 2010). In addition, there appeared to be an association with obesity and an increased body mass index and the development of PAH.

### 1.2.4 Pulmonary arterial hypertension arteriopathy

Along the media of the pulmonary artery there is a heterogeneous population of phenotypically distinct vascular cells. The main pulmonary artery is composed of three distinct layers of cells as mentioned previously; endothelial cells in the tunica intima, heterogeneous smooth muscle cells within the tunica media and both muscular and non-muscular cells in the tunica adventitia (Frid *et al.*, 1994; Stiebellehner *et al.*, 2003). As the artery extends from the extra-lobar pulmonary artery and into the intra-pulmonary artery the lumen and the arterial wall narrow with fewer vascular cell types. In the distal pulmonary artery only a homogeneous population of smooth muscle cells exists (Stiebellehner *et al.*, 2003). The smooth muscle cell layer eventually ceases and only a thin layer of endothelial cells remains (occasionally with a single smooth muscle cell or pericytes: smooth muscle cell precursors).

In utero, the initial development of larger blood vessels involves the recruitment of precursor smooth muscle cells by endothelial cells in the mesoderm. Smooth muscle cells will proliferate and undergo differentiation and maturation into the quiescent adult smooth muscle cell (Stenmark & Mecham, 1997). Pulmonary vascular remodeling is a key feature of PAH and is defined as any structural changes that occur within the vascular wall and can occur within all three vascular layers. In particular, a key feature of re-structured pulmonary arteries includes an increase in smooth muscle cells and endothelial cells. It appears that in the vasculature normally quiescent cells resistant to mitogenic stimulation exhibit cellular responses similar to developmental processes when injured (Stenmark & Mecham, 1997). Non-muscular pulmonary arteries are typically comprised of endothelial cells and in some cases, pericytes. In response to injury, pericytes can differentiate into vascular smooth muscle cells, which contributes to muscularisation of previously non-muscular arteries. Injurious insults include inflammation, hemodynamic stress (increased shear stress), mechanical injury and hypoxia.

There is a general acceptance that the distal pulmonary arteries are the most crucial mediators of increased vascular resistance that precede the development of RVH. However, recent indications have challenged this notion, suggesting that stiffening of the proximal pulmonary artery by deposition of collagen may impact PAPs and RVH in the absence of any structural changes in the distal pulmonary circulation (Vanderpool *et al.*, 2013). Interestingly, distal smooth muscle cells have a very low proliferative capacity compared to proximal smooth muscle cells. Furthermore, hypoxia actually reduces their

proliferative capacity (Stiebellehner *et al.*, 2003). Thus, a phenotypic switch in the homogeneous population of smooth muscle cells in the distal pulmonary arteries is presumed to occur to permit vascular proliferation and remodeling. Phenotypic switching is defined as a change in the gene expression of a cell that alters its behavioural response to various stimuli. For example, a previously non-proliferative cell may undergo phenotypic-switching into a highly proliferative cell. In addition, mature vascular endothelial cells can also transdifferentiate into smooth muscle cells through a mesenchymal transition (Frid *et al.*, 2002). Alternatively, proliferative smooth muscle cells of the proximal artery may migrate and extend into previously non-muscular pulmonary arteries contributing to distal pulmonary vascular remodeling.

The lung is composed of more than 40 different cell types that are essential to facilitate gas exchange and metabolic and endocrine functions. The lung has a remarkable regenerative capacity after injurious insults, yet the cell types that contribute to this effect remain obscure. There is now evidence for resident stem cells within the lung (Kajstura *et al.*, 2011) implicating that the phenotypically distinct smooth muscle cells that appear in the distal artery could also be differentiated stem cells. Alternatively, the origin of these cells could be from distinct regions, such as blood-borne progenitor cells or bone marrow-derived progenitor cells (Toshner *et al.*, 2009). However, there is currently much speculation of the role of progenitor cells in PAH as to whether they play a role in repairing damage that has occurred or whether they are indeed intricate to the pathogenesis of PAH (Toshner & Morrell, 2010).

The pathological features observed in PAH are primarily within the pulmonary arteries with the veins unaffected. PAH pathology includes pulmonary arterial vascular lesions within the distal pulmonary arteries (<500µm in diameter), characterised by medial hypertrophy, adventitial thickening, inflammation, complex vascular lesion (plexiform) formation and thrombotic lesions (Galie *et al.*, 2009).

Medial hypertrophy of both muscular and elastic arteries is a common pathological feature of all categories of PH (Pietra *et al.*, 1989; Pietra *et al.*, 2004). Alongside, dilatation of elastic pulmonary arteries and intimal atheromas and RVH are all manifestations of PH. Medial hypertrophy is an increase in the size of the vessel wall by hyperplasia and hypertrophy of both pre- and intra-acinar arteries eventually extending into previously non-muscularised acinar arteries (Pietra *et al.*, 2004). The pulmonary artery runs parallel to the respiratory tree and the pulmonary acinus is the region beyond the terminal bronchus. The

pulmonary acinus consists of the most delicate arterial structure with a discontinuous smooth muscle cell layer, which eventually ceases to exist (Pietra *et al.*, 2004).

Plexiform, dilatation and arteritis have been classified as complex vascular lesions that occur as part of the arteriopathy associated with PH (Pietra *et al.*, 2004). Plexiform lesions are formed by extensive hyperplastic and hypertrophic responses of cells that constitute the arterial wall. Within their structures, vascular channels, lined with numerous proliferating endothelial cells are a typical feature (Jonigk *et al.*, 2011). Plexiform lesions consist of numerous cell types, including smooth muscle and inflammatory cells but predominantly consist of endothelial cells (Tuder *et al.*, 1994;Jonigk *et al.*, 2011). Plexiform lesions can occur in both pre- and intra-acinar regions of the pulmonary arterial tree, but typically occur at arterial branching points (Pietra *et al.*, 2004) and are present in 90% of patients with PAH (Stacher *et al.*, 2012). It is, however, difficult to determine the stage at which plexiform lesions start to occur as we are unable to assess the presence of lesions prior to lung transplantation. Thus, plexiform lesions may only be present at end-stage disease.

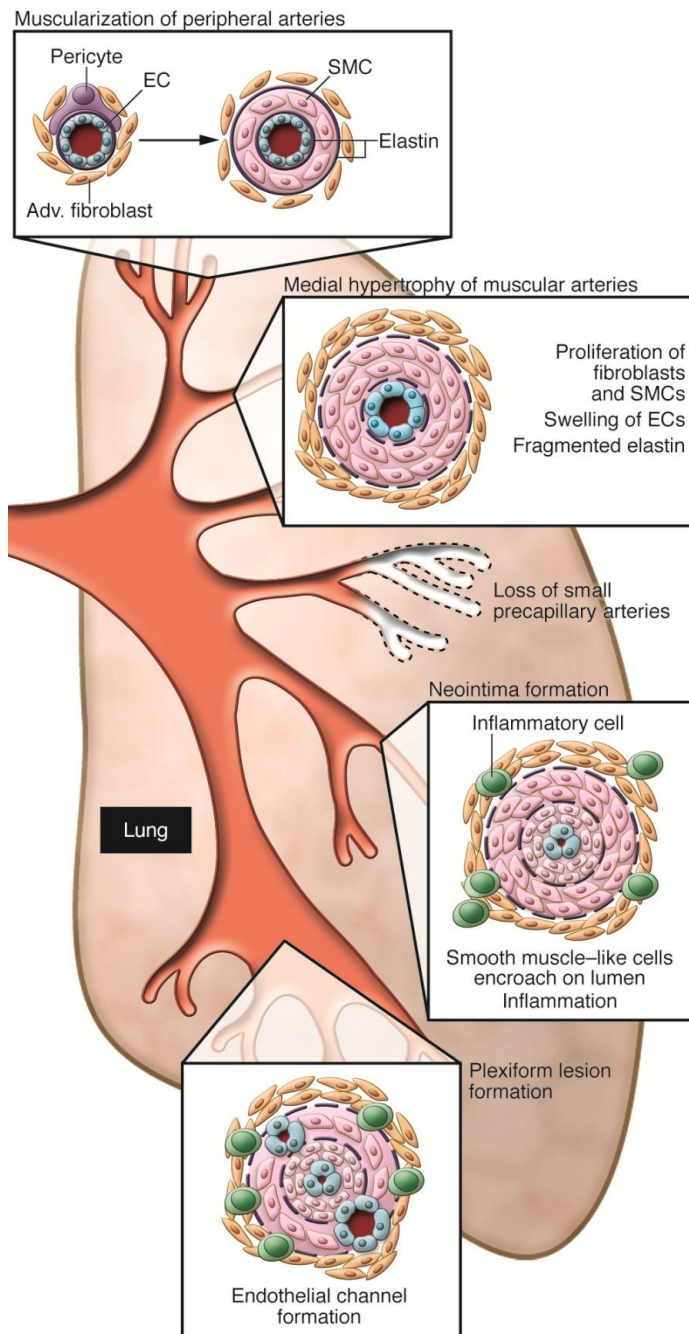


**Figure 1-1 Pulmonary arterial hypertension arteriopathy**

Pulmonary arterial hypertension (PAH) is a complex arteriopathy that includes muscularisation of peripheral pulmonary arteries, medial hypertrophy of muscular arteries, neointima formation, plexiform lesion formation and loss of precapillary arteries. SMC, smooth muscle cell; EC, endothelial cell. Reproduced with permission from Dr. Marlene Rabinovitch and the Journal of Clinical Investigation (Rabinovitch, 2012).

### 1.2.5 The right heart

In utero, the pulmonary circulation is vasoconstricted and the right ventricle is hypertrophied. At birth, the pulmonary pressures fall and the right ventricular structure is switched to an adult phenotype within weeks (Haddad *et al.*, 2011). The left and right ventricles of the heart are structurally and functionally unique. The right ventricle has a much thinner wall and whilst the volume of blood that is pumped out of the heart (stroke volume) is the same, it does this with less force due to the low resistance of the pulmonary arteries (Voelkel *et al.*, 2006). Chronic PAH results in a pressure overload on the right ventricle that initially leads to adaptive hypertrophy. Consistent constraint on the right ventricle eventually results in dilatation, contractile dysfunction and heart failure (maladaptive right ventricular remodeling). Right ventricular function is the most critical factor in the survival of patients with PH (D'Alonzo *et al.*, 1991; Sandoval *et al.*, 1994). Several mechanisms have now been identified to contribute to maladaptive right ventricular remodeling, including a switch from  $\alpha$ -myosin heavy chain ( $\alpha$ -MHC) to  $\beta$ -myosin heavy chain ( $\beta$ -MHC) as the main contractile protein, as well as mitochondrial, metabolic and electrical remodeling (Haddad *et al.*, 2011). In particular, RVH is associated with altered metabolic gene expression suggesting a switch from fatty acid metabolism to glucose metabolism as the main energy source (Sharma *et al.*, 2004).

Remarkably, despite dramatic alterations in right ventricular structure and function during PH, patients with severe PH who have received single-lung transplants show sustained improvement in right ventricular function in terms of ejection fraction and right ventricular wall thickness (Ritchie *et al.*, 1993). The mechanism by which the right ventricle repairs itself are still unclear but may be related to the mechanisms that occur after birth (Voelkel *et al.*, 2006).

### 1.2.6 Inflammation and pulmonary arterial hypertension

Inflammatory insults represent well-defined triggers of PAH. For example, HIV is associated with the development of PAH in ~0.5% of patients (Sitbon *et al.*, 2008). Perhaps the most common cause of PAH recognised is the parasite schistosomiasis which migrates through the skin into the venous system where it matures into an adult worm before migrating into the lung causing an inflammatory response. 1% of patients infected by schistosomiasis will develop PAH, supporting a functional role for inflammation in PAH (reviewed by Graham *et al.*, 2010). Furthermore, there is a direct correlation with the development of PAH in patients with inflammatory conditions, such as systemic lupus

erythematous and scleroderma (reviewed by Johnson & Granton, 2011). Interestingly, it has been estimated that approximately 78% of patients affected with autoimmune diseases are women, suggesting that female hormones may drive disease pathogenesis and inflammatory responses (Fairweather *et al.*, 2008). The importance of inflammation in PAH can also be observed in BMPR-2 haploinsufficient mice. These mice do not develop a spontaneous PAH phenotype, yet under inflammatory stress these mice are more susceptible to a PAH phenotype than wild-type mice (Song *et al.*, 2005).

The role of inflammation in PAH is further supported by the increased production of inflammatory mediators in both experimental and human PAH (reviewed by Price *et al.*, 2012) and is therefore under intense investigation. T cells, B cells and macrophages are observed in the complex vascular lesions that are associated with PAH (Tuder *et al.*, 1994). Additionally, perivascular mast cells and dendritic cells are also increased in patients with IPAH (Savai *et al.*, 2012).

Cytokines are key mediators of inflammation and are also dysregulated in the setting of PAH. Serum cytokines, including the interleukins and tumour necrosis factor  $\alpha$  (TNF $\alpha$ ) levels are increased in both IPAH and HPAH and are indicative of survival in patients, thereby representing potential useful biomarkers (Soon *et al.*, 2010). Furthermore, chronic overexpression of TNF $\alpha$  is associated with the development of PAH (Fujita *et al.*, 2002) and TNF $\alpha$  administration to isolated rat pulmonary arteries increases vasoconstriction (Stevens *et al.*, 1992). Overexpression of interleukin-6 (IL-6) is associated with the development of severe PAH with the formation of neointimal occlusive angioproliferative vascular lesions (Steiner *et al.*, 2009). Taken together, this provides evidence for an association of inflammation with PAH, whether being of a causative nature or a secondary mediator.

### **1.2.7 Treatments**

The current therapeutic strategy in PH is aimed at targeting the underlying cause of the disease as well as the symptoms. Treating WHO group 1 PH, both IPAH and HPAH is complicated by the lack of understanding of its complex pathology. Advanced treatments are used to improve the symptoms and thereby the quality of life in this subset of patients. PH is a multifactorial process with various aetiologies and the treatment regimen will therefore depend on the PH classification. The majority of patients will receive Ca<sup>2+</sup> channel blockers, endothelin receptor antagonists, prostanoids or phosphodiesterase type 5

(PDE5) inhibitors alone or in combination. Patients will also be evaluated to receive supportive therapy including oral anticoagulants, diuretics, oxygen and digoxin. Currently available treatments are suboptimal and have considerable unmet clinical needs as mortality rates remain unacceptably high (Benza *et al.*, 2012) and the need for improved therapies is urgently required.

#### 1.2.7.1 $Ca^{2+}$ channel blockers

$Ca^{2+}$  channel blockers, such as nifedipine or diltiazem, inhibit the influx of  $Ca^{2+}$  through voltage gated  $Ca^{2+}$  channels. Consequently, the hyperpolarisation of vascular smooth muscle cells by the accumulation of  $Ca^{2+}$  inside the cell that results in a contraction is inhibited. This aims to reduce the increased pulmonary vascular tone and pressure. Acute vasodilator testing during right heart catheterisation is necessary in most patients (certainly in IPAH patients) to identify patients that will respond to long-term  $Ca^{2+}$  channel blocker therapy (Galiè *et al.*, 2013).

The use of  $Ca^{2+}$  channel blockers to treat patients with PAH was first reported in 1987 by Rich and Brundage where they treated a small cohort of patients with a high dose of a  $Ca^{2+}$  channel blocker. This led to reductions in PAPs and a regression of RVH as measured by electro- and echocardiography (Rich & Brundage, 1987). This provided rationale to assess the long-term effectiveness of  $Ca^{2+}$  channel blockers in PAH. In this study, 26% of patients responded to the treatment and it vastly improved the 5-year survival in these patients (Rich *et al.*, 1992). In a more recent study, the characteristics of IPAH patients whom respond to long-term  $Ca^{2+}$  channel blocker therapy were evaluated. Less than 10% of IPAH patients responded to the therapy, and all these patients had responded to the initial vasodilator test with either epoprostenil or NO (Sitbon *et al.*, 2005). Additionally, favourable responses to  $Ca^{2+}$  channel blockers has been reported in anorexigen-associated PAH, but was absent in PAH associated with HIV, portal hypertension, congenital heart disease and connective tissue disease (Montani *et al.*, 2010). Therefore, the use of  $Ca^{2+}$  channel blockers is limited in PAH as it is only effective in a very small subset of patients.

#### 1.2.7.2 Endothelin receptor antagonists

ET-1 is a potent vasoconstrictor that is produced and released predominantly by vascular endothelial cells, which was characterised by Yanagisawa and colleagues in 1988 (Yanagisawa *et al.*, 1988). Subsequently, elevated plasma levels of ET-1 were reported in

patients with PH (Stewart *et al.*, 1991). Importantly, the expression of ET-1 by vascular endothelial cells is also increased in PH (Giaid *et al.*, 1993).

ET-1 exerts its effects through binding with either endothelin receptor-A (ETA) or endothelin receptor-B (ETB), which are both G-protein coupled receptors (GPCR). In larger conduit arteries ET-1 induces vasoconstriction which is predominantly mediated by the ETA receptor. In contrast, in the smaller resistance vessels, the ETB mediates vasoconstriction (Maclean *et al.*, 1994). Subsequently, it was found that at lower concentrations the effects of ET-1 are mediated by the ETB, but at higher concentrations responses are mediated via ETA (McCulloch *et al.*, 1996). ET-1 mediates vasoconstriction through the ETA and ETB receptor by activation of phospholipase C resulting in an increase in intracellular inositol triphosphate, diacylglycerol and intracellular  $Ca^{2+}$  leading to sustained vasoconstriction and activation of mitogenic pathways (Galié *et al.*, 2004). In contrast, the ETB receptor also mediates vasodilation by stimulating the production of NO and prostacyclin (Hirata *et al.*, 1993). However, the pulmonary vasoconstriction observed in response to ET-1 stimulation is mediated by both receptors, as dual blockade is necessary for maximal effects (Galié *et al.*, 2004).

Pre-clinical studies suggested that the use of the non-selective endothelin receptor antagonist, bosentan, might be beneficial in the treatment of PH (Chen *et al.*, 1995; Eddahibi *et al.*, 1995). Bosentan is an orally active drug and has a half-life of approximately 5 hours. Clinical trials using bosentan have reported improvements in pulmonary haemodynamics, 6-minute walking distance and survival. However, a main adverse side effect of bosentan is hepatotoxicity and patients therefore need to be carefully monitored to assess their liver function. There is also evidence to suggest that women respond better to endothelin receptor antagonists than men, and going forward, this will need to be taken into consideration when evaluating treatment effectiveness (Gabler *et al.*, 2012).

The use of selective ETA-receptor antagonists has also been evaluated in PAH. For example, monotherapy with ambrisentan, an ETA selective antagonist has proven beneficial in haemodynamic parameters and 6 minute walking distance with low reported hepatotoxicity (Blalock *et al.*, 2010; Oudiz *et al.*, 2009). Whether selective antagonism has a therapeutic advantage over non-selective antagonism requires further elucidation.

### 1.2.7.3 Prostanoids

Prostacyclin is a member of the prostanoid family. It is a metabolite of arachidonic acid by the cyclooxygenase pathway and is predominantly synthesized by endothelial cells. Prostacyclin binds with vascular prostacyclin receptors which are GPCR. This increases intracellular cyclic adenosine monophosphate (cAMP), which activates protein kinase A (PKA) resulting in smooth muscle cell relaxation and inhibition of platelet aggregation. Prostacyclins are therefore potent vasodilators in vascular beds and are one of the most effective treatments in PAH. Prostacyclins are synthesized by the enzymatic activity of prostacyclin synthase and its expression is decreased in PAH (Tuder *et al.*, 1999). Prostacyclin and its analogues are therefore utilised in the management of PAH due to their vasodilator properties, which can counteract the effects of a shift towards the production of vasoconstrictor mediators, such as ET-1. Prostacyclins are therefore a very powerful tool in the treatment of PAH.

The clinical use of prostacyclin is limited by its very short half-life. Prostacyclin analogues have therefore been generated to improve their pharmacokinetic properties. There are three types of prostacyclin analogues approved for the treatment of PAH; Epoprostenol, iloprost and treprostinil are synthetic prostacyclin analogues that have been approved for the treatment of PAH. The administration of poprostenol is invasive and requires an intravenous catheter and a portable pump. In contrast, iloprost and treprostinil are available as inhalation agents. Treprostinil may also be administered subcutaneously. Beraprost is the only prostacyclin analogue that is available for oral administration, but has currently not been approved for the treatment of PAH. Although prostacyclins have improved survival and exhibit favourable vasodilator properties, they cannot prevent the manifestation of advanced plexiform lesions (Pogoriler *et al.*, 2012). Furthermore, there are several limitations with prostacyclin analogues including inconvenient routes of administration, non-specific activation of receptors and short-half-lives (Sitbon & Morrell, 2012).

### 1.2.7.4 Phosphodiesterase 5 inhibitors

The cyclic nucleotides, cAMP and cyclic guanosine monophosphates (cGMP) are important mediators of pulmonary vasodilation by activation of PKA and protein kinase G (PKG), respectively. It is well established that NO is a mediator involved in the activation of the cGMP/PKG pathway. Phosphodiesterases (PDEs) catalyse the hydrolysis of cAMP and cGMP. PDEs inhibitors are considered an attractive therapeutic to promote

vasodilation by increasing the intracellular concentration of cAMP and cGMP. Furthermore, PDE isoforms are differentially expressed within tissues allowing for selective targeting (Murray *et al.*, 2011). PDE5 is expressed in abundance within the lung (Corbin *et al.*, 2005) and PDE5 inhibitors that promote the activation of the vasodilatory cGMP/PKG pathway have been very effective in the management of PAH. In addition to their vasodilatory properties, PDE5 inhibitors have also shown anti-proliferative effects (Wharton *et al.*, 2005) which are highly favourable in this proliferative vasculopathy. PDE5 inhibitors including sildenafil, tadalafil and vardenafil are commonly known for their application in patients with erectile dysfunction. All three inhibitors are approved for the treatment of PAH and show positive therapeutic effects (Galiè *et al.*, 2013).

There are numerous PDE isoforms that mediate cyclic nucleotide levels within target tissues, yet only PDE5 inhibitors have been used to elevate cGMP levels and prostacyclin analogues to indirectly regulate cAMP levels through its receptors. More recently, in a comprehensive analysis of PDE isoforms within human pulmonary arterial smooth muscle cells (hPASMCs) from control and PAH samples demonstrated that the expression of PDE1A, PDE1C, PDE3B, and PDE5A were increased in patients with PAH (Murray *et al.*, 2007). Moreover, hPASMCs from PAH patients had a significant reduction in cAMP production in response to agonist stimulation with forskolin and PDE1 and PDE3 activity were largely accountable for this (Murray *et al.*, 2007). Specifically, inhibition of PDE1C resulted in an accumulation of cAMP and a reduction in hPASMC proliferation, highlighting this as a novel therapeutic target to modulate cyclic nucleotide levels in PAH (Murray *et al.*, 2007).

#### 1.2.7.5 Adempas® approved to treat pulmonary arterial hypertension

In late 2013 Adempas® (riociguat) was approved by the U.S. Food and Drug Administration (FDA) for the treatment of PAH based on promising phase 3 clinical trials. Riociguat is a soluble guanylate cyclase stimulator and acts in synergy with NO that results in vasodilation thereby reducing PAPs. Riociguat was shown to significantly improve exercise capacity and clinical end-points in a phase 3 clinical trial in patients with PAH (Ghofrani *et al.*, 2013).

### 1.2.8 Emerging therapies

The therapeutic strategy in PAH is two-fold. First, we have to selectively target the disease mediators. Second, we have to promote regeneration of the lost distal pulmonary arteries

and reverse the extensive remodeling of the pulmonary arterial network that is likely to have occurred. Ideally, therapies should also be selective for the pulmonary circulation to maximise the therapeutic effects and prevent off-target effects. Current therapies are mainly considered for their vasodilatory properties and more recently, the potential anti-proliferative effects. It has been postulated that for the successful management of PAH, the strategy should be to obtain therapies that are pro-apoptotic, regenerative and anti-inflammatory (Michelakis *et al.*, 2008).

### **1.3 Genetic basis of pulmonary arterial hypertension**

In 1951 Dresdale provided the first unique evidence that PAH may have a heritable basis, where a mother, her sister and her son all presented with symptoms of PAH (Dresdale *et al.*, 1951). More than ten years ago, a genetic basis for the development of PAH was finally confirmed and was a remarkable discovery that has paved the way for understanding the underlying disease mechanisms (Deng *et al.*, 2000; Lane *et al.*, 2000). It was later identified that more than 70% of patients with HPAH carried a mutation in the BMPR-2 gene (Machado *et al.*, 2006a). Globally, this identification has made significant contributions to our understanding of how such mutations contribute to disease pathogenesis.

#### **1.3.1 Bone morphogenic protein receptor type II**

In 1997, Nichols and colleagues (Nichols *et al.*, 1997) identified six families where there was evidence for PAH in the absence of any secondary cause. Inspection of the pedigree charts of the six families indicated an autosomal dominant mode of inheritance. By linkage mapping, they identified a gene associated with PAH on the long arm of chromosome 2. Aforementioned, in 2000 the first gene associated with PAH was identified. Mutations in the BMPR-2 gene that encode the bone morphogenic protein receptor type II (BMPR-2), a member of the TGF- $\beta$ , leading to dysregulated signaling were identified (Lane *et al.*, 2000). The penetrance of HPAH is low with only 20% of carriers actually developing the disease (Hamid *et al.*, 2009). Patients with IPAH also have reduced gene and protein expression of BMPR-2, although this is more enhanced in HPAH patients (Atkinson *et al.*, 2002).

In an attempt to establish the mode of inheritance in patients with HPAH in a large number of families, several striking observations were made (Lloyd *et al.*, 1995). Firstly, at birth there was an abnormal gender ratio, with a greater proportion of female births, suggesting

selective loss of male offspring. Secondly, in this cohort studied, the ratio of females to males was 2.7:1. Thirdly, if disease had been passed from an asymptomatic heterogeneous mother, the mean age of death was strikingly lower than if the disease had been acquired from an asymptomatic heterogeneous father. Fourthly, and perhaps the most intriguing observation, more females were carriers and more females had PAH (Loyd *et al.*, 1995). This provides evidence that an aspect of female gender is implicated in both the development and the progression of PAH.

Bone morphogenic proteins (BMPs) exhibit a plethora of biological activities including regulation of growth, differentiation and apoptosis. They are members of the TGF- $\beta$  signaling superfamily that signal through Smad and Smad-independent pathways. On the extracellular surface BMPs bind to the tetrameric complex that consists of the type II receptor, BMPR-2 and its co-type I receptor (such as BMPR1A, BMPR1B or ALK-1) (Machado *et al.*, 2011). Specific ligands for BMPR-2 are BMPs, specifically BMP-2, BMP-4, BMP-6, BMP-7 and growth differentiation factors (GDF) -5 and -6 (Morrell, 2006). Upon activation, the type I receptor undergoes phosphorylation which can activate several signaling pathways including phosphorylation of Smad1/5/8, p38 mitogen activated protein kinase (p38 MAPK), ERK1/2, c-Jun N-terminal kinase (JNK) and Akt/phosphoinositide 3-kinase (PI3K) (as reviewed by Massague, 2003; Morrell, 2006; Rabinovitch, 2012). Signaling via Smads requires interaction with Smad4 (co-Smad) in order to translocate to the nucleus where it can bind with deoxyribonucleic acid (DNA) and alter transcription.

In addition to mutations identified in the BMPR-2 gene, other mutations in the TGF- $\beta$  signaling pathway have also been confirmed. Mutations in ALK-1 (a type I receptor cognate to BMPR-2) (Harrison *et al.*, 2003) and ENG (Chaouat *et al.*, 2004) are present in patients with hemorrhagic telangiectasia and PAH (Harrison *et al.*, 2003). Rare mutations in Smad 9 have also been associated with the development of HPAH (Nasim *et al.*, 2011).

#### 1.3.1.1 *BMPR-2 signaling in the pulmonary vasculature*

Germline mutations in the BMPR-2 gene are accountable for at least 70% of heritable PAH (HPAH) and 10% to 40% of apparently sporadic cases of IPAH (Lane *et al.*, 2000; Machado *et al.*, 2001; Thomson *et al.*, 2000). As a consequence of non-missense BMPR-2 mutations there is either reduced trafficking of the receptor to the cell surface or compromised phosphorylation of BMP type 1 receptors, which are essential for activation

of Smads (Morrell, 2006). In contrast, missense mutations retain normal trafficking to the cell surface and ability to activate Smad signaling, but have compromised ability in signal transduction via Smads (Morrell, 2006).

BMPR-2 is expressed in all cell types that comprise the pulmonary vascular wall, but is predominantly expressed within endothelial cells (Atkinson *et al.*, 2002). Here they maintain normal endothelial cell function by regulating endothelial cell motility, survival and proliferation (Valdimarsdottir *et al.*, 2002; de Jesus Perez *et al.*, 2009). Gene silencing of BMPR-2 in endothelial cells induces apoptosis (Teichert-Kuliszewska *et al.*, 2006) through, in part, recruitment of non-canonical Wnt signaling (de Jesus Perez *et al.*, 2009). Phosphorylation of Smads by BMPR-2 in the endothelium activates proliferation (de Jesus Perez *et al.*, 2009) and promotes tube formation and migration (Valdimarsdottir *et al.*, 2002; de Jesus Perez *et al.*, 2009).

In pulmonary arterial smooth muscle cells (PASMCs) BMPR-2 is present, yet it is much less densely populated here than what is observed in endothelial cells (Atkinson *et al.*, 2002). In this vascular cell, their function confers depending on whether the cell type resides in the proximal or distal part of the pulmonary artery (Yang *et al.*, 2005). In the proximal pulmonary artery, BMP-4 stimulation inhibits proliferation, yet in the distal pulmonary arteries it stimulates proliferation. The inhibitory effects on PASMCs were subsequently found to be mediated via Smad1, which is markedly reduced in PAH patients, irrespective of BMPR-2 status (Yang *et al.*, 2005). In the setting of a BMPR-2 mutation, endothelial cells become susceptible to apoptosis, resulting in a leaky barrier that permits entry of circulating factors to the underlying smooth muscle cells (Yang *et al.*, 2005).

Despite advances in our understanding of the BMPR-2 pathway, there are still no drugs that aim to rescue this pathway. Recently, a promising target was identified (Spiekerkoetter *et al.*, 2013). Using a high-throughput luciferase reporter assay, FDA approved drugs were screened to assess their ability to rescue BMPR-2 signaling. Tacrilomus (FK506), an immunosuppressive drug, was able to recapitulate the function of BMP-4 by activating pSmad 1/5/8 and the inhibitor of DNA binding-1 (ID-1) in endothelial cells. Targeting this pathway may provide a promising therapeutic strategy in the management of HPAH and also in cases of IPAH where BMPR-2 signaling is reduced.

## 1.3.2 Genetic modifiers

### 1.3.2.1 *The serotonin transporter*

Elevated levels of serotonin have been associated with the pathology of both experimental and clinical PAH and these effects are mediated in part via the SERT. Polymorphisms within the SERT gene have been identified as a genetic risk factor in PAH. SERT is encoded by the soluble carrier family 6, member 4 (SLC6A4) and is localised to chromosome 17q11.1-17q12 (Ramamoorthy *et al.*, 1993). A short (S) and long (L) polymorphism in the upstream regulatory region of SERT affects its transcriptional regulation and is a common polymorphism (Lesch *et al.*, 1996). The short polymorphism confers reduced transcriptional efficiency of the SERT gene promoter and the long variant increases transcriptional efficiency.

In 2001, Eddahibi and colleagues (Eddahibi *et al.*, 2001b) reported that the L-allelic variant of the SERT promoter was present in 65% of patients with PAH whereas it was only present in 27% of controls. In HPAH patients, patients homozygous for the LL genotype present at an earlier age of diagnosis than patients with either the SS or LS genotypes (Willers *et al.*, 2006). In patients with PH secondary to heart failure, the LL variant is also associated with higher PAPs (Olson *et al.*, 2007). Given the incomplete penetrance (approximately 20% to 30%) that is observed in patients with BMPR-2 mutations (Newman *et al.*, 2001; Newman *et al.*, 2004), we therefore assume a multiple-hit hypothesis whereby an additional insult may be present. SERT polymorphisms represent one such 'insult' and this data provides evidence for this. In contrast, no associations with SERT polymorphisms were reported in patients with IPAH (Willers *et al.*, 2006). Other studies have also failed to identify any association with SERT polymorphisms and PAH (Baloira *et al.*, 2012; Machado *et al.*, 2006b). There is therefore still much speculation whether SERT polymorphisms contribute to PAH pathobiology.

### 1.3.2.2 *Cytochrome P450 1B1*

In 2008, West and colleagues identified another modifier gene in PAH, cytochrome P450 1B1, CYP1B1 (West *et al.*, 2008), a xenobiotic and estrogen metabolizing enzyme. Subsequently, they genotyped for the CYP1B1 polymorphism that substitutes an asparagine for a serine in position 453 in patients with BMPR-2 mutations with and without evidence for PAH (Austin *et al.*, 2009). This polymorphism is associated with increased proteosomal degradation of CYP1B1 (Bandiera *et al.*, 2005). Interestingly,

female patients with BMPR-2 mutations that had been diagnosed with PAH had a 4-fold higher penetrance for the wild-type genotype (Austin *et al.*, 2009). This suggests that CYP1B1 activity is associated with the development of PAH amongst BMPR-2-mutant carriers and represents another potential ‘second-hit’ factor. The contribution of this in experimental PAH is intriguing and remains to be determined.

### **1.3.3 Newly identified genetic mutations**

#### *1.3.3.1 Potassium channel, subfamily K, member 3 (Ma et al., 2013)*

In 2013, mutations in KCNK3 (also known as TASK-1), a pH sensitive potassium channel that regulates the resting membrane potential was identified as a mutation associated with PAH (Ma *et al.*, 2013). All the mutations identified in this channel in patients with PAH results in a loss-of-function. KCNK3 is postulated to be important in regulating pulmonary vascular tone. Furthermore, hypoxia blocks KCNK3 and treprostinil (an FDA approved drug for the treatment of PAH) can activate the channel (Olschewski *et al.*, 2006). In addition, a phospholipase inhibitor can also rescue the function of this channel and represents a novel mechanism by which potassium channel activity can be rescued in patients with PAH (Ma *et al.*, 2013).

## **1.4 Animal models of pulmonary arterial hypertension**

When describing animal models of PAH, they will be defined as PH (although these animals do develop a PAH phenotype). However, the classical models that are utilized are currently under scrutiny as to whether they are direct models of human PAH and therefore to avoid confusion, they will be termed PH.

### **1.4.1 Hypoxic-induced pulmonary hypertension**

Brisket disease is a severe and costly disease that occurs in cattle residing at high altitude, named suitably after the swelling that occurs in the brisket. Glover and Newsom in 1915 first described this phenomenon in cattle living at high altitude with symptoms including weakness, dyspnoea on exertion, diarrhoea and oedema (Glover & Newsom, 1915). Upon autopsy, abnormalities were reported in the heart structure, including enlargement and thin, dilated walls. Furthermore, it appeared that returning the cattle to a lower altitude was sufficient to reverse the disease (Glover & Newsom, 1915). Based on these findings, together with consistent reports of RVH in brisket disease (Alexander & Jensen, 1959),

Will and co-workers pioneered the studies investigating the effect of hypoxic exposure on the pulmonary circulation (Will *et al.*, 1962). The effects of high altitude on pulmonary haemodynamics were assessed over time in normal cattle. The cattle developed the so-called brisket disease and all had elevated pulmonary pressures, which increased over time. Despite a consistent development of PH in all the animals studied, there was a wide-spread in the degree of PH with some animals reaching PAPs of 45mmHg, whilst others reached over 100mmHg (Will *et al.*, 1962). Furthermore, there was evidence that the response to hypoxia was very species dependent, which led on to a very unique study that addressed the effect of hypoxia in various species (Tucker *et al.*, 1975). In response to chronic hypoxia, pigs and calves developed severe PH, rabbits and rats developed moderate PH whereas sheep, guinea pigs and dogs developed mild PH. In trying to identify the underlying mechanism for these interspecies variations, the researchers identified the medial thickness of the small pulmonary arteries in control animals as being strongly correlated with the severity of PH developed (Tucker *et al.*, 1975). This identified a key role for vascular smooth muscle in the development of hypoxia-induced PH. The extreme ease at inducing PH in animals by exposure to chronic hypoxia has made this an extremely popular model utilized by researchers.

#### **1.4.2 Monocrotaline-induced pulmonary hypertension**

The oral administration of *crotalaria spectabilis* seeds results in the development of PH and RVH and is associated with a medial increase in the pulmonary trunk and muscular pulmonary arteries (Kay *et al.*, 1967). A single injection of monocrotaline (MCT) derived from the *crotalaria spectabilis* plant is sufficient to induce severe PH and RVH in rats (Ghodsi & Will, 1981). MCT is activated to dehydromonocrotaline in the liver by the activity of cytochrome P450 3A4 (CYP3A4) (Reid *et al.*, 1998). MCT results in endothelial damage and extension of smooth muscle into normally non-muscular pulmonary arteries (Rosenberg & Rabinovitch, 1988). Despite the evidence for endothelial cell damage, this model is characterised by medial smooth muscle thickening in the absence of endothelial cell angio-obliterative lesions (Gomez-Arroyo *et al.*, 2012b).

### 1.4.3 Development of pulmonary hypertension in animal models that display heightened serotonin activity

#### 1.4.3.1 Serotonin transporter overexpressing mice

Female mice that overexpress the serotonin transporter (SERT<sup>+</sup> mice) develop spontaneous increases in RVSP and pulmonary vascular remodeling at 5-6 months of age, which is absent in male SERT<sup>+</sup> mice (White *et al.*, 2011b). Interestingly, despite increases in RVSP and PVR, this occurs in the absence of RVH (White *et al.*, 2011b).

#### 1.4.3.2 S100 Ca<sup>2+</sup> binding protein A4 overexpressing mice

The S100 Ca<sup>2+</sup> binding protein, S100A4/mts1, is expressed in neointimal and complex vascular lesions of patients with PAH. Additionally, in approximately 5% of mice that overexpress the S100A4/mts1 gene, there have been identified lesions that exhibit similar vascular arteriopathy to human PAH (Greenway *et al.*, 2004). Serotonin stimulates the release of S100A4/mts1, which enhances the proliferation and migration of hPASMCs via the receptor for advanced glycation end products (RAGE). Further upstream, nuclear transport of phosphorylated ERK via a serotonin receptor, the 5-HT1B receptor, is mediated by SERT and is essential for the up-regulation of S100A4/mts1 (Lawrie *et al.*, 2005). In parallel with the SERT<sup>+</sup> model, only female mice develop elevated RVSP and pulmonary vascular remodeling at 5 months of age, and this effect is absent in male mice. Additionally, the development of neointimal lesions was only observed in female mice. Again, there appeared to be no effect on RVH as a consequence of S100A4/mts1 overexpression (Dempsey *et al.*, 2011).

#### 1.4.3.3 The SUGEN-Hypoxic Model of pulmonary arterial hypertension

Combined inhibition of the vascular endothelial growth factor receptor (VEGF-R) with the increased shear stress caused by hypoxia results in apoptosis of endothelial cells, releasing vascular endothelial growth factor (VEGF) and TGF- $\beta$ . This stimulates proliferation and inhibits apoptosis of the underlying smooth muscle cell layer. In mice, exposure to SUGEN5416 (SU5416 (SU); VEGF-R inhibitor) and hypoxia for three weeks results in the formation of occluded vascular lesions. However, when returned to normoxic conditions, the developed phenotype reverses to baseline characteristics (Ciuclan *et al.*, 2011). In contrast, rats develop more severe lesions after just three weeks and this progressively worsens to a severe PH phenotype that recapitulates human PAH arteriopathy when returned to normoxic conditions (Abe *et al.*, 2010). Interestingly, serotonin activity is

heightened in this model (Ciucan *et al.*, 2011; Ciucan *et al.*, 2012). In fact, the development of SU-hypoxic induced PAH is dependent on peripheral serotonin synthesis, as mice devoid of tryptophan hydroxylase 1 (TPH1), the rate limiting enzyme in the synthesis of serotonin, do not develop a PAH phenotype (Ciucan *et al.*, 2012). Furthermore, female rats also develop a more severe disease phenotype in this model compared to male rats (Tofovic *et al.*, 2012).

#### 1.4.3.4 Dexfenfluramine-induced pulmonary hypertension

Dexfenfluramine is an indirect serotonergic agonist that is an identified risk factor for the development of PAH (Abenhaim *et al.*, 1996; Kramer & Lane, 1998). Dexfenfluramine is a SERT substrate that causes release of serotonin from intracellular stores (Rothman *et al.*, 1999). Dexfenfluramine also inhibits the reuptake of serotonin into cells thereby increasing extracellular concentrations of serotonin (Eddahibi *et al.*, 2001a). In animals, dexfenfluramine induces a PAH phenotype in female mice only, again with no effect reported on RVH (Dempsey *et al.*, 2013).

## 1.5 Serotonin signaling

Serotonin is a neurotransmitter and a hormone that is derived from tryptophan. The majority of the body's serotonin is produced by the enterocromaffin cells that line the gut. Serotonin is released into the bloodstream where it is rapidly taken-up and stored in platelets via the SERT, resulting in extremely low circulating plasma levels. Furthermore, serotonin is rapidly metabolized by monoamine oxidase to 5-hydroxyindoleacetic acid. There is substantial evidence suggesting that TPH1 activity, the rate limiting step in the synthesis of serotonin, contributes to experimental PAH (Abid *et al.*, 2012; Ciucan *et al.*, 2012; Izikki *et al.*, 2007; Morecroft *et al.*, 2007; Morecroft *et al.*, 2012). Pulmonary arterial endothelial cell expression of TPH1 is increased in both experimental and clinical PAH, increasing local serotonin production which can act in a paracrine fashion on underlying PASMCs to facilitate proliferation predominantly via the SERT (Eddahibi *et al.*, 1999) and the 5-HT<sub>1B</sub> receptor (Maclean *et al.*, 1996).

#### 1.5.1.1 The serotonin transporter and pulmonary arterial hypertension

The SERT is a member of the sodium/chloride (Na<sup>+</sup>/Cl<sup>-</sup>) family of transporters, which also includes noradrenergic, dopamine,  $\gamma$ -aminobutyric acid (GABA) and glycine transporters. As mentioned above, SERT is encoded by the SLC6A4, and is localised to chromosome

17q11.1-17q12 (Ramamoorthy *et al.*, 1993). Serotonin uptake by the SERT is mediated by the co-transport of one Na<sup>+</sup> and one Cl<sup>-</sup> ion, which is regulated by the Na<sup>+</sup>/K<sup>+</sup> ATPase (Torres *et al.*, 2003).

Serotonin is a potent smooth muscle mitogen and vasoconstrictor that is released from the vascular endothelium or from adrenergic stimulation in the pulmonary arteries. There is now a wealth of evidence to support a role for serotonin in the pathobiology of PAH. The original 'serotonin-hypothesis' of PAH arose from the PAH epidemic in patients taking the anorectic drugs, aminorex and dexfenfluramine (Abenhaim *et al.*, 1996). Both aminorex and dexfenfluramine are substrates for the SERT and cause release of serotonin from intracellular stores (Rothman *et al.*, 1999). This is supported by studies in mice where dexfenfluramine induces a PH phenotype, which is dependent on peripheral serotonin synthesis as mice deficient in TPH1 do not develop a PH phenotype (Dempsey *et al.*, 2008). Polymorphisms in the SERT gene that are associated with an increased expression of SERT are correlated with an earlier age of diagnosis in patients with BMPR-2 mutations, yet not in patients with IPAH (Willers *et al.*, 2006). One study reported that the L-allelic variant of the SERT gene that increases its expression was more common in patients with IPAH compared to controls (Eddahibi *et al.*, 2001b). Furthermore, SERT expression was increased in a small cohort of pulmonary arterial smooth muscle cells (PASMCs) from patients with PAH (Eddahibi *et al.*, 2001b). However, further comprehensive analyses have failed to find any significant associations between SERT alleles and PAH (Machado *et al.*, 2006b; Willers *et al.*, 2006). Overexpression of the SERT gene in mice, thereby increasing its activity, is sufficient to induce a PH phenotype (Maclean *et al.*, 2004; White *et al.*, 2011b; Guignabert *et al.*, 2006; Machado *et al.*, 2006b). Intriguingly, this is only evident in female mice and has subsequently been found to be dependent on circulating 17 $\beta$ -estradiol (17 $\beta$ -E2), the predominant circulating premenopausal hormone (White *et al.*, 2011b). Overexpression of the human SERT gene in mice has dramatic effects on gene expression profiles in the pulmonary arteries resulting in an up-regulation of 71 genes and a down-regulation of 84 genes (White *et al.*, 2011a). One gene that was up-regulated by SERT overexpression in mice was CYP1B1 (White *et al.*, 2011a), which is a major estrogen metabolizing enzyme. This suggests that that altered 17 $\beta$ -E2 metabolism may underlie the pathogenic effects of 17 $\beta$ -E2 in this model. On the other hand, mice deficient in the SERT gene develop less severe PH phenotypes in response to chronic hypoxia (Eddahibi *et al.*, 2000).

Although the precise mechanism by which SERT mediates proliferation of pulmonary vascular cells remains incompletely defined, serotonin-induced proliferation is heightened in PASMCs derived from PAH patients which is associated with an increased expression of SERT (Marcos *et al.*, 2004). Although, inhibition of SERT may offer some therapeutic value, extracellular concentrations of serotonin available to bind with the 5-HT<sub>1B</sub> receptor may increase, mediating vasoconstriction in human pulmonary arteries (Morecroft *et al.*, 1999) and proliferation of hPASMCs (Lawrie *et al.*, 2005). Additionally, there is evidence for cross-talk between the SERT and the 5-HT<sub>1B</sub> receptor. For example, the 5-HT<sub>1B</sub> receptor nuclear transportation of phosphorylated ERK1/2 is mediated by the SERT and is essential for the up-regulation of the Ca<sup>2+</sup> binding protein S100A4/mts1, which is associated with proliferation and migration of PASMCs (Lawrie *et al.*, 2005). Therefore, a greater therapeutic effect may be offered by dual inhibition of the SERT and the 5-HT<sub>1B</sub> receptor. Indeed, the combined 5-HT<sub>1B</sub> and SERT antagonist LY393558 is more effective than SERT inhibition alone in hypoxia-induced PH and SERT+ mice (Morecroft *et al.*, 2010).

## 1.6 Steroidogenesis

Both epidemiological studies and recent studies in animal models of PAH have highlighted a potential role for steroid hormones in the pathogenesis of this devastating vasculopathy. Steroid hormones have multi-factorial functions throughout the body and are synthesized from cholesterol in the gonads, adrenal glands and placenta and to a lesser extent in the adipose tissue, liver and skin. Progesterone, 17 $\beta$ -E2 and testosterone are synthesised by oxidative activity of the cytochrome P450 (CYP) enzymes and the hydroxysteroid dehydrogenases. The synthesis of steroid hormones is, in part, regulated by the hypothalamic-pituitary axis. Gonadotroph cells in the anterior pituitary gland synthesize and secrete leutenizing hormone (LH), which regulates estrogen and testosterone synthesis in the gonads.

Estrogens are small lipophilic compounds that have genomic and non-genomic activities that are produced from the pre-cursor cholesterol, providing the backbone of all steroid hormones. The cholesterol for this process can be obtained from the cell membrane, synthesized from acetate or obtained from the circulation from high density lipoproteins (HDL) or low density lipoproteins (LDL) (Scott *et al.*, 2009). Enzymatic activity of various CYP enzymes and the steroidogenic acute regulatory protein (StAR) metabolise cholesterol to pregnenolone which is then further metabolised to

dehydroepiandrosteredione (DHEA) by CYP catalytic activity. Activity of the  $3\beta$  hydroxysteroid dehydrogenase ( $3\beta$ -HSD) metabolises DHEA to androstenedione. Androstenedione can then be converted to testosterone by  $17\beta$ -hydroxysteroid dehydrogenase 3 ( $17\beta$ -HSD3). Testosterone may also be interconverted back to androstenedione by the activity of  $17\beta$ -HSD2. Alternatively, androstenedione can be metabolised to  $16\alpha$ -hydroxyandrostenedione by CYP2C11. Androstenedione, testosterone and  $16\alpha$ -hydroxyandrostenedione can undergo oxidative metabolism by CYP19A1 (aromatase) in the presence of nicotinamide adenine dinucleotide phosphate (NADPH) to the active estrogens, estrone (E1),  $17\beta$ -E2 and  $17\beta$ -,  $16\alpha$ -estriol (E3 or  $16\alpha$ -OHE1), respectively. The steroidogenic pathway for the synthesis of estrogens from cholesterol is summarized in Figure 1-2.

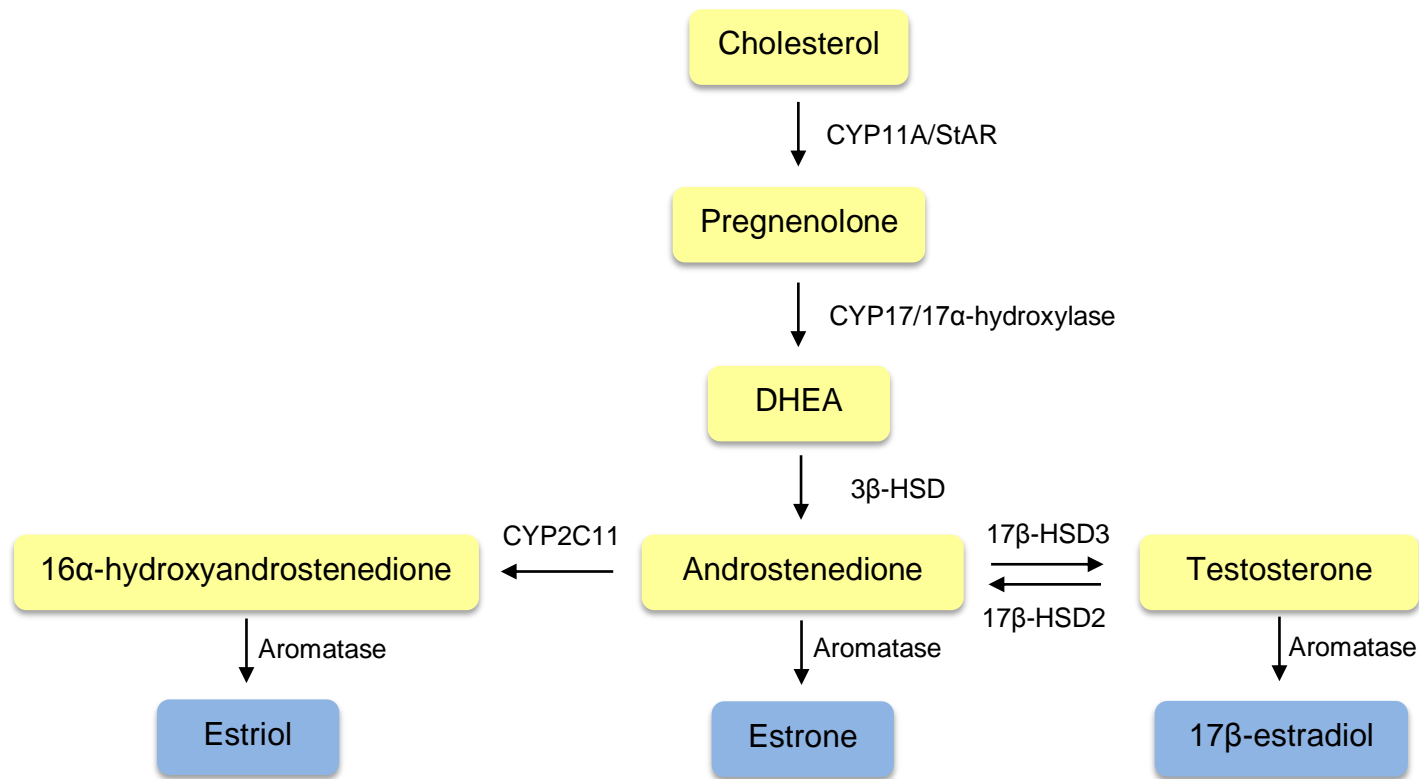


**Figure 1-2 Synthesis of estrogens from cholesterol**

Cholesterol is converted to pregnenolone by the activity of CYP11A and the steroidogenic acute regulatory protein (StAR). Pregnenolone is converted to dehydroepiandrosterone (DHEA) by the activity of CYP17 and 17 $\alpha$ -hydroxylase. DHEA is converted to androstenedione by 3 $\beta$ -hydroxysteroid dehydrogenase (3 $\beta$ -HSD). Androstenedione can then be converted to testosterone by 17 $\beta$ -hydroxysteroid dehydrogenase 3 (17 $\beta$ -HSD3) and/or 16 $\alpha$ -hydroxyandrostenedione by CYP2C11. 16 $\alpha$ -hydroxyandrostenedione, androstenedione and testosterone can then be converted to estrogens by the activity of aromatase to estriol, estrone and 17 $\beta$ -estradiol, respectively.

### 1.6.1 Aromatase

Aromatase is the critical enzyme in the synthesis of estrogens from androgens mediating the formation of E1 and 17 $\beta$ -E2 from androstenedione and testosterone, respectively (Figure 1-3). In pre-menopausal women, the primary site of estrogen synthesis occurs in the ovaries. In post-menopausal women and in men, the principal site of estrogen synthesis is extra-gonadal sites, such as the adipose tissue. Circulating C19 precursors act as a reservoir for the synthesis of estrogens within extra-gonadal sites. The principal pre-cursors are androstenedione, DHEA and DHEA-sulphate (DHEAS) which circulate at relatively high concentrations within the plasma in both men and women (Simpson, 2003). These pre-cursors are then converted into testosterone and estrogens within target tissues. The catalytic activity of aromatase removes a methyl group from the first carbon ring of testosterone, creating an aromatic ring resulting in the formation of 17 $\beta$ -E2 (Figure 1-3). Tissue specific expression of aromatase is therefore a powerful regulator of local estrogen synthesis in extra-gonadal sites. Locally synthesized estrogens can act in a paracrine or intracrine fashion creating a potentially potent estrogenic milieu that may be superior to the effects of circulating levels. Although it is difficult to correlate local estrogen synthesis with circulating levels, it has been predicted that the concentration of 17 $\beta$ -E2 in breast tumours in post-menopausal women is twenty times greater than levels circulating in the plasma (Pasqualini *et al.*, 1996). Local estrogen synthesis may therefore have a much greater impact on steroidogenic effects within target cells independent of circulating levels. It has been hypothesized that excess estrogens or aberrant activity are involved with tumorigenesis by exerting pro-proliferative effects and/or postulated that they act as pro-carcinogens by inducing genotoxicity (Tsuchiya *et al.*, 2005).

The regulation of aromatase is tissue-specific and is achieved through the use of different gene promoters (Simpson, 2003). Follicle stimulating hormone (FSH) regulates aromatase expression through cAMP in the proximal promoter II in the ovaries and retinoids regulate aromatase expression via the distal promoter I.1 in the placenta (Simpson, 2003). In contrast, within the adipose tissue and bone, aromatase expression is regulated by glucocorticoids, cytokines and TNF $\alpha$  by the distal promoter I.4 (Simpson *et al.*, 1997). In response to various injurious stimuli, such as inflammatory mediators, enhanced aromatase expression and subsequent estrogen synthesis is mediated via promoter switching from the distal promoter I.4 to the proximal promoter II (Agarwal *et al.*, 1996; Zhao *et al.*, 1996). More recently, hypoxia-inducible factor-1 $\alpha$  (HIF-1 $\alpha$ ) has been found to drive increased

aromatase expression in breast adipose tissue via promoter switching to the proximal promoter II (Samarajeewa *et al.*, 2013).

In other hormone-sensitive tissues, such as the lung and uterus, estrogens also present as a risk factor. For example, women are more likely to develop non-small cell lung cancer (NSCLC) than men, although in contradiction, women have a better 5-year survival rate (Cerfolio *et al.*, 2006). It has therefore been suggested that both endogenous and exogenous sources of estrogens may be associated with the development of lung cancer. Aromatase expression is increased in human NSCLC cells and  $17\beta$ -E2 stimulates proliferation within these cells (Marquez-Garban *et al.*, 2009). Furthermore, aromatase inhibition in NSCLC xenografted nude mice reduced tumour progression, suggesting that endogenously produced estrogens are in fact mediating pathogenic effects in NSCLC (Marquez-Garban *et al.*, 2009).

More recently, a genetic study has provided evidence that aromatase activity may be associated with PAH pathobiology. Portopulmonary hypertension (PPHTN) is a subcategory of PAH that occurs secondary to portal hypertension. Two promoter single nucleotide polymorphisms (SNPs) in aromatase have been associated with an increased risk of PPHTN and these SNPs are associated with elevated plasma  $17\beta$ -E2 levels (Roberts *et al.*, 2009). Furthermore, the aromatase inhibitor anastrozole has shown remarkable therapeutic potential in the SU-hypoxic rat model where it successfully reversed the PAH phenotype in female rats and this correlated with reduced plasma  $17\beta$ -E2 levels (Mair *et al.*, 2013; Tofovic *et al.*, 2013).

Aromatase inhibitors are already clinically approved for the treatment of estrogen-sensitive cancers and are the first line therapy against early and metastatic breast cancer in post-menopausal women. The application of this line of therapy in PAH may therefore be an attractive therapeutic strategy on the basis that PAH is an estrogen-sensitive vasculopathy. Anastrozole is currently being evaluated in a phase 2 clinical trial for its safety, ability to reduce circulating  $17\beta$ -E2 levels and to improve right ventricular function in patients with PAH.

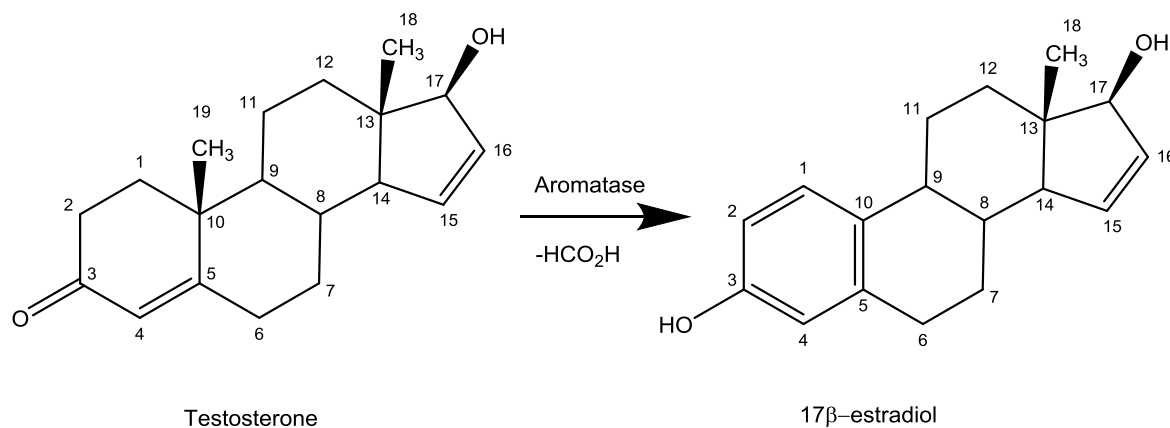


**Figure 1-3 Aromatisation of testosterone to 17β-estradiol**

## 1.6.2 Estrogens

There are three major subtypes of estrogens: 17β-E2, E1 and E3. In premenopausal women, the predominant circulating estrogen is 17β-E2. In women, circulating levels of 17β-E2 vary depending on the estrous cycle. In the follicular phase, circulating concentrations of 17β-E2 are about 100pg/mL (~0.37nM) and during ovulation these levels rise to about 600pg/mL (~2.20nM). After menopause, 17β-E2 levels are dramatically reduced up to 20-fold lower (Mendelsohn & Karas, 1999). We are all exposed to exogenous estrogen sources in various forms including contraception's, hormone-replacement therapy, dietary sources and chemical products. Furthermore, vascular cells can modulate their own estrogenic milieu by the local conversion of testosterone or androstenedione to 17β-E2 and E1 respectively (Harada *et al.*, 1999).

Estrogens (and androgens) circulate in the blood bound to the sex hormone binding globulin (SHBG), regulating circulating concentrations of free steroids and their transport to target tissues. The androgens, testosterone and dihydrotestosterone (DHT) have the highest binding affinities for SHBG followed by 17β-E2, E1 and E3 (Dunn *et al.*, 1981). In contrast, androstenedione has a relatively low binding affinity for SHBG (Dunn *et al.*, 1981). It is thought that steroids reach their target sites by binding of the SHBG with its receptor on the plasma membrane thereby resulting in either co-internalisation or release of the steroid. The true identification of the SHBG receptor and the mechanisms that underlie transport of steroids to target tissues still remains uncertain. Steroids may also circulate bound to albumin or other plasma proteins. It is assumed that only free unbound steroids are biologically active.

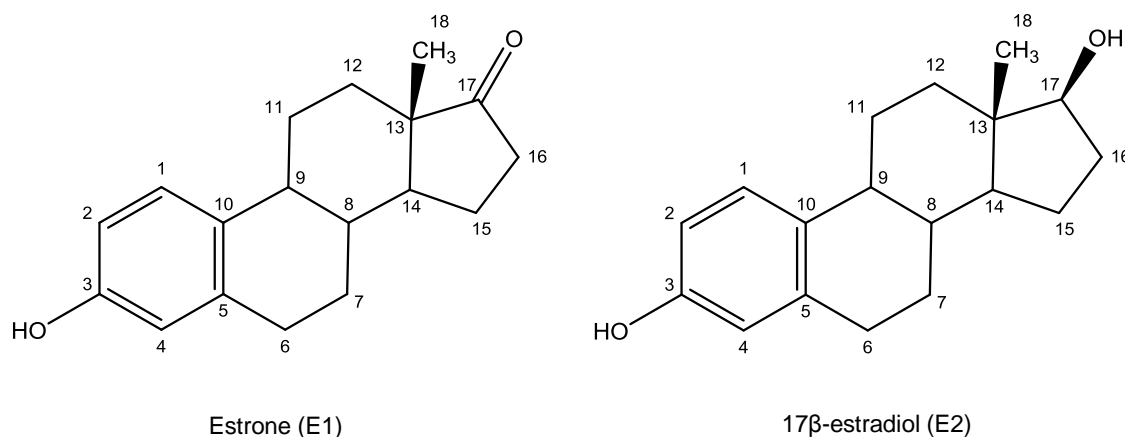


**Figure 1-4 Chemical structure of estrone and 17β-estradiol**

### 1.6.3 Tissue regulation of estrogens

The formation of biologically active estrogens within target tissues may also occur via the sulfatase and hydroxysteroid dehydrogenase pathways. Estrone-sulfate (E1-S) acts a reservoir for estrone synthesis through the sulfatase pathway. Steroid sulfatase hydrolyses both E1S and dehydroepiandrosterone-sulfate (DHEA-S). The estrone formed by this reaction can then be converted to 17β-E2 by the activity of 17β-hydroxysteroid dehydrogenase 1 (17β-HSD1). In a similar fashion, 17β-E2 can also be converted to E1 by the activity of 17β-HSD2. Thus, multiple pathways exist in maintaining the estrogenic milieu within target cells and fluctuations in enzyme activity and expression can therefore have dramatic consequences on the estrogenic potential of a cell.

Aromatase inhibitors have been successfully used in the management of breast cancer but endocrine resistance remains a problem associated with cancer relapse. Both steroid sulfatase inhibitors and 17β-HSD inhibitors are therefore currently being evaluated for their treatment in breast cancer. In breast cancer tumours, it appears that the sulfatase pathway may be superior to the aromatase pathway in regulating intra-tumoral 17β-E2 levels as its activity for estrone synthesis was dramatically higher than aromatase activity (Santer *et al.*, 1984). STX64 is a potent irreversible steroid sulfatase inhibitor that has been evaluated in a phase I clinical trial (Stanway *et al.*, 2006). After a five-day dosing period, steroid sulfatase activity in peripheral blood and breast cancer tissue was decreased almost 100% and E1, 17β-E2, androstenediol, DHEA, testosterone and androstenedione levels were significantly decreased (Stanway *et al.*, 2006). Patients that had previously had breast cancer progression with aromatase inhibitor therapy, showed evidence of a stable disease

with STX64 therapy (Stanway *et al.*, 2006). STX64 is currently being evaluated for its potential in reducing breast cancer growth and its safety and effectiveness in estrogen receptor positive and metastatic breast cancer.

As discussed previously, estrogenic E1 which is synthesized by steroid sulfatase and aromatase is converted to the potent estrogen 17 $\beta$ -E2 by the activity of 17 $\beta$ -HSD1. Inhibitors of 17 $\beta$ -HSD1 may therefore be a useful tool in regulating levels of 17 $\beta$ -E2 within tissues. 17 $\beta$ -HSD1 activity is associated with enhanced breast cancer cell proliferation by increasing 17 $\beta$ -E2 synthesis and inactivating dihydrotestosterone (DHT) (Aka *et al.*, 2010). Increased levels of 17 $\beta$ -HSD1 in breast cancer have been associated with a worse prognosis (Gunnarsson *et al.*, 2008; Oduwole *et al.*, 2004). Interestingly, in NSCLC, a high intra-tumoral expression of both 17 $\beta$ -HSD1 and 17 $\beta$ -HSD2 were positively associated with tumour stage (Verma *et al.*, 2013). Accordingly, a high intra-tumoral E1 concentration was associated with a high expression of 17 $\beta$ -HSD2 and a low intra-tumoral E1 concentration was associated with a high expression of 17 $\beta$ -HSD1 (Verma *et al.*, 2013). However, 17 $\beta$ -E2 intra-tumoral concentrations did not vary with isoform expression (Verma *et al.*, 2013). This study highlights a key role for both 17 $\beta$ -HSD isoforms within NSCLC.

#### 1.6.4 Estrogen receptors

Estrogens are small lipophilic compounds that play critical roles in sexual development and reproductive function. However, it is now recognised that estrogens contribute to a plethora of mechanisms in physiology and disease in both sexes. It has become increasingly apparent that estrogens can influence multiple biological functions, including inflammatory responses (Straub, 2007), cardiovascular function (Mendelsohn & Karas, 1999) and bone homeostasis (Weitzmann & Pacifici, 2006). Estrogens are lipophilic and can therefore penetrate the cell membrane into the cytosol. Once inside the cell, estrogens can be further metabolised by various CYP enzymes to active metabolites or can interact with its nuclear receptors, estrogen receptor  $\alpha$  (ER $\alpha$ ) or estrogen receptor  $\beta$  (ER $\beta$ ), encoded by the ESR1 and ESR2 gene, respectively. ER $\alpha$  and ER $\beta$  are transcription factors that alter gene expression upon activation. Alternatively, estrogens can also signal through non-genomic (do not affect gene transcription) mechanisms either by ER $\alpha$  or ER $\beta$  tethered on the plasma cell membrane (Simoncini *et al.*, 2000) or the orphan GPCR, GPR30/GPCR-estrogen receptor (GPER-1), mediating acute effects. ER $\alpha$  is a 66kDa protein whereas ER $\beta$  is a 59kDa protein. ER $\alpha$  and ER $\beta$  both have a DNA binding domain, a ligand binding

domain in the COOH terminal and a NH<sub>2</sub> terminal domain, through which they interact with regulatory binding proteins (Heldring *et al.*, 2007). There is significant homology amongst the two receptors in the DNA binding domain and the ligand binding domain. In contrast, ER $\alpha$  and ER $\beta$  differ in the terminal domain, activation function-1 (AF-1), which regulates target gene transcription. The functionally unique aspect of signaling through ER $\alpha$  and ER $\beta$  is that it is dependent on the environment in which it is activated. Therefore, the response will be different in a 'normal' cell compared to a 'diseased' cell. As hormones are key modulators of transcription, its activity depends on the signaling pathways that are activated when the ligand binds with the receptor, as well as the cellular composition of co-regulatory proteins and the promoters on estrogen responsive genes (Heldring *et al.*, 2007).

#### *1.6.4.1 Ligand-mediated regulation of estrogen receptor signaling*

Estrogen binding with either of its nuclear receptors results in its translocation to the nucleus where it regulates gene transcription. ER $\alpha$  and ER $\beta$  have distinct, often opposing effects on gene transcription. Thus, the relative expression of each receptor subtype within a cell may underlie the pleiotropic effects that are often observed with estrogens. Estrogen binds with the activation function-2 (AF-2) within the ligand binding domain of the estrogen receptor which results in a conformational change that promotes homodimerization and binding to the estrogen response element (ERE) within the promoters of target genes. The resultant increase or decrease in gene expression is mediated by the recruitment (tethering) of either co-activators or co-repressors. Estrogen can also regulate gene expression indirectly by tethering with other transcription factors, such as activator protein-1 (AP-1), and by protein-protein interactions (Murphy, 2011). This process has recently been demonstrated to be dependent on ligand-mediated induction of transcription factors (Heldring *et al.*, 2011).

#### *1.6.4.2 Ligand-independent regulation of estrogen receptor signaling*

In addition to the direct and indirect effects of ligand-mediated regulation of transcription through the estrogen receptors, estrogen receptors can undergo post translational modification including phosphorylation, acetylation ubiquitilation and sumoylation (Murphy *et al.*, 2011). Phosphorylation of the estrogen receptors can occur by various growth factors or membrane-bound estrogen receptors which permits binding to the ERE. Phosphorylation at specific serine sites within the receptor has been demonstrated to facilitate transcription. For example, phosphorylation at serine 118 (Ser118) by mitogen activated protein kinases (MAPK) of the estrogen receptor regulates the activity of the AF-

1 (Kato *et al.*, 1995). Phosphorylation can also occur at other serine residues including Ser104 and Ser106, amongst others. The exact role of phosphorylation of estrogen receptors remains under-investigated, yet it is thought to contribute to drug resistance to selective estrogen receptor modulators (Murphy *et al.*, 2011).

#### 1.6.4.3 Non-genomic signaling effects of estrogen receptors

Estrogen receptors that are localised on the plasma membrane as well as GPER-1 mediate non-genomic effects by acute activation of signaling kinases.  $17\beta$ -E2 has been associated with the stimulation of adenylate cyclase activity, cAMP, MAPK and PI3K signaling pathways. Activation of these pathways results in rapid cellular effects, such as activation of eNOS. For example, ER $\alpha$  binds to a regulatory subunit of PI3K in a ligand-dependent manner, thereby increasing its activity and the activation of eNOS (Simoncini *et al.*, 2000).

GPER-1 is a 7-transmembrane GPCR that regulates secondary messenger pathways. GPER-1 is unique in that it couples to a stimulatory and an inhibitory G protein, G $\alpha_s$  and G $\alpha_{i/o}$  respectively, regulating intracellular levels of cAMP. GPER-1 is an important mediator of the rapid, transient non-genomic effects of  $17\beta$ -E2 by ERK1/2 activation, which is dependent on transactivation of the epidermal growth factor receptor (Filardo *et al.*, 2000). Furthermore, GPER-1 mediates increases in cAMP in response to  $17\beta$ -E2 to restore epidermal growth factor activated ERK (Filardo *et al.*, 2000). GPER-1 is ubiquitously expressed in both normal and malignant tissues, with high levels in the heart, lungs, liver, ovaries and brain (Prossnitz *et al.*, 2008). In addition, GPER is also expressed in vascular endothelial cells and smooth muscle cells (Prossnitz *et al.*, 2008). Several studies have reported the expression of GPER-1 in cancerous tissues and its contribution to  $17\beta$ E2 induced cellular proliferation (Prossnitz *et al.*, 2008). GPER-1 protein expression has also been positively correlated with tumour size (Filardo *et al.*, 2006). It should however be noted that estrogen is not the sole activator of GPER-1 signaling which has also been shown to be activated by other mediators including aldosterone (Gros *et al.*, 2011).

In addition to GPER, several truncated isoforms of ER have been identified on the plasma membrane and are thought to contribute to the rapid, non-genomic effects of  $17\beta$ -E2.

#### 1.6.4.4 Estrogen receptor variants and their signaling

Estrogens mediate a plethora of activities within target cells and a persistent challenge is that not all findings can be understood through known properties of the 'classical' estrogen receptors. This complexity can be, in part, explained by the existence of splice variants of the estrogen receptors. At least two splice variants of ER $\alpha$  have been identified, ER36 (Wang *et al.*, 2005) and ER46 (Flourirot *et al.*, 2000). These are truncated ER $\alpha$  receptors that lack the NH<sub>2</sub> terminal domain. Both ER36 and ER46 can form heterodimers with ER $\alpha$  and regulate target gene transcription.

Estrogen receptors on the plasma membrane are important regulators of the rapid non-genomic signaling of estrogens, in particular by mediating the formation of eNOS and subsequent NO synthesis. ER46 is expressed in abundance within endothelial cells and is localized on the plasma membrane, cytosol and nucleus (Li *et al.*, 2003). In particular ER46 is localised within plasmalemmal caveolae and has been found to be a more potent inducer of eNOS than ER $\alpha$  (Li *et al.*, 2003). ER46 can also regulate genomic effects contributing to cellular proliferation. In estrogen receptor negative tissues, transfection of ER46 results in the activation of ER $\alpha$ -related genes and in ER $\alpha$  positive tissues, ER46 forms a heterodimer with ER $\alpha$  and acts as a competitive inhibitor of DNA binding thereby reducing transcription (Flourirot *et al.*, 2000). Moreover, the proliferative status of MCF-7 (breast cancer) cells is altered depending on the ratio of ER $\alpha$  to ER36 suggesting that ER46 plays a role in cellular proliferation (Flourirot *et al.*, 2000).

More recently, ER36 was characterised and cloned (Wang *et al.*, 2005). ER36 contains myristoylation sites giving it the potential to be localized within the plasma membrane (Wang *et al.*, 2005). Later studies confirmed that ER36 is predominantly a membrane-associated receptor (Wang *et al.*, 2006). ER36 lacks the transcriptional domains of ER $\alpha$  and functionally cannot regulate transcription in the absence or presence of 17 $\beta$ -E2 (Wang *et al.*, 2006). Moreover, ER36 inhibits the genomic signaling pathways of 17 $\beta$ -E2 - independent and -dependent transactivation activities of both ER $\alpha$  and ER $\beta$  (Wang *et al.*, 2006). ER36 is associated with the rapid, non-genomic effects of 17 $\beta$ -E2 and results in dramatic elevations in phosphorylated ERK1/2. These effects are mediated via a membrane-bound receptor as BSA-conjugated 17 $\beta$ -E2 (a membrane impermeable 17 $\beta$ -E2) was also found to dramatically induce ERK1/2 phosphorylation (Wang *et al.*, 2006). Interestingly, ER36 is expressed in triple-negative estrogen receptor breast cancer tumours and mediates 17 $\beta$ -E2 induced mitogenic signaling by cross-talk with the epidermal growth

factor receptor, Src and ERK (Zhang *et al.*, 2011). This challenges the convention that estrogen-receptor negative breast cancer is not associated with pathogenic estrogen signaling. Further contributing to the complexity of estrogen signaling is the presence of splice variants of ER $\beta$  (ER $\beta$ 2, -4, -5,  $\Delta$ exon5).

#### 1.6.4.5 Estrogen and the cardiovascular system

In contrast to the numerous pathogenic effects of estrogen signaling in hormone-sensitive cancers, 17 $\beta$ -E2 is renowned for its protective effects against cardiovascular disease in premenopausal women. However, it appears that fluctuations from physiological levels present as risk factors in a myriad of cardiovascular diseases (Barros & Gustafsson, 2011).

Estrogen receptors have been identified throughout the cardiovascular system in the endothelium, smooth muscle, adventitia and macrophages. Whilst estrogen signaling is probably a complex process that involves signaling through receptors, metabolism and non-receptor mediated effects, studies on estrogen receptor knock-out mice have been extremely informative to delineate its functions. Conditional knock-out of ER $\beta$  in mice causes right and left ventricular hypertrophy (Forster *et al.*, 2004), systemic hypertension (Zhu *et al.*, 2002), ovarian dysfunction (Cheng *et al.*, 2002) and fewer alveoli in the lungs (Patrone *et al.*, 2003). Interestingly, at 5 months of age, both male and female ER $\beta$  deficient mice have fibrosis in their lungs and underdeveloped alveoli (Morani *et al.*, 2006).

Studies using estrogen receptor knock-out mice have revealed that ER $\alpha$  is the predominant receptor mediating the cardio-protective effects of 17 $\beta$ -E2 on the heart by regulation of VEGF (Jesmin *et al.*, 2010). VEGF is a cytokine, mitogen and pro-survival factor for endothelial cells and its reduction is associated with the pathogenesis of numerous cardiovascular diseases, including PAH (Farkas *et al.*, 2009). In ER $\alpha$  and ER $\beta$  knock-out mice there is a reduced expression of VEGF and its receptors, signaling effectors endothelial nitric oxide synthase (eNOS) and the serine/threonine protein kinase akt, although the effects are much more pronounced in ER $\alpha$  knock-out mice (Jesmin *et al.*, 2010).

17 $\beta$ -E2 is recognized to mediate protective effects on the heart via inhibition of angiotensin II (Ang II). Ang II infusions results in left ventricular hypertrophy in female mice and this is exacerbated by ovariectomy (Pedram *et al.*, 2008). These effects are predominantly mediated via the ER $\beta$  as exogenously administered 17 $\beta$ -E2 partially

reversed the hypertrophy in ER $\beta$  knock-out mice, but inhibited this in wild-type and ER $\alpha$  knock-out mice (Pedram *et al.*, 2008).

In systemic vascular smooth muscle cells (VSMC), 17 $\beta$ -E2 inhibits cell proliferation by increasing the mitochondrial antioxidant enzyme, manganese superoxide dismutase (MnSOD) (Sivritas *et al.*, 2011). Furthermore, 17 $\beta$ -E2 reduces aortic neointima formation through MnSOD, which is dependent on the transcriptional activation of Kruppel-like factor-4 (KLF-4) (Sivritas *et al.*, 2011). The transcriptional activation of KLF-4 is mediated via ER $\alpha$  (Sivritas *et al.*, 2011). Interestingly, whilst 17 $\beta$ -E2 mediates protective effects in the cardiovascular system, these effects are lost in patients with diabetes mellitus (Orchard, 1996), suggesting that hyper/hypoglycaemia may affect 17 $\beta$ -E2 signaling. High glucose is associated with an accelerated rate of VSMC proliferation (Yasunari *et al.*, 1996). Interestingly, 17 $\beta$ -E2 inhibits VSMC proliferation under normal glucose levels (5.5mM) and has no effects in high glucose conditions (25mM) (Ortmann *et al.*, 2011). Selective activation of ER $\alpha$  with the agonist MPP inhibits high-glucose-induced VSMC proliferation, which is overcome with dual activation of ER $\alpha$  and ER $\beta$  (Ortmann *et al.*, 2011). Furthermore, these selective inhibitory effects mediated by activation of ER $\alpha$  are associated with a decrease in intracellular reactive oxygen species (ROS) formation and ERK activation (Ortmann *et al.*, 2011). Others have shown an importance for 17 $\beta$ -E2 in glucose homeostasis by studying aromatase knock-out (estrogen-deficient) mice. Both male and female aromatase knock-out mice have reduced glucose oxidation and increased insulin levels (Jones *et al.*, 2000).

## 1.7 Cytochrome P450 Enzymes

CYP heme-thiolate monooxygenase enzymes are catalytic molecules commonly known for their role in drug detoxification processes in the liver. As such they are abundantly expressed in the liver. CYP enzymes also play an extremely important role in the synthesis and metabolism of various endogenous compounds. The lung, aside from its major role in gas exchange, acts as a protective filter from the external environment and contains numerous CYP enzymes. Whilst CYP enzymes are detoxifying enzymes, they paradoxically lead to the formation of reactive intermediates that can induce cellular and DNA damage. In addition to their vast role in xenobiotic metabolism, CYP enzymes are critical in the metabolism of eicosanoids, the synthesis of cholesterol and the synthesis and metabolism of steroids, amongst others. Metabolism by the activity of CYP enzymes has a genotoxic capacity via the generation of reactive oxygen intermediates (ROMs) that can

interact with nucleic acids and proteins and initiate tumourigenesis (Nebert & Dalton, 2006).

CYP enzymes are haemoproteins in that they contain an iron ( $\text{Fe}^{3+}$ ), serving as a docking site for oxygen, which in the presence of NADPH is reduced to  $\text{Fe}^{2+}$ . CYP enzymes are part of a super-family subdivided according to sequence homology whereby if 40% of their sequence are identical then they belong to the same family (Gibson & Skett, 2001). Conserved sequence homology amongst CYP enzymes is only about 10-30%. CYP enzymes are critical enzymes in the phase 1 metabolism of drugs and endogenous compounds that lead to hydroxylated products. This is the first step in preparing a compound for elimination by increasing its polarity thereby making it more soluble in water. The liver is the prime site for CYP activity. Other prominent organs capable of CYP metabolism include the lung, kidney and brain, amongst others (Gibson & Skett, 2001). CYP enzymes are found in abundance within the microsomal fraction of the endoplasmic reticulum.

Numerous drugs and compounds are hydroxylated by the mixed-function oxidase (MFO) reaction which is catalysed by the activity of CYP enzymes. The criterion for substances to be metabolized by this pathway appears to be high lipophilicity, such as steroid compounds (Gibson & Skett, 2001). The overall chemical reaction is characterised by the following:



where RH represents an oxidisable substance such as a drug or steroid compound and ROH is the hydroxylated compound. This MFO reaction is catalysed and dependent on the activity of CYP enzymes.

### 1.7.1 Catalytic cycle of cytochrome P450 enzymes

Exogenous and endogenous compounds can undergo oxidation by the catalytic activity of CYP enzymes, including the estrogens,  $17\beta\text{-E}_2$  and  $\text{E}_1$  (Figure 1-5). The first step in the catalytic cycle involves binding of the estrogens with the oxidised ferric ( $\text{Fe}^{3+}$ ) of the CYP enzyme. NADPH-cytochrome P450 is a reducing agent that donates an electron for CYP hydroxylation resulting in  $\text{Fe}^{2+}$ . Molecular oxygen binds to the  $\text{Fe}^{2+}$ -steroid complex. Thereafter, electron rearrangement occurs between the oxygen and the iron and a second electron is introduced by the reduction reaction of NADPH-cytochrome P450. Subsequently a hydroxylated (-OH) product of the parent compound is released.

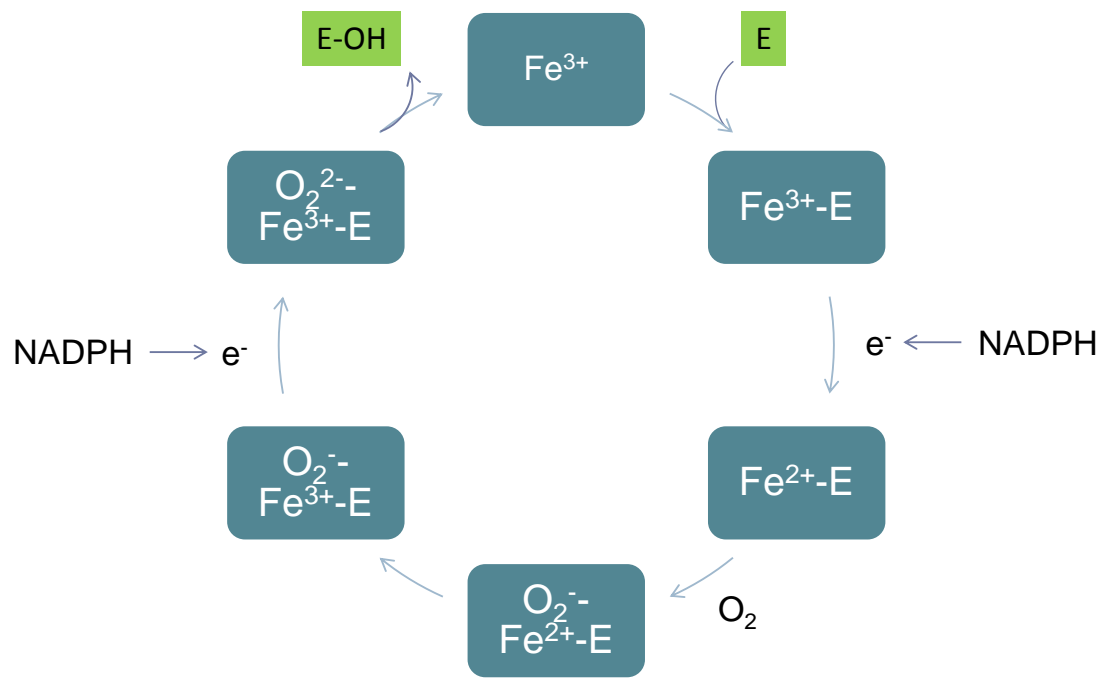


**Figure 1-5 Catalytic cycle of cytochrome P450 enzymes**

E represents an estrogen (either  $17\beta$ -estradiol or estrone) and Fe represents iron. NADPH, nicotinamide adenine dinucleotide phosphate.

### 1.7.2 Oxidative metabolism of estrogens: 17 $\beta$ -estradiol and estrone

CYP enzymes that metabolize estrogens are present in various target tissues and can dramatically alter the function of estrogens. Metabolites can exert biological effects by interactions with estrogen receptors and/or receptor-independent effects. 17 $\beta$ -E2 and E1 undergo oxidative metabolism by CYP enzymes in the presence of NADPH to their corresponding hydroxylated metabolites (Figure 1-6). Accumulating evidence suggests that certain estrogen metabolites formed by this pathway are biologically active and estrogenic and possess unique biological functions that may not be directly associated with their parent hormone. CYP enzymes are expressed in abundance within the liver and this is therefore a prime site of estrogen metabolism. CYP enzymes promote the hydroxylation (addition of an -OH group) on a carbon at any position within the chemical structure. Different CYP isoforms exhibit differential hydroxylation activities at different positions within the carbon structure of both 17 $\beta$ -E2 and E1. Therefore, the unique expression of CYP enzymes within target tissues can modulate metabolite formation. The consequences of estrogen metabolism can therefore have dramatic consequences for vascular cell fate by in part, regulating the formation of either anti- or pro-proliferative metabolites. The predominant hydroxylation pathways of 17 $\beta$ -E2 and E1 include 2-, 4- and 16 $\alpha$ -hydroxylations.

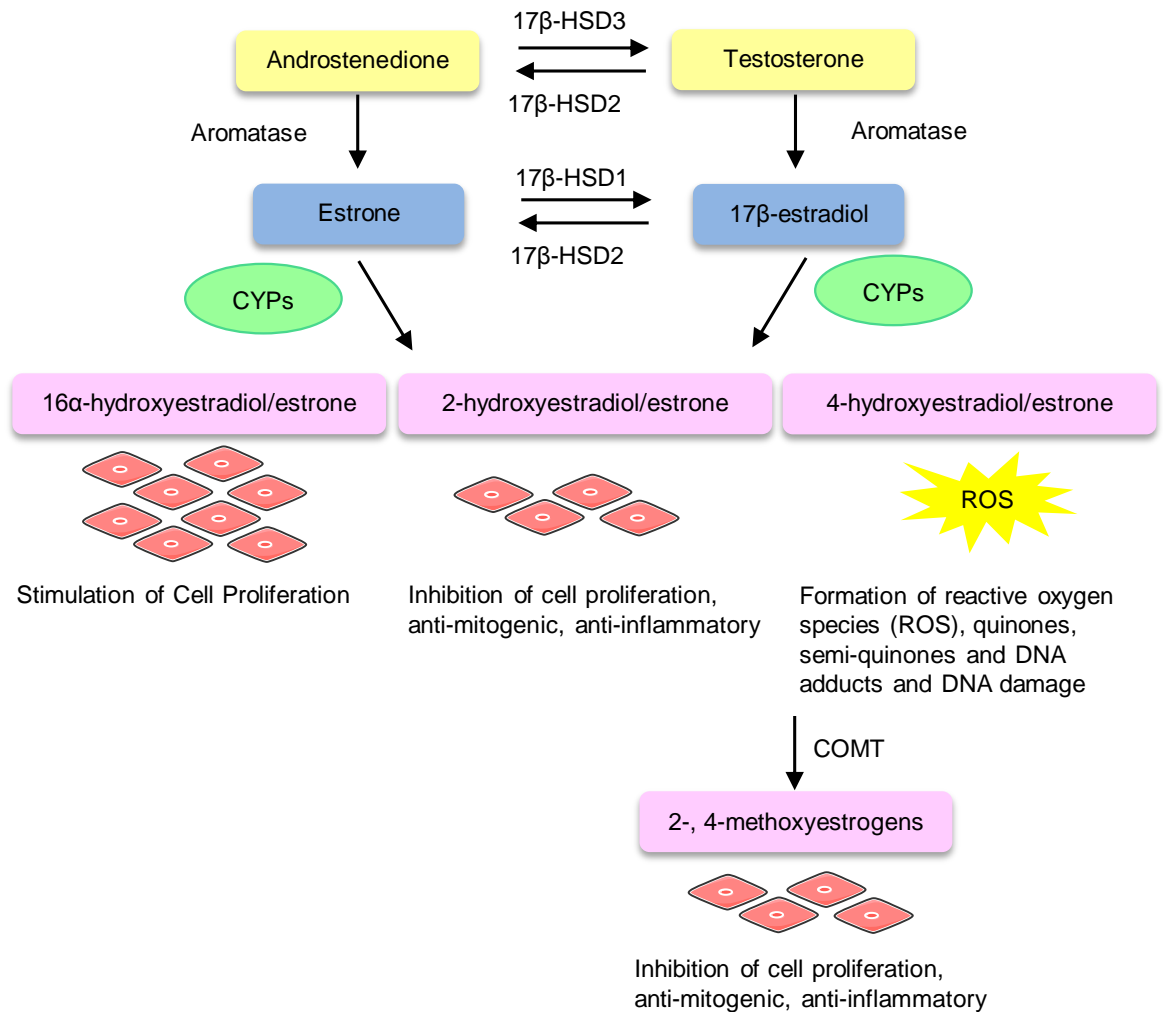


**Figure 1-6 Metabolism of estrone and 17β-estradiol and the effects of downstream metabolites**

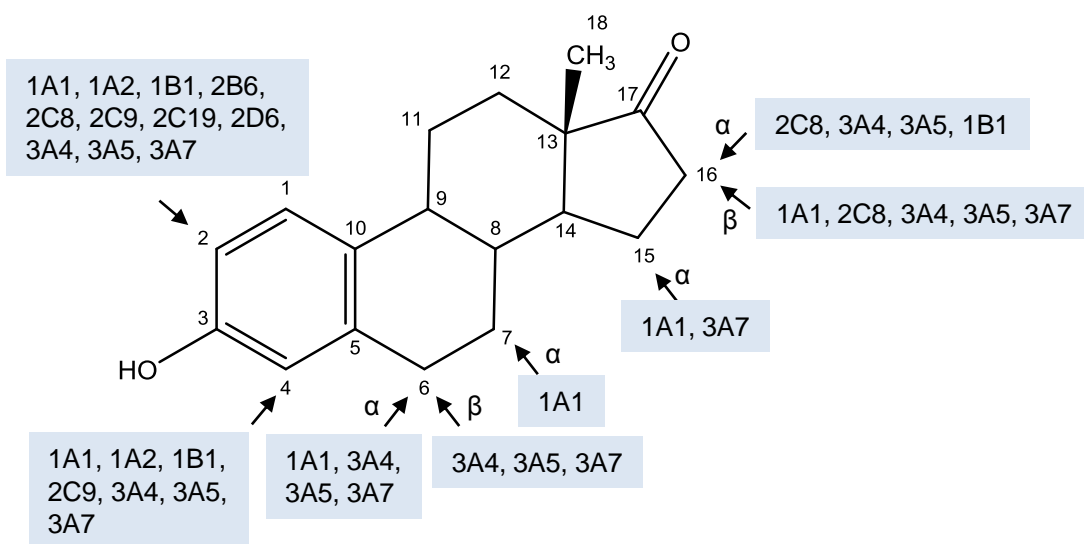
Estrone (E1) and 17β-estradiol (17β-E2) are synthesized from androstenedione and testosterone respectively by the activity of aromatase. E1 and 17β-E2 can then be further metabolized by the activity of cytochrome P450 enzymes (CYPs) to the 16α-, 2-, 4-hydroxylated estrogens. The 2- and the 4-hydroxylated estrogens can then be further metabolized by the activity of catechol-O-methyl transferase (COMT) to the 2- and 4-methoxyestrogens.

### 1.7.2.1 *The oxidative metabolism of 17 $\beta$ -estradiol*

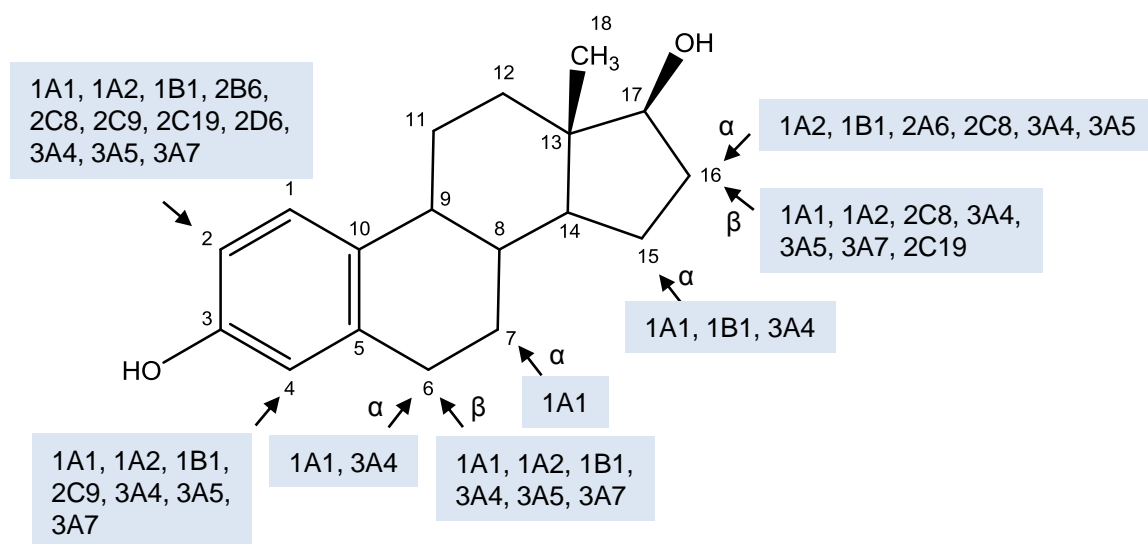
CYP1A1, CYP1A2, CYP3A4 and CYP3A5 have preferential 2-hydroxylation (hydroxylation at the second carbon) activities for 17 $\beta$ -E2 (Lee *et al.*, 2003). CYP1A1 also catalyses the formation of 15 $\alpha$ -, 6 $\alpha$ -, 4- and 7 $\alpha$ -hydroxyestradiol (15 $\alpha$ -OHE2, 6 $\alpha$ -OHE2, 4-OHE2 and 7 $\alpha$ -OHE2, respectively) and CYP1A2 and CYP3A5 can also mediate formation of 4-OHE2 (Lee *et al.*, 2003). CYP3A4 also catalyses the formation of 4-OHE2 and 16 $\beta$ -hydroxyestradiol (16 $\beta$ -OHE2) (Lee *et al.*, 2003). In contrast, CYP1B1 exhibits preferential catalytic activity for the 4-hydroxylation of 17 $\beta$ -E2, but has the additional capacity to generate 2-hydroxyestradiol (2-OHE2) and 16 $\alpha$ -hydroxyestradiol (16 $\alpha$ -OHE2) (Badawi *et al.*, 2001; Hanna *et al.*, 2000; Lee *et al.*, 2003). CYP2A6, CYP2B6, CYP2C8, CYP2C9 and CYP2D6 all have low estrogenic oxidative activities of 17 $\beta$ -E2 (Lee *et al.*, 2003).

### 1.7.2.2 *The oxidative metabolism of estrone*

A similar oxidative metabolic pathway by the activity of CYP enzymes is observed with E1. CYP1A1, CYP1A2 and CYP3A4 predominantly catalyses the formation of 2-hydroxyestrone (2-OHE1) followed by 4-hydroxyestrone (4-OHE1) CYP1B1 preferentially catalyses the formation of 4-OHE1 (Lee *et al.*, 2003). CYP2A6, CYP2B6, CYP2C8, CYP2C9 and CYP2D6 have low estrogenic oxidative activities for the C2 position (Lee *et al.*, 2003). The formation of 16 $\alpha$ -hydroxyestrone (16 $\alpha$ -OHE1) is catalysed predominantly by CYP1A1, CYP2C19 and CYP3A5 (Cribb *et al.*, 2006).



Estrone (E1)

17 $\beta$ -estradiol (E2)**Figure 1-7 Cytochrome P450 mediated metabolism of estrone and 17 $\beta$ -estradiol**

The metabolism of estrone (E1) and 17 $\beta$ -estradiol (17 $\beta$ -E2) by the catalytic activity of various cytochrome P450 (CYP) enzymes. Diagram modified and reproduced with permission from Professor Bao-Ting Zhu (Lee *et al.*, 2003)

### 1.7.3 CYP1B1

There are three members of the CYP1 family (CYP1A1, CYP1A2 and CYP1B1) and these are key enzymes in the metabolism and activation of hydrophobic xenobiotic pro-carcinogens. The aryl hydrocarbon receptor (AHR) regulates the expression of the CYP1 family (Figure 1-8). CYP1B1 is a member of the cytochrome P450 enzyme family I, subfamily B, polypeptide 1.

#### 1.7.3.1 Regulation of CYP1B1

CYP1B1 transcriptional activity is predominantly regulated by the AHR (Figure 1-8). Various endogenous and exogenous compounds including dioxins and poly aromatic hydrocarbons bind with the AHR complex (consisting of the AHR, AHR-interacting protein (AIP) and heat shock proteins (hsp90)). Upon binding, the AHR dissociates from its AIP and hsp90 and translocates into the nucleus where it dimerizes with the AHR nuclear translocator (ARNT). This complex then binds to specific DNA enhancer sequences known as dioxin-response elements (DRE) which results in transcription of the CYP1 family, including CYP1B1.

17 $\beta$ -E2 is a substrate for CYP1B1 and can regulate its transcriptional activity. In Ishikawa cells (human endometrial adenocarcinoma cells), over-expression of ER $\alpha$  induces the transcriptional activation of CYP1B1 in the presence of 17 $\beta$ -E2 and this may be via a direct interaction with ER $\alpha$  and estrogen responsive elements on CYP1B1 rather than via the AHR pathway (Tsuchiya *et al.*, 2004). In hPASCs, 17 $\beta$ -E2 at physiologically relevant concentrations (1nM) increases the protein expression of CYP1B1 (White *et al.*, 2011a). In addition, the profound PAH insults serotonin and dexfenfluramine also increase the expression of CYP1B1 in hPASCs (Dempsey *et al.*, 2013; White *et al.*, 2011b). In vascular endothelial cells, increased shear stress increases the expression of CYP1B1 (Conway *et al.*, 2009). Additionally, the transcription of CYP1B1 is induced by the environmental toxics 2,3,7,8-tetrachlorodibenzo-p-dioxin (TCDD) and benzo(a)pyrene. Co-treatment of TCDD with 17 $\beta$ -E2 in human lung cells results in an accumulation of 4-methoxyestradiol (4-MeOE2), a key downstream metabolite indicative of CYP1B1 activity (Cheng *et al.*, 2007).

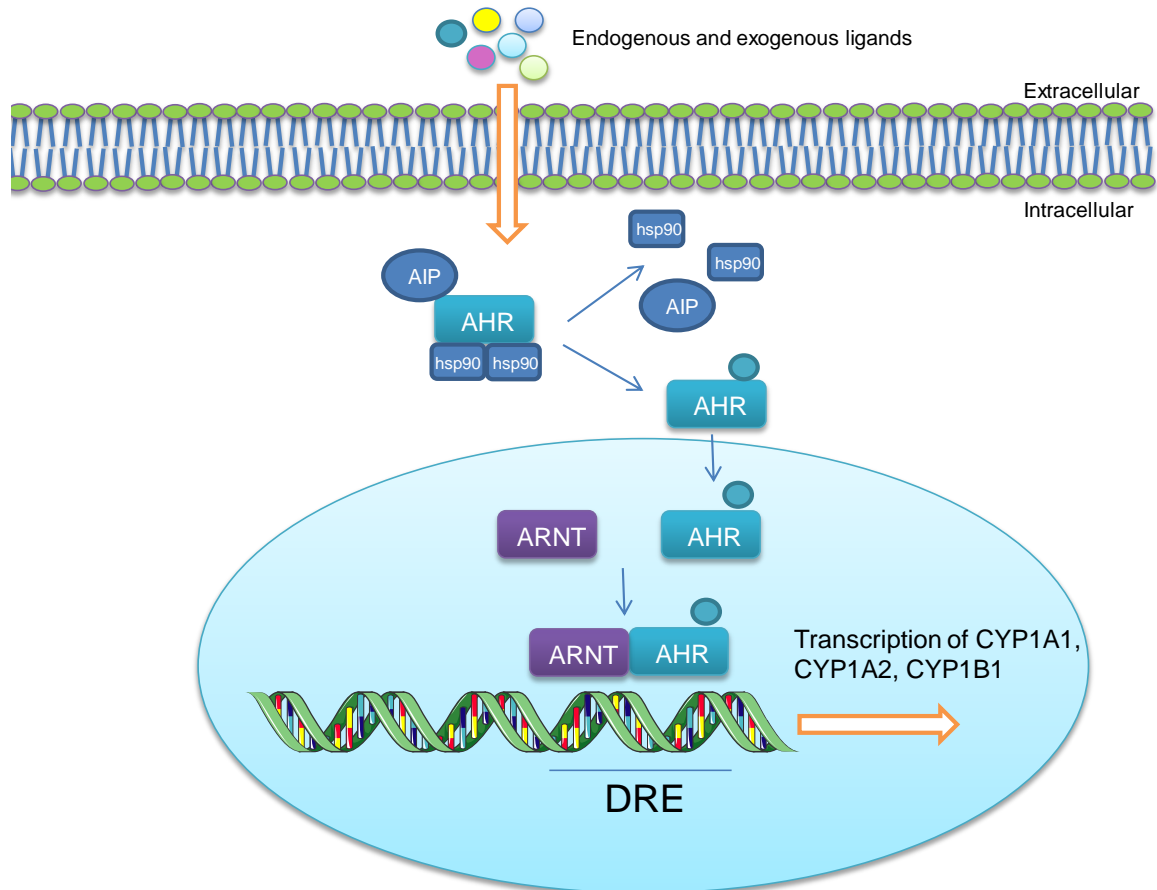


**Figure 1-8 Transcriptional activation of cytochrome P450 enzymes by the aryl hydrocarbon receptor**

Endogenous and exogenous compounds bind with the aryl hydrocarbon receptor (AhR) dissociating it from its complex consisting of AhR-interacting protein (AIP) and heat shock proteins (hsp90) and translocates to the nucleus. The AhR associates with the AhR nuclear translocator (ARNT) and binds with specific DNA enhancer sequences known as dioxin-responsive elements (DRE) which results in transcriptional activation of the CYP1 family.

### 1.7.3.2 CYP1B1 and cancer

Increased CYP1B1 expression has been reported in virtually all types of cancer including breast cancer (McKay *et al.*, 1995), lung cancer (Murray *et al.*, 1997) and ovarian cancer (McFadyen *et al.*, 2001). The relatively low expression of CYP1B1 within normal tissues makes this an attractive therapeutic target. This suggests that CYP1B1 activity could be used to bio-transform anti-cancer agents into their active form specifically only within target tissues. Furthermore, the therapeutic value of CYP1B1 inhibition in cancer is currently under phase 2 clinical trials (Luby, 2008). CYP1B1 is predominantly an extra-hepatic enzyme that hydroxylates 17 $\beta$ -E2 and E1 predominantly to the catechol 4-hydroxyestrogens (4-OHE2 and 4-OHE1, respectively). CYP1B1 is expressed within estrogen target tissues including the mammary, ovary and uterus (Tsuchiya *et al.*, 2005). The 4-hydroxyestrogens are recognised to contribute to tumorigenesis via the formation of ROS resulting in the formation of quinones and semiquinones that can cause DNA damage via the formation of depurinating DNA adducts (Nutter *et al.*, 1991;Nutter *et al.*, 1994). Although steroids may influence cellular function in terms of proliferation, a genotoxic event that induces cellular damage is essential for the initiation of cancer (Cavalieri *et al.*, 1997). The abundant expression of CYP1B1 in cancerous tissues including breast, colon, lung, oesophagus, skin, lymph node, brain and testis supports a pathological role for CYP1B1 in tumorigenesis, in particular since its expression was undetectable in normal tissues (Murray *et al.*, 1997). This is further supported by a high concentration of 4-hydroxylated estrogens in uterine leiomyoma and breast cancer (Lemon *et al.*, 1992;Liehr *et al.*, 1995;Liehr & Ricci, 1996). In human breast cancer biopsies, 4-hydroxylated estrogens are up to three times higher than 2-hydroxylated estrogens (Rogan *et al.*, 2003). In line with this, catechol estrogen quinone levels were also three times higher in breast cancer specimens compared to control (Rogan *et al.*, 2003). In addition to its 4-hydroxylation activity, CYP1B1 has the additional capacity to hydroxylate at the C2 and C16 positions on the carbon ring of 17 $\beta$ -E2 and E1.

In the liver, 4-hydroxylation is a minor metabolic pathway of estrogens with 2-hydroxylation being the predominant pathway (Hammond *et al.*, 1997;Suchar *et al.*, 1995). However, in extrahepatic tissues, 4-hydroxylase activity is much more profound. For example, in uterine myometrium and myomata (tumour tissue), 4-hydroxylation of 17 $\beta$ -E2 is the predominant pathway for catechol estrogen formation and this is elevated in myomata (Liehr *et al.*, 1995). Certain target tissues are susceptible to 17 $\beta$ -E2-induced carcinogenesis including the Syrian hamster kidney (Liehr *et al.*, 1986), CD-1 mouse

uterus (Newbold *et al.*, 1990) and the rat pituitary (Clifton & Meyer, 1956). More interestingly, in all these tissues the 4-hydroxylation pathway of catechol estrogen formation predominates, suggesting that metabolic activation of this pathway is associated with carcinogenesis (Bui & Weisz, 1989; Weisz *et al.*, 1992; Paria *et al.*, 1990). Microsomes isolated from human mammary adenocarcinomas and fibroadenoma show elevated 4-hydroxylation activities compared to normal tissue (Liehr & Ricci, 1996). However, more recently, in a comprehensive analysis of estrogen metabolites within breast cancer tissue and urine, there appeared to be no evidence for 4-hydroxylation activity in breast tissue, although 4-OHE1 was detected within in the urine (Taioli *et al.*, 2010). Both 4-OHE1 and 4-OHE2 retain strong estrogenic activity and have high binding affinities at both estrogen receptors ER $\alpha$  and ER $\beta$  (Zhu *et al.*, 2006).

CYP1B1 also has the additional capacity to promote the 2-hydroxylation of estrogens, although this is a relatively minor pathway. In contrast to the carcinogenic effects observed with the 4-hydroxylation pathway, both 2-OHE1 and 2-OHE2 lack carcinogenic activity. This is possibly due to its prompt and exceptionally high metabolic clearance rate by the activity of catechol-O-methyl transferase (COMT) to its methoxylated metabolites (Ball *et al.*, 1983; Merriam *et al.*, 1980). The products formed by this reaction, 2-methoxyestrone (2-MeOHE1) and 2-methoxyestradiol (2-MeOHE2), possess little estrogenic activity with a low binding affinity for estrogen receptors (Zhu *et al.*, 2006). Furthermore, 2-MeOHE2 has distinct antimitogenic, antiangiogenic, anti-inflammatory and apoptotic effects that are mediated independently of the estrogen receptors and has therefore been considered as an anti-cancer agent (Lakhani *et al.*, 2003).

16 $\alpha$ -hydroxylation represents a potentially pathogenic pathway that may be activated by CYP1B1 activity (Badawi *et al.*, 2001; Hanna *et al.*, 2000). In contrast to the evidence of a pathogenic role for the 4-hydroxylation pathway in cancer, the evidence for 16 $\alpha$ -hydroxylation is less concrete. 16 $\alpha$ -OHE1 binds to the estrogen receptor in two different ways. First, it binds in a similar non-covalent fashion to that of 17 $\beta$ -E2 and second, it forms an irreversible covalent bond with the receptor (Swanek & Fishman, 1988). Furthermore, 16-hydroxylated metabolites stimulate proliferation of breast cancer cells (Seeger *et al.*, 2006; Lippert *et al.*, 2003). An increased ratio of 2-OHE1/16 $\alpha$ -OHE1 has been inversely associated with an increased risk of breast cancer in some studies (Muti *et al.*, 2000; Dallal *et al.*, 2013) whereas other studies have failed to report any correlation (Cauley *et al.*, 2003; Eliassen *et al.*, 2008).

### 1.7.3.3 CYP1B1 and cardiovascular diseases

Within the cardiovascular system, the contribution of estrogen metabolism by CYP1B1 in the pathogenesis of cardiovascular diseases is less well-defined. However, a pathogenic role of CYP1B1 activity is thought to mediate the development of hypertension, cardiac hypertrophy and fibrosis. However, these effects are not through estrogen metabolism, but rather through arachidonic acid metabolism. However, given the profound effects that estrogens mediate within the cardiovascular system, it is likely that in the coming years an increasing role for estrogen metabolism may emerge.

Arachidonic acid metabolism is mediated via the activity of CYP1B1 *in vitro* towards the formation of epoxyeicosatrienoic acids (EETs) and hydroxyeicosatetraenoic acids (HETEs) (Choudhary *et al.*, 2004). In the vasculature, CYP1B1 is predominantly expressed within smooth muscle cells, yet its expression is increased by shear stress within the vascular endothelium (Conway *et al.*, 2009). In vascular smooth muscle cells, Ang II and arachidonic acid cause migration, proliferation and hypertrophy which is inhibited by the highly potent and selective CYP1B1 inhibitor, 2,3',4,5'-tetramethoxystilbene (TMS) (Yaghini *et al.*, 2010). This is associated with a reduced formation of ROS and its downstream signaling molecules ERK1/2 and p38MAPK (Yaghini *et al.*, 2010).

Ang II and deoxycorticosterone acetate (DOCA)-salt induced hypertension, cardiac hypertrophy and fibrosis are inhibited by CYP1B1 inhibition with TMS (Jennings *et al.*, 2010; Sahan-Firat *et al.*, 2010). Furthermore, increases in mean arterial pressures and cardiac hypertrophy by Ang II is reduced in CYP1B1<sup>-/-</sup> mice (Jennings *et al.*, 2010). The increased vascular reactivity associated with Ang II and DOCA-salt induced hypertension in aortic, mesenteric and femoral arteries is inhibited in CYP1B1<sup>-/-</sup> mice and by TMS treatment (Jennings *et al.*, 2010; Sahan-Firat *et al.*, 2010). Ang II induces aortic endothelial dysfunction as assessed by an impairment in the vasorelaxant response to acetylcholine and this is prevented with TMS (Jennings *et al.*, 2010).

Ang II induced hypertension and cardiac hypertrophy is associated with an increase in NADPH oxidase activity and ROS formation and this is inhibited by CYP1B1 inhibition and in CYP1B1<sup>-/-</sup> mice (Jennings *et al.*, 2010). The elevated ROS signaling by Ang II is potentially mediated via the metabolism of arachidonic acid by the activity of CYP1B1 resulting in increased activity of the downstream signaling effectors ERK1/2 and p38MAPK (Malik *et al.*, 2012).

Taken together, this provides evidence that CYP1B1 is associated with the pathology of cardiovascular diseases in particular through elevated ROS signaling. This highlights a therapeutic potential of CYP1B1 inhibition within cardiovascular diseases.

#### 1.7.3.4 Physiological role for CYP1B1

The formation of genotoxic intermediates by the activity of CYP1B1 together with its activity towards the formation of ROS via hydroxylation of estrogens and metabolism of arachidonic acids has uncovered speculation of why such a detrimental enzyme would exist. There appears to be no beneficial effects associated with the activity of CYP1B1. In support of this, the CYP1B1<sup>-/-</sup> mouse has a normal phenotype and is protected against the toxic effects of many poly aromatic hydrocarbons which are known to induce malignancies (Nebert & Dalton, 2006). However, the CYP1B1<sup>-/-</sup> mouse exhibits key pathological features associated with primary congenital glaucoma, including abnormalities in ocular drainage and the trabecular meshwork in the eye (Vasiliou & Gonzalez, 2008). This highlights at least one physiological advantage of normal CYP1B1 activity.

### 1.7.4 Phase 2 metabolism of hydroxylated estrogens

Catechol estrogens (the 2- and 4-hydroxylated estrogens) are further metabolized by methylation by the activity of COMT. The activity of COMT represents a key deactivation process, in particular by reducing the ability of 4-hydroxylated estrogens to generate quinones and semiquinones that have the capacity to induce harmful DNA transformations (Acharya *et al.*, 2010). Catechol estrogens can also be metabolized by other conjugation reactions including sulfation and glucuronidation.

## 1.8 Gender and pulmonary arterial hypertension

In 1951, Dresdale reported a greater incidence of PAH in females (Dresdale *et al.*, 1951). These findings were later confirmed by the national institutes of health (NIH) registry, which reported 1.7:1 female to male ratio (Rich *et al.*, 1987). More recently, large-scale epidemiological studies from registries in France, UK/Ireland and the USA have reported an even higher incidence of PAH amongst females at ~65%, 70% and 80%, respectively (Badesch *et al.*, 2010;Humbert *et al.*, 2006;Ling *et al.*, 2012). However, despite an increased prevalence amongst females, better survival is reported in females and in younger patients (Benza *et al.*, 2010;Humbert *et al.*, 2010). More recently, a comprehensive study characterised the relationship of sex and haemodynamics in PAH

(Ventetuolo *et al.*, 2014). In young patients (<45 years), male patients had higher mean PAPs compared to females and these differences were attenuated in older patients. Furthermore, mean PAPs were higher in younger patients compared to older patients, despite survival being reportedly poorer in the older patients.

The cardio-protective effects of  $17\beta$ -E2 may contribute to the improved survival in female patients compared to males as improved right ventricular systolic function is superior in both healthy and PAH-affected women compared to men and is associated with higher circulating levels of  $17\beta$ -E2 (Kawut *et al.*, 2009; Ventetuolo *et al.*, 2011).

In addition, a few reports have described an association with physiological and pharmacological estrogen exposure. Morse and colleagues reported an interesting scenario that highlighted a risk for estrogen exposure and the development of HPAH (Morse *et al.*, 1999). They reported the significant onset of PAH in a 46-year old obligate carrier after 3 months on hormone replacement therapy. Interestingly, HPAH had been diagnosed in several of her family members, all of which were female. More recently, a survey was conducted to measure prolonged exogenous estrogen exposure in patients attending the 8<sup>th</sup> international Pulmonary Hypertension Association (Sweeney & Voelkel, 2009). More than 81% of patients reported prior use of hormone therapy and 70% reported prolonged use (more than 10 years) (Sweeney & Voelkel, 2009). Whilst this may provide a link between exogenous estrogen exposure and PAH, the study did not compare PAH patients with the general population. In another study, there was evidence that hormone replacement therapy prevented the development of PAH in patients with systemic sclerosis (Beretta *et al.*, 2006). In PPHTN, circulating  $17\beta$ -E2 levels are increased, which is associated with a single nucleotide polymorphism (SNP) in aromatase, as discussed previously (Roberts *et al.*, 2009). The reason for these sexual dimorphisms in reported incidence and survival is incompletely understood and under-investigated.

In review of epidemiological findings, it was initially hypothesized that estrogens, particularly  $17\beta$ -E2, would be associated with the pathogenesis of PAH. However, numerous pre-clinical studies suggest that  $17\beta$ -E2 mediates protective effects in the pulmonary circulation and on the right ventricle. Previously, the majority of pre-clinical studies have utilised male rodents as they develop a much more robust and severe disease phenotype (Rabinovitch *et al.*, 1981). Additionally, it provides a basis to study molecular pathways in the absence of any influence of female-derived hormones. Recently, in light of epidemiological studies, there has been increased interest in assessing the role of steroids,

in particular, female-derived hormones on the development and progression of PAH. However, there has been conflicting reports of the role of estrogens in PAH, which has so far obscured and diffused our understanding of the relative impact that female hormones, or lack thereof, may have in PAH.

## 1.8.1 Estrogens and experimental pulmonary hypertension

### 1.8.1.1 Estrogens and monocrotaline-induced pulmonary hypertension

Several lines of evidence converge to support a protective role for  $17\beta$ -E2 in the MCT model of PH. In particular, ovariectomy exacerbates the PH phenotype, suggesting a protective role for  $17\beta$ -E2 in this model (Ahn *et al.*, 2003; Farhat *et al.*, 1993; Tofovic *et al.*, 2006; Umar *et al.*, 2011; Yuan *et al.*, 2013). MCT disrupts the vascular endothelium in the pulmonary artery, leading to microvascular leakage which is prevented by  $17\beta$ -E2 (Farhat *et al.*, 1993). Other studies have shown that  $17\beta$ -E2 can reverse established severe MCT-induced PH leading to 100% survival, mediated by the estrogen receptor, ER $\beta$  (Umar *et al.*, 2011). The protective effects of  $17\beta$ -E2 in this model included suppression of inflammation as assessed by a reduction in the inflammatory marker ED-1 as well as a reduction in IL-6 (Umar *et al.*, 2011). Circulating IL-6 levels are increased in PAH (Humbert *et al.*, 1995) and overexpression of IL-6 in the lungs induces PH in mice (Steiner *et al.*, 2009). Furthermore,  $17\beta$ -E2 reversed blood vessel loss in both the lungs and right ventricle and even promoted angiogenesis (Umar *et al.*, 2011).

2-MeOHE2 is a CYP/COMT metabolite of  $17\beta$ -E2 that is a more potent inducer of prostacyclin synthesis and inhibitor of ET-1 production in human umbilical vein endothelial cells than its parent compound (Seeger *et al.*, 1999; Dubey *et al.*, 2001). This metabolic pathway therefore highlights a potential protective pathway. Indeed, 2-MeOHE2 prevents the development of MCT-induced PH and reverses established MCT-induced PAH (Tofovic *et al.*, 2005). However, whilst 2-MeOHE2 increases prostacyclin production in human umbilical vein endothelial cells,  $16\alpha$ -OHE1 caused the most profound induction of prostacyclin synthesis (Seeger *et al.*, 1999). Elevated circulating levels of  $16\alpha$ -OHE1 has been associated with the incidence of HPAH (Austin *et al.*, 2009). It is likely that estrogen metabolites may infer divergent signaling in diverse cell types. Thus, further studies are needed to confirm the effects of estrogen metabolites on prostacyclin synthesis in the pulmonary artery.

### 1.8.1.2 Estrogens and hypoxic-induced pulmonary hypertension

The sexual dimorphism in response to hypoxia has been reported in chickens (Burton *et al.*, 1968), swine (McMurtry *et al.*, 1973) and rats (Rabinovitch *et al.*, 1981). Whilst reports of gender differences in hypoxic PAH in humans is lacking, we can obtain insight from individuals living at high altitude (a hypoxic environment). Whilst most studies have been carried out in men, or have not segregated for gender, one study characterised a gender difference in high-altitude PH in the Kyrgyz population from Central Asia living 3,000m above sea level (Aldashev *et al.*, 2002). Electrocardiograms were performed in 347 males and 394 females and signs of cor pulmonale were reported in 23% of males and 6% of females, indicating a greater effect of hypoxia on males in humans. However, it should be noted that 43% of the men were smokers compared to none in the females. Further studies are required to confirm these findings, as this would have implications for the use of this model in studying IPAH and HPAH, which predominates in females (Badesch *et al.*, 2010; Humbert *et al.*, 2006; Ling *et al.*, 2012). Nonetheless, this model has provided a basis to study the molecular pathways that may underpin disease pathogenesis.

Both gender and the menstrual cycle can affect pulmonary arterial reactivity. Pulmonary artery rings from pro-estrous females (high levels of circulating  $17\beta$ -E2) reduce pulmonary arterial vasoconstrictions under both normoxic and hypoxic conditions (in comparison to estrous and di-estrous female and male pulmonary artery rings) (Lahm *et al.*, 2007). However, only high doses of exogenous  $17\beta$ -E2 (500 $\mu$ M and 1mM) attenuate hypoxic and phenylephrine-induced pulmonary arterial vasoconstriction, independent of sex or estrous cycle and were likely through a non-genomic effect as the response was observed instantly (Lahm *et al.*, 2008b). Further studies have provided evidence that the protective effects of  $17\beta$ -E2 in hypoxic-induced PH are mediated by the ER $\alpha$  and are independent of  $17\beta$ -E2 metabolism, as the general CYP inhibitor, 1-aminobenzotriazole (ABT) has no effects (Lahm *et al.*, 2012). Initially, it was reported that intermittent hypoxia increased the expression of both ER $\alpha$  and ER $\beta$  in rats (Wu *et al.*, 2008). In contrast, chronic hypoxia increased the expression of ER $\beta$ , whereas levels of ER $\alpha$  were unchanged (Lahm *et al.*, 2012). ER $\beta$  inhibition abolished the beneficial effects of  $17\beta$ -E2 on the right ventricle (Lahm *et al.*, 2012). This is consistent with reports that ER $\beta$  knockout mice have RVH (Forster *et al.*, 2004).  $17\beta$ -E2 treated hypoxic rat lungs displayed a reduction in phosphorylated ERK and increased expression of p27<sup>kip</sup>, a cell cycle inhibitor (Lahm *et al.*, 2012).

ET-1 is a potent vasoconstrictor produced from the vascular endothelium and its synthesis is decreased by  $17\beta$ -E2 (Akishita *et al.*, 1996). Hypoxia is a potent inducer of ET-1 synthesis (Rakugi *et al.*, 1990) and it is regulated by the AHR (Lund *et al.*, 2008). Interestingly, transcriptional activity of the precursor to ET-1, pre-pro ET-1, is increased in the lungs of ovariectomized rats but not in rats with intact ovaries (Earley & Resta, 2002), suggesting that circulating estrogens are suppressing ET-1 synthesis. In addition,  $17\beta$ -E2 replacement in rats prevents increases in ET-1 mRNA and protein expression by interfering with hypoxia-inducible factor (HIF) activity (Earley & Resta, 2002).

Endothelium-dependent relaxation is an important physiological response that is impaired by exposure to chronic hypoxia and is thought to contribute to PAH. Phytoestrogens are plant-derived estrogen-like compounds that have the ability to restore the function of the endothelium by promoting relaxation. In pulmonary arteries isolated from chronically hypoxic male rats, the phytoestrogens genistein and daidzen (derived from soy) can restore the impaired vasorelaxation response to agonists that stimulate release of NO (Karamsetty *et al.*, 2001).

#### *1.8.1.3 Estrogens in genetically-susceptible and drug-induced pulmonary hypertension*

Whilst  $17\beta$ -E2 appears to exert protective effects in the classical models of PH (MCT and hypoxic), in genetically susceptible and drug-induced pulmonary hypertensive models,  $17\beta$ -E2 appears to be a risk factor. These models are therefore perhaps much more relevant to studying the gender effects associated with the development of IPAH and HPAH.

Overexpression of the human SERT gene in mice leads to a spontaneous PH phenotype in female mice at 5-6 months of age (White *et al.*, 2011b). To establish whether these effects are facilitated by ovarian-derived estrogens, female SERT<sup>+</sup> mice were ovariectomized and assessed for a PH phenotype after 12 weeks. Ovariectomy successfully attenuated the PH phenotype as assessed by pulmonary vascular remodeling and RVSPs in these mice and this could be re-established by exogenous administration of  $17\beta$ -E2. In contrast, administration of  $17\beta$ -E2 in male SERT<sup>+</sup> mice had no effects (White *et al.*, 2011b). Decreased expression of the estrogen metabolizing enzyme CYP1B1 has been reported in patients harbouring mutations in the Bmpr-2 gene (West *et al.*, 2008). In contrast, a CYP1B1 genetic polymorphism Asn453Ser (N453S) which is associated with an increased post-transcriptional proteosomal degradation of CYP1B1 (Bandiera *et al.*, 2005) is more common in patients without any evidence of PAH, despite harbouring mutations in the

BMPR-2 gene (Austin *et al.*, 2009). In female SERT+ mice and in IPAH, CYP1B1 expression is increased (White *et al.*, 2011a). Differential estrogen metabolism may be species and gender specific and may therefore contribute to the divergent effects of exogenous  $17\beta$ -E2 in male and female SERT+ mice.

Another model that displays female selectivity is the mouse model that overexpresses a member of the S100A4/mts1 (Dempsey *et al.*, 2011). Additionally, complex vascular-like lesions were present in approximately 25% of females (Dempsey *et al.*, 2011). Serotonin induces the expression and release of S100A4/mts1 in hPASMC, inducing cellular proliferation via RAGE (Lawrie *et al.*, 2005).  $17\beta$ -E2 increases the expression of S100A4/mts1, whilst soluble RAGE (which can bind RAGE agonists) inhibits the proliferative capacity of  $17\beta$ -E2. This suggests that  $17\beta$ -E2 mediates an increased expression of S100A4/mts1 which can then bind to RAGE promoting PASMC proliferation.

#### 1.8.1.4 Estrogens in SU-hypoxic-induced pulmonary arterial hypertension

The combined vascular insult SU5416 with hypoxia in rats is to date the model that most closely and robustly recapitulates human PAH pathology, with dramatically elevated pressures and the formation of complex vascular lesions. In contrast to the classical models of PH, female SU-hypoxic rats develop a more severe PAH phenotype compared to male rats as measured by RVSP, yet develop less pronounced RVH (Tofovic *et al.*, 2012). Whilst both genders developed occlusive vascular lesions, female rats developed complex vascular lesions (Tofovic *et al.*, 2012). In this model, ovariectomy reduced the elevated RVSP, yet worsened the degree of RVH (Tofovic *et al.*, 2013). To further support a pathogenic role for  $17\beta$ -E2 in this model, rats were dosed with an aromatase inhibitor anastrozole, which inhibits endogenous synthesis of  $17\beta$ E2. Similar with ovariectomy, aromatase inhibition significantly reduced RVSP, yet only had a modest effect on right ventricular remodeling (Mair *et al.*, 2013;Tofovic *et al.*, 2013).

#### 1.8.1.5 Estrogens and dexfenfluramine-induced pulmonary hypertension

Finally, chronic administration of the anorectic drug dexfenfluramine in mice leads to increased RVSP in female mice only (Dempsey *et al.*, 2013). In contrast, in female obese rats, dexfenfluramine did cause a decrease in the weight of the animals but did not cause PH (Mitani *et al.*, 2002). Interestingly, paradoxical effects were observed in MCT treated female rats, where dexfenfluramine attenuated the effects of MCT (Mitani *et al.*, 2002).

Dexfenfluramine alone induced the activity of elastase, an enzyme that is pathobiologically linked to the development and progression of PAH, and conversely, in combination with MCT, reduced its activity (Mitani *et al.*, 2002). More recently, synergistic effects have been observed in hPASMCs treated with dexfenfluramine and  $17\beta$ -E2 leading to enhanced cellular proliferation (as measured by thymidine incorporation), suggesting that the effects of dexfenfluramine may be facilitated via  $17\beta$ -E2 (Dempsie *et al.*, 2013). Given that  $17\beta$ -E2 exerts protective effects in the MCT model of PH, dexfenfluramine may be enhancing these effects. Additionally,  $17\beta$ -E2 metabolism by activity of CYP enzymes may contribute to these divergent effects in the MCT model and requires clarification.

#### 1.8.1.6 Estrogen effects *in vitro*

In isolated perfused rat lungs,  $17\beta$ -E2 potentiates vasoconstriction to a TXA2 mimic (U-46619) (Farhat & Ramwell, 1992). Additionally, the vasoconstrictive effects to U-46619 alone were enhanced in sexually mature female rats compared to sexually mature male rats (Farhat & Ramwell, 1992). Removal of the pulmonary endothelium increases thymidine uptake (a measure of cell mitosis) in canine PASMC and this effect is abolished in the presence of an intact endothelium (Farhat *et al.*, 1992). In distal hPASMCs, cellular proliferation assays revealed that of the three main estrogens, (E1,  $17\beta$ -E2, E3) and progesterone,  $17\beta$ -E2 is the only estrogen to stimulate increased proliferation as measured by thymidine incorporation assays (White *et al.*, 2011b).

Arachidonic acid stimulates endothelium-dependent contractions in both male and female pulmonary arteries from rabbits, yet these effects are potentiated in females and mediated by  $17\beta$ -E2 (Pfister, 2011). Arachidonic acid is the pre-cursor in the production of eicosanoids, such as thromboxanes, leukotrienes and prostacyclin. In female rabbit pulmonary arteries, there is a greater expression of 5- and 15-lipoxygenase which leads to an increased production of 5- and 15-HETE, respectively, which stimulates contraction of the pulmonary artery (Pfister, 2011).

The expression of BMPR-2 is decreased by about 25% in human female cultured lymphocytes compared to males and  $17\beta$ -E2 suppresses BMPR-2 expression in both cultured lymphocytes and human microvascular endothelial cells (Austin *et al.*, 2012). Under normoxic conditions in pulmonary endothelial cells,  $17\beta$ -E2 can increase BMP signaling (phosphorylation of Smad1/5/8), whilst under hypoxic conditions,  $17\beta$ -E2 suppresses BMP signaling via estrogen receptor signaling and Hypoxia-inducible factor  $1\alpha$

(HIF1 $\alpha$ ) (Ichimori *et al.*, 2013). These divergent findings may be partly explained by the different anatomical locations of the endothelial cells studied (microvascular vs. large pulmonary arterial endothelial cells). In contrast, in hypoxic pulmonary microvascular endothelial cells, 17 $\beta$ -E2 reduces the phosphorylation of ERK, increases the expression of the cell cycle inhibitor, p27<sup>kip1</sup> and decreases VEGF secretion and cell proliferation (Lahm *et al.*, 2012).

### 1.8.2 Progesterone and pulmonary hypertension

Pregnenolone is converted to either DHEA or progesterone. Progesterone is the pre-cursor to aldosterone. In both male and female rat coronary and pulmonary arteries, progesterone is a potent vasodilator (English *et al.*, 2001). In this study, the vasodilatory properties of 17 $\beta$ -E2, progesterone, testosterone and cortisol were compared in the different vascular beds. All steroids were associated with an acute vasodilatory response, although differences were noted between genders and the vascular bed studied. In the pulmonary arteries, progesterone was the most potent vasodilator, followed by testosterone, cortisol and then 17 $\beta$ -E2 (English *et al.*, 2001). In rabbit pulmonary arteries, the vasodilatory properties of progesterone are endothelium-dependent and associated with elevations in NO and cGMP (Li *et al.*, 2001). In rats deficient of gonadal estrogens by ovariectomy, progesterone has been shown to attenuate the development of MCT-induced PH, RVH and pulmonary vascular remodeling (Tofovic *et al.*, 2009a). Progesterone receptors have been detected within the complex vascular lesions of a patient with PAH (Barberis *et al.*, 1995), although this has never been repeated in a larger cohort of patients. Further studies are merited to understand the role of progesterone in PAH.

However, the use of progesterone therapy in PAH should be approached with caution as it is the pre-cursor to aldosterone. In patients with PAH, plasma aldosterone levels are increased (Maron *et al.*, 2013). Aldosterone interacts with the mineralocorticoid receptor and its antagonist spironolactone prevents PASMC proliferation and attenuates experimental PH (Preston *et al.*, 2013). This highlights a potential detrimental pathway that may be activated by progesterone therapy.

### 1.8.3 Androgens and pulmonary hypertension

Whilst the incidence of PAH is more common in women than in men, in patients older than 60 years of age, the estimated 2-year survival in male patients is significantly less compared to female patients (Shapiro *et al.*, 2012). Young male patients (<45 years old)

with IPAH have been reported to have higher mean PAPs and pulmonary vascular resistance compared with females, whilst in older patients there were no differences in pulmonary haemodynamics (Ventetuolo *et al.*, 2014). Interestingly, older patients (>45 years) with IPAH, had significantly lower mean PAPs and pulmonary vascular resistance compared with younger patients, and this was observed in both sexes (Ventetuolo *et al.*, 2014). However, survival is worse in male patients (Shapiro *et al.*, 2012). These sexual dimorphisms suggest that both estrogens and androgens may influence the pathogenesis of PAH. The levels of androgens and estrogens decline with age, with a dramatic reduction in estrogens in females after menopause. In PAH, the function of the right ventricle is a key determinant in the survival of patients (D'Alonzo *et al.*, 1991; Sandoval *et al.*, 1994). Thus it appears that both estrogens and androgens may adversely affect pulmonary haemodynamics in younger patients whilst promoting the function of the right ventricle. In contrast, in older patients, the reduction in estrogens and androgens may be associated with the lower mean PAPs and pulmonary vascular resistance compared with younger patients. Overall, these epidemiological differences in survival suggest that androgens may influence disease pathogenesis.

Androgens are primarily synthesized within the gonads and the adrenal cortex. Testosterone is the primary androgenic steroid hormone that mediates its effects through the androgen receptor. Testosterone is metabolized to its potent, active metabolite dihydrotestosterone by 5 $\alpha$ -reductase which can also activate the androgen receptor. As mentioned previously, right ventricular function is the most important prognostic factor in PAH (D'Alonzo *et al.*, 1991). Androgen receptors have been identified in both the left and the right ventricle (Lizotte *et al.*, 2009). Both aromatase and 5 $\alpha$ -reductase expression are increased in cardiac hypertrophy which is associated with an enhanced production of dihydrotestosterone (Thum & Borlak, 2002). The contractile protein  $\alpha$ -MHC has also been found to be reduced in cardiac hypertrophy and can be restored with administration of testosterone (Thum & Borlak, 2002).

Testosterone is a potent vasodilator of the pulmonary vascular beds in both males and females (Rowell *et al.*, 2009; Smith *et al.*, 2005). In fact, it is a more potent vasodilator of the pulmonary arteries than 17 $\beta$ -E2 (English *et al.*, 2001). These effects are rapid and have been shown to occur independently of the androgen receptor (Jones *et al.*, 2002). The precise mechanism by which testosterone exerts these vasodilatory actions are incompletely understood. However, there is evidence to suggest that testosterone acts as a

calcium antagonist as the dilatation to testosterone is increased in vessels pre-constricted with agents that activate voltage-gated calcium channels (Jones *et al.*, 2002).

The relatively low levels of testosterone in females may provide rationale for the increased incidence of PAH amongst females. Studies examining the effects of testosterone on the pulmonary vasculature and right ventricle are limited. In mice, castration results in reduced RVH and myocyte diameter in response to pulmonary arterial banding, and testosterone successfully normalised these parameters (Hemnes *et al.*, 2012). Pulmonary artery banding is a surgical technique that mimics right ventricular pressure overload by ligation of the pulmonary artery. Additionally, survival was improved in castrated mice that underwent pulmonary artery banding compared with pulmonary artery banding alone, despite testosterone having minimal effects on pulmonary haemodynamics (Hemnes *et al.*, 2012). In a healthy cohort of patients, increased testosterone levels were associated with increased stroke volume and right ventricular mass and volume (Ventetuolo *et al.*, 2011). In male patients, right ventricular ejection fractions worsen in males after initiating therapy, whereas it improves in females with IPAH, which may explain the sex differences in survival (Jacobs *et al.*, 2013).

DHEA is the pre-cursor to androstenedione. The formation of testosterone from androstenedione is mediated by the activity of 17 $\beta$ -hydroxysteroid dehydrogenase 3 (17 $\beta$ -HSD3). DHEA is synthesized primarily in the adrenal glands from cholesterol and is the most abundant adrenal steroid. In addition, the gonads also participate in DHEA synthesis. It commonly circulates in its sulfated form, DHEA-S, which acts as an internal reservoir for DHEA synthesis. DHEA-S is converted to DHEA by the activity of sulfotransferases within tissues. Men have higher levels of DHEA and DHEA-S than women (~50% more) and these decline with age (Parker, 1999). DHEA and DHEA-S are potent inhibitors of cell proliferation in several cell lines by halting cells in the G0/G1 phase (Jiang *et al.*, 2005). In the hypoxic rat model of PAH, DHEA prevented the development of pulmonary arterial remodeling, RVH and PH (Bonnet *et al.*, 2003). In vitro cellular studies in PASMCs have implicated that DHEA mediates its effects by reducing the levels of intracellular calcium and the activation of voltage gated potassium channels (Bonnet *et al.*, 2003). In the SU-Hypoxic model of PAH, DHEA treatment inhibited right ventricular apoptosis, fibrosis and oxidative stress by a reduction in NADPH levels (Alzoubi *et al.*, 2013). Thus, DHEA mediates anti-oxidant effects by reducing the availability of NADPH to generate ROS. Furthermore, DHEA is a potent suppressor of induced-CYP1B1 expression *in vivo* (Ciolino *et al.*, 2003). A clinical trial in patients with chronic obstructive pulmonary

disease associated PH has shown promising results for DHEA as a therapy by significantly increased 6-minute walking tests and pulmonary haemodynamics (de La Roque *et al.*, 2012).

#### 1.8.4 CYP1B1 and pulmonary hypertension

The fact that PAH is more common in women than in men has led to the hypothesis that estrogens, in particular  $17\beta$ -E<sub>2</sub>, the main pre-menopausal hormone, may be facilitating the development and pathogenesis of PAH. One hypothesis is that estrogen metabolism is pathologically altered in disease. Increased CYP1B1 activity has been associated with the development of numerous cancers and cardiovascular diseases, as discussed previously. However, its contribution to the development and pathogenesis of PAH remains obscure. CYP1B1 expression is decreased by 10-fold in Epstein-Barr virus immortalized B lymphocytes harvested from patients with HPAH associated with a BMPR-2 mutation (West *et al.*, 2008). In contrast, in female mice that over-express the human SERT gene and in hPASMCs derived from patients with IPAH, CYP1B1 expression is increased (White *et al.*, 2011a). A genetic polymorphism in CYP1B1 (Asn453→Ser; N453S), which is associated with an increased rate of degradation of CYP1B1 (Bandiera *et al.*, 2005) is more common in patients with a BMPR-2 mutation without any evidence of PAH (Austin *et al.*, 2009). This implicates that the activity of CYP1B1 is a requisite/second-hit factor for the development of PAH in patients harbouring a BMPR-2 mutation. Furthermore, in this cohort of patients the urinary 2-OHE1/16 $\alpha$ -OHE1 ratio was lower compared to unaffected mutation carriers, suggesting that estrogen metabolism by this CYP1B1 polymorphism yields increases in 16 $\alpha$ -OHE1. Taken together, this suggests that CYP1B1 may be a pathological mediator in PAH, yet the functional importance of CYP1B1 has never been critically evaluated. Despite paramount evidence that highlights a greater risk of PAH amongst females suggesting that a female component may be influencing disease pathogenesis, there is a paucity of investigation of estrogens and their metabolism in PAH.

## 1.9 Aims

PAH is more common in women than in men (Badesch *et al.*, 2010;Humbert *et al.*, 2006;Ling *et al.*, 2012) and new insights suggest that estrogen metabolism may contribute to the pathogenesis of PAH. The principal aim of this research was therefore to investigate the role of estrogen metabolism, in particular by CYP1B1, on the development and pathogenesis of PAH. This was addressed by the following project aims:

1. To functionally and molecularly characterise the impact of estrogen metabolism by CYP1B1 on the development of PH in vitro and in vivo
2. To characterise the mechanisms that underlie CYP1B1 pathogenic activity in PH
3. To develop a method to quantitatively measure estrogen metabolism in pulmonary vascular cells
4. To determine the metabolic fate of  $17\beta$ -E2 in hPASCs from naïve cells and PAH-PASCs in both males and females

## **Chapter 2**

### **Methods**

## 2.1 Chemicals reagents and equipment

All chemical reagents were supplied by Sigma-Aldrich, Dorset, UK unless otherwise stated. All organic and aqueous solvents were supplied by Fisher Scientific Limited, Loughborough, UK. Materials for protein expression analysis and RNA expression were purchased from Invitrogen, Paisley, UK and Qiagen, UK, respectively unless otherwise stated. All materials used were of the highest grade obtainable. All cell culture plastics were provided by Corning (supplied by Fischer Scientific Limited, Loughborough, UK).

## 2.2 Animals

All experimental procedures were carried out in accordance with the United Kingdom Animal Procedures Act (1986) and with the "Guide for the Care and Use of Laboratory Animals" published by the US National Institutes of Health (NIH publication No. 85-23, revised 1996). All *in vivo* procedures were performed under the project license 60/4404 (previously 60/3773) held by Professor Margaret MacLean at the University of Glasgow and under the personal license 60/12704 held by Anne Katrine Z. Johansen. All animals were maintained in the same environmental conditions and subject to a continuous 12 hour light/dark cycle and had access to fresh food and water ad libitum. Some animals were housed at the Central Research Facility at the University of Glasgow and others were housed in Professor Margaret MacLeans' chamber suite. For genetically modified mice, tail samples were provided by the Central Research Facility for genotyping to confirm genetic background.

### 2.2.1 General experimental design

Where possible, animals were randomized into their respective study groups and studied blindly. Group identity was revealed after results had been analyzed. No mortalities were reported in any of the studies apart from the monocrotaline study, which have been summarized within the result section.

### 2.2.2 Cytochrome P450 1B1 knockout mice

Homozygote CYP1B1 knockout (CYP1B1<sup>-/-</sup>) mice were kindly provided by the National Institutes of Health/National Cancer Institute, Bethesda, USA. CYP1B1<sup>-/-</sup> mice were generated as described by Buters and colleagues (Buters *et al.*, 1999). Briefly, a genomic clone of 10.5kb containing two of the three exons of murine CYP1B1 was generated using

a 1.7kb cassette. One of the exons was non-coding and the other two exons were targeted to disrupt the function of CYP1B1. The genomic clone was electroporated into embryonic stem cells, grown and transfected into blastocysts from C57BL/6 mice. These cells were then injected into pseudopregnant mice and bred with C57BL/6 to obtain CYP1B1<sup>-/-</sup> mice (Buters *et al.*, 1999). Wild-type mice (C57BL/6) were purchased from Harlan Laboratories (Oxon, UK) and studied as controls.

### **2.2.3 Serotonin transporter overexpressing mice**

Mice overexpressing the human serotonin transporter (SERT<sup>+</sup> mice) were generated and kindly provided by Professor Tony Harmar from the University of Edinburgh. C57BL/6 x CBA wild-type mice were used to generate this mouse model. A 500kb yeast artificial chromosome (YAC35D8) was modified to contain the human SLC6A4 gene (encodes SERT) flanked by 150kb at the 5' and 300kb at the 3' region (Shen *et al.*, 2000). A hemagglutinin epitope tag was incorporated into the yeast chromosome at the C-terminus of the SLC6A4 gene (Shen *et al.*, 2000). The YAC clones were amplified and purified and injected into the pro-nuclei of fertilized eggs from C57BL/6 x CBA female mice to generate human SERT<sup>+</sup> mice (Shen *et al.*, 2000).

## **2.3 Models of pulmonary hypertension**

Both the MCT and the hypoxic models of PH were studied. Whilst these “classical” animal models have and continue to contribute to our understanding of the molecular mechanisms that contribute to the pathobiology of the pulmonary hypertensive process, these models are generally no longer considered direct models of human PAH. Therefore, PH will be used when referring to animal models and PAH will be used when referring to human PAH.

### **2.3.1 Monocrotaline-induced pulmonary hypertension**

10-16 male and female wistar rats (Harlan Laboratories, Oxon, UK) at 10-12 weeks old at termination procedure were studied per group. Where appropriate, rats were injected with the pneumotoxin, MCT pyrrole (Sigma-Aldrich, Dorset, UK). MCT was dissolved in 1mol/L hydrogen chloride (HCl) at a concentration of 100 mg/mL, neutralized with 1mol/L sodium hydroxide (NaOH), and diluted with sterile distilled water to 6 mg/mL. Rats were randomly subdivided to receive either vehicle or MCT at a dose of 60mg/kg by subcutaneous injection in the flank of the rat at day 0. All animals were weighed every day

and monitored for any signs of discomfort. Animals that were deemed unwell by the Central Research Facility staff were terminated by a schedule 1 procedure.

### *2.3.1.1 2,3',4,5'-Tetramethoxystilbene study*

14 days post MCT injection animals were randomly allocated to receive either the highly potent and selective CYP1B1 inhibitor, TMS (Tocris, UK) at 3mg/kg/day or its vehicle (~4% (v/v) ethanol: distilled water) by intra-peritoneal injection for an additional 14 days. TMS was prepared freshly daily prior to use under sterile conditions. TMS was pre-dissolved in 100% ethanol and diluted with distilled water to achieve 0.6mg per 1900µl solution. A 200g rat was injected with 1900µl of the drug solution and the volume was altered according to the weight of the animal to achieve a 3mg/kg dose.

## **2.3.2 Chronic hypobaric hypoxia**

To study the effects of hypoxia on the cardiopulmonary unit, CYP1B1<sup>-/-</sup>, SERT<sup>+</sup> and wild-type mice were exposed to 2 weeks of hypobaric hypoxia. On day 0, mice were placed into the hypobaric chamber and the pressure was gradually reduced to 750mbar (50mbar every 30 minutes) to allow for acclimatization. On day 1, the pressure was further reduced to 550mbar (50mbar every 30 minutes). This pressure is approximately equivalent to 10% oxygen, stimulating hypoxic pulmonary vasoconstriction in the lungs, which leads to the development of a moderate, yet consistent pulmonary hypertensive phenotype. Every 5 days, the chamber was brought back up to atmospheric pressure to replenish food and water and change caging (50mbar every 5 minutes). For dosing experiments, the chamber was brought to atmospheric pressure every day for a maximum of 30 minutes. Room temperature, humidity and the chamber pressure were monitored and recorded carefully throughout the entire study period.

### *2.3.2.1 2,3',4,5'-Tetramethoxystilbene study in hypoxic pulmonary hypertension*

To assess the therapeutic viability of CYP1B1 in hypoxia-induced PH, 10-12 week old mice (Harlan Laboratories, Oxon, UK) were administered TMS (3mg/kg/day) or vehicle (~4% (v/v) ethanol: distilled water) via intra-peritoneal injection for the 14 day duration of chronic hypoxia exposure. All solutions were prepared fresh daily under sterile conditions. TMS was pre-dissolved in ethanol and diluted in distilled water to 0.06mg per 200µl. 200µl was injected by intra-peritoneal injection to achieve a 3mg/kg dose in a 20g mouse

and adjusted accordingly. Mice maintained under normoxic conditions were studied as controls.

### 2.3.2.2 *2,3',4,5'-Tetramethoxystilbene study in SERT+ pulmonary hypertension*

Female SERT+ mice develop a robust PH phenotype at 5 months of age (MacLean *et al.*, 2004; White *et al.*, 2011b). To assess the contribution of CYP1B1 to SERT+ PH, 5-6 month old female SERT+ mice (normoxic and hypoxic) were administered TMS (1.5mg/kg/day) or vehicle (~4% (v/v) ethanol: distilled water) via intra-peritoneal injection for 14 days. This was studied in both normoxic and hypoxic conditions. All solutions were prepared fresh daily under sterile conditions. TMS was pre-dissolved in ethanol and diluted in distilled water to achieve a 0.03mg per 100µl solution. 100µl was injected by intra-peritoneal injection to achieve a 1.5mg/kg dose in a 20g mouse and adjusted accordingly.

### 2.3.2.3 *Effect of CYP1B1 metabolites in pulmonary hypertension*

Female and male 10- to 12-week-old C57BL/6 littermate mice were administered 16 $\alpha$ -hydroxyestrone (16 $\alpha$ -OHE1; Steraloids, US; 1.5 mg/kg/day) or vehicle (~4% ethanol v/v distilled H<sub>2</sub>O) daily via intraperitoneal injection for 28 days before the assessment of PH. In a separate study, female 10- to 12-week-old C57BL/6 littermate mice were administered 4-hydroxyestradiol (4-OHE2; Steraloids, US; 1.5 mg/kg/day) or vehicle (~4% ethanol v/v distilled H<sub>2</sub>O) daily via intraperitoneal injection for 28 days before the assessment of PH

## **2.4 Assessment of pulmonary hypertension**

### **2.4.1 Anaesthesia**

Mice were anaesthetised in an anaesthetic box with 3% (v/v) isoflurane (Abbot Laboratories, Berkshire, UK) supplemented with oxygen at a flow rate of 0.5L/min to assist in the flow of the anaesthetic gas. Mice were immediately weighed and transferred to a facemask continuously administering ~1.5% (v/v) isoflurane supplemented with oxygen at a flow rate of 0.5L/min. The required depth of anaesthesia was confirmed by the absence of a hind-limb or tail reflex. Throughout the procedure, anaesthesia was carefully monitored to ensure that the depth of anaesthesia neither became too shallow or too deep. This was monitored by continuous assessment of reflexes and observation of heart rate and breathing rates.

## 2.4.2 Systemic arterial pressure

Once the required level of anaesthesia had been achieved, an incision was made in the skin at the ventral neck to expose the first layer of muscle which was carefully teased away to reveal the trachea. The left common carotid artery is located dorsal and slightly to the left of the trachea and is identifiable as a large bright red pulsating vessel. The artery was isolated from the vagus nerve which has a white appearance and runs alongside the vessel and cleaned up of any tissue by carefully manipulating the forceps alongside the vessel. Once isolated, surgical non-sterile nylon black monofilament suture size 5-0 (Harvard Apparatus, Massachusetts, USA) was placed underneath the artery and tied at the proximal end of the artery with a single knot, pulled back and taped down to expose an extended arterial length. A second piece of suture was placed underneath the artery and left untied. Thereafter, the right ventricular pressure (RVP; described below) was obtained. Once a steady reading of at least 5 minutes had been obtained for the RVSP, the systemic arterial pressure (SAP; Figure 2-1) was obtained. Using a microsurgical clip (Fine Science Tools, Heidelberg, Germany, FST#18055-04), the vessel was carefully clamped at the proximal end of the carotid artery. A small incision was made at the distal end of the artery just below where the suture had been tied. Using forceps, an opening was manipulated to allow a smooth insertion of a calibrated fluid-filled micro-cannula (Harvard Apparatus, Massachusetts, USA) which was advanced to the base of the clip. Using the second piece of suture, a knot was tied around the cannula and the artery. At this point, the three-way tap was turned on to allow the flow of heparinised saline (Heparin Sodium, Wockhardt, UK; 20units/ml) and the clip was removed to obtain a pressure reading for the SAP.

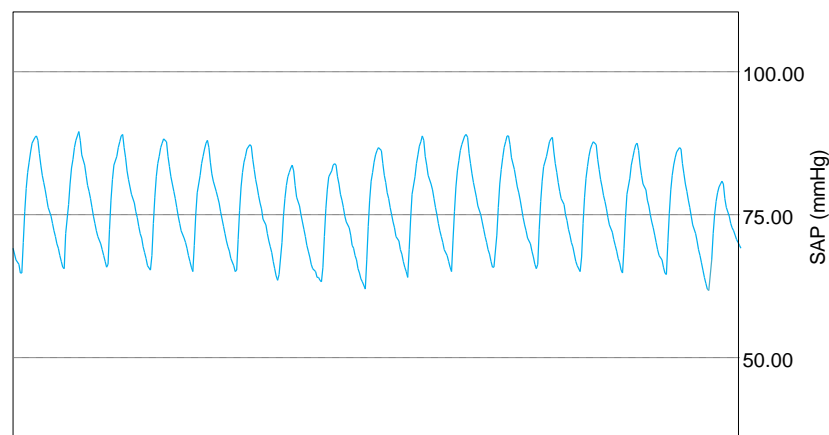


**Figure 2-1 Representative mean systemic arterial pressures**

Systemic arterial pressure (SAP; mmHg) taken from a 5-month old normoxic female wild-type mouse.

## 2.4.3 Right ventricular pressure

### 2.4.3.1 *In mice*

RVP were measured by diaphragmatic catheterisation in mice. It is technically challenging to accurately obtain PAP by this method, and therefore RVP were taken as an indirect assessment of the PAP. After isolating and tying off the left common carotid artery, an incision was made right above the sternum. Heparinised saline (20units/mL) was flushed through the line and the attached calibrated 25mm gauge needle to ensure that there were no air bubbles in the system that may obscure the result. The needle was then advanced underneath the sternum, a couple of mm to the right hand-side at approximately a 100° angle using a micromanipulator (Warner Instruments, Connecticut, USA). Pressure recordings were monitored carefully to estimate the location of the needle. Initially, a drop in pressure was observed as the needle advances through the diaphragm and into the abdominal cavity. The right heart was then catheterised with the needle which should produce a reading that has even oscillations, with diastolic values of near zero (Figure 2-2). Every few seconds, breathing artefacts will appear in the trace (these were not included in the analysis). An upward shift of the diastolic and systolic values is typically a pressure that is observed in the left ventricle. If the needle is resting against the septum of the heart, this can sometimes cause an ambiguous reading. Therefore, if such a pressure was obtained, the needle was first carefully moved slightly to the left. If this did not improve the pressure reading, it is a good indication that the needle had entered the left side of the heart as opposed to the right.

### 2.4.3.2 *In rats*

In rats, anaesthesia was maintained at ~2% (v/v) isoflurane supplemented with oxygen at a flow rate of 1L/min. To maintain a constant body temperature, rats were placed on a heat mat throughout the entire procedure and their temperature was monitored with a temperature probe. Systemic arterial pressures (SAP) were obtained by microcannulation of the left common carotid artery, as previously described prior to cannulation of the right ventricle. Due to the larger size of the artery surgical non-sterile nylon black monofilament suture size 4-0 (Harvard Apparatus, Massachusetts, USA) was used. RVP were obtained by catheterisation of the right ventricle via the right jugular vein using a fluid-filled cannula (with heparin; 20units/ml).

All pressure readings were obtained with Biopac Systems MP35 using a SS132 Blood pressure transducer (Biopac Systems Inc, California, USA). Blood pressure traces were analysed using BSL Pro 3.7 (Biopac Systems Inc, California, USA).

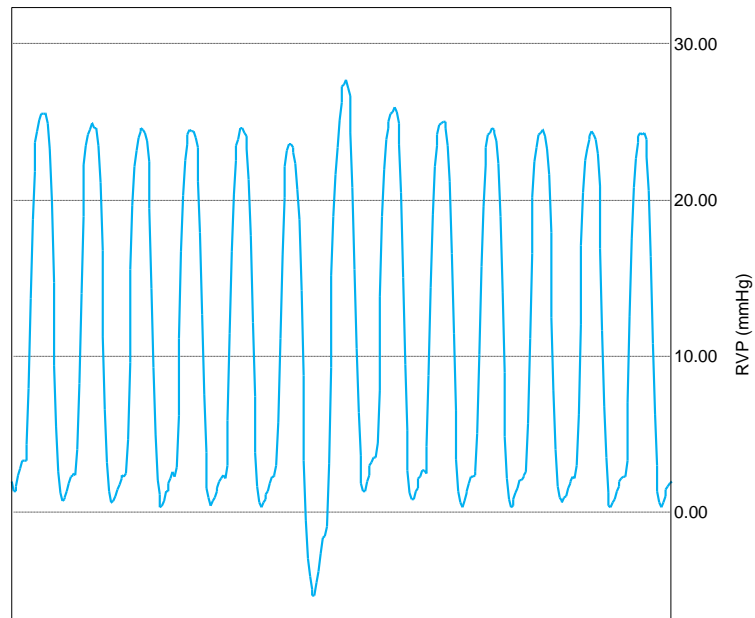


**Figure 2-2 Representative right ventricular pressure**

A representative trace of right ventricular pressure (RVP; mmHg) obtained by transdiaphragmatic right heart catheterisation in a normoxic 3 month-old wild-type female mouse.

#### 2.4.4 Tissue harvest

Immediately following sacrifice, the heart and lungs were gently flushed with ice-cold Dulbecco's phosphate buffered saline (DPBS) solution (Sigma-Aldrich, Dorset, UK) through the right ventricle. For molecular analysis, the lobes of the right lung were flash frozen in liquid nitrogen (polymerase chain reaction (PCR), protein and ELISA) and stored at  $-80^{\circ}\text{C}$ . For experiments where small vessel wire myography was performed, a lung lobe was retained for immunohistochemical analysis and the left lung was used for myography. For other experiments, the left lung was gently inflated with  $\sim 0.5\text{ml}$  (in mice) 10% (v/v) neutral buffered formalin (NBF; 90% (v/v) distilled water, 10% (v/v) formalin, 33mmol/L monosodium phosphate ( $\text{NaH}_2\text{PO}_4$ ), 45mmol/L disodium phosphate ( $\text{Na}_2\text{HPO}_4$ )) and kept under gentle agitation in 10% NBF for a minimum of 4 hours prior to paraffin embedding (see section 2.6.1). Urine samples were collected by puncture of the bladder with BD Micro-Fine™ needle (BD, Oxford, UK) and immediately snap frozen. The uterus and ovaries were isolated and excised for assessment of dry weights and subsequently snap frozen.

Other tissues were collected for the tissue repository (including kidneys, spleen and liver). Blood was collected in 100 $\mu\text{L}$  heparin sodium DPBS (10units of heparin). Cells were removed from the blood by centrifugation for 10 minutes at 2,000 $\times g$  in a chilled centrifuge ( $4^{\circ}\text{C}$ ) to obtain plasma. The plasma supernatant was pipetted into a chilled eppendorf and snap frozen.

#### 2.4.5 16 $\alpha$ -hydroxyestrone urinary analysis

16 $\alpha$ -OHE1 concentration in urine samples was quantified by an enzyme linked immunosorbent assay (ELISA) (ESTRAMET 2/16, Demeditec Diagnostics, Germany) as per manufacturers' instructions. Briefly, 16 $\alpha$ -OHE1 was assayed with specific alkaline-phosphatase-labelled conjugation, and quantification was determined by 405-nm spectrophotometry analysis (SpectraMax M2, Molecular Devices, US).

#### 2.4.6 Right ventricular hypertrophy

RVH was assessed in all animal studies using Fultons' Index (Fulton *et al.*, 1952), by expressing the dry weight of the right ventricle over the dry weight of the left ventricle + septum (RV/LV+S).

## 2.5 Small vessel wire myography

### 2.5.1.1 Isolation of the intra-pulmonary artery

The main pulmonary artery branches into the left and right extra-pulmonary arteries from which the intra-pulmonary arteries descend (~200µm). The dorsal surface of the lung was carefully pinned down facing up. From this view, the hilum where the primary bronchi and pulmonary artery enter the lungs is visible. The pulmonary artery runs posterior to the bronchi along its length. The pulmonary artery was carefully excised from any peri-adventitial tissue and cleaned up of parenchymal tissue.

### 2.5.1.2 Vessel mounting onto a myograph

The vessel bath chamber of each individual myograph unit (Multi Wire Myograph System – 610M; Danish Myo Technology A/S, Aarhus, Denmark) was filled with Krebs-Henseleit buffer (pH 7.4, mmol/L deionised water: 119 sodium chloride (NaCl), 4.7 potassium chloride (KCl), 1.2 magnesium sulphate (MgSO<sub>4</sub>), 25 sodium bicarbonate (NaHCO<sub>3</sub>), 1.2 monopotassium phosphate (KH<sub>2</sub>PO<sub>4</sub>), 1.25 calcium chloride (CaCl<sub>2</sub>) and 11mM D-glucose). Krebs-Henseleit solution was always prepared fresh on the day of isolation of vascular tissues. To obtain the optimal pH, the solution was oxygenated by a gas mixture containing 95% oxygen and 5% carbon dioxide. The myograph chamber was set to 37°C and equilibrated and maintained with a constant gas flow of 16% oxygen, 5% carbon dioxide and 79% nitrogen. This gas composition was selected as it reflects the partial pressure of the lungs. Freshly isolated pulmonary arteries were maintained in Krebs-Henseleit buffer and cut into ring segments of 2mm. The vessel was then cannulated with two pieces of 40µm diameter stainless steel wire (Danish Myo Technology A/S, Aarhus, Denmark) carefully to prevent damage to the endothelium. The vessel was mounted into the myograph chamber and secured in place and left to equilibrate in the buffer for 20 minutes.

### 2.5.1.3 Pressure Standardization

Using the micrometer on the myograph, the pressure applied to the vessel was altered to mimic the transmural pressure present *in vivo*. All myography experiments performed were done in animals where RVSPs had been obtained and the pressure was set accordingly to this. To calculate the transmural pressure, P, the following equation was used (Mulvany & Halpern, 1977):

$P = 2\pi \times \text{wall tension (t)}/\text{internal vessel circumference (L)}$

$t = \text{force (f)}/2 \times \text{vessel length (v)}$

$L = (X_i - X_o) \times 2 + 205.6$ ; where  $X_i$  = applied tension;  $X_o$  = relaxed tension

$P/0.13333 = \text{pressure in mmHg (0.1333kPa = 1mmHg)}$

The internal circumference when the wires are touching is equal to  $2 + \pi \times 40\mu\text{m}$  (wire diameter size) = 205.6.

Once the required transmural pressure had been achieved by gradual increments, the artery was left to stabilize for 30 minutes. The pulmonary arteries were contracted with 50nM KCl twice, with a wash step after the contraction had plateaued. Cumulative concentration response curves were then determined for serotonin (Sigma-Aldrich, Dorset, UK) at bath concentrations from 1nM to 100 $\mu\text{M}$ , incrementing in half log doses. The contraction to serotonin is represented as a % of the contractile response to the second KCl contractile response.

All myography data was recorded and analysed using MyoDaq 20 (Danish Myo Technology A/S, Aarhus, Denmark).

## 2.6 Immunohistochemistry

### 2.6.1 Tissue Fixation and Paraffin Embedding

Tissue samples were immediately placed in NBF and placed on a shaker under gentle agitation for a minimum of 4 hours, depending on the size of the tissue. Formalin-fixed paraffin embedded tissue is optimum to help reduce background caused by expression of endogenous biotins. After fixation, tissue samples were dehydrated through a water-histoclear gradient and then embedded in wax in a Citadel 1000 tissue processor (Thermo Scientific, UK), summarised in Table 2-1. Immediately prior to cutting for section-mounting onto slides, tissue blocks were placed in  $-20^{\circ}\text{C}$  to help solidify the wax. Sections were cut at  $3\mu\text{m}$  using a microtome (Leica RM2125, Leica Microsystems, Milton Keynes, UK), placed in water at  $37^{\circ}\text{C}$  to gently melt the wax and then placed onto a polylysine-coated slide (Sakura Finetek, Netherlands) to improve tissue adherence. For particularly sensitive antibodies, sections were cut, left to dry and then stored in the fridge and used within one week. For more commonly used antibodies, such as  $\alpha$ -smooth muscle actin ( $\alpha\text{SMA}$ ), sections could be stored at room temperature for several months prior to staining.

**Table 2-1 Process for paraffin-embedding small animal tissues**

<b>Condition</b>	<b>Small Tissue Samples</b>	<b>Larger Tissue Samples</b>
10% NBF	4 hours	8 hours
70% Ethanol: Water	15 minutes	45 minutes
80% Ethanol: Water	15 minutes	45 minutes
95% Ethanol: Water	25 minutes	45 minutes
95% Ethanol: Water	25 minutes	1 hour
100% Ethanol: Water	15 minutes	1 hour
100% Ethanol: Water	15 minutes	1 hour
100% Ethanol: Water	15 minutes	1 hour
Histoclear	30 minutes	1 hour
Histoclear	30 minutes	1 hour
Paraffin	30 minutes	1 hour
Paraffin	30 minutes	1 hour

Samples were maintained for a minimum of 4 hours in 10% neutral buffered formalin (NBF). Samples were however routinely maintained in NBF overnight.

## 2.6.2 Immunohistochemistry

Sections were dewaxed in xylene for 30 minutes and rehydrated through an alcohol-water gradient (100% ethanol for 10 minutes, 100% ethanol for 5 minutes, 90% ethanol for 2 minutes and 70% for 2 minutes). Sections were then washed in running water for 10 minutes to ensure adequate rehydration. Antigen retrieval was performed using 10mM citric acid buffer (Citric acid monohydrate dissolved in distilled water; Sigma-Aldrich, Dorset, UK), adjusted to pH 6.0 with 5M sodium hydroxide (NaOH), in a microwave for 4 x 5 minutes and then left to cool at room temperature for 20 minutes. Formalin fixing of tissue can cause cross-linking of proteins which can mask the antigen site of interest and this step is therefore essential to prevent masking of proteins. The advantage of this type of fixing is that it preserves a good cellular morphology. Sections were then washed in running water for 10 minutes before blocking for 30 minutes in 3% (w/v) hydrogen peroxide solution (Sigma, Dorset, UK) to block endogenous peroxidase activity, which can be present at high levels in tissues and would yield a high background and non-specific staining. Sections were washed in running water before blocking with ready-to-use 2.5% (v/v) normal horse serum (ImmPRESS kit, Vector Labs, Peterborough, UK) for 1 hour at room temperature in a humidified chamber. Sections were then incubated with the relevant primary antibody overnight at 4°C in a humidified chamber (see Table 2-2 for details on experimental conditions). The primary antibody diluent consisted of 1% (w/v) bovine serum albumin (BSA) in 10mM phosphate buffered saline (PBS) pH 7.4 (made using Sigma-Aldrich (Dorset, UK) tablets (2.7 mmol/L KCl, 137 mmol/L NaCl pH; 1 tablet dissolved in 200mL distilled water). The primary antibody was washed off in 3 x 10 minute washes in tris-buffered saline (TBS) pH 8.4 (50mmol/L Tris, 150mmol/L NaCl) before incubation with an anti-rabbit Ig peroxidase polymer secondary antibody (ImmPRESS Kit, Vector Labs, Peterborough, UK) for 1 hour at room temperature. Excess secondary antibody was washed off in 3 x 10 minute washes with TBS. Positive immunolocalization was then visualised with a suitable chromagen for 2-15 minutes under the microscope (either 3,3'-diaminobenzidine (DAB) or Vector® VIP substrate kits, Vector Labs, Peterborough, UK). The reaction was terminated by immersion into running water once a positive signal had occurred with minimal background staining. Sections were then dehydrated through a water-ethanol gradient (70%, 90%, and 2 x 100% ethanol v/v) for 5 minutes in each solution, followed by 2 x 5 minutes in histo-clear (National Diagnostics, Georgia, USA) before mounting of slide sections on to cover slips using Tissue-Tek (Sakura Finetek, Netherlands). Staining was visualised and photographed using

a Zeiss Imager M.1 AX10 and axiovision Rel. 4.8 (Carl Zeiss Microscopy Ltd, Cambridge, UK).

#### *2.6.2.1 Haematoxylin and eosin counter-staining*

Rat sections were counter-stained with haematoxylin (nuclear stain) and eosin (cytoplasm and collagen) prior to dehydration and embedding. Sections were immersed in haematoxylin for 5 minutes and then rinsed in running water. Sections were differentiated in 1% acid-alcohol to remove excess stain. To enhance the blue stain, sections were placed into luke warm water followed by 3 minutes in eosin. Sections were rinsed in running tap water and then dehydrated through an ethanol gradient before mounting, as described above.

**Table 2-2 Antibody manufacturers and optimal concentrations for immunohistochemistry**

<b>Antibody</b>	<b>Supplier</b>	<b>Antibody Dilution</b>
CYP1B1 (rabbit pAb)	Abcam-ab33586	1µg/mL
α-SMA (rabbit pAb)	Abcam-ab5694	0.4µg/mL
vWF (rabbit pAb)	Dako-A0082	3.1µg/mL

To check for non-specific binding rabbit immunoglobulin G (IgG) were used at the same concentration as the primary antibody. All antibodies were polyclonal (pAb) and raised in rabbits. The secondary used for all immunohistochemistry experiments was therefore anti-rabbit. αSMA, α-smooth muscle cell actin; vWF, von willebrand factor.

### 2.6.2.2 Quantitative Analysis of CYP1B1 Immunoreactivity

Positive CYP1B1 immunoreactivity in murine and human pulmonary arteries was semi-quantified by colorimetric analysis (MetaMorph, version 6.1, Molecular Devices, USA). The average pixel intensity of each image correlated to a greyscale range of 0 (black) to 255 (white), with intermediate intensities being assigned an appropriate grey level. Preliminary studies were carried in randomly selected arteries to determine the pixel intensity range that corresponded with positive CYP1B1 staining. The colour threshold was selected to detect pixel intensity between 0 and 156 as representative of CYP1B1 staining. Pulmonary arteries <80µm in mice and <200µm in human were selected and specifically analysed. The percentage threshold area detected was then expressed as the percentage of positive CYP1B1 immunoreactivity within the vessel wall. For both human and murine lung sections, a total of 15 pulmonary arteries from each lung were assessed. All immunoquantification was performed by Dr. Kirsty Mair.

### 2.6.3 Pulmonary vascular remodeling

Pulmonary vascular remodeling was assessed in 3µm sagittal lung sections stained with elastic picro-sirius red and pulmonary arteries <80µm external diameter was microscopically assessed for degree of muscularisation in a blinded fashion. The number of remodeled arteries was expressed over the total number of arteries present within the section and expressed as a percentage. To visualise the degree of muscularisation, 3µm sagittal lung sections were stained with α-SMA (Abcam, Cambridge, UK) as described above (see section 2.6.2).

#### 2.6.3.1 Elastic picro-sirius red staining

Sections were dewaxed in histo-clear for 20 minutes and rehydrated through an alcohol-water gradient (100% ethanol for 5 minutes, 100% ethanol for 5 minutes, 90% ethanol for minutes and 70% for 5 minutes). Sections were then washed in running water for 5 minutes to ensure adequate rehydration. The tissue section was then immersed into a 0.5% (w/v) potassium permanganate (KMNO<sub>4</sub>) solution for 5 minutes for oxidation to enhance staining. The sections were then rinsed in water and immersed into 1% (w/v) oxalic acid to decolorize the sections from the KMNO<sub>4</sub> followed by an additional wash step. Sections were rinsed in 95% ethanol and then placed in Millers Elastin Stain (Thermo Scientific, UK) for 2 hours. Excess stain was removed by rinsing in 95% ethanol and then running tap water. Sections were counterstained with picro-sirius red for 3 minutes and then briefly

rinsed in water. Sections were dehydrated rapidly through a water-ethanol gradient (70% ethanol for 1 minute, 90% ethanol for 1 minute, 2 x 100% ethanol for 5 minutes each and then 2 x histo-clear for 5 minutes each. Sections were mounted onto cover slips as previously described. Staining was visualised using a Zeiss Imager M.1 AX10. The staining results in a black appearance of elastic fibres, a deep red colour in collagen and the cytoplasm, muscular cells, red blood cells and fibrin appear yellow.

## **2.7 Sodium dodecyl sulphate – polyacrylamide gel electrophoresis**

### **2.7.1 Protein solubilization**

All tissue samples were homogenized in ice-cold 1% (v/v) lauryl maltoside (LM) buffer (Abcam, Cambridge, UK) in DPBS using a hand-held ultrasonic tissue homogenizer (Misonix XL-2000, Fisher Scientific, UK). Samples were kept on ice for 30 minutes to encourage protein solubilization, followed by ice-sonication. Samples were centrifuged to remove cellular debris at 10,000xg for 10 minutes at 4°C and the supernatant was collected for protein estimation by a bicinchoninic acid (BCA) protein assay.

### **2.7.2 Bicinchoninic acid protein assay**

Protein concentrations were determined using a BCA protein assay (Thermo Scientific, UK). The standard solutions ranged from 0-2mg/ml bovine serum albumin (BSA) solution, diluted in 1% (v/v) LM buffer in DPBS as required. In this reaction, copper in the reagent mix is reduced by the protein which reacts with the BCA to form a purple solution (green→purple). Therefore, the more protein there is, the more intense the purple colour appears. Both the standards and the samples of interest were loaded onto a clear 96 well plate. Reagent A and Reagent B were mixed in the ratio 4.9ml to 0.1ml, respectively. 200µl of this mixture was added to each well and left on a gentle shaker for 20-30mins. The plate was read at 562 nm using a POLARstar OPTIMA microplate reader (BMG Labtech, Germany). A representative standard curve is shown in Figure 2-3.

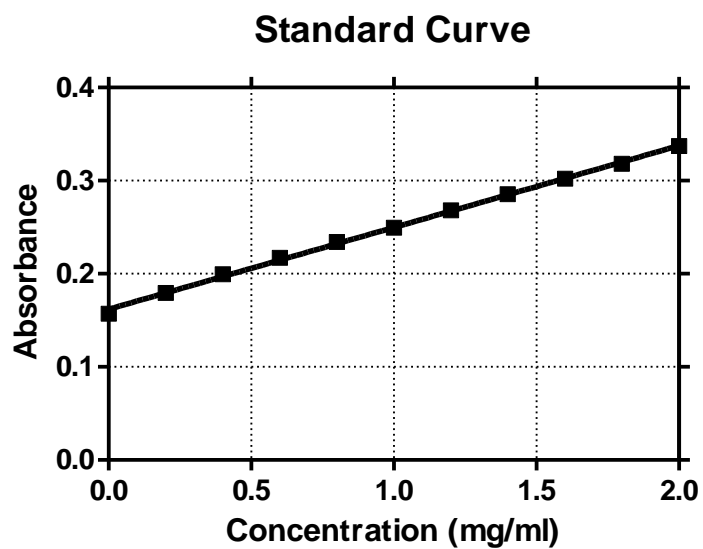


**Figure 2-3 A representative bicinchoninic acid protein assay standard curve**

A representative standard curve obtained for BSA solution (0-2mg/ml) using a bicinchoninic acid (BCA) protein assay. Samples performed in duplicate.

### 2.7.3 Western blotting

NuPAGE reducing agent was added to protein samples together with a sample buffer containing a blue dye for loading visualisation (NuPAGE lithium dodecyl sulfate sample buffer). Samples were heated for 15 minutes at 70°C in a heat block. This ensures adequate denaturing and reducing of protein disulphide bonds effectively exposing proteins to allow for efficient antibody binding. Samples were loaded onto Novex NuPAGE 4-12% polyacrylamide gels and separated according to protein size by a constant flow of an electrical current at 150volts in NuPAGE MOPS running buffer containing 1% (v/v) antioxidant using electrophoresis. See blue pre-stained protein standard was used as the protein ladder to determine approximate protein size. Once adequately separated, the proteins were transferred on to a polyvinylidene difluoride (PVDF) membrane (Millipore Corporation, Massachusetts, USA), which had been pre-activated by emersion in 100% methanol. This was performed using wet electroblotting in a transfer tank containing a transfer buffer consisting of 5% (v/v) NuPAGE transfer buffer, 20% (v/v) methanol, and 1% (v/v) antioxidant prepared in distilled water. This was run at 30volts for 2 hours to allow for sufficient transfer of proteins onto the PVDF membrane. To check for transfer efficiency, blots were immersed in Ponceau S solution (0.1% (w/v) Ponceau S in 5% (v/v) acetic acid). This stains all proteins to allow for visualisation. This was subsequently washed off with water, reactivated with methanol and the membranes were transferred into a 5% (w/v) non-fat milk solution (marvel) in 0.1% (v/v) Tween 20 (Fisher Scientific, Loughborough, UK) in TBS (TBST: pH 7.6) to block the membrane to prevent non-specific binding of the antibody for 1 hour at room temperature. Blots were rinsed in TBST and then incubated with the primary antibody overnight in either 5% (w/v) marvel in TBST or 5% BSA in TBST overnight at 4°C (See Table 2-3 for details). The unbound primary antibody was then washed off the blot by 3 consecutive washes in TBST each lasting 10 minutes. The corresponding secondary antibody to which the first antibody was raised in (see Table 2-3 for details), linked with horseradish peroxidase (HRP) was then applied to the membrane at a 1:5000 dilution in 5% marvel TBST for 1 hour at room temperature with gentle rocking. The membrane was washed 3 times in TBST for ten minutes and antibody binding was detected by enhanced chemiluminescent (ECL) using Pierce ECL (Thermo Scientific, UK) or Immobilon western chemiluminescent HRP substrate (Merck Millipore, Massachusetts, USA) and developed onto film. The membranes were then washed and stripped using Restore western blot stripping buffer (Thermo Scientific, UK) and re-probed with a loading control (Glyceraldehyde 3-phosphate dehydrogenase,

GAPDH). For quantification, the densitometry was analysed using TotalLab 1D gel analysis (TotalLab, UK).

**Table 2-3 Experimental details for antibodies used for protein analysis by western blotting**

Antibody	Supplier	Antibody dilution human	Detected band size
CYP1B1 (rabbit pAb)	Abcam-ab33586	0.2µg/mL in 5% non-fat milk	61kDa
Aromatase (rabbit pAb)	Abcam-ab69653	1µg/mL in 5% non-fat milk	58kDa
COMT	Sigma-HPA001169	1µg/mL in 5% non-fat milk	28kDa
17β-HSD1	HPA021032	1µg/mL in 5% non-fat milk	35kDa
GAPDH (mouse mAb)	Abcam-ab9484	0.2µg/mL in 5% non-fat milk	40kDa

Experimental details of antibodies used for protein analysis by western blotting. All antibodies were prepared in 5% non-fat milk in 0.1% tween tris buffered saline. A dilution factor is provided where the antibody concentration is not supplied by the manufacturer. Specified next to the primary antibody is the species that the antibody was raised in. pAb, polyclonal antibody; mAb, monoclonal antibody; GAPDH (loading control), glyceraldehyde-3-phosphate dehydrogenase.

## 2.8 RNA analysis

### 2.8.1 RNA extraction

To extract RNA from tissue samples, lysis was performed using QIAzol lysis reagent and extracted with the miRNEASY extraction kit according to manufacturer's instructions. For both cell extractions and tissue extractions 700µl QIAzol was used. Where required, tissues were homogenised with a TissueLyser II using stainless steel beads for a total of 2 minutes, with 30 second intervals every 30 seconds (to prevent overheating of the samples risking RNA degradation). Samples were left at bench top for 5 minutes to promote dissociation of nucleoprotein complexes. To extract the RNA, 140µl of high grade chloroform was added and shaken vigorously. Samples were left for a further 3 minutes to encourage sample separation of RNA from DNA, proteins and lipids and then centrifuged at 12,000xg for 15 minutes at 4°C. The upper aqueous layer formed contains the RNA which was carefully transferred into a 1.5ml eppendorf and the remaining products were discarded. The RNA suspension is then precipitated with 1.5 x volumes of 100% high grade RNA-free ethanol and mixed by pipetting the mixture up and down. Half the sample is transferred into a spin column, which is provided in the extraction kit. The column contains a silica membrane that binds the RNA from the sample. The sample was centrifuged at 8,000xg for 15 seconds at room temperature and the resulting elute was discarded and the process was repeated with the remaining sample. The captured RNA on the membrane is then washed with RWT buffer. To ensure adequate clean-up of contaminating DNA, DNase was added to the membrane and left at room temperature for 15 minutes. The sample was then washed again with RWT buffer followed by a wash with RPE buffer. All washes were removed by centrifugation at 8,000xg for 15 seconds at room temperature. The spin column was then transferred into a new 1.5ml eppendorf. 30µl of RNase free water was pipetted directly onto the RNA-enriched membrane and eluted by centrifugation for 1 minute at 8,000xg. The isolated samples were immediately transferred to ice. To determine RNA concentrations and purity, samples were analysed by a NanoDrop, ND-1000 spectrophotometer (Thermo Scientific, UK) prior to storage in -80°C. The NanoDrop measures the absorbance of a sample. RNA absorbs light at a wavelength of 260nm, whilst proteins absorb at a wavelength of 280nm. Thus the purity of the sample can be determined by expressing the absorbance at 260nm/280nm. All samples analysed had a 260/280 ratio of ~2.

## 2.8.2 Reverse transcription

Extracted RNA samples were reverse transcribed with TaqMan® reverse transcription reagents (Life Technologies, Paisley, UK) as per manufacturers' instructions. 1µg RNA was transcribed per sample in a cocktail of RT-buffer, 25mM magnesium chloride (MgCl<sub>2</sub>), deoxynucleotide triphosphates (dNTPs), random hexamers, RNase inhibitors and Multiscribe. Reverse transcription was performed using the Veriti® Thermal Cycler (Life Technologies, Paisley, UK) under the following cycling conditions: 10 minutes at 25°C (maximised primer RNA template binding), 30 minutes at 48°C for reverse transcription and 5 minutes at 95°C to deactivate reverse transcription.

## 2.8.3 Quantitative real time-polymerase chain reactions

Gene expression was determined using TaqMan® mastermix and primers for mouse *cyp1b1* (Mm00487229\_m1) and normalised to  $\beta$ 2-microglobulin (Mm00437762\_m1). Samples were analysed using the ViiA7™ Real-Time PCR System (Life Technologies, Paisley, UK) with the following cycling conditions: 50°C for 2 minutes to activate uracil N glycosylase (degrades DNA), 95°C for 10 minutes to activate DNA polymerase followed by 50 cycles of 95°C for 15 seconds for denaturation and 60°C for annealing and extension.

## 2.9 Cell culture

### 2.9.1 Human pulmonary arterial smooth muscle cells

HPASMCs were generated at the University of Cambridge and kindly provided by Professor Nicholas W. Morrell (University of Cambridge). HPASMCs were explanted from the distal pulmonary microvasculature (vessels with <1mm external diameter) from subjects with no reported presence of PH and patients with either HPAH or IPAH. Control samples were obtained from unused donor tissues. PAH hPASMCs were obtained at lung or heart-lung transplantations. Both male and female samples were used in these studies as specified within text. The smooth muscle cell phenotype was confirmed by positive  $\alpha$ -SMA staining by immunofluorescence. All tissue culture experiments were carried out under sterile conditions in a class II laminar flow hood.

Distal hPASMCs were isolated as previously described by either microdissection or magnetic isolation (Wharton et al., 2000) and provided by Professor Nicholas Morrell (University of Cambridge). Samples were stored in liquid nitrogen facilities in 10%

dimethyl sulfoxide (DMSO) (v/v) in 10% (v/v) fetal bovine serum (FBS) Dulbecco's modified eagle medium (DMEM). DMSO is a cryoprotectant that aids in reducing cell death during the slow-freezing process to liquid nitrogen (-196°C). HPASMCs brought up from liquid nitrogen were kept on dry ice before rapidly defrosting the cells by dipping the bottom part of the vial into a 37°C water bath. Once the contents in the vial had thawed, the exterior of the vial was wiped with 70% ethanol to prevent contamination. Even dispersion of the cells was ensured by pipetting the suspension up and down. To determine the number of viable cells present, 20µL of the cell suspension was diluted in an equal volume of Trypan Blue 0.4% solution (Sigma-Aldrich, Dorset, UK) and counted using a haemocytometer, counting each 16 squares in the four different corners to obtain an average. Trypan blue detects cell viability as viable cells do not absorb the dye, whilst dead cells are permeable to the dye and appear a dark blue colour. The haemocytometer is designed so that the number of cells in one set of 16 squares is equivalent to the number of cells  $\times 10^4/\text{mL}$ . Cells were diluted in 10% FBS (v/v; Sera Laboratories International, West Sussex, UK) 1% antibiotic antimycotic (AA) DMEM at the required cell density. Cells were plated at a density of 10,000 cells per  $\text{cm}^3$  in a T75 flask. Cells were then incubated at 37°C, 5%  $\text{CO}_2$ , 95% air humidified cell culture incubator. Cells were left to adhere for a minimum of 24 hours and thereafter fed fresh media every 24 or 48 hours. DMEM contains phenol red, a pH indicator which progresses from a red colour to a yellow colour as the pH of the medium decreases which can be a result of a bacterial infection, cellular death or more commonly just a gradual reduction in pH in response to waste products released from the cells. All cell culture medium contained 1% (v/v) AA (10,000 unit's penicillin, 10 mg streptomycin and 25µg amphotericin B per mL). Penicillin prevents bacterial cell growth by inhibiting cell wall synthesis. Streptomycin is a bacterial protein synthesis inhibitor and amphotericin B is an anti-fungal agent.

#### *2.9.1.1 Sub-culturing of human pulmonary arterial smooth muscle cells*

Cells were grown until near confluency and sub-cultured for further experiments and studied between passages 3 and passages 8. The cell culture medium was aspirated from the flasks and washed twice with sterile DPBS. 2mL of 0.25% trypsin/EDTA solution (0.1% (w/v) EDTA in PBS, Life Technologies, Paisley, UK) was added to the flask and swirled to distribute the solution over the entire surface of the flask. Trypsin cleaves proteins, thereby detaching them from the flask. The flask is returned to the cell culture incubator for approximately 3 minutes until all of the cells have developed a round morphology, whereby the flask is gently tapped to dislodge the cells. Immediately, 8mLs

of fresh 10% FBS DMEM was added to the flask to terminate the effects of trypsin. Cells were sub-cultured into 6 well plates at a density of 7,500 to 10,000 cells per cm<sup>2</sup>. The cell culture medium was replaced the following day and then every 24 or 48 hours after. All cells were grown to the required level of confluency for subsequent experiments prior to cell-cycle synchronisation by serum deprivation in 0.2% charcoal-stripped (CS)-FBS in phenol-red free (PRF) DMEM for 24 hours. The cell culture medium was replenished after 24 hours and the relevant agonists or antagonists were added to the wells for cell growth assays.

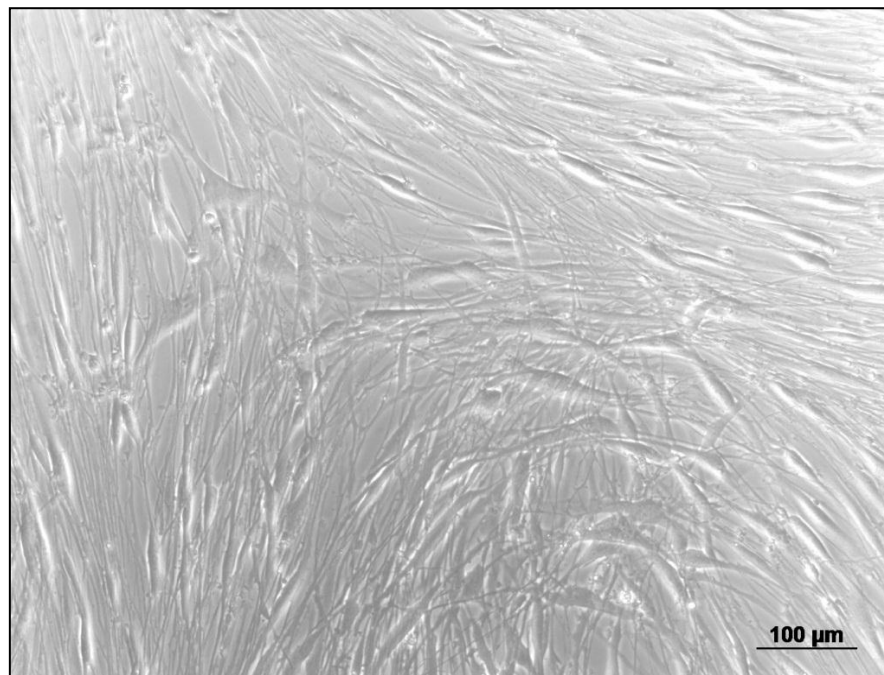


**Figure 2-4 Distal human pulmonary arterial smooth muscle cell morphology**

Microphotograph of distal female control human pulmonary arterial smooth muscle cells grown in a 96 well culture dish.

## 2.9.2 Charcoal-stripped fetal bovine serum

Endogenous estrogens present in FBS were removed by charcoal stripping. Dextran-activated charcoal selectively removes non-polar components from serum including hormones. Dextran-coated charcoal (Sigma-Aldrich, Dorset, UK) was added to FBS at a concentration of 1g/100mL and left at 4°C under gentle agitation. Samples were subsequently centrifuged at 1,811xg at 4°C for 30 minutes. The stripped serum was decanted and filtered through a 0.22µm filter. This process was repeated and samples were aliquoted and frozen until use. Successful removal of 17β-E2 was determined by a competitive based immunoassay (Cayman Chemical, Michigan, USA; see section 2.12). This serum was used in all cell culture experiments.

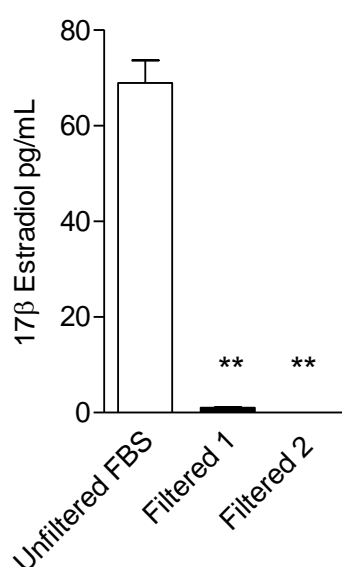


**Figure 2-5 Removal of 17β-estradiol from foetal bovine serum**

17β-estradiol (17β-E2) was removed from foetal bovine serum (FBS) by charcoal stripping twice with dextran-coated charcoal. Samples were filtered to remove charcoal from samples with a 0.22µm filter and assayed by a competitive 17β-E2 specific ELISA.

## 2.10 Thymidine incorporation assay

To measure cellular proliferation, the incorporation of  $^3\text{H}$ -labelled thymidine into chromosomal strands of replicating DNA during mitosis was measured. HPASMCs were seeded in 24-well plates at a density of 7,500 cells per  $\text{cm}^2$ . Cells were grown to ~60% confluency in 10% DMEM and then quiesced for 24 hours to arrest the cell cycle and synchronise the cells in 0.2% (v/v) CS-FBS, PRF-DMEM. Cell culture medium was replaced with 1% charcoal stripped PRF-DMEM and stimulated with agonists/antagonists for 72 hours. To investigate effects of antagonists, drugs were incubated with the cells for 30 minutes prior to addition of an agonist. Drugs and media were replaced every 48 hours.  $^3\text{H}$ -Thymidine (Perkin Elmer, Cambridgeshire, UK) was added to the culture medium (0.1 $\mu\text{Ci}$ ) for the last 24 hours.

To terminate the experiment, the medium was removed and the cell monolayer was washed twice with DPBS. Protein samples were purified by protein precipitation with 0.5mL 5% (w/v) trichloroacetic acid washes 3 times followed by cell lysis with 0.5ml 0.3M NaOH for a minimum of 30 minutes. The cell lysate was collected in 1mL Ecoscint A scintillation fluid (National Diagnostics, Georgia, USA), vortexed and left to settle for 2 hours. The total  $^3\text{H}$  thymidine was measured using a Tri-Carb 2800TR  $\beta$ -scintillation counter (Perkin Elmer, Cambridgeshire, UK).

## 2.11 CellTiter-Glo® luminescent cell viability assay

To determine the number of viable cells, the CellTiter-Glo® luminescence cell viability assay (Promega, Wisconsin, USA) was used, as described in the manufacturers' protocol. This assay measures the amount of adenosine triphosphate (ATP) present in the cells using beetle luciferin, which undergoes oxidation by luciferase in the presence of ATP, magnesium and oxygen, emitting a luminescent signal. Therefore the amount of luminescence is directly proportional to the amount of ATP present in the cells which strongly correlates with cell number.

Briefly, cells were plated in 96-well opaque walled clear-bottomed plates (Greiner Bio One, Stonehouse, UK) at a density of 7,500 cells per  $\text{cm}^2$  in 10% (v/v) FBS DMEM. At 60% confluency, cells were quiesced in 0.2% (v/v) CS-FBS DMEM for 24 hours prior to addition of relevant agonists/antagonists, as described previously for thymidine incorporation assays (see section 2.10). The cell culture plates were removed from

controlled incubators and allowed to equilibrate to room temperature for about 30 minutes. An equal volume of the CellTiter Glo® reagent to the amount of media present in the wells was added to each well, alongside 3 blanks containing only cell culture medium (no cells for background luminescence). The plate was placed onto an orbital shaker to induce cell lysis and approximately 10 minutes was allowed for stabilisation of the luminescent signal. Luminescence was recorded using a luminometer (POLARStar OPTIMA, BMG Labtech, Germany).

## 2.12 17β-estradiol immunoassay

The levels of 17β-E2 were determined by competitive based immunoassay in whole lung samples from female wild-type and SERT+ mice and in hPASCs from control and PAH patients. All tissue samples were homogenized in ice-cold 1% (v/v) LM buffer in DPBS using a hand-held ultrasonic tissue homogenizer (Misonix XL-2000, Fisher Scientific, UK). Samples were kept on ice for 30 minutes to encourage protein solubilization, followed by ice-sonication. Samples were centrifuged to remove cellular debris at 10,000xg for 10 minutes at 4°C and the supernatant was collected for protein estimation by a BCA protein assay (see section 2.7.2). 400μg of protein were loaded for mouse lung samples and 30μg of protein was loaded for hPASCs samples. Each sample was performed in duplicate. 17β-E2 levels were determined by a 17β-E2 enzyme-linked immunosorbent assay kit as per manufacturer's instructions (Cayman Chemical, Michigan, USA), which is summarized in Figure 2-6. Briefly, a constant amount of 17β-E2 acetylcholinesterase conjugate (17β-E2 tracer) competes with 17β-E2 for binding with 17β-E2 antiserum. Therefore, the amount of bound 17β-E2 tracer is inversely proportional to the concentration of 17β-E2 present in the sample. The plate supplied is pre-coated with a mouse monoclonal anti-rabbit IgG which binds free 17β-E2 antiserum. The plate was then washed with UltraPure Water (Cayman Chemical, Michigan, USA) five times to remove any unbound reagents. The activity of the acetylcholinesterase bound to the plate is measured by addition of Ellman's reagent and read at a wavelength of 405nm for kinetic and end point measurements (SpectraMax M2 plate reader, Molecular Devices, California, USA).

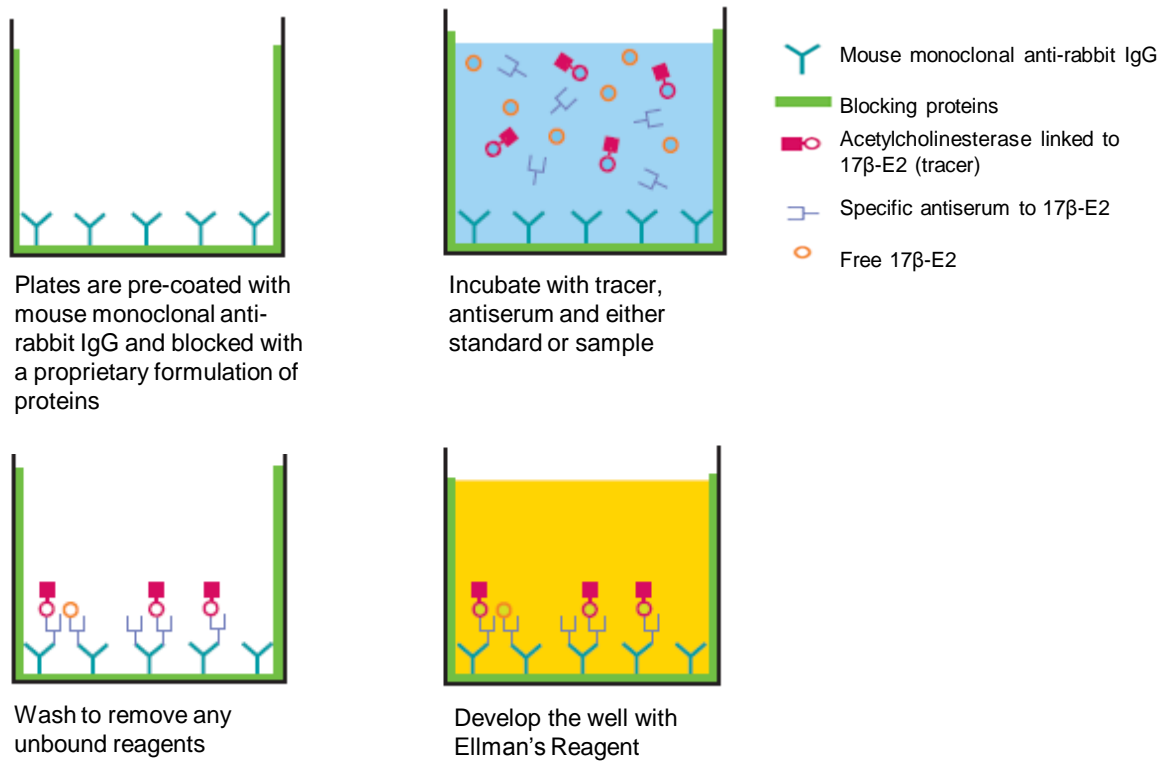


**Figure 2-6 Schematic of the 17β-estradiol immunoassay**  
 Image kindly provided by Cayman Chemical, Michigan, USA

### 2.12.1 17 $\beta$ -estradiol levels in extracellular medium

There is evidence that suggests that synthesis and metabolism of estrogens is increased in PAH. Thus, we investigated 17 $\beta$ -E2 uptake into cells by measuring the depletion from the extracellular medium as an indirect measurement of 17 $\beta$ -E2 metabolism in cells. Female hPASCs derived from PAH patients and non-diseased controls were plated at a density of 10,000 cells per cm<sup>2</sup> in 6-well plates and grown until near confluency. Cells were quiesced in 0.2% (v/v) CS-FBS PRF-DMEM for 24 hours and then stimulated with 1nM 17 $\beta$ -E2 (544.76pg) for 10 minutes and 24 hours. At the termination of the experiment, cells were placed on ice and the spent medium was collected and the intact cells were lysed in 1% (v/v) LM solution in DPBS for protein correction using a BCA protein assay. Levels of 17 $\beta$ -E2 in the medium were determined using the 17 $\beta$ -E2 EIA, as previously described (see section 2.12).

## 2.13 High performance liquid chromatography

All aqueous and organic solvents were glass-distilled, high performance liquid chromatography high performance liquid chromatography (HPLC) grade.

There is evidence that altered estrogen synthesis and metabolism may figure prominently in PAH. However, to date, limited knowledge is available on the dynamic regulation of estrogen metabolism in PAH. This is partly due to challenges in measuring steroid compounds and a lack of availability of immunoassays. To address this question, we developed a methodology to quantitatively measure estrogen metabolism in cell cultures using HPLC with ultraviolet (UV) and radiochemical detection.

### 2.13.1 Optimisation of separation of estrogen metabolites by high performance liquid chromatography

Fifteen estrogens and estrogen metabolites, including oestrone (E1), 17 $\beta$ -estradiol (17 $\beta$ -E2), estriol/16 $\alpha$ -hydroxyestradiol (16 $\alpha$ -OHE2), 17 $\alpha$ -estradiol (17 $\alpha$ -E2), 16-epiestriol (16-epi-E3), 17-epiestriol (17-epi-E3), 2-hydroxyestrone (2-OHE1), 2-hydroxyestradiol (2-OHE2), 4-hydroxyestrone (4-OHE1), 4-hydroxyestradiol (4-OHE2), 2-methoxyestrone (2-MeOHE1), 2-methoxyestradiol (2-MeOHE2), 4-methoxyestrone (4-MeOHE1), 4-methoxyestradiol (4-MeOHE2), 16 $\alpha$ -hydroxyestrone (16 $\alpha$ -OHE1) were obtained from Steraloids, Inc. (Newport, USA). All steroids were dissolved in 0.1% ascorbic acid (w/v) methanol at a concentration of 0.25mg/ml. Ascorbic acid was added to the samples to

prevent non-specific oxidation. Samples were diluted in a mobile phase consisting of water (W), acetonitrile (A) and methanol (M) in the ratio 50-30-20, respectively (WAM) to 10 $\mu$ g/mL. Initially, all steroids were separated by HPLC and detected by UV light. HPLC separation was carried out on a Sunfire C18 column (150mm x 4.6mm internal diameter column packed with 5 $\mu$ m C18 particles, Waters, Hertfordshire, UK), maintained at 25°C. A total of 200 $\mu$ l of each steroid standard solution (equivalent to 2 $\mu$ g) was injected onto the HPLC column at a flow rate of 1ml per minute using a ASI-100 automated sample injector (Dionex, California, USA) and a P680 HPLC pump (Dionex, California, USA). Samples were initially analysed on a HPLC photo diode array detector (PDA) Dionex PDA-100 at wavelengths  $\lambda$ 190nm to  $\lambda$ 220nm (Dionex, California, USA) to determine the optimum UV that delivers the best spectral profile and maximal absorbance.

Due to the structural similarity of estrogen compounds, including structural isomers (for example, 17 $\beta$ -E2 and 17 $\alpha$ -E2), to obtain a single chromatogram of all 15 estrogen metabolites, it was essential to use a gradient elution mode. This utilizes graded mobile phase compositions to improve the separation of the compounds. The interaction of the compounds with the column stationary phase and the mobile phase will determine its unique elution profile. All estrogen metabolites were successfully separated on gradient elution mode at 25°C and detected at  $\lambda$ 200nm. The initial mobile phase consisted of 50-10-40 WAM which was maintained for 1 minute. The mobile phase was altered to 55-40-4 over a gradient from 1 to 8 minutes and maintained for 2 minutes under these conditions. The mobile phase was then switched to 50-30-20 in a ballistic gradient over 1 minute and maintained in these conditions for a subsequent 9 minutes. The mobile phase reverted back to the initial conditions for stabilisation of the UV signal for 10 minutes.

### **2.13.2 Optimization of estrogen metabolite extraction**

Prior to HPLC analysis, estrogens were extracted from their biological matrix to remove interferences and maximise recoveries. Initially, we wished to assess the optimal extraction method for complete recovery of all the estrogen metabolites. We tested both solvent extractions and solid phase extraction (SPE) using Oasis® HLB Columns (Waters, Hertfordshire, UK).

#### *2.13.2.1 Solvent Extractions*

To assess the ability of solvent extractions to extract estrogen metabolites we used ethyl acetate, diethyl ether and dichloromethane in the ratios (aqueous: solvent) 1:1, 1:5 and 1:10

(except for dichloromethane where we were unable to separate the solvent from the biological matrix at the ratio 1:1). A mixture of all the standards (dissolved in 0.1% (w/v) ascorbic acid methanol) was added to 500µl of the biological matrix; 0.1% (w/v) ascorbic acid, 1% CS-FBS PRF-DMEM. Medium samples with an equal volume of 0.1% (w/v) ascorbic acid in methanol was also prepared for extraction. The former is known as pre-spiking, where the standards are added into the biological matrix prior to the extraction. This can then be compared to the latter, where the standard solution is added to the sample after the extraction (post-spiking). This tests the efficiency of the extraction method. To each mixture, the relevant solvent was added and thoroughly vortexed and then allowed to separate on the bench top. Ethyl acetate and diethyl ether are less dense than the biological matrix and form the upper layer of the separation, which was carefully removed. In contrast, dichloromethane is denser and thus separates into the bottom layer. The mixture of estrogen standards was then added to the post-spiked samples. The samples were reduced to dryness under a gentle stream of oxygen free nitrogen gas at room temperature and reconstituted in the initial mobile phase (WAM 50-10-40).

#### *2.13.2.2 Oasis SPE Extraction*

A mixture of all the standards (dissolved in 0.1% (w/v) ascorbic acid methanol) was added to 10mL of the biological matrix; 0.1% (w/v) ascorbic acid, 1% CS-FBS PRF-DMEM. The Oasis® HLB reverse-phase cartridges 3 cubic centimetres 60 mg (Waters, Hertfordshire, UK) were placed onto a vacuum manifold to encourage flow (Waters extraction manifold, Waters, Hertfordshire, UK). The sorbent bed was preconditioned with 3mL methanol and 3mL water prior to loading the sample (steroid standards in biological matrix and the biological matrix without any steroids), which was allowed to pass through the cartridge. The steroids were retained on the column which was subsequently re-equilibrated with 3mL water followed by a 3mL wash with 5% (v/v) methanol in 95% water. All organic and aqueous solvents contained 0.1% (w/v) ascorbic acid. The steroids were then eluted through the cartridge with 0.1% (w/v) ascorbic acid in 100% methanol. The eluted samples were dried under a gentle stream of oxygen free nitrogen gas at room temperature and reconstituted in the initial mobile phase (50-10-40 WAM). This methodology is summarised in Table 2-4.

Extraction recovery percentages for both solvent extractions and SPE were calculated by dividing the mean integrated peak areas from pre-spiked samples by the mean integrated

peak areas from post-spiked samples and control samples (no extraction) and multiplied by 100.

**Table 2-4 Oasis® HLB extraction of Estrogen metabolites**

<b>Solid phase extraction with Oasis® HLB</b>	
Condition	3mL Methanol 3mL Water
Loading	Sample
Re-equilibrate	3mL Water
Wash	3mL 95% water in methanol
Elution	3mL methanol

### 2.13.2.3 High performance liquid chromatography

100µl of sample was injected onto the HPLC column and run under a gradient elution mode, as previously described (See section 2.13.1).

### 2.13.2.4 Extraction of radiolabelled $^{14}\text{C}$ -17β-estradiol and optimisation of concentration required for optimum detection

$^{14}\text{C}$ -4C-17β-E2 ( $^{14}\text{C}$ -17β-E2) specific activity, 55mCi/mmol; concentration, 0.1mCi/mL) was obtained from American Radiolabelled Chemicals, Inc. (Missouri, USA).  $^{14}\text{C}$ -17β-E2 was selected as the suitable isotope as the deuterated form ( $^3\text{H}$ -17β-E2) may lose deuteriums during CYP metabolism. The Oasis® HLB columns obtained the best recoveries of all estrogen metabolites (Chapter 5). The same methodology was therefore tested for the extraction of radiolabelled 17β-E2.

To determine the optimal concentration of 17β-E2 to use for subsequent experiments, we required a concentration that provided maximal peak intensity in the radiolabelled detector without saturation of the signal (to allow greatest chance of detection of metabolite formation). The molar concentration of  $^{14}\text{C}$ -17β-E2 is calculated by dividing the radioactivity concentration by the specific activity (1.818mmol/L). The maximum peak intensity was obtained with 0.074µl of  $^{14}\text{C}$ -17β-E2. The optimal concentration was 50nM in 10mL (136.19ng), which was used for all subsequent experiments. This concentration allowed us to run the sample in replicate, a minimum of 3 times. Radioactivity (counts

per minute) was determined by a radio HPLC detector (Berthold LP509, Berthold Technologies, Bad Wilbad, Germany).

### 2.13.3 Estrogen metabolism in cells

HPASMCs (passages 3-6) were seeded in 100mm tissue culture plates at a density of 10,000 cells per cm<sup>2</sup> and grown to near confluency. Cells were synchronised by serum deprivation for 24 hours in 0.2% CS-FBS, PRF-DMEM. After 24 hours, the cell culture media was replaced with 1% CS- FBS, PRF-DMEM to maintain adequate growth. To assess 17 $\beta$ -E2 metabolism, cells were exposed to <sup>14</sup>C-17 $\beta$ -E2 at the pre-optimized concentration of 50nM (136.19ng) for various time-points (0, 10, 30 minutes, 1, 2, 4, 24, 48 hours). At the end-point, cell culture plates were placed on ice; the spent, metabolite-enriched medium was collected with 0.1% ascorbic acid to prevent oxidation of the extremely sensitive catechol estrogens and frozen at -20°C prior to SPE extraction (see section 2.13.2.2) and HPLC analysis. After SPE extraction, standards were added to the sample at a concentration of 10 $\mu$ g/mL for peak identification. The cell monolayer was washed twice with 10mL of ice cold DPBS, and lysed with a 1% LM (v/v) in DPBS. Cells were carefully scraped from the surface of the culture dish and placed in a pre-chilled eppendorf for 30 minutes. Cells were then further lysed by sonication in an ice bath (3 x 30 seconds), centrifuged at 10,000xg for 10 minutes at 4°C. The supernatant was removed and placed in a fresh, ice-chilled eppendorf and frozen at -20°C, prior to BCA analysis to determine the protein concentration for normalisation of results.

#### 2.13.3.1 High performance liquid chromatography

100 $\mu$ l of the extracted product and steroids applied to the column was separated by HPLC and detected by a UV and radio-labelled detection system. The sample was separated using a Sunfire C18 column and maintained at 25°C. To confirm peak identity, the samples were also separated with an Allure Biphenyl 5 $\mu$ m, 4.6 x 150mm column (Thames Restek, Buckinghamshire, UK) at 30°C with reverse phase chromatography in isocratic mode using water and methanol in the mobile phase (32% water:78% methanol). All peak integrations for quantification were obtained from the sample run in the Allure Biphenyl column.

All HPLC data analysis was performed with Chromeleon 6.5 chromatography data system (Dionex, California, USA).

## 2.14 Statistical analysis and data handling

Data was processed and analyzed using GraphPad Prism 5 (California, USA). Data is represented as the groups mean  $\pm$  the standard error of the mean (SEM). Data was analyzed by a student's t test (where there were only two groups) or a Bonferroni's Post Hoc test (when comparing across all groups).

## **Chapter 3**

# **The Estrogen Metabolizing Enzyme Cytochrome P450 1B1 Influences the Development of Pulmonary Arterial Hypertension**

### 3.1 Introduction

Despite the complexity and multi-factorial pathology associated with PAH, the incidence of both IPAH and HPAH is more common in women than in men (Badesch *et al.*, 2010; Ling *et al.*, 2012; Shapiro *et al.*, 2012). This suggests that sex hormones may be mediating pathological effects in the presence and absence of genetic susceptibilities. This is supported by evidence that estrogens are important during lung development, normal physiology and pathophysiology (reviewed by Carey *et al.*, 2007; Townsend *et al.*, 2012).

17 $\beta$ -E2, the main pre-menopausal hormone, is metabolised by various CYP enzymes to both pro- and anti-proliferative metabolites. Aberrant expression of CYP1B1, a major extra-hepatic estrogen-metabolizing enzyme, has been reported in both pre-clinical models of PAH (White *et al.*, 2011a) and in human PAH (Austin *et al.*, 2009). A genetic polymorphism in CYP1B1 (Asn453 $\rightarrow$ Ser; N453S), which is associated with an increased rate of degradation of CYP1B1 (Bandiera *et al.*, 2005) is more common in patients with a BMPR-2 mutation without any evidence of PAH (Austin *et al.*, 2009). This suggests that CYP1B1 activity is involved in the development of PAH in patients harbouring a BMPR-2 mutation. Epidemiological evidence highlights a detrimental role for female gender in PAH, yet there is a paucity of understanding of the basis of this. Altered metabolism by aberrant CYP1B1 activity may underlie this, yet its contribution to PAH has so far been undetermined.

In premenopausal women, the predominant circulating estrogen is 17 $\beta$ -E2. In women, circulating levels of 17 $\beta$ -E2 vary depending on the estrous cycle. In the follicular phase, circulating concentrations of 17 $\beta$ -E2 are about 100pg/mL (~0.37nM) and during ovulation these levels rise to about 600pg/mL (~2.20nM). After menopause, 17 $\beta$ -E2 levels are dramatically reduced up to 20-fold lower (Mendelsohn & Karas, 1999). Furthermore, vascular cells can modulate their own estrogenic milieu by the local conversion of testosterone or androstenedione to 17 $\beta$ -E2 and E1 respectively (Harada *et al.*, 1999). 17 $\beta$ -E2 and E1 can be interconverted to one another by the activity of 17 $\beta$ -HSD enzymes. In hPASCs 17 $\beta$ -E2 at 1nM increases the expression of CYP1B1 and cellular proliferation (White *et al.*, 2011a).

CYP1B1 is a member of the CYP superfamily, which are monooxygenase enzymes that substitute a hydrogen atom to a hydroxyl group in the presence of oxygen and NADPH. CYP1B1 preferentially hydroxylates at the C4 position of the aromatic ring of 17 $\beta$ -E2 and

to a lesser extent, at the C2 and C16 positions (Badawi *et al.*, 2001; Hanna *et al.*, 2000; Lee *et al.*, 2003). CYP metabolites can then undergo further metabolism by the activity of COMT to their methylated metabolites. Increased activity and expression of CYP1B1 has already been reported in many diseases including breast cancer (McKay *et al.*, 1995), lung cancer (Murray *et al.*, 1997), ovarian cancer (McFadyen *et al.*, 2001), and systemic hypertension (Jennings *et al.*, 2010). Yet, the contribution of CYP1B1 to the development of PAH remains uncertain.

Here, we investigate the potential pathological contribution of CYP1B1 metabolism of 17 $\beta$ -E2 on the development of PAH. We demonstrate increased CYP1B1 expression in both experimental and clinical PAH which may direct the intrinsically regulated metabolism of 17 $\beta$ -E2 towards the formation of pro-proliferative metabolites. Furthermore, we demonstrate an essential function of CYP1B1 on the development of experimental PAH supporting a putative pathological role of CYP1B1 metabolism in this highly prevalent disease in females. We provide evidence for gender differences in PAH, that suggests estrogen-related therapies, particularly through inhibition of pathological metabolism through CYP1B1, may be a promising therapeutic strategy in some patients.

Aims of this chapter

1. To functionally and molecularly characterise the impact of estrogen metabolism by CYP1B1 to the development of PAH in vivo

## 3.2 Results

### 3.2.1 Hypoxia alters the estrogen metabolic axis in human pulmonary arterial smooth muscle cells

Hypoxia is a mediator in PAH pathogenesis and we therefore wished to investigate whether oxygen deprivation alters components of the estrogen-metabolic axis in hPASMCs. CYP1B1 transcription is predominantly mediated by translocation of the AhR to the nucleus where it associates with the ARNT and binds to DRE. HIF1 $\alpha$  is a master regulator of hypoxia-induced gene expression. HIF1 $\alpha$  mediates gene transcription in response to hypoxia by the AhR pathway by binding of the HIF1 $\alpha$ -ARNT complex to hypoxia-response genes. There is therefore a close link between the AhR pathway, hypoxia and CYP1B1 and we were therefore interested to investigate the effect of hypoxia (1% oxygen) on CYP1B1 expression. Hypoxia increased the expression of CYP1B1 (Figure 3-1a). 17 $\beta$ -HSD1 regulates internal reservoirs of E1 by converting them into 17 $\beta$ -E2. We report an increased expression of 17 $\beta$ -HSD1 following exposure to chronic hypoxia (Figure 3-1b), which suggests there is increased formation of 17 $\beta$ -E2 in response to hypoxia in these cells. This can then be further metabolised by increased CYP1B1 expression. Activity of COMT methylates hydroxylated estrogens to their less active metabolites. Here, the expression of COMT was unchanged following hypoxic exposure (Figure 3-1c).

### 3.2.2 Pulmonary CYP1B1 expression is increased in experimental and clinical PAH

Chronic hypoxia and SU-hypoxia increased CYP1B1 mRNA and protein expression in murine pulmonary arteries compared to their normoxic counterparts (White *et al.*, 2012). Immunohistochemistry analysis revealed that CYP1B1 was localised within all cells that comprise the vascular wall (Figure 3-2 - Figure 3-3). In human PAH, CYP1B1 protein and mRNA expression was increased in PASMCs compared to control (White *et al.*, 2012). Similarly, CYP1B1 immunolocalisation and quantification revealed increased CYP1B1 expression in the pulmonary arteries of patients with PAH compared to controls (Figure 3-4). CYP1B1 was localised to all layers of the pulmonary arterial wall including  $\alpha$ -SMA (smooth muscle cells) and von Willebrand positive cells (endothelial cells) (Figure 3-5). Patient characteristics are listed in Table 3-1.

**Table 3-1 Patient characteristics of human lung sections**

Clinical data of patients with PAH including their sex, age, mean pulmonary arterial pressure (mPAP) and drug therapy that were used for Immunolocalisation and semi-quantification of CYP1B1 in the pulmonary arteries of lung sections.

<b>Sex</b>	<b>Age</b>	<b>Patient Information</b>	<b>mPAP (mmHg)</b>	<b>Drug Therapy</b>
F	26	HPAH	67	Nifedipine
F	30	HPAH	46	Iloprost, sildenafil
F	38	HPAH	56	Epoprostenol
F	44	IPAH	44	Epoprostenol
F	51	IPAH	49	Prostacyclin
F	23	IPAH	57	Iloprost
M	23	HPAH	54	Iloprost and sildenafil
M	56	IPAH	N/A	N/A

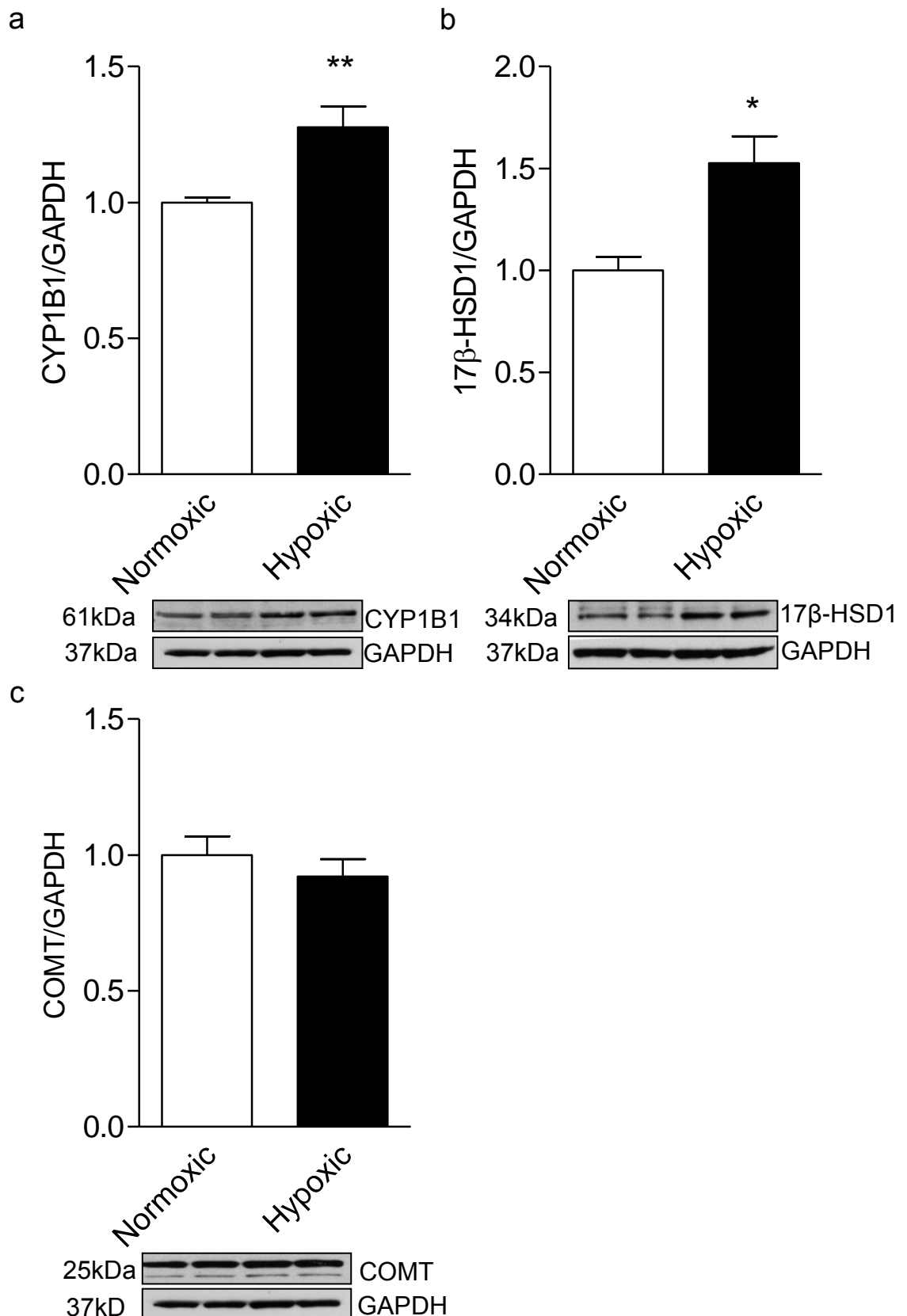


**Figure 3-1 Effect of hypoxia on protein expression of CYP1B1, COMT and 17β-HSD1 in human pulmonary arterial smooth muscle cells (hPASMCs)**

Female control hPASMCs were quiesced for 24 hours and then exposed to either normoxic or hypoxic conditions (1% oxygen) for 24 hours. Cell homogenates were assayed for protein expression by western blotting for CYP1B1 (a), 17β-HSD1 (b) and COMT (c) and analysed by densitometric analysis. GAPDH was used as the internal loading control. Full western blots are shown in appendix 1. n=2 patients, repeated 2 times per condition, \*P<0.05, \*\*P<0.01, t-test, data is expressed as the mean ± SEM.

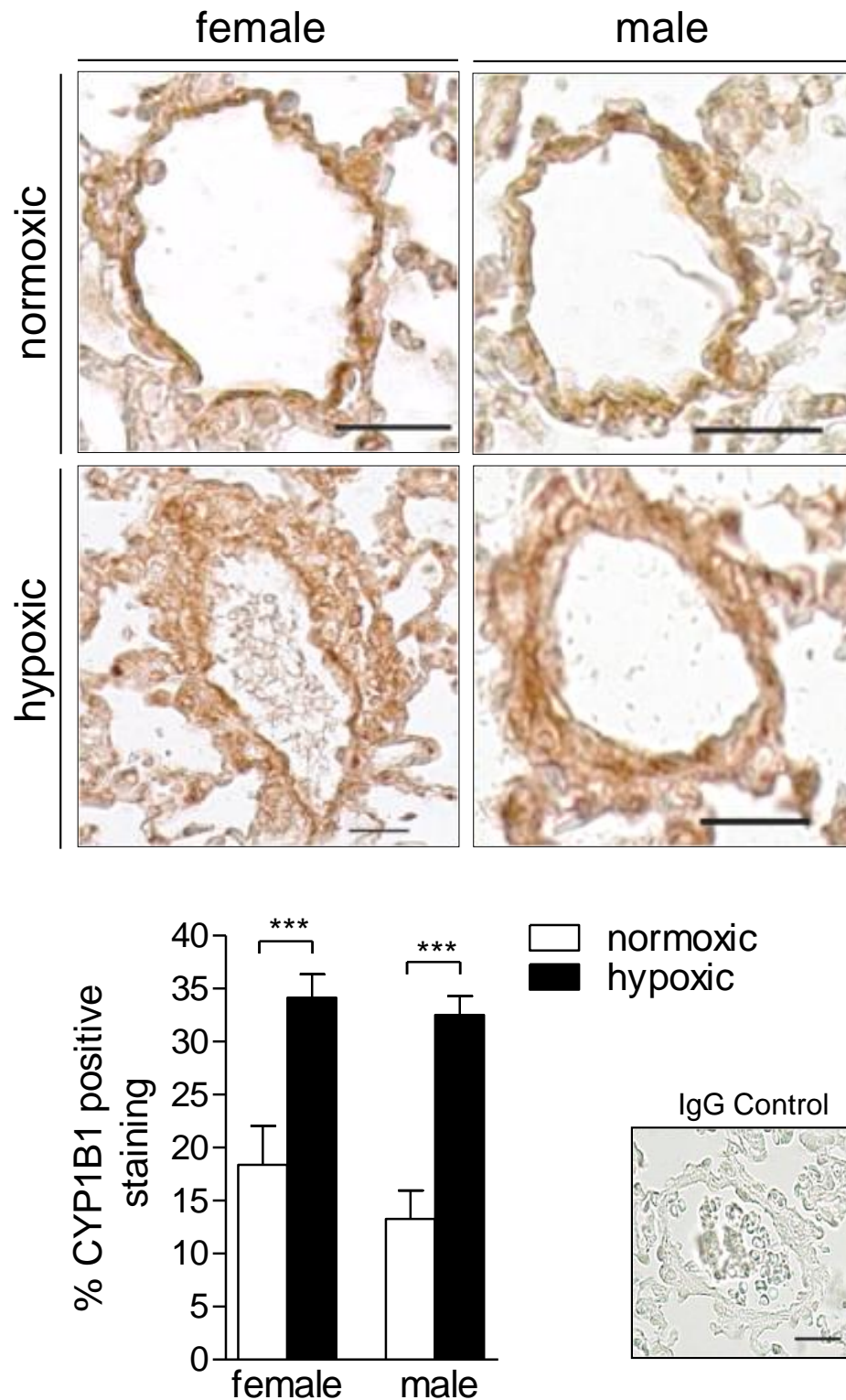


**Figure 3-2 Immunolocalisation of CYP1B1 in normoxic and hypoxic murine pulmonary arteries**

Female and male C57BL/6 mice were exposed to hypoxia (10% oxygen) or kept in room air for 2 weeks. Representative immunohistochemistry for CYP1B1 in the small pulmonary arteries and quantification of the % positive CYP1B1 staining within the vessel wall. CYP1B1 expression is visualized by DAB staining (dark orange/brown stain).  $n=4$  mice per group,  $***P<0.001$ , One-way ANOVA with a Bonferroni's post-hoc test. Data is expressed as the mean  $\pm$  SEM. IgG control reveals no non-specific binding. Scale bar =  $20\mu\text{m}$ .

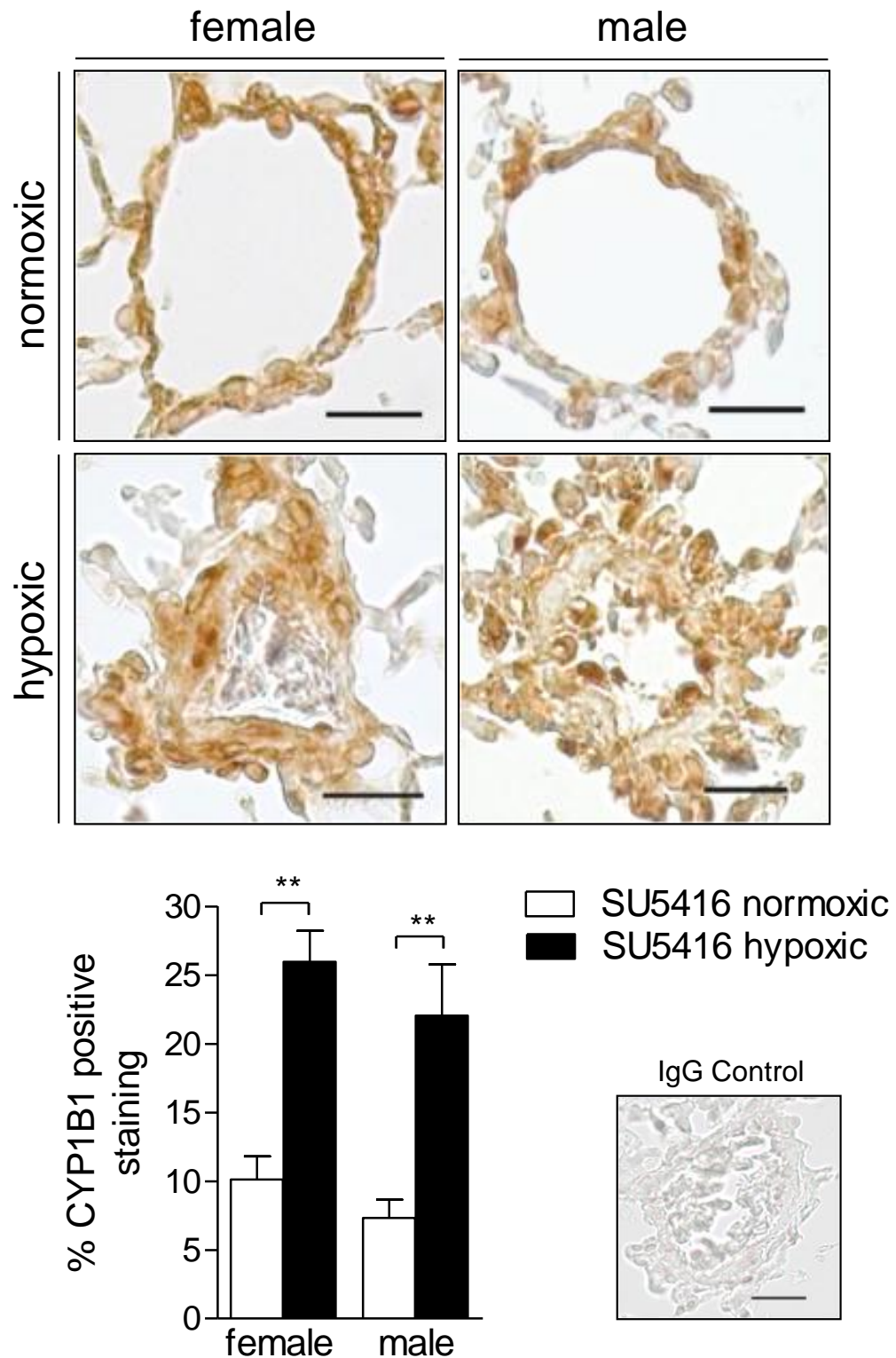


**Figure 3-3 Immunolocalisation of CYP1B1 in SU-hypoxic murine pulmonary hypertension**

Female and male (C57BL/6) mice were exposed to hypoxia (10% oxygen) or kept in room air for 3 weeks and given SU5416 (20mg/kg) at 0, 7 and 14 days. Representative immunohistochemistry for CYP1B1 in the small pulmonary arteries and quantification of the % positive CYP1B1 staining within the vessel wall. CYP1B1 expression is visualized by DAB staining (dark orange/brown stain). n=5 mice per group, \*\*P<0.01, One-way ANOVA with a Bonferroni's post-hoc test. Data is expressed as the mean  $\pm$  SEM. IgG control reveals no non-specific binding. Scale bar = 20 $\mu$ m.

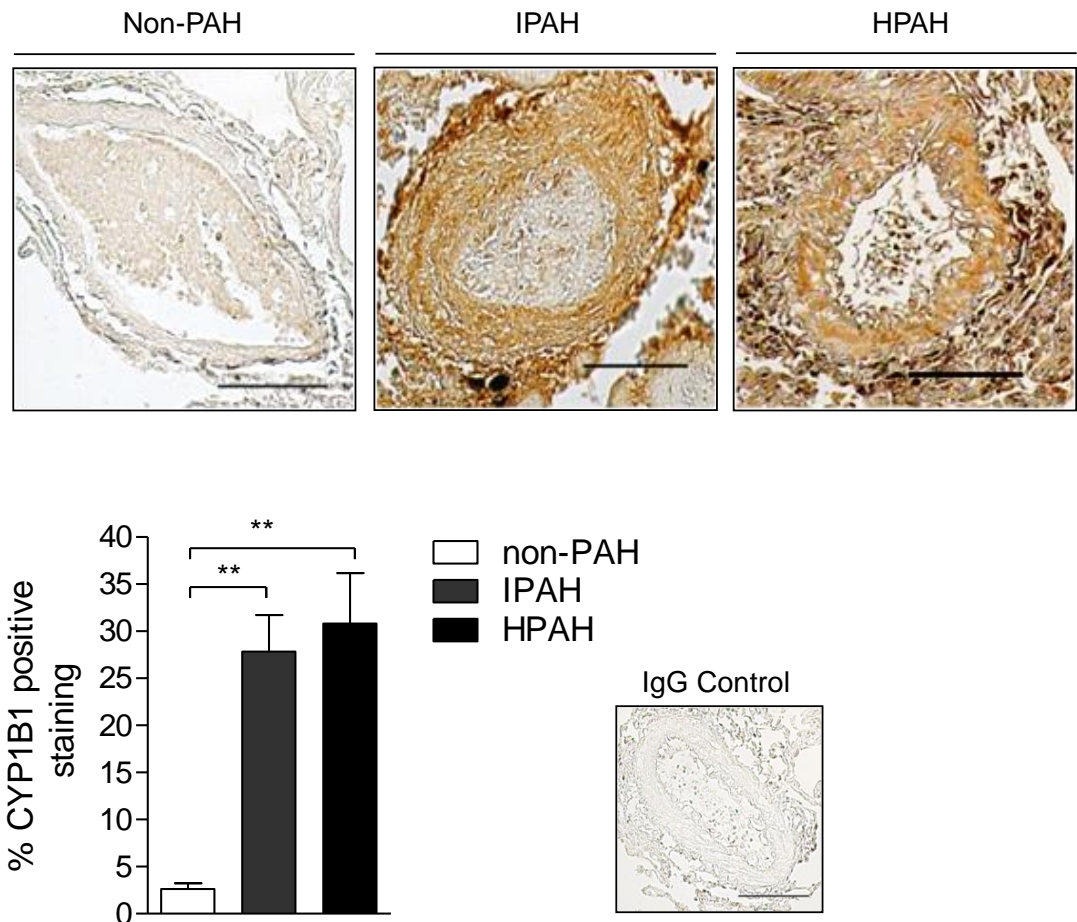


**Figure 3-4 Immunolocalisation of CYP1B1 in pulmonary arteries from patients with PAH**

CYP1B1 immunolocalisation and quantification of the % CYP1B1 staining in non-PAH, idiopathic PAH (IPAHA) and heritable PAH (HPAH) pulmonary arteries. CYP1B1 expression is visualized by DAB staining (dark orange/brown stain). The IPAHA artery is from a 56 year old male patient and the HPAH patient is a 26 year old female patient with a BMPR-2 mutation. Quantification was from n=4 patients per group (see Table 3-1 for patient characteristics). \*\*P<0.01, One-way ANOVA with a Bonferroni's post-hoc test. Data is expressed as the mean ± SEM. IgG control revealed absence of non-specific binding. Scale bars = 100µm.

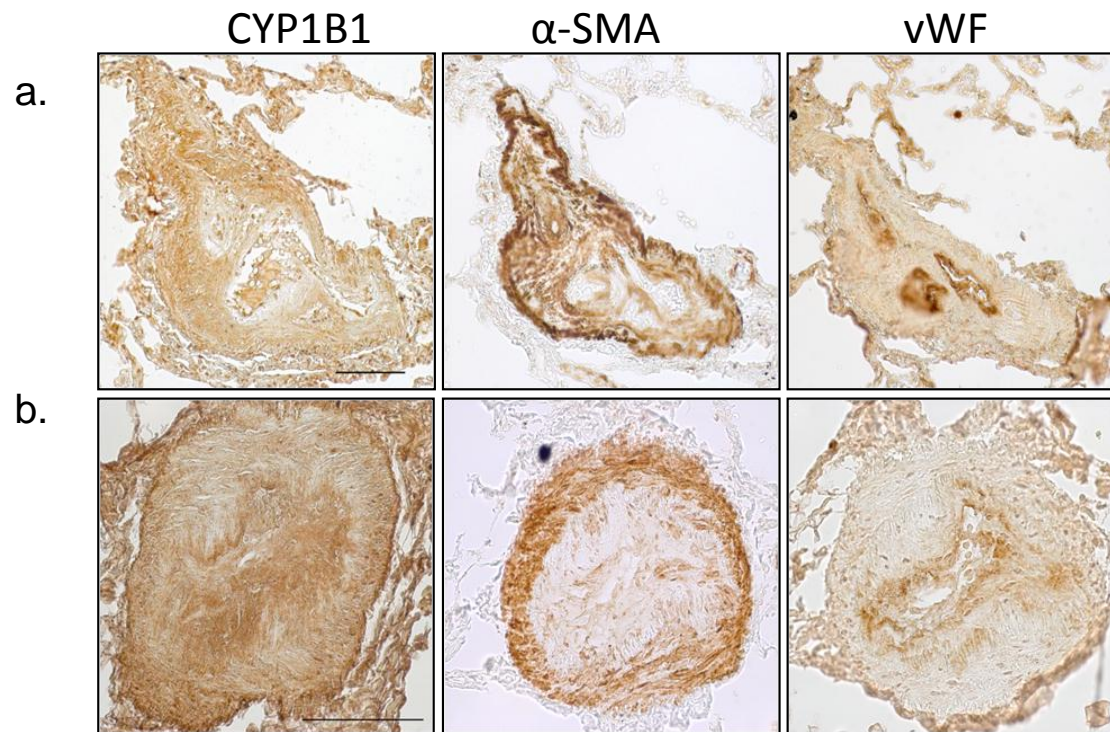


**Figure 3-5 Cellular localisation of CYP1B1 in human vascular lesions**

The expression of CYP1B1,  $\alpha$ -SMA (smooth muscle cell marker) and vWF (endothelial cell marker) in 5 $\mu$ m consecutive human pulmonary arteries as visualized by the chromagen DAB which appears as a brown/orange stain. CYP1B1,  $\alpha$ -SMA and vWF immunolocalisation in a complex vascular lesion from a 38 year old female heritable PAH (HPAH) patient (a) and a 26 year old male HPAH patient (b). Scale bar = 100 $\mu$ m.

### 3.2.3 Effect of chronic hypoxia in CYP1B1 deficient mice

To test the function of CYP1B1 in hypoxia-induced PAH, CYP1B1<sup>-/-</sup> mice were exposed to chronic hypobaric hypoxia for 14 days. Under basal conditions (normoxia), no differences in the ratio of RV/LV+S were observed between wild-type and CYP1B1<sup>-/-</sup> female mice. In contrast, male CYP1B1<sup>-/-</sup> mice had a reduced RV/LV+S ratio compared to wild-type mice. Following hypoxic exposure, both male and female wild-type mice develop increased RVH. In contrast, the degree of RVH induced by hypoxia was significantly less in male and female CYP1B1<sup>-/-</sup> mice compared to their wild-type controls (Figure 3-6). No baseline differences were observed in RVSPs between wild-type and CYP1B1<sup>-/-</sup> mice. Hypoxia induced increases in RVSP in wild-type mice and this effect was greater in male mice. CYP1B1<sup>-/-</sup> male mice exhibited an attenuated RVSP in response to hypoxia. No effect was observed in the female CYP1B1<sup>-/-</sup> mice (Figure 3-7). Hypoxia had no significant effects on the mean right ventricular pressure (mRVP) in female mice, whilst in male mice this was significantly increased (Table 3-2).

Pulmonary arterial remodeling in the distal vasculature is a prominent feature of hypoxic-induced PH and was therefore examined in lung sections obtained from these mice (Figure 3-8 - Figure 3-9). Under normoxic conditions, no differences in vascular remodeling were observed in CYP1B1<sup>-/-</sup> mice compared to their wild-type controls. Hypoxia increased remodeling in the distal vasculature in both male and female wild-type mice. CYP1B1<sup>-/-</sup> female mice exhibited a similar degree of vascular remodeling as was observed in the wild-type mice. In male CYP1B1<sup>-/-</sup> mice, the degree of vascular remodeling in response to hypoxia was significantly less than in the wild-type mice.

mSAP, heart rate and body weights were monitored for any off-target effects of hypoxia or genetic ablation of CYP1B1 (Table 3-2). Exposure to hypoxia caused an increase in mSAP in male mice. This was not observed in any of the other groups studied. Female CYP1B1<sup>-/-</sup> mice had reduced heart rates compared to their wild-type counterparts under normoxic conditions. In male CYP1B1<sup>-/-</sup> mice, a reduced heart rate was reported following hypoxic exposure compared to wild-type mice. Female CYP1B1<sup>-/-</sup> mice were on average heavier than their respective wild-type mice under normoxic conditions. In contrast male CYP1B1<sup>-/-</sup> mice weighed less than their wild-type controls under both normoxic and hypoxic conditions.

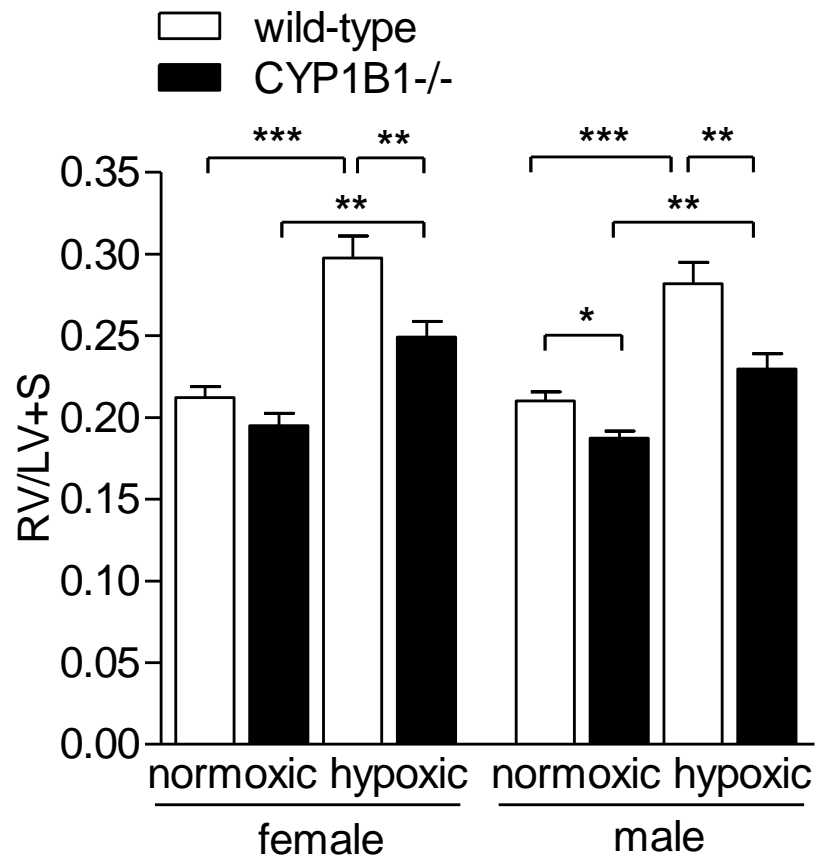


**Figure 3-6 Right ventricular hypertrophy in chronically hypoxic CYP1B1<sup>-/-</sup> mice**

Female and male wild-type (C57BL/6) and CYP1B1<sup>-/-</sup> mice were exposed to hypoxia (10% oxygen) or kept in room air for 2 weeks. Right ventricular hypertrophy was assessed by expressing the dry weight of the right ventricle over the left ventricle and septum (RV/LV+S; Fultons index). n=8-12 per group, \*P<0.05, \*\*P<0.01, \*\*\*P<0.001, One-way ANOVA with a Bonferroni's post-hoc test. Data is expressed as the mean ± SEM.

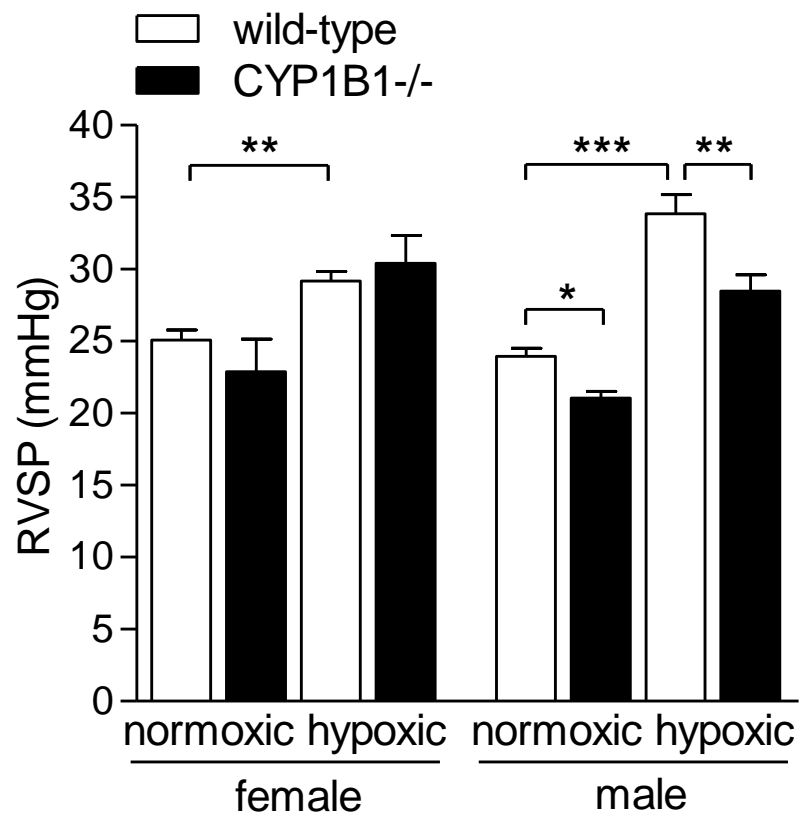


**Figure 3-7 Right ventricular systolic pressures in chronically hypoxic CYP1B1-/- mice**

Female and male wild-type (C57BL/6) and CYP1B1-/- mice were exposed to hypoxia (10% oxygen) or kept in room air for 2 weeks. Right ventricular systolic pressures (RVSP) were measured by right heart catheterisation. n=7-11 per group, \*P<0.05, \*\*P<0.01, \*\*\*P<0.001, One-way ANOVA with a Bonferroni's post-hoc test. Data is expressed as the mean  $\pm$  SEM.

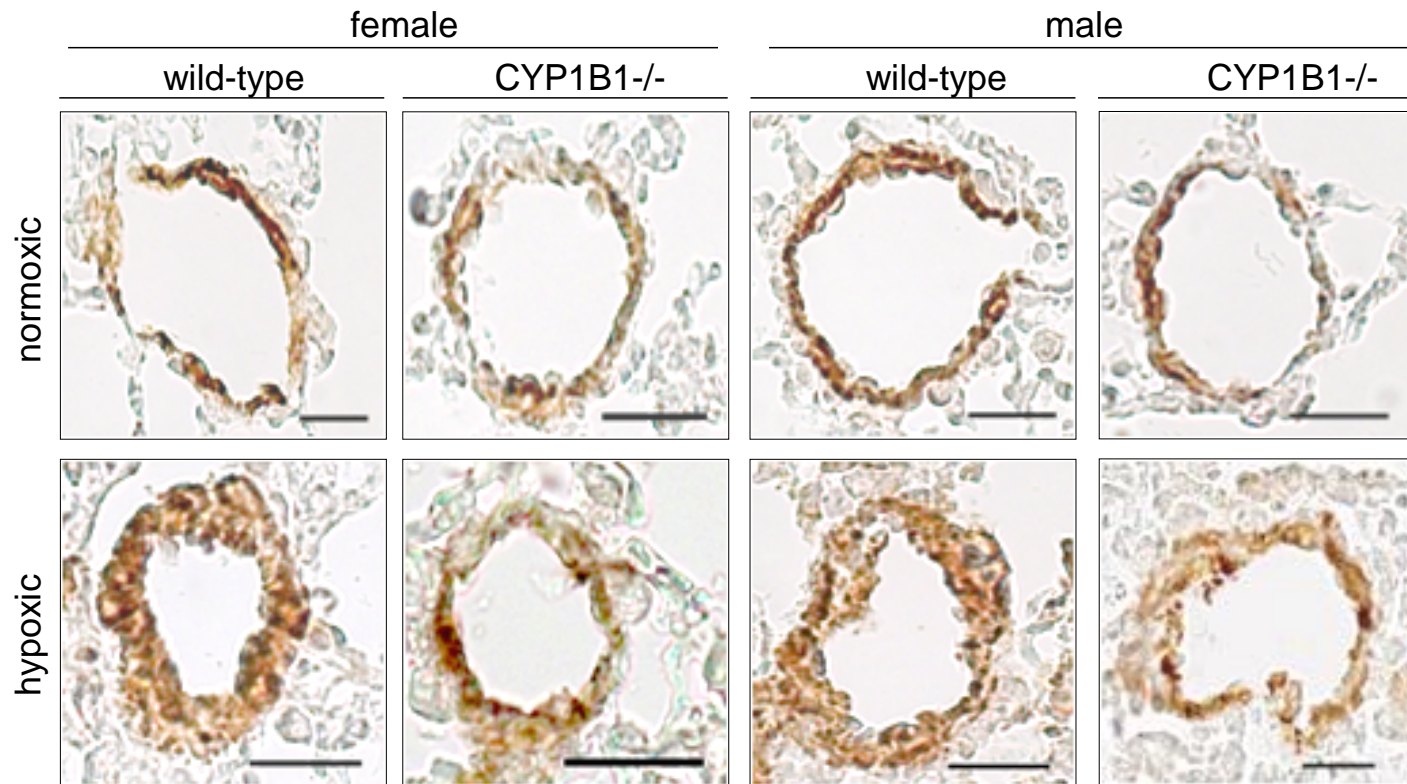


**Figure 3-8 Representative expression of  $\alpha$ -smooth muscle actin positive cells in response to hypoxia in wild-type and CYP1B1<sup>-/-</sup> mice**

Female and male wild-type (C57BL/6) and CYP1B1<sup>-/-</sup> mice were exposed to hypoxia (10% oxygen) or kept in room air for 2 weeks. The degree of vascular muscularisation was visualized by  $\alpha$ -smooth muscle actin ( $\alpha$ -SMA) staining in the distal vasculature.  $\alpha$ -SMA expression was visualised by DAB staining (dark orange/brown stain). Scale bar = 20 $\mu$ m

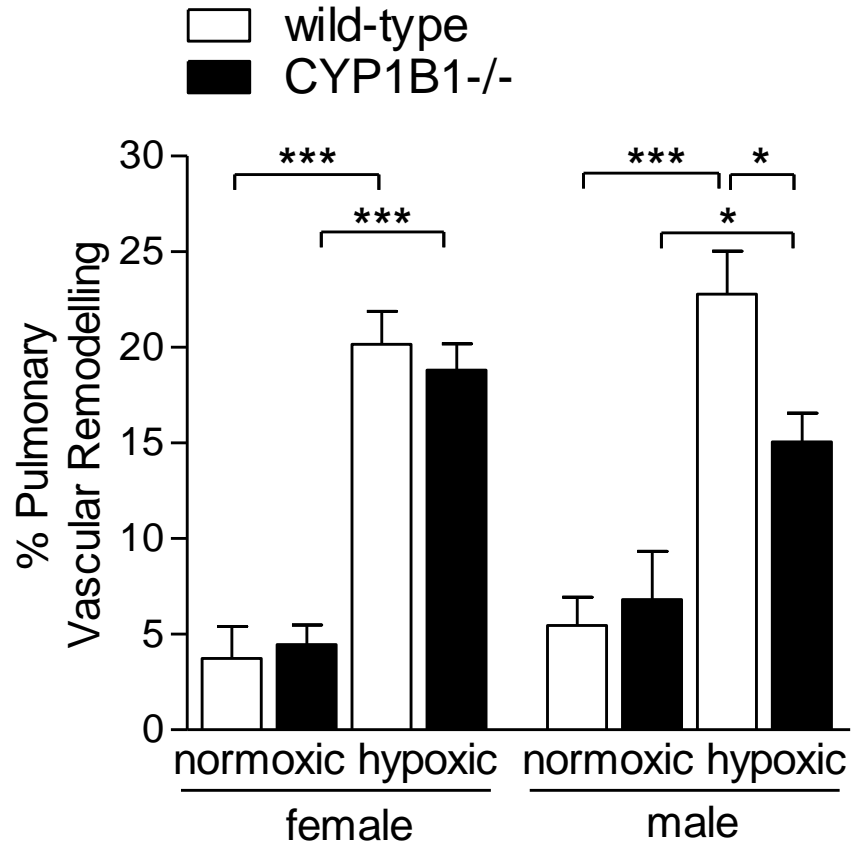


**Figure 3-9 Pulmonary vascular remodeling in chronically hypoxic CYP1B1<sup>-/-</sup> mice**

Female and male wild-type (C57BL/6) and CYP1B1<sup>-/-</sup> mice were exposed to hypoxia (10% oxygen) or kept in room air for 2 weeks. The degree of pulmonary arterial remodeling was assessed by counting the number of remodeled and non-remodeled arteries in a lung section and expressed as the % of remodeled vessels over the total number of vessels. n=4-5 per group, \*P<0.05, \*\*P<0.01, One-way ANOVA with a Bonferroni's post-hoc test. Data is expressed as the mean ± SEM.

### **3.2.4 Intra-pulmonary arterial vasoconstriction in CYP1B1<sup>-/-</sup> Mice**

Vasoconstriction of intra-pulmonary arteries is increased following hypoxic exposure. To investigate the contribution of CYP1B1 on the contractile response of the pulmonary artery, contractile responses to the potent vasoconstrictor serotonin were examined in arteries isolated from wild-type and CYP1B1<sup>-/-</sup> mice after normoxic and hypoxic exposure. In arteries from normoxic mice, there were no differences in pulmonary vasoconstriction across groups. (Figure 3-10a) Following hypoxic exposure, female wild-type and CYP1B1<sup>-/-</sup> mice displayed similar contractile responses to serotonin. In contrast, male CYP1B1<sup>-/-</sup> mice had reduced serotonin-induced contractile responses compared to male wild-type mice (Figure 3-10b).

### **3.2.5 Effect of CYP1B1 on uterine + ovary weights**

Given the prominent role of estrogen metabolism by CYP1B1, we were interested in assessing the effects of hypoxia (elevated CYP1B1 activity) and CYP1B1<sup>-/-</sup> (reduced CYP1B1 activity) on dry uterus and ovary weights. No changes were observed across the groups studied (Figure 3-11).

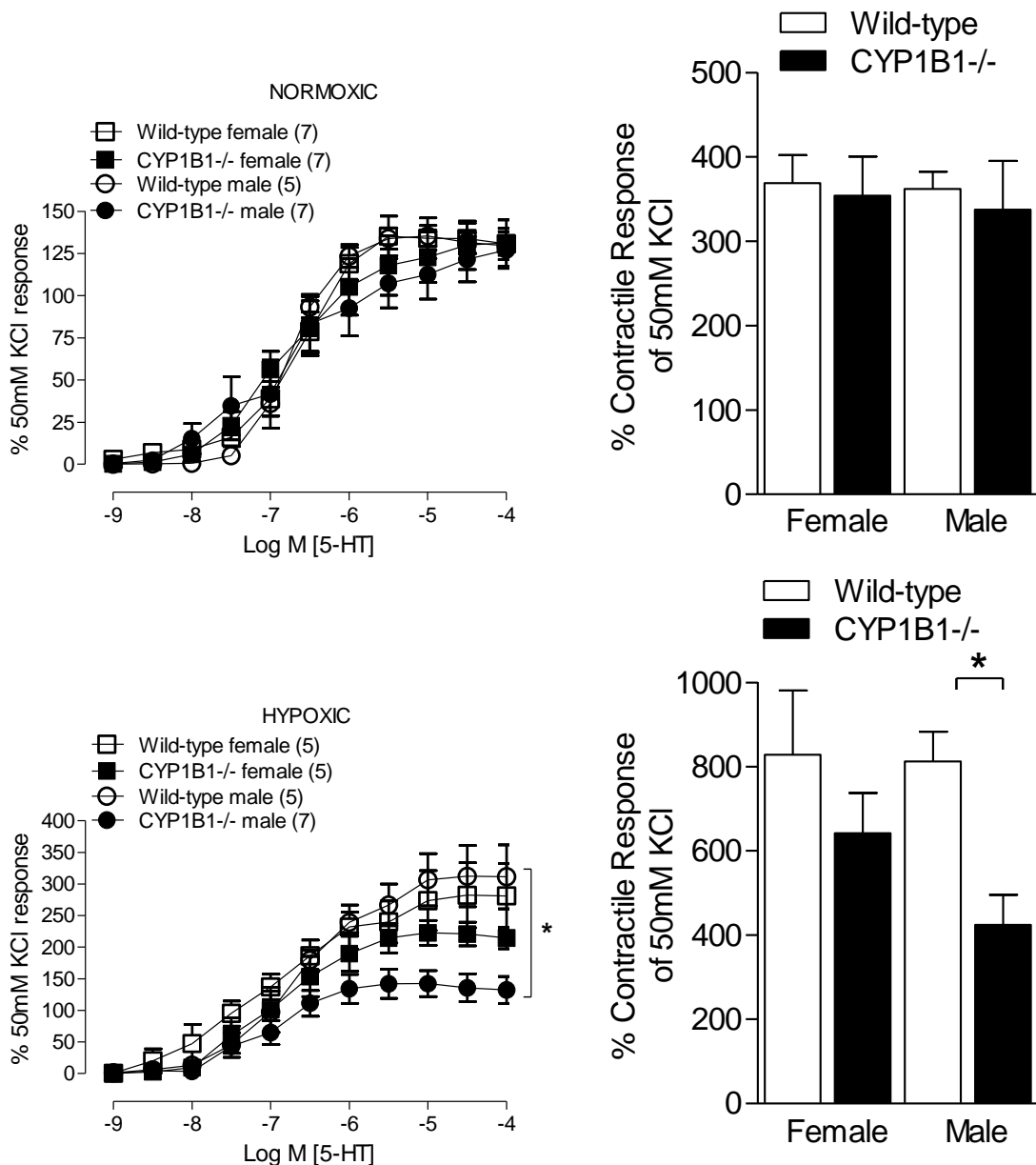


**Figure 3-10 Vasoreactivity of the intrapulmonary arteries in chronically hypoxic CYP1B1<sup>-/-</sup> mice**

Female and male wild-type (C57BL/6) and CYP1B1<sup>-/-</sup> mice were exposed to hypoxia (10% oxygen) or kept in room air for 2 weeks. The intra-pulmonary arteries were isolated from mice at sacrifice and mounted in a myograph. The arteries were constricted twice by increasing extracellular concentrations to 50mM potassium chloride (KCl). The second response was used as a reference constriction to calculate the % vasoconstriction in response to serotonin. Following a wash-out and re-stabilization, cumulative concentration response curves to serotonin were constructed. Serotonin-induced pulmonary arterial vasoconstriction in mice maintained in normoxic conditions (a). Serotonin-induced pulmonary arterial vasoconstriction mice exposed to hypoxia (b); biological replicates are indicated above dose response curves in the legend; Bars are n=5-7, \*P<0.05, One-way ANOVA with a Bonferroni's post-hoc test. Data is expressed as the mean  $\pm$  SEM.

**Table 3-2 Phenotypic data from wild-type and CYP1B1<sup>-/-</sup> mice**

Animal Group	mSAP (mmHg)	mRVP (mmHg)	Heart rate (bpm)	Body Weight (g)
Female wild-type normoxic	91.37 ± 2.52 (7)	12.36 ± 0.47 (7)	489.3 ± 23.09 (6)	19.89 ± 0.17 (10)
Female CYP1B1 <sup>-/-</sup> normoxic	80.10 ± 1.82 (5)	12.22 ± 0.91 (5)	369.8 ± 21.54§ (6)	22.33 ± 0.34§ (10)
Female wild-type hypoxic	98.98 ± 2.26 (9)	14.31 ± 0.53 (9)	416.6 ± 18.65 (9)	20.16 ± 0.36 (10)
Female CYP1B1 <sup>-/-</sup> hypoxic	93.18 ± 2.45 (7)	14.05 ± 0.48 (6)	357 ± 28.43 (8)	21.32 ± 0.48 (10)
Male wild-type normoxic	88.99 ± 2.40 (8)	11.48 ± 0.8 (8)	472.8 ± 16.6 (8)	28.50 ± 0.60 (9)
Male CYP1B1 <sup>-/-</sup> normoxic	90.53 ± 2.70 (4)	9.86 ± 0.9 (9)	415.9 ± 20.74 (11)	25.82 ± 0.85§ (10)
Male wild-type hypoxic	106.9 ± 2.03* (7)	15.23 ± 1.18* (8)	517 ± 15.37 (9)	28.66 ± 0.73 (8)
Male CYP1B1 <sup>-/-</sup> hypoxic	95.14 ± 7.52 (6)	12.88 ± 0.55 (10)	386 ± 16.00§§§ (9)	25.69 ± 0.34§§ (10)

Female and male wild-type (C57BL/6) and CYP1B1<sup>-/-</sup> mice were exposed to hypoxia (10% oxygen) or kept in room air for 2 weeks. Mean systemic arterial pressures (mSAP) were measured by cannulation of the carotid artery. Mean right ventricular pressures (mRVP) were calculated from the right ventricular pressure obtained by right heart catheterisation. n numbers are indicated in brackets. \*P<0.05, P<0.01 c.f. normoxic; §P<0.05, §§§P<0.01 c.f. wild-type, One-way ANOVA with a Bonferroni's post-hoc test. Data is expressed as the mean ± SEM.

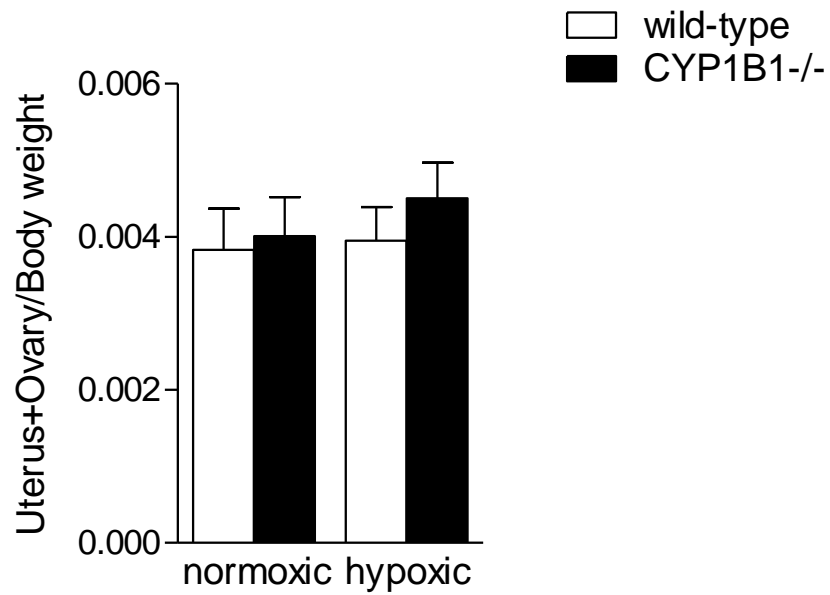


**Figure 3-11 The dry weights of the uterus and ovaries in chronically hypoxic female CYP1B1-/- mice**

Female and male wild-type (C57BL/6) and CYP1B1-/- mice were exposed to hypoxia (10% oxygen) or kept in room air for 2 weeks. The dry weight of the uterus and ovaries were expressed over the body weight. n=8-9, One-way ANOVA with a Bonferroni's post-hoc test. Data is expressed as the mean  $\pm$  SEM.

### **3.2.6 Inhibition of CYP1B1 is protective on the development of hypoxia-induced PAH**

Gene knockout may lead to compensatory mechanisms and as such, we wished to test the effect of CYP1B1 inhibition in mice. We therefore studied the effects of the highly potent and selective CYP1B1 inhibitor TMS in hypoxic-induced PH to determine the role of CYP1B1. The dosing procedures and the *in vivo* component (RVP, RVH, SAP) of this study were a joint collaborative effort with Ms. Emma Wallace, Ms. Annabel Campbell and Dr. Kevin White. TMS reduced the degree of RVSP, RVH and pulmonary vascular remodeling in both male and female mice exposed to chronic hypoxia (Figure 3-12 - Figure 3-15). Both hypoxia and TMS had no effects in mSAPs. Whilst no effects were observed on hypoxia on the average heart rates, TMS significantly increased the heart rate in female mice exposed to hypoxia, in comparison to their age-matched vehicle-control groups (Table 3-3).

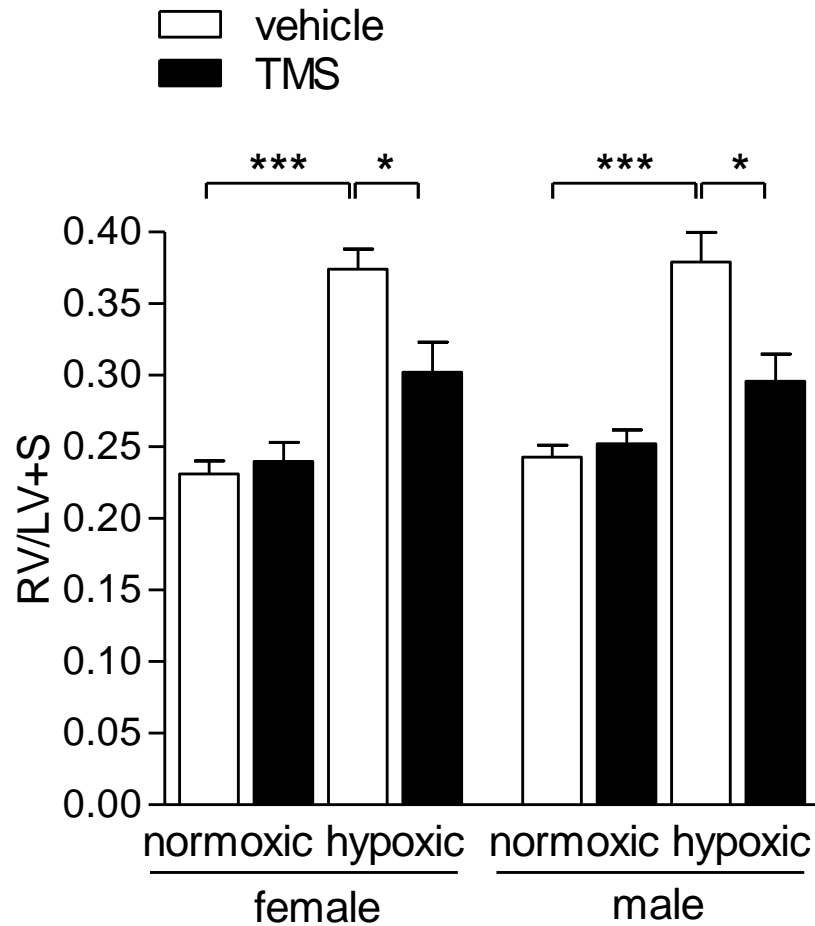


**Figure 3-12 The CYP1B1 inhibitor 2,3',4,5'-tetramethoxystilbene (TMS) attenuates the development of chronic hypoxia-induced right ventricular hypertrophy in mice**

Female and male wild-type mice were exposed to hypoxia (10% oxygen) or kept in room air for 2 weeks. Mice were either injected with 3mg/kg/day TMS or vehicle (~5% ethanol in saline) during the 2 week study. Right ventricular hypertrophy (RVH) was assessed by expressing the dry weight of the right ventricle over the left ventricle and septum (RV/LV+S; Fultons index) in normoxic and chronically hypoxic vehicle- and TMS-treated female and male C57BL/6 mice. n=7-10, \*P<0.05, \*\*P<0.01, \*\*\*P<0.001, One-way ANOVA with a Bonferroni's post-hoc test. Data is expressed as the mean ± SEM.

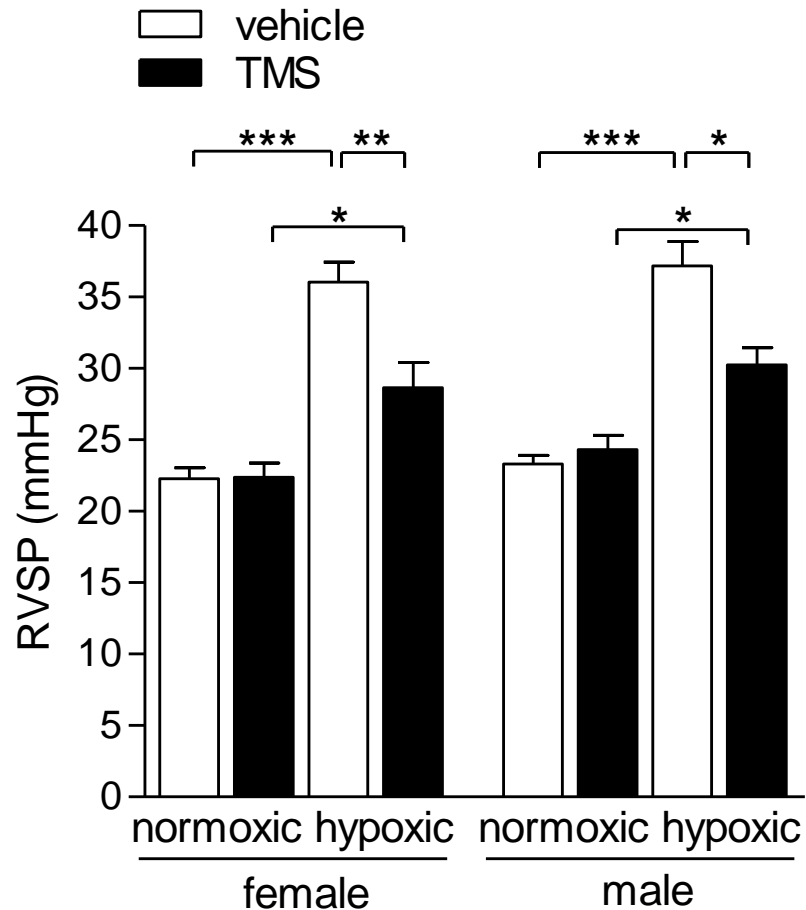


**Figure 3-13 The CYP1B1 inhibitor 2,3',4,5'-tetramethoxystilbene (TMS) attenuates the development of chronic hypoxia-induced right ventricular systolic pressures in mice**

Female and male wild-type mice were exposed to hypoxia (10% oxygen) or kept in room air for 2 weeks. Mice were either injected with 3mg/kg/day TMS or vehicle (~5% ethanol in saline) during the 2 week study. Right ventricular systolic pressures (RVSP) were measured by right heart catheterization in normoxic and chronically hypoxic vehicle- and TMS-treated female and male C57BL/6 mice. n=7-10, \*P<0.05, \*\*P<0.01, \*\*\*P<0.001, One-way ANOVA with a Bonferroni's post-hoc test. Data is expressed as the mean  $\pm$  SEM.

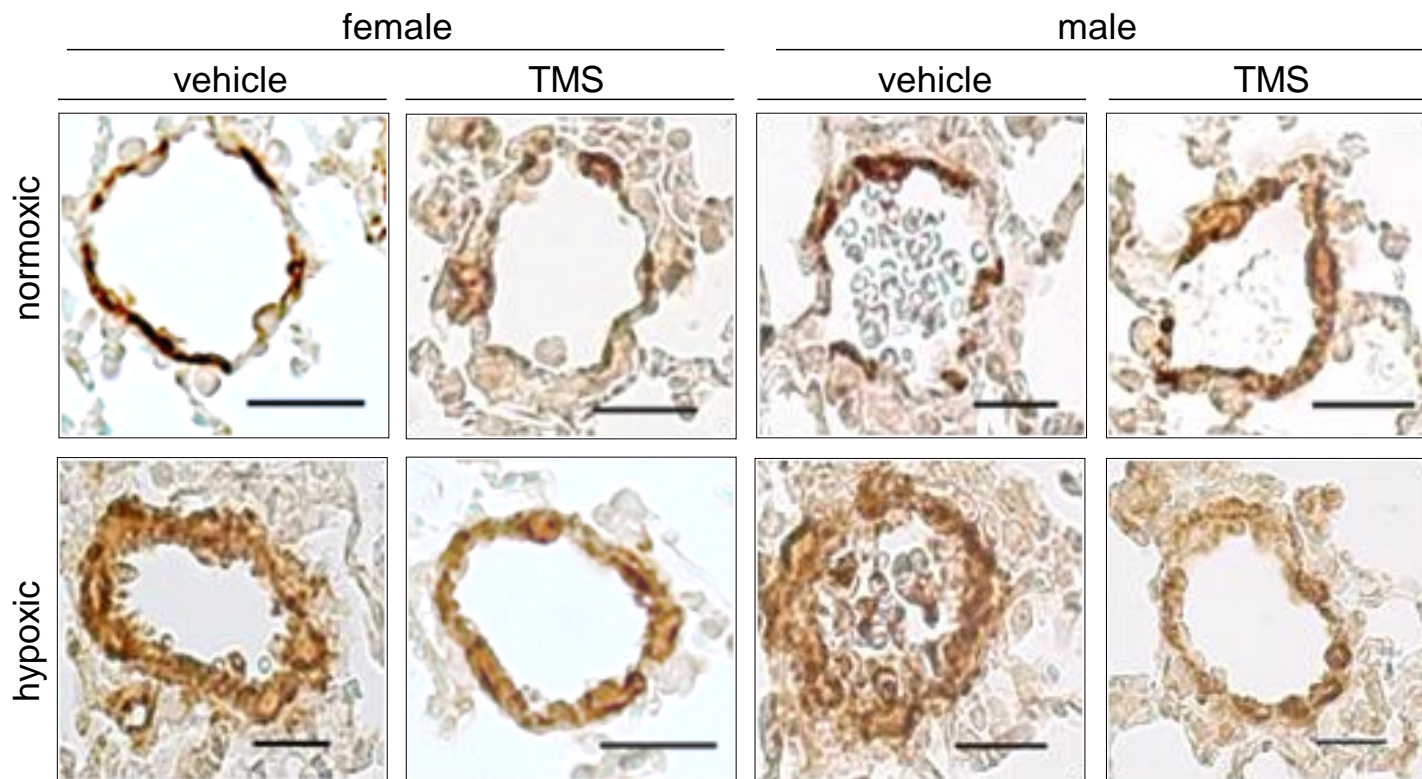


**Figure 3-14 Representative  $\alpha$ -smooth muscle actin–stained pulmonary arteries in normoxic and chronic hypoxic C57BL/6 mice dosed with vehicle- or the CYP1B1 inhibitor 2,3',4,5'-tetramethoxystilbene (TMS)**

Female and male wild-type mice were exposed to hypoxia (10% oxygen) or kept in room air for 2 weeks. Mice were either injected with 3mg/kg/day TMS or vehicle (~5% ethanol in saline) during the 2 week. The degree of vascular muscularisation was visualized by  $\alpha$ -smooth muscle actin ( $\alpha$ -SMA) staining in the distal vasculature.  $\alpha$ -SMA expression was visualized by DAB staining (dark orange/brown stain). Scale bar = 20 $\mu$ m.

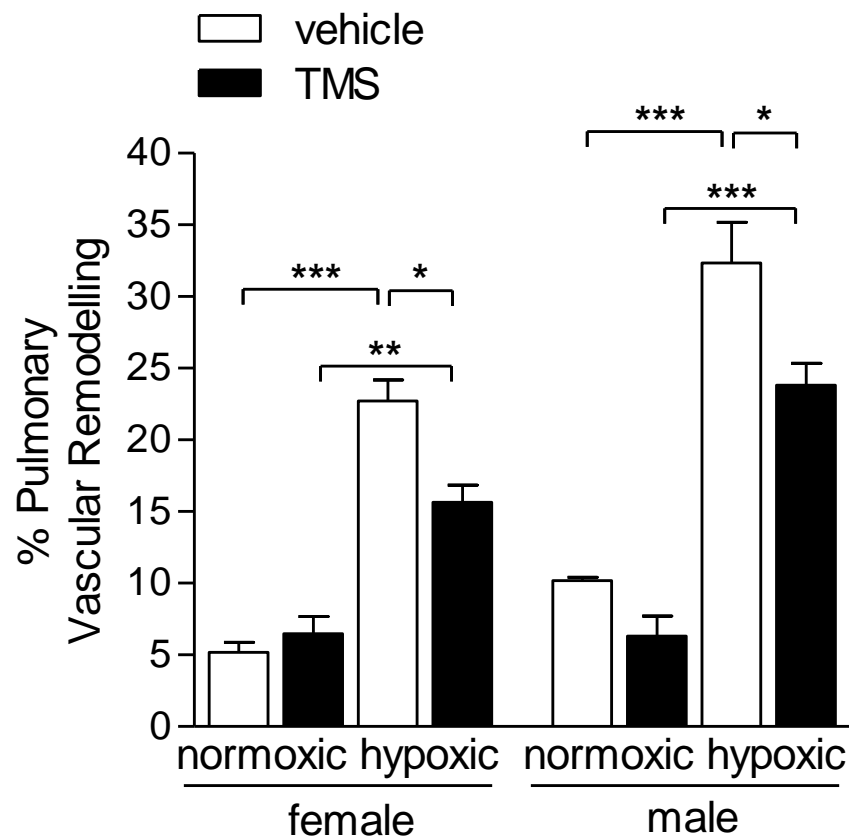


**Figure 3-15 The CYP1B1 inhibitor 2,3',4,5'-tetramethoxystilbene (TMS) attenuates the development of chronic hypoxia-induced pulmonary vascular remodeling**

Female and male wild-type mice were exposed to hypoxia (10% oxygen) or kept in room air for 2 weeks. Mice were either injected with 3mg/kg/day TMS or vehicle (~5% ethanol in saline) during the 2 week study. The degree of pulmonary arterial remodeling was assessed by counting the number of remodeled and non-remodeled arteries in a lung section and expressed as the % of remodeled vessels over the total number of vessels. n=4-7, \*P<0.05, \*\*P<0.01, \*\*\*P<0.001, One-way ANOVA with a Bonferroni's post-hoc test. Data is expressed as the mean ± SEM.

**Table 3-3 Effect of CYP1B1 inhibitor 2,3',4,5'-tetramethoxystilbene (TMS) in normoxic and hypoxic C57BL/6 mice on haemodynamics and phenotypes**

Animal Group	mSAP (mmHg)	mRVP (mmHg)	Heart rate (bpm)	Body Weight (g)
Female Wild-type normoxic	91.07 ± 1.53 (9)	15.71 ± 0.49 (9)	428.2 ± 16.92 (9)	19.40 ± 0.20 (10)
Female TMS normoxic	95.49 ± 1.63 (6)	12.47 ± 0.59 (10)	404.4 ± 14.70 (10)	18.30 ± 0.42 (10)
Female wild-type hypoxic	98.59 ± 2.72 (8)	19.73 ± 1.13* (10)	366.0 ± 21.43 (9)	18.69 ± 0.31 (10)
Female TMS hypoxic	100.70 ± 3.91 (6)	16.01 ± 1.06§ (10)	477.4 ± 21.30§§ (10)	15.66 ± 0.18§§§ (10)
Male wild-type normoxic	100.90 ± 0.76 (8)	13.06 ± 0.89 (7)	441.8 ± 21.21 (8)	26.56 ± 0.51 (10)
Male TMS normoxic	103.02 ± 4.00 (6)	13.00 ± 0.74 (6)	473.4 ± 14.15 (6)	26.31 ± 0.42 (10)
Male wild-type hypoxic	100.50 ± 0.77 (5)	16.26 ± 1.103 (7)	485.5 ± 33.59 (7)	26.14 ± 0.73 (10)
Male TMS hypoxic	107.40 ± 2.10 (7)	14.20 ± 1.01 (6)	439.1 ± 26.09 (8)	24.57 ± 0.39 (10)

Female and male wild-type mice were exposed to hypoxia (10% oxygen) or kept in room air for 2 weeks. Mice were either injected with 3mg/kg/day TMS or vehicle (~5% ethanol in saline) during the 2 week study. Mean systemic arterial pressures (mSAP) were measured by cannulation of the carotid artery. Mean right ventricular pressures (mRVP) were calculated from the right ventricular pressure obtained by right heart catheterisation. n numbers are indicated in brackets. \*P<0.05, \*\*P<0.01 cf. normoxic; §P<0.05, §§§P<0.001 cf. vehicle, One-way ANOVA with a Bonferroni's post-hoc test. Data is expressed as the mean ± SEM.

### 3.2.7 Monocrotaline-induced PH is moderately altered by TMS treatment in male but not female rats

Having demonstrated CYP1B1 as an integrative mediator of hypoxia-induced PH, we wanted to assess its function in a severe inflammatory model of the disease, induced by the pneumotoxin MCT. Assistance was provided for the dosing procedures of this study and the majority of the female *in vivo* component (RVP, RVH and SAP) was carried out by Ms. Katie Hood, Dr. Ian Morecroft, Ms. Margaret Nilsen and Dr. Kirsty Mair. Both females and males develop RVH in response to MCT although this effect is more pronounced in the male rats. No effect was observed in response to TMS treatment in the female rats, yet male rats had a slight, yet non-significant reduction in RVH to a similar level to that observed in the female rats with TMS treatment (Figure 3-16). Here, we report that both female and male rats develop substantial increases in RVSP in response to MCT, and this effect was unaltered by CYP1B1 inhibition (Figure 3-17).

Despite the severity of MCT-induced-PH, this occurs in the absence of the complex pulmonary arteriopathy that is a key feature in human PAH. However, vascular remodeling is present to a much greater extent than what is observed in hypoxic-induced-PH in mice with medial narrowing present. We therefore investigated the extent of pulmonary vascular remodeling in the distal vasculature of these animals. MCT induced substantial increases in arterial remodeling in both male and female rats (Figure 3-19). Although there were no significant effects observed by TMS treatment, the effect of MCT on arterial remodeling when comparing vehicle-TMS to MCT-TMS was non-significant in females, suggesting a moderate effect of TMS treatment in this group. Similarly, in male rats there was less significance when comparing vehicle-TMS with MCT-TMS as compared with vehicle-vehicle to MCT-vehicle. When examining the degree of muscularisation in the distal vasculature, all rats developed neointimal lesions in response to MCT, yet these appeared much more pronounced in the vehicle group compared to TMS treated groups (Figure 3-18). This may account for the improved survival in TMS treated rats (see below).

To determine whether the effects of MCT and TMS were specific to the cardio-pulmonary unit, mSAP were monitored in all groups (Table 3-4). The mSAPs were increased in female rats in response to MCT whereas no effect was observed in male rats. This was unaffected by TMS treatment. MCT reduced the heart rate in male rats and this effect was improved by TMS treatment. No effect was observed in the female rats (Table 3-4). MCT and TMS had no effects on dry uterus + ovary weights (Figure 3-20).

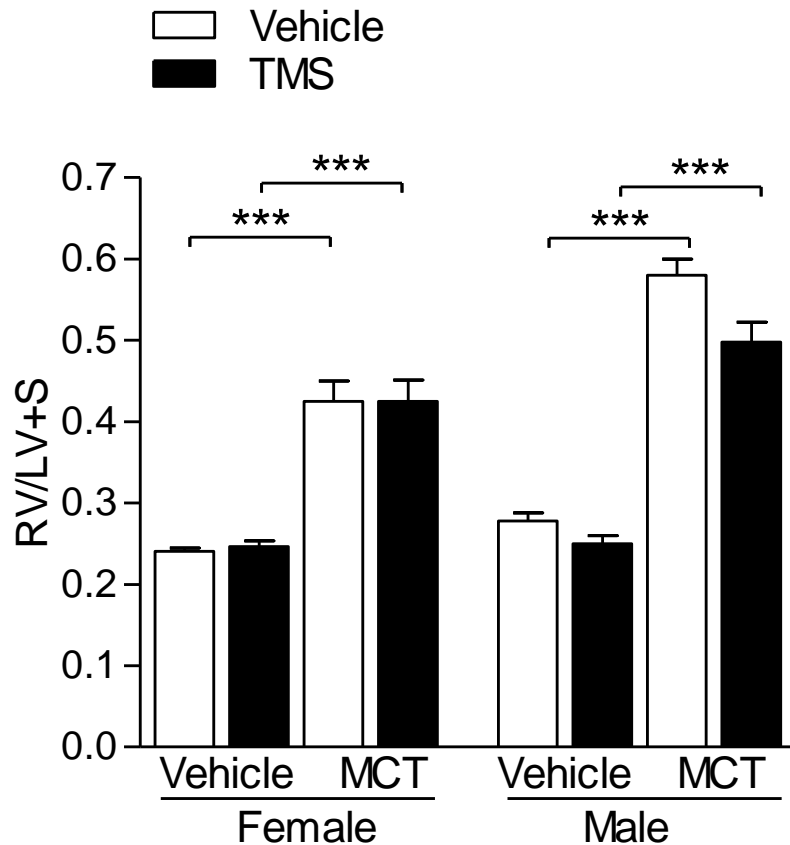


**Figure 3-16 Monocrotaline induces right ventricular hypertrophy and this is unaffected by the CYP1B1 inhibitor 2,3',4,5'-tetramethoxystilbene (TMS)**

Female and male wistar rats were injected with a single injection of monocrotaline (MCT; 20mg/kg) or vehicle (see methods for a detailed description) on day 0. After 2 weeks, rats were injected with 3mg/kg/day TMS or vehicle (~5% ethanol in saline) for a further 2 weeks. Right ventricular hypertrophy (RVH) was assessed by expressing the dry weight of the right ventricle over the left ventricle and septum (RV/LV+S; Fultons index). n=8-16, \*\*\*P<0.001, One-way ANOVA with a Bonferroni's post-hoc test. Data is expressed as the mean ± SEM.

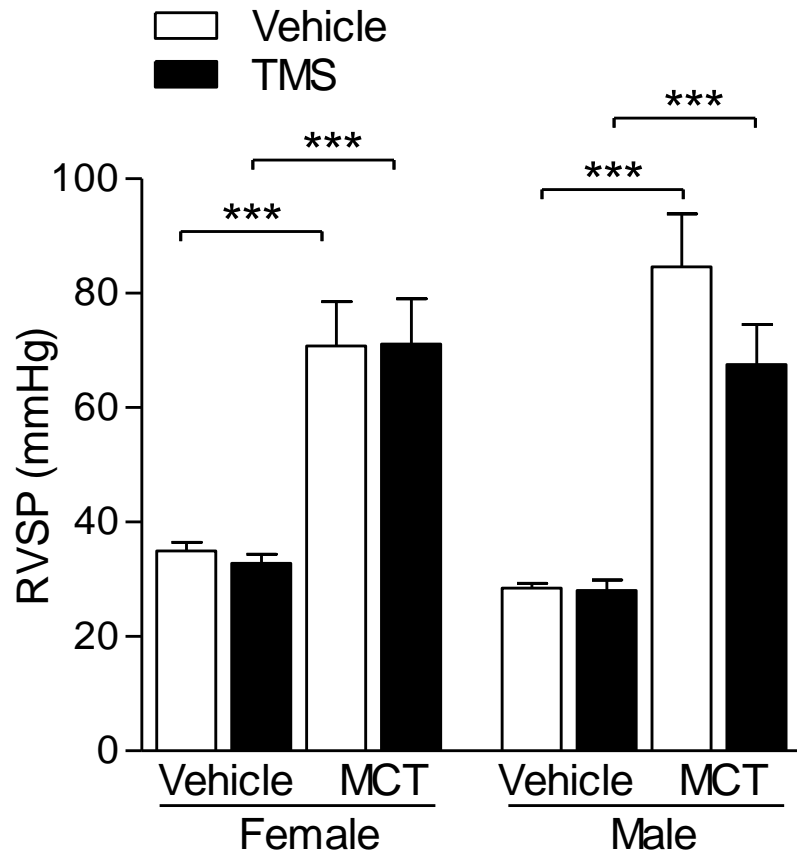


**Figure 3-17 Monocrotaline induces increases in right ventricular pressures and this is unaffected by the CYP1B1 inhibitor 2,3',4,5'-tetramethoxystilbene (TMS)**

Female and male wistar rats were injected with a single injection of monocrotaline (MCT; 20mg/kg) or vehicle (see methods for a detailed description) on day 0. After 2 weeks, rats were injected with 3mg/kg/day TMS or vehicle (~5% ethanol in saline) for a further 2 weeks. Right ventricular systolic pressures (RVSP) were measured in rats by right heart catheterisation through the jugular vein. n=5-11, \*\*\*P<0.001, One-way ANOVA with a Bonferroni's post-hoc test. Data is expressed as the mean  $\pm$  SEM.

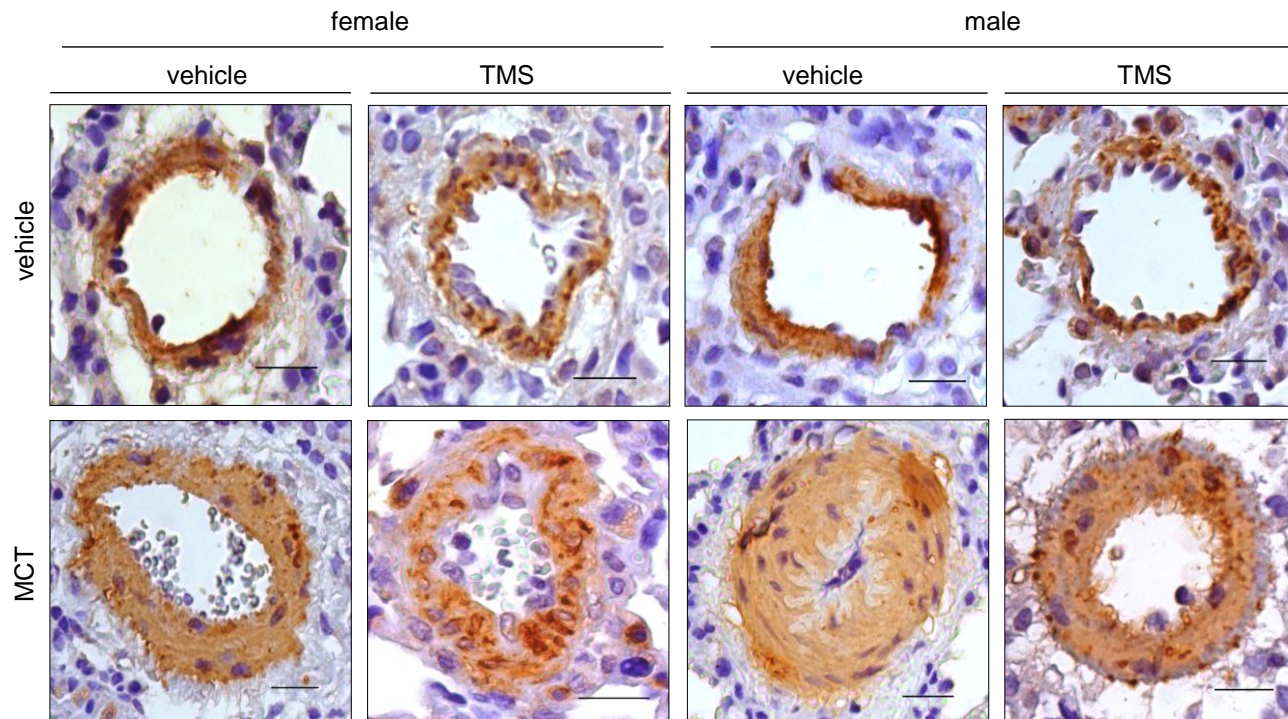


**Figure 3-18 Representative  $\alpha$ -smooth muscle actin–stained pulmonary arteries in monocrotaline (MCT) rats treated with vehicle- or the CYP1B1 inhibitor 2,3',4,5'-tetramethoxystilbene (TMS)**

Female and male wistar rats were injected with a single injection of monocrotaline (MCT; 20mg/kg) or vehicle (see methods for a detailed description) on day 0. After 2 weeks, rats were injected with 3mg/kg/day TMS or vehicle (~5% ethanol in saline) for a further 2 weeks. The degree of vascular muscularisation was visualized by  $\alpha$ -smooth muscle actin ( $\alpha$ -SMA) staining in the distal vasculature.  $\alpha$ -SMA expression was visualised by DAB staining (dark orange/brown stain). Sections have been counterstained with haematoxylin and eosin. Scale bar = 20 $\mu$ m

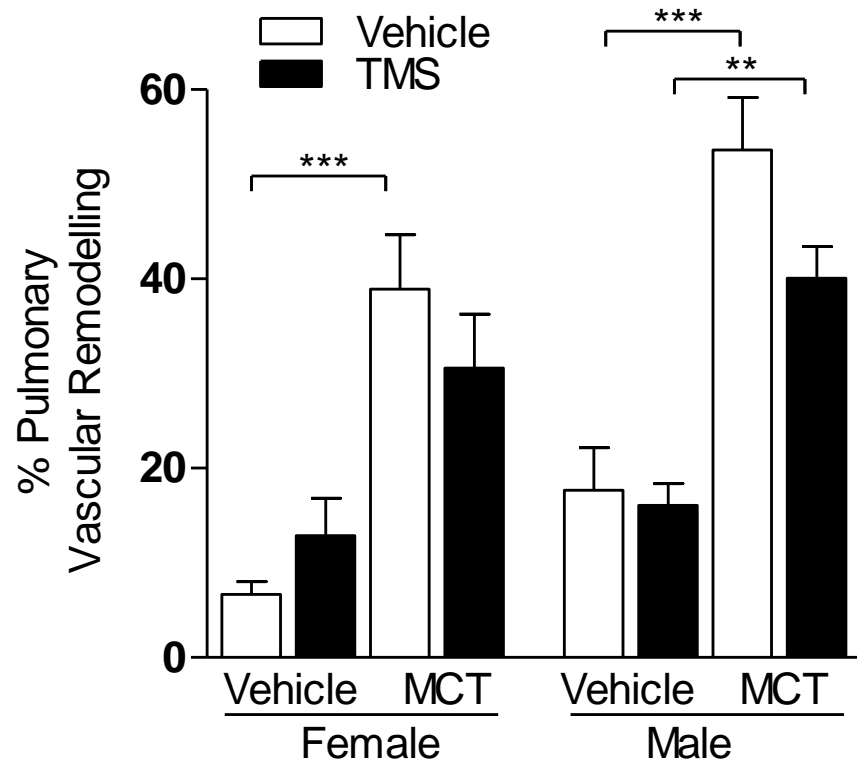


**Figure 3-19 Monocrotaline increases pulmonary vascular remodeling and this is unaffected by the CYP1B1 inhibitor 2,3',4,5'-tetramethoxystilbene (TMS)**

Female and male wistar rats were injected with a single injection of monocrotaline (MCT; 20mg/kg) or vehicle (see methods for a detailed description) on day 0. After 2 weeks, rats were injected with 3mg/kg/day TMS or vehicle (~5% ethanol in saline) for a further 2 weeks. The degree of pulmonary arterial remodeling was assessed by counting the number of remodeled and non-remodeled arteries in a lung section and expressed as the % of remodeled vessels over the total number of vessels. n=6-7, \*\*P<0.01, \*\*\*P<0.001, One-way ANOVA with a Bonferroni's post-hoc test. Data is expressed as the mean ± SEM.

**Table 3-4 Phenotypic data from monocrotaline wistar rates treated with vehicle or the CYP1B1 inhibitor 2,3',4,5'-tetramethoxystilbene (TMS)**

Animal Group	mSAP (mmHg)	mRVP (mmHg)	Heart rate (bpm)	Body Weight (g)
Female vehicle-vehicle	103.6 ± 5.001 (8)	12.71 ± 1.247 (7)	406.9 ± 10.78 (8)	191.4 ± 4.63 (9)
Female vehicle-TMS	109.6 ± 7.025 (6)	12.95 ± 1.149 (6)	402.6 ± 14.19 (6)	195.3 ± 3.75 (9)
Female MCT-vehicle	126.8 ± 10.15 (7)	27.52 ± 3.177** (8)	414.4 ± 6.46 (8)	209.3 ± 4.46 (12)
Female MCT-TMS	122 ± 8.243 (7)	30.62 ± 3.661*** (11)	393.7 ± 8.64 (12)	191.2 ± 4.40 (11)
Male vehicle-vehicle	98.38 ± 2.548 (9)	11.52 ± 0.2759 (8)	397.2 ± 8.41 (9)	301.3 ± 9.74 (9)
Male vehicle-TMS	106.6 ± 4.284 (9)	11.65 ± 0.4779 (7)	398.2 ± 18.43 (9)	293.2 ± 9.72 (9)
Male MCT-vehicle	83.86 ± 1.716 (5)	36.65 ± 1.143*** (5)	301.8 ± 14.06*** (7)	298.9 ± 10.71 (9)
Male MCT-TMS	95.71 ± 5.047 (11)	31.83 ± 2.6*** (8)	360.1 ± 12.07§ (11)	280.0 ± 6.96 (12)

Female and male wistar rats were injected with a single injection of monocrotaline (MCT; 20mg/kg) or vehicle (see methods for a detailed description) on day 0. After 2 weeks, rats were injected with 3mg/kg/day TMS or vehicle (~5% ethanol in saline) for a further 2 weeks. Mean systemic arterial pressures (mSAP) were measured by cannulation of the carotid artery. Mean right ventricular pressures (mRVP) were calculated from the right ventricular pressure obtained by right heart catheterisation. n numbers are indicated in brackets. \*\*P<0.01; \*\*\*P<0.001 c.f. vehicle control; §P<0.05 c.f. MCT-V, One-way ANOVA with a Bonferroni's post-hoc test. Data is expressed as the mean ± SEM.

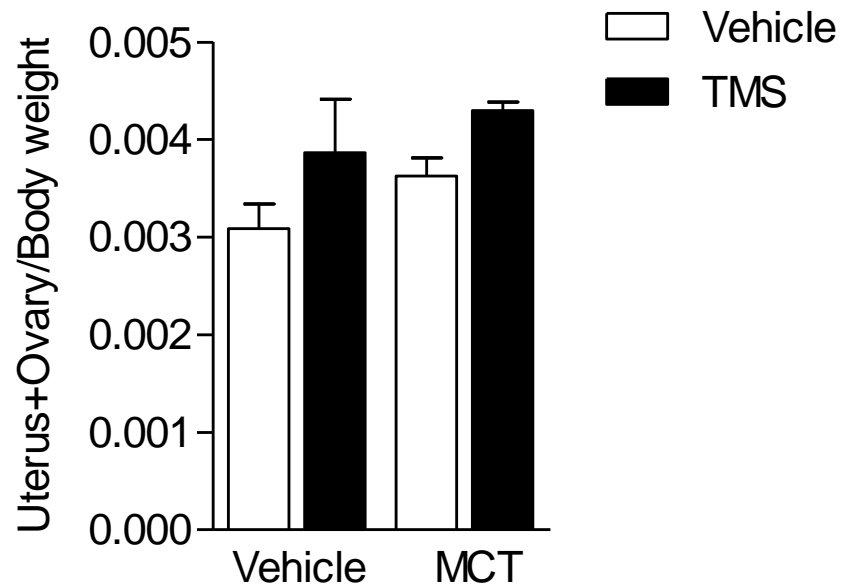


**Figure 3-20 Monocrotaline and CYP1B1 inhibition with 2,3',4,5'-tetramethoxystilbene (TMS) on uterus+ovary weights/body weights**

Female and male wistar rats were injected with a single injection of monocrotaline (MCT; 20mg/kg) or vehicle (see methods for a detailed description) on day 0. After 2 weeks, rats were injected with 3mg/kg/day TMS or vehicle (~5% ethanol in saline) for a further 2 weeks. The dry weight of the uterus and ovaries were expressed over the body weight. n=5-9.

### 3.2.8 Survival is improved in rats treated with TMS

Due to the severity of the MCT model, mortality rates increase substantially after about 20 days post induction, from suspected right heart failure. Mortalities were reported in male rats treated with MCT after 23 days and after 26 days in female rats. TMS treatment delayed the onset of death in male rats and completely prevented this effect in female rats (Figure 3-21).

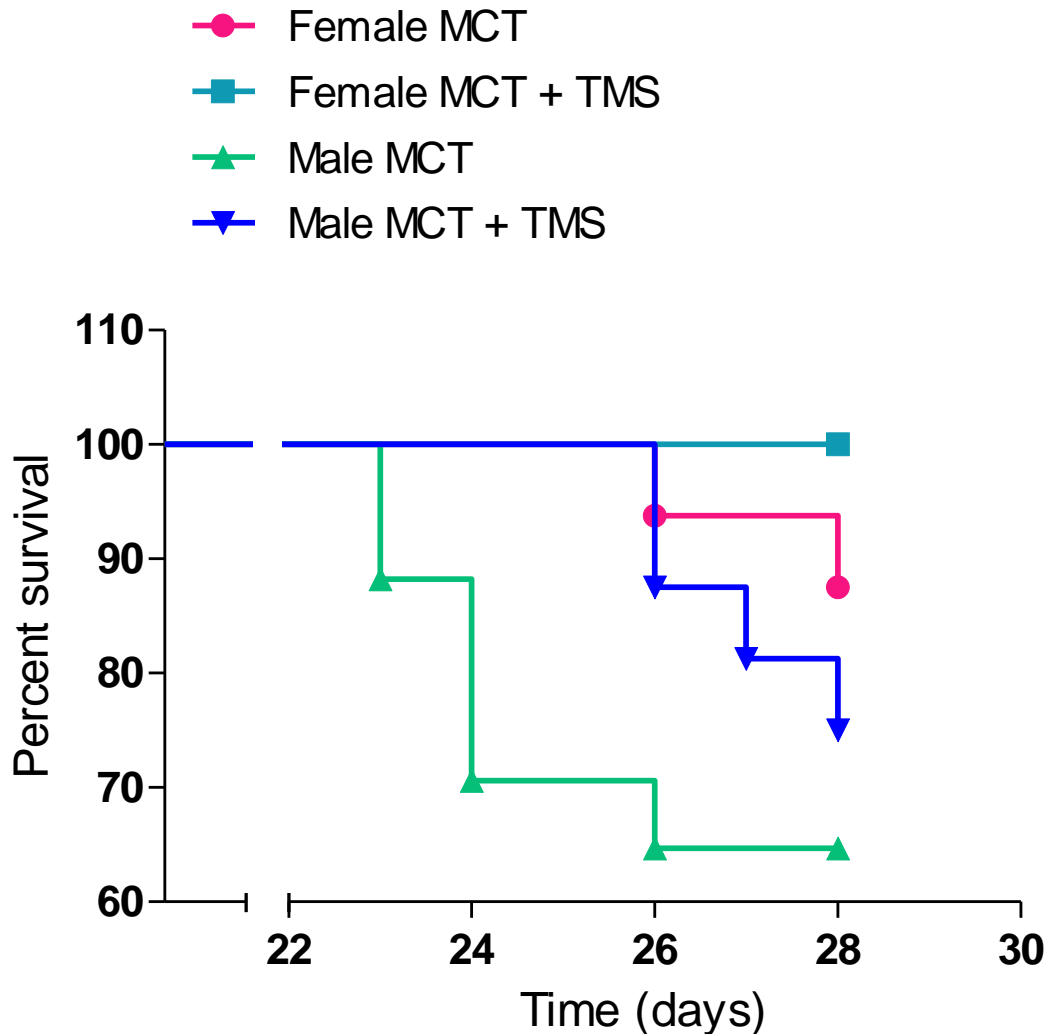


**Figure 3-21 CYP1B1 inhibition with 2,3',4,5'-tetramethoxystilbene (TMS) improves survival in monocrotaline treated rats as assessed by Kaplan-Meier survival analysis**

Female and male wistar rats were injected with a single injection of monocrotaline (MCT; 20mg/kg) or vehicle (see methods for a detailed description) on day 0. After 2 weeks, rats were injected with 3mg/kg/day TMS or vehicle (~5% ethanol in saline) for a further 2 weeks. Each group had 16 rats at the start of the experiment.

### 3.2.9 Estrogen synthesis and metabolism is dysregulated in female SERT+ mice

We have previously reported evidence for dysregulated estrogen metabolism in hypoxic-associated PH and in human PAH (Chapter 3 and White et al., 2012). Here, we provide evidence that estrogen metabolism is dysregulated in female mice that overexpress the SERT. This model is unique in that it displays female susceptibility via the effects of  $17\beta$ -E2 (White et al., 2011b). Firstly, we demonstrated that the expression of the estrogen-synthesizing enzyme, aromatase is increased in the lungs of female SERT+ mice compared to wild-type mice (Figure 4 1b). Based on this observation, we next determined the levels of endogenous  $17\beta$ -E2 in the lungs of these mice. Despite increased protein expression of aromatase, whole lung levels of  $17\beta$ -E2 were unchanged (Figure 4 1b)

$17\beta$ -E2 can undergo further metabolism via activity of CYP enzymes or may be interconverted to E1 by activity of  $17\beta$ -HSD1. Previously we identified a critical role for CYP1B1 in PH pathogenesis (Chapter 3 and White et al., 2012). Furthermore the expression of CYP1B1 has been reported as increased in the proximal pulmonary arteries from female SERT+ mice at 2 months of age (when no PH phenotype is evident) (White et al., 2011a). As SERT+ mice do not develop the PH phenotype until 5 months of age, we wished to determine whether the expression of CYP1B1 was altered at this age. We studied the distal section of the lung as most of the key pathological changes associated with PH occur within the distal pulmonary arteries (Yuan & Rubin, 2005). CYP1B1 mRNA and protein expression was increased in the lungs of female SERT+ mice (Figure 4 2)

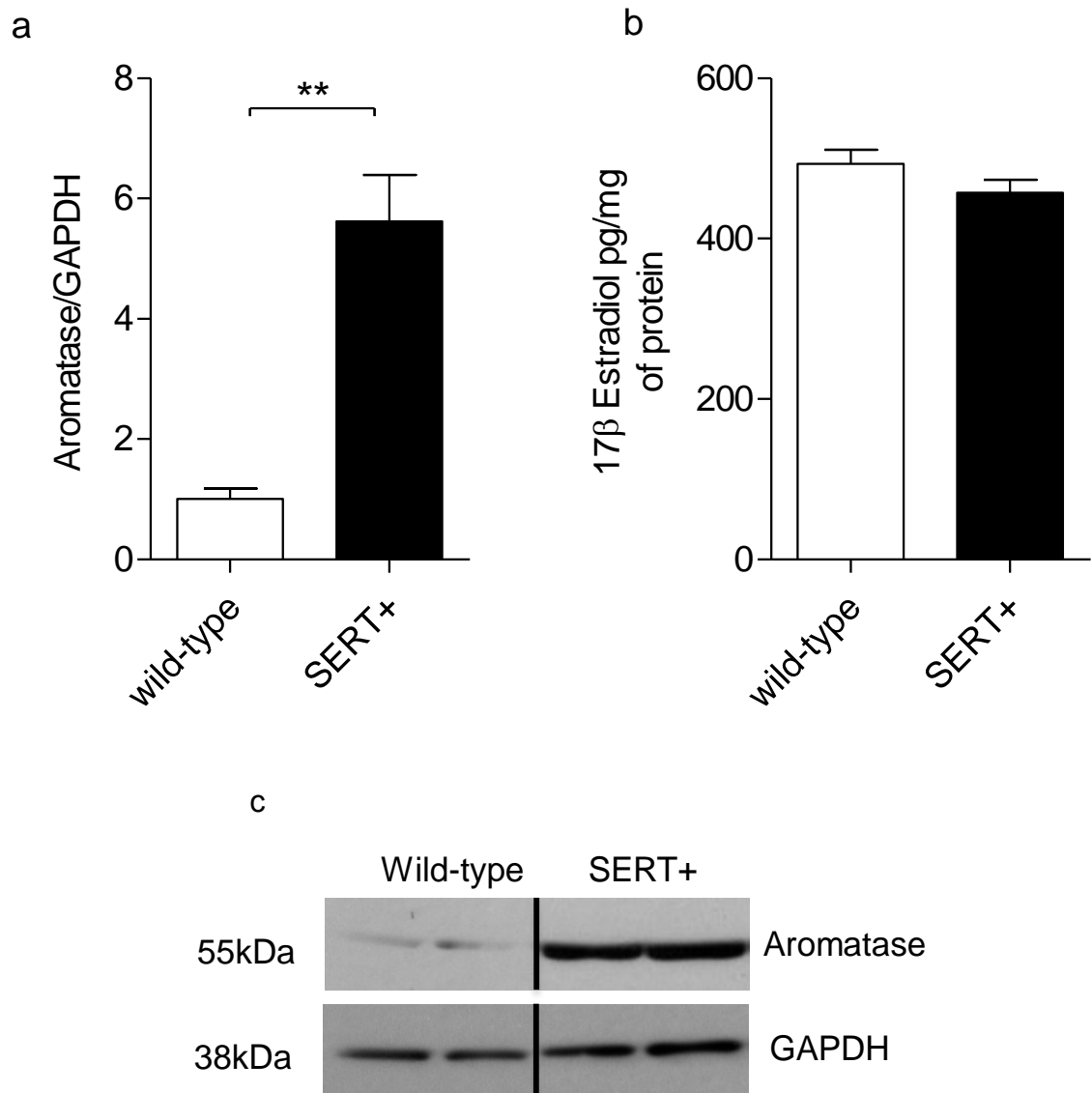


**Figure 3-22 Overexpression of SERT+ on aromatase expression and 17β-estradiol concentrations in whole lung homogenates**

5-6 month old female wild-type (C57BL/6 x CBA) and SERT+ mice lung homogenates were analyzed for aromatase expression and concentrations of 17β-estradiol (17β-E2). Western blot and densitometric analysis of aromatase expression. GAPDH was used as the internal loading control (a, c). Full western blots are shown in appendix 1. ELISA analysis of 17β-E2 concentrations in whole lung homogenates. 400μg of protein was loaded per well and assayed in duplicate. n=4-5, \*\*P<0.01, t-test. Data is expressed as the mean ± SEM

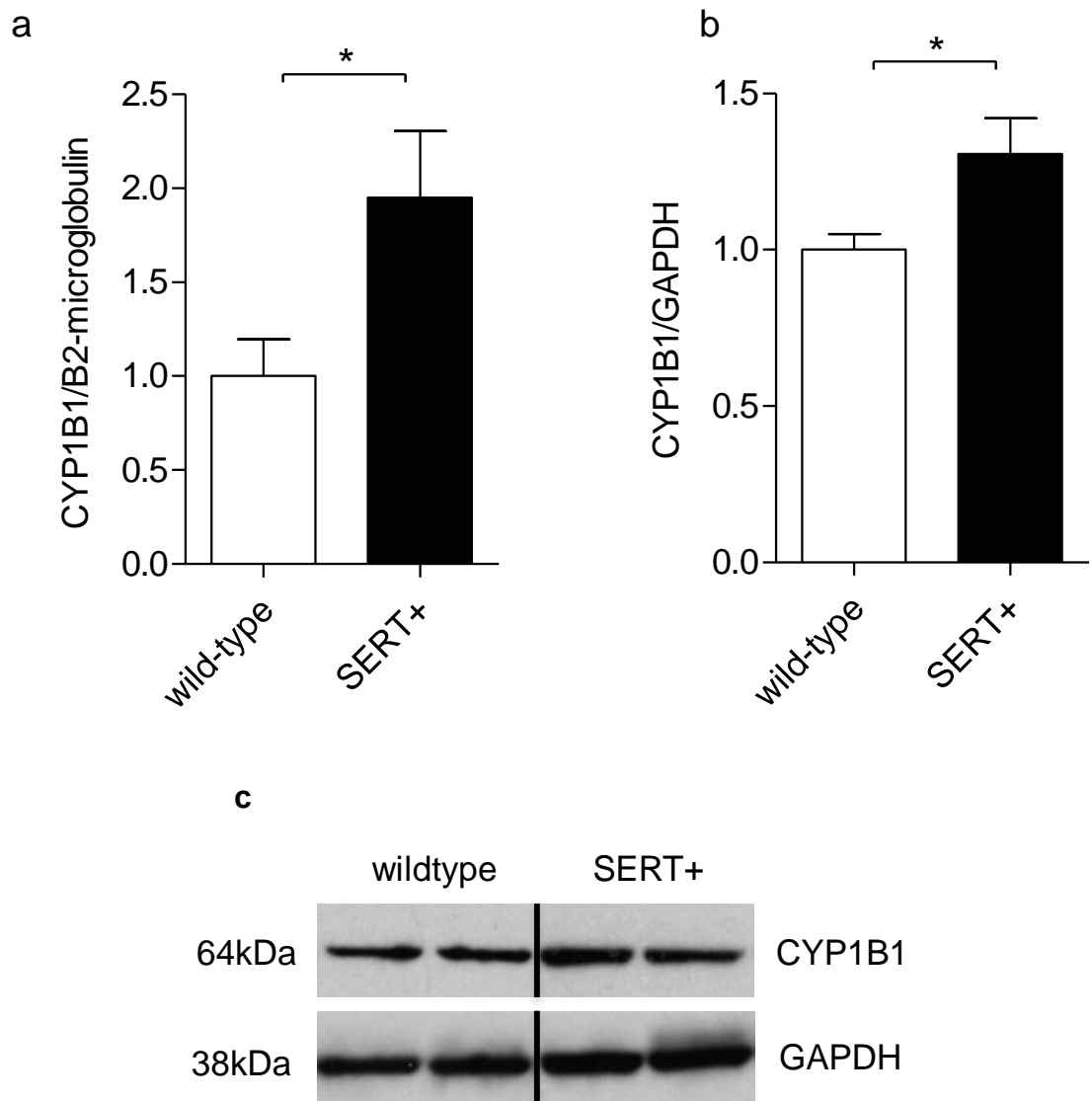


**Figure 3-23 Lung CYP1B1 expression is increased in female SERT+ mice**

5-6 month old female wild-type (C57BL/6 x CBA) and SERT+ mice lung homogenates were analyzed for CYP1B1 expression. qRT-PCR for mRNA of CYP1B1 expression normalized to B2-microglobulin (a). Western blot and densitometric analysis of CYP1B1 expression in whole lung samples from female wild-type and SERT+ mice. GAPDH was used as the internal loading control (b-c). Full western blots are shown in appendix 1. n=5-6, \*P<0.05, t-test. Data is expressed as the mean  $\pm$  SEM

### **3.2.10 Inhibition of CYP1B1 regresses pulmonary hypertension in female SERT+ mice**

Female SERT+ mice exhibit an established PH phenotype at 5-6 months of age (White *et al.*, 2011a). We have previously reported that CYP1B1 is involved in the development of both hypoxic and SU-hypoxic induced PH. Here, we provide evidence that CYP1B1 influences the disease pathogenesis in a serotonin/estrogen-dependent model of PH.

Female SERT+ mice have elevated RVSP compared to age-matched wild-type controls and this effect is exaggerated by exposure to chronic hypoxia. Inhibition of CYP1B1 in these mice reverses these elevated pressures under both normoxic and hypoxic conditions (Figure 3-24 -Figure 3-25). Despite elevated RVSP, female SERT+ mice do not develop RVH measured by RV/LV+S. However, on exposure to hypoxia, female SERT+ mice develop exaggerated RVH compared to wild-type mice. Inhibition of CYP1B1 with TMS (1.5mg/kg/day for 14 days) did not affect RVH in either normoxic or hypoxic conditions (Figure 3-26). Pulmonary vascular remodeling was increased in the distal vasculature in female SERT+ mice compared to wild-type mice in both normoxic and hypoxic conditions. This effect was completely reversed by CYP1B1 inhibition (Figure 3-28). In line with this, pulmonary arterial muscularisation was increased in female SERT+ mice and this was reduced by TMS treatment under both normoxic and hypoxic conditions (Figure 3-27) mSAP were unchanged by SERT overexpression, CYP1B1 inhibition and/or hypoxia (Table 3-5). Female SERT+ mice have a reduced heart rate, which is returned to rates similar to wild-type mice by TMS therapy. No other effects on heart rate were reported (Table 3-5). Interestingly, female SERT+ mice had dramatically lower body weights under both normoxic and hypoxic conditions.

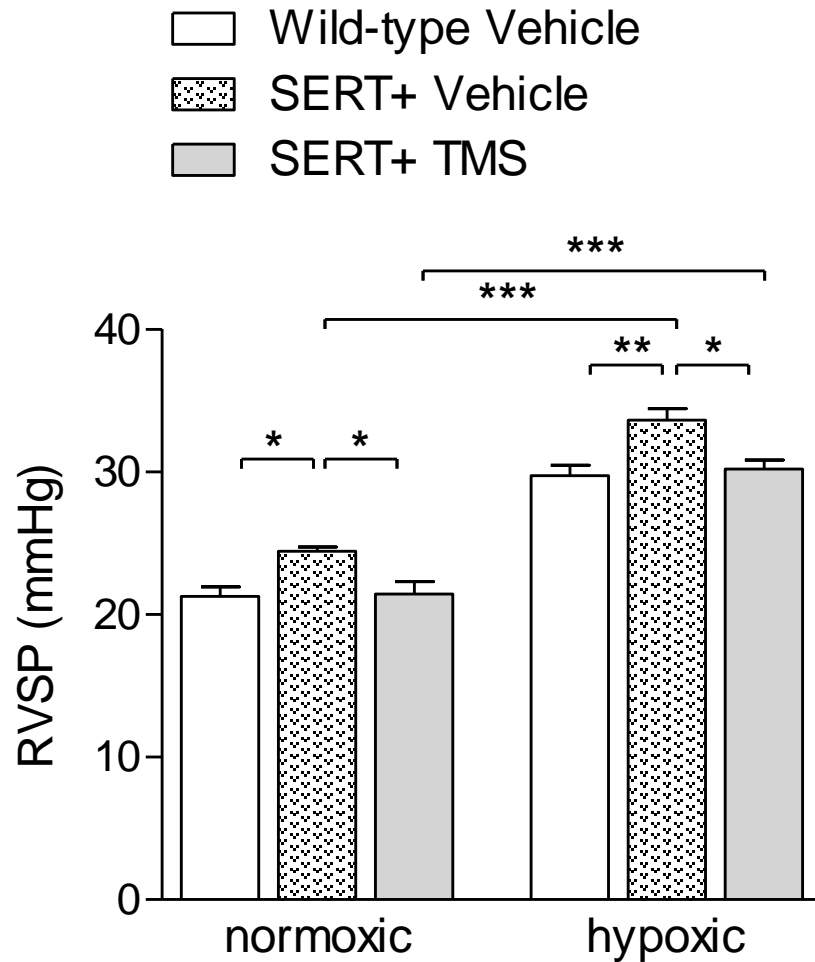


**Figure 3-24 SERT mice have increased right ventricular systolic pressures which are exacerbated by hypoxia and reversed by CYP1B1 inhibition with 2,3',4,5'-tetramethoxystilbene (TMS)**

Female wild-type C57BL/6 x CBA and SERT+ mice were exposed to hypoxia (10% oxygen) or kept in room air for 2 weeks. SERT+ mice were either injected with 1.5mg/kg/day TMS or vehicle (~5% ethanol in saline) during the 2 week study. Right ventricular systolic pressures (RVSP) were assessed by right heart catheterisation. n=7-10, \*P<0.05; \*\*P<0.01; \*\*\*P<0.001, One-way ANOVA with a Bonferroni's post-hoc test. Data is expressed as the mean  $\pm$  SEM.

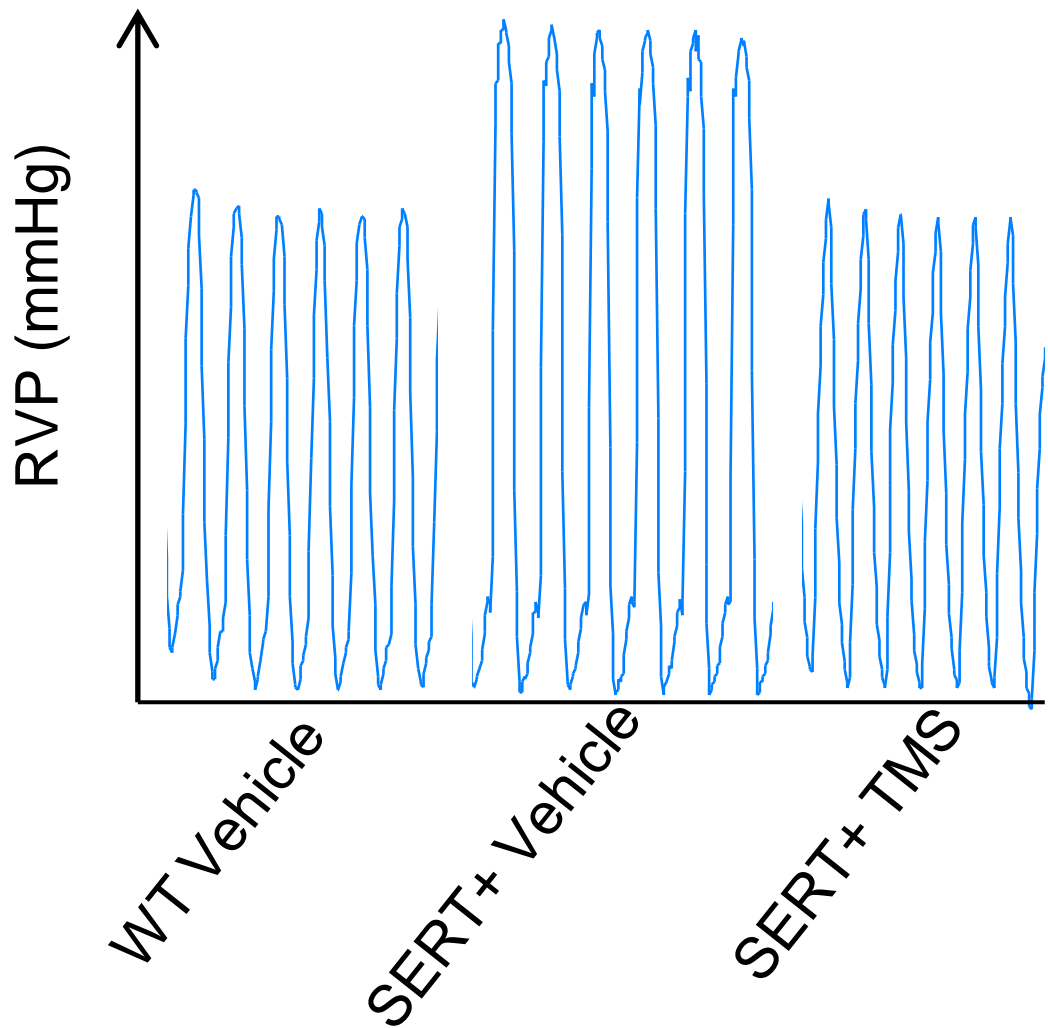


**Figure 3-25 Representative right ventricular pressure traces from wild-type, SERT+ and SERT+ mice treated with the CYP1B1 inhibitor 2,3',4,5'-tetramethoxystilbene (TMS)**

Representative right ventricular pressures from 5-6 month old female wild-type C57BL/6 x CBA, SERT+ mice and SERT+ mice treated with the CYP1B1 inhibitor TMS (1.5mg/kg/day) for 2 weeks. Traces were selected at random from each group.

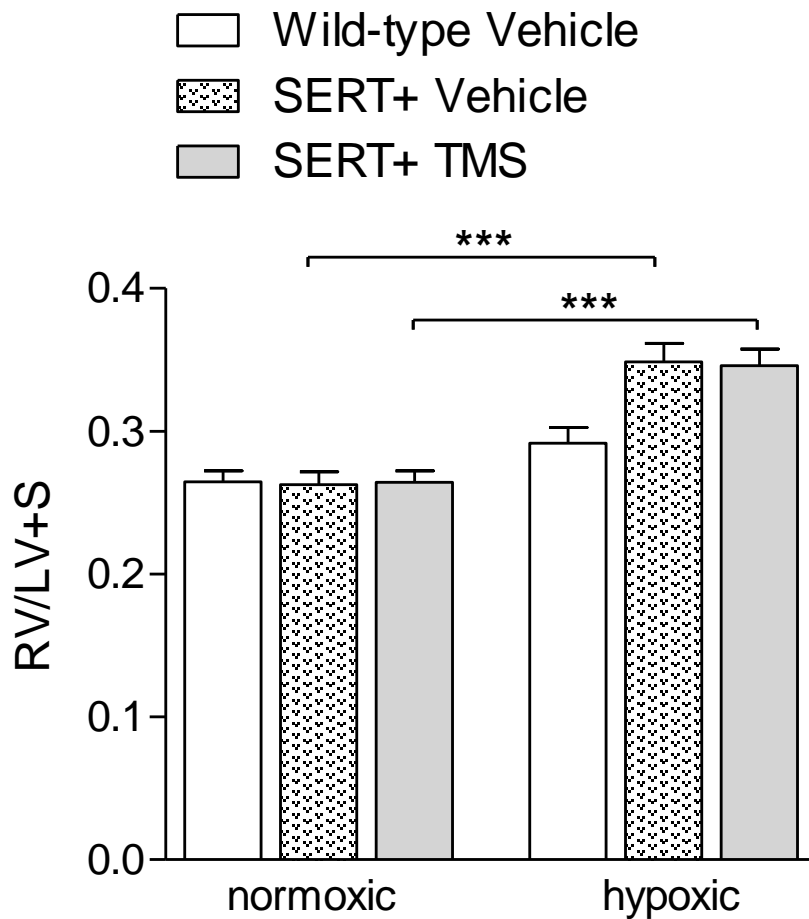


**Figure 3-26 Right ventricular hypertrophy in female SERT+ mice in normoxic and hypoxic conditions and the effect of CYP1B1 inhibition with 2,3',4,5'-tetramethoxystilbene (TMS)**

Female wild-type C57BL/6 x CBA and SERT+ mice were exposed to hypoxia (10% oxygen) or kept in room air for 2 weeks. SERT+ mice were either injected with 1.5mg/kg/day TMS or vehicle (~5% ethanol in saline) during the 2 week study. Right ventricular hypertrophy (RVH) was assessed by expressing the dry weight of the right ventricle over the left ventricle and septum (RV/LV+S; Fultons index). n=9-11, \*\*\*P<0.001, One-way ANOVA with a Bonferroni's post-hoc test. Data is expressed as the mean  $\pm$  SEM.

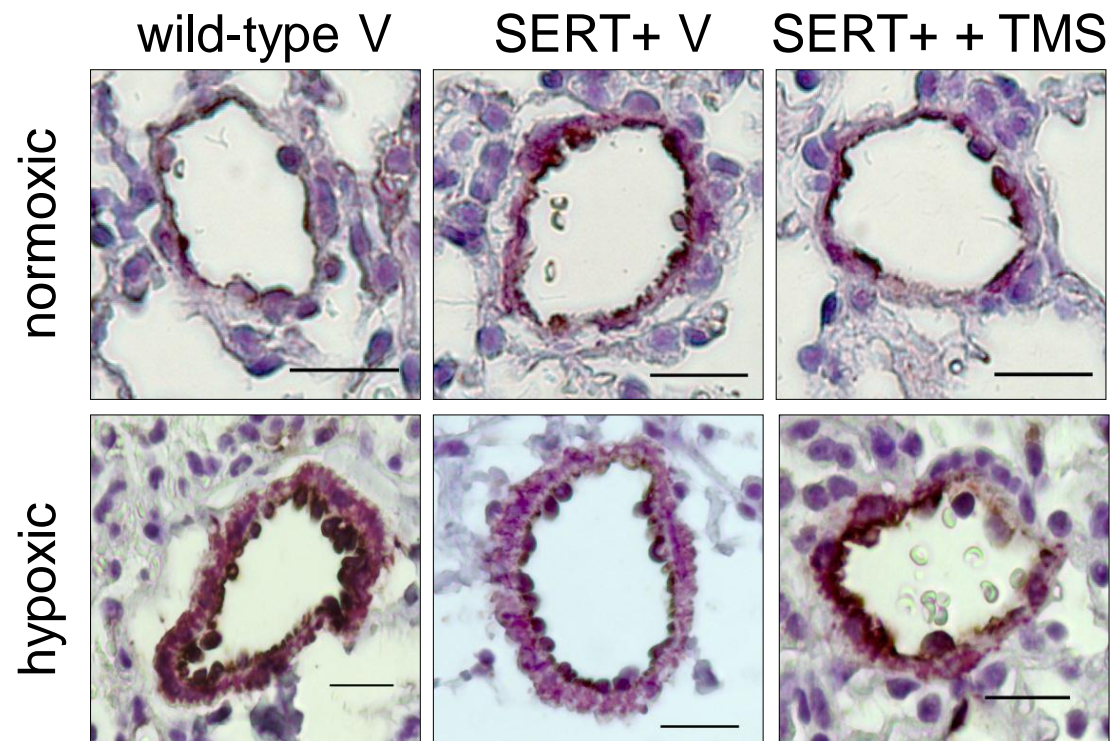


**Figure 3-27 Representative  $\alpha$ -smooth muscle actin- and von-Willebrand stained pulmonary arteries in wild-type and SERT+ mice treated with vehicle- or the CYP1B1 inhibitor 2,3',4,5'-tetramethoxystilbene (TMS)**

Female wild-type C57BL/6 x CBA and SERT+ mice were exposed to hypoxia (10% oxygen) or kept in room air for 2 weeks. SERT+ mice were either injected with 1.5mg/kg/day TMS or vehicle (~5% ethanol in saline) during the 2 week study. Pulmonary arterial endothelial cells and smooth muscle cells are visualised by von Willebrand staining (DAB; dark brown colour) and  $\alpha$  smooth muscle actin ( $\alpha$ -SMA; VIP, pink/purple staining), respectively. V=vehicle. Scale bar = 20 $\mu$ m

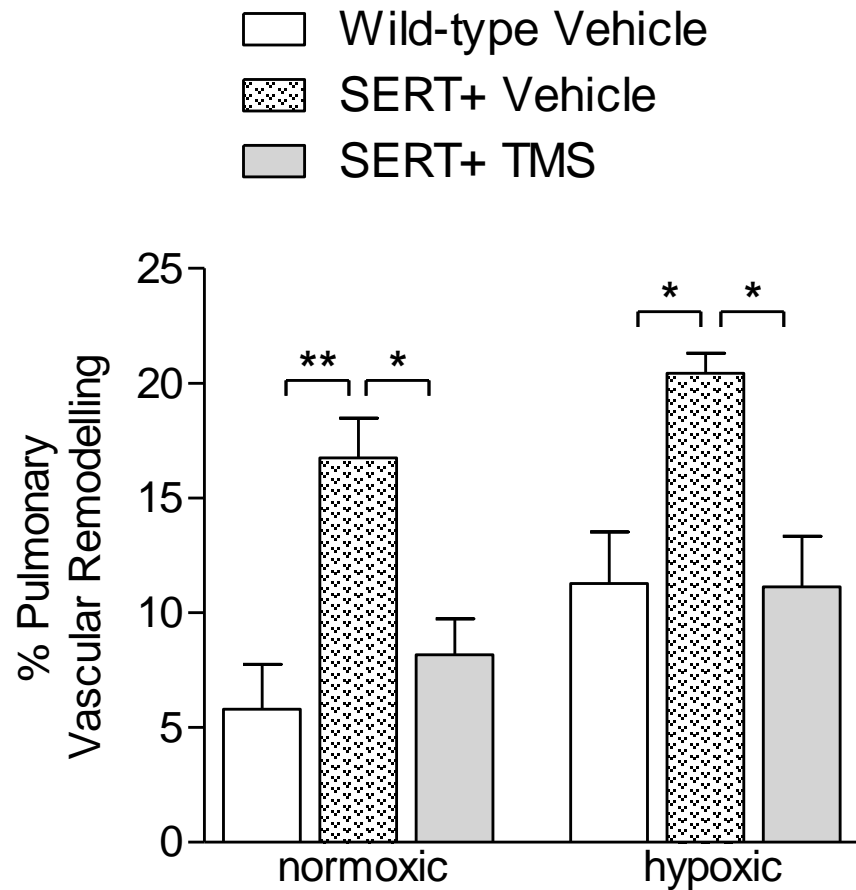


**Figure 3-28 SERT mice have increased pulmonary vascular remodeling and this is reversed by CYP1B1 inhibition with 2,3',4,5'-tetramethoxystilbene (TMS)**

Female wild-type C57BL/6 x CBA and SERT+ mice were exposed to hypoxia (10% oxygen) or kept in room air for 2 weeks. SERT+ mice were either injected with 1.5mg/kg/day TMS or vehicle (~5% ethanol in saline) during the 2 week study. The degree of pulmonary arterial remodeling was assessed by counting the number of remodeled and non-remodeled arteries in a lung section and expressed as the % of remodeled vessels over the total number of vessels. n=4-6, \*P<0.05; \*\*P<0.01, One-way ANOVA with a Bonferroni's post-hoc test. Data is expressed as the mean  $\pm$  SEM.

**Table 3-5 Effect of SERT overexpression, hypoxia and TMS on mean systemic arterial pressures and heart rate**

Animal Group	mSAP (mmHg)	mRVP (mmHg)	Heart rate (bpm)	Body Weight (g)
Wild-type vehicle normoxic	76.99 ± 2.64 (7)	11.84 ± 0.73 (8)	427.70 ± 6.79 (9)	26.31 ± 1.14 (9)
SERT+ vehicle normoxic	85.16 ± 3.82 (10)	13.99 ± 0.56 (7)	322.80 ± 18.22§ (7)	20.23 ± 0.80§§§ (8)
SERT+ TMS normoxic	90.49 ± 4.58 (9)	13.49 ± 0.62 (9)	395.30 ± 21.37 (9)	17.96 ± 0.98 (10)
Wild-type vehicle normoxic	85.63 ± 2.35 (8)	18.10 ± 0.61*** (10)	415.60 ± 29.16 (10)	25.01 ± 0.82 (10)
SERT+ vehicle hypoxic	92.13 ± 5.45 (6)	16.20 ± 0.73 (10)	405.40 ± 17.15 (9)	17.87 ± 0.53§§§ (10)
SERT+ TMS hypoxic	85.98 ± 2.85 (6)	16.00 ± 0.43 (9)	395.00 ± 24.37 (10)	18.16 ± 0.48 (10)

Female wild-type C57BL/6 x CBA and SERT+ mice were exposed to hypoxia (10% oxygen) or kept in room air for 2 weeks. SERT+ mice were either injected with 1.5mg/kg/day TMS or vehicle (~5% ethanol in saline) during the 2 week study. Mean systemic arterial pressures (mSAP) were measured by cannulation of the carotid artery. Mean right ventricular pressures (mRVP) were calculated from the right ventricular pressure obtained by right heart catheterisation. n numbers are indicated in brackets. \*\*\*P<0.001 vs. normoxic control, §P<0.05, §§§P<0.001 vs wild-type control.

### 3.3 Discussion

The incidence of IPAH and HPAH is more common in women than in men suggesting that estrogens and/or their metabolites may be integrated in the pathogenesis of PAH. Whilst protective effects of  $17\beta$ -E2 have been reported in both hypoxic and MCT-induced PH (Lahm *et al.*, 2012;Umar *et al.*, 2011;Xu *et al.*, 2010), our present findings suggest that altered estrogen metabolism by up-regulation of CYP1B1 influences the development of PAH in both sexes. We show that CYP1B1 expression is increased in both experimental and clinical pulmonary vascular disease. Moreover, we provide the first unique evidence that estrogen metabolism by CYP1B1 is involved in the development of experimental PH. The increased cellular expression of CYP1B1 in the pulmonary arteries of patients with PAH suggests that its activity may be pertinent to disease pathogenesis and illustrates a potential attractive therapeutic target in this thus far un-curable cardiovascular disease.

Hypoxia is a key mediator in PAH. Thus we wished to investigate the crude effects of oxygen deprivation on the estrogen-metabolic axis in healthy hPASMCs. Following a 24 hour hypoxic exposure,  $17\beta$ -HSD1 and CYP1B1 protein expression were increased, whilst no effects were observed in COMT expression (Figure 3-1). This suggests that elevated pathogenic metabolism of  $17\beta$ -E2 via CYP1B1 may play a role in the development of PAH. Furthermore, increased expression of  $17\beta$ -HSD1 suggests increased conversion of the less active E1 to the more active  $17\beta$ -E2, which can then be further metabolised by CYP1B1.

Given that hypoxia increased CYP1B1 expression in a homogenous population of hPASMCs, we next investigated the effects of chronic hypobaric hypoxia for 14 days on CYP1B1 expression in murine pulmonary arteries. Here, we show that CYP1B1 expression was consistently up-regulated in both male and female mice by hypoxia (Figure 3-2). In addition, combined VEGF-R inhibition with hypoxia for 21 days also increased CYP1B1 expression in the distal pulmonary arteries of both male and female mice (Figure 3-3). Importantly, CYP1B1 expression was also increased in both male and female pulmonary arteries from patients with IPAH and HPAH (Figure 3-4 - Figure 3-5). CYP1B1 expression was localised in both endothelial and smooth muscle cells (Figure 3-5). Furthermore, CYP1B1 protein and RNA expression is also increased in pre-clinical and human PAH (White *et al.*, 2011a;White *et al.*, 2012).

Given the profound vascular expression of CYP1B1, we next wished to investigate the role of CYP1B1 on the development of PAH in animal models of PAH. We assessed the development of hypoxia-induced PH in CYP1B1<sup>-/-</sup> mice (Figure 3-6 - Figure 3-10) and also examined the effect of chronic inhibition with the selective and potent CYP1B1 inhibitor, TMS (Figure 3-12 - Figure 3-15). Hypoxia-induced increases in RVSP, RVH, pulmonary vascular remodeling and pulmonary intra-arterial vasoconstriction were attenuated in male CYP1B1<sup>-/-</sup> mice. In contrast, RVH was the only PAH parameter that was attenuated in female CYP1B1<sup>-/-</sup> mice in response to chronic hypoxia. CYP1B1 is expressed during embryonic development and is constitutively expressed in several adult tissues (Choudhary *et al.*, 2003). This highlights a critical role of this enzyme and suggests that genetic deletion of CYP1B1 may result in compensatory effects, which may be necessary considering the importance of this enzyme in xenobiotic metabolism. We therefore wished to investigate the effects of the selective and potent CYP1B1 inhibitor, TMS in the hypoxic model of PH to determine if the effects of selective CYP1B1 inhibition were different from CYP1B1 gene knockout. Additionally, we wanted to assess the therapeutic potential of TMS therapy in PAH. We demonstrated that inhibition of TMS attenuated the development of hypoxia-induced PH in both male and female mice, as assessed by RVSP, RVH and pulmonary vascular remodeling.

Although, hypoxia-induced PH is a useful pre-clinical model of PAH, it fails to recapitulate the complex arteriopathy that is seen in human PAH. In collaboration with Novartis Pharmaceuticals in Horsham, we investigated the role of CYP1B1 in SU-hypoxia induced-PAH (White *et al.*, 2012) which is associated with the formation of occluded vascular lesions (Ciuclan *et al.*, 2011), which are absent in the classic hypoxic model of PH. TMS attenuated the development of SU-hypoxic induced increases in RVSP, RVH, pulmonary vascular remodeling and the formation of occluded vascular lesions, further supporting a pathogenic effect of CYP1B1 activity *in vivo* (White *et al.*, 2012).

Inflammation is a well-documented component associated with the disease pathology of PAH (reviewed by Price *et al.*, 2012). MCT is a plant-derived alkaloid that targets and disrupts the vascular endothelium which elicits an inflammatory response. It therefore drives a distinct disease pathology compared to the hypoxic and SU-hypoxic models of PAH. To assess the function of CYP1B1 activity on the progression of PH, we investigated the ability of CYP1B1 inhibition on reversal of established PH in the MCT model of PH (Figure 3-16 - Figure 3-19). Despite large increases in RVSP and RVH in both males and females, there was no development of the complex arteriopathy that is observed in end-

stage human disease, albeit neointimal lesions were present. The results presented here suggest that CYP1B1 inhibition for 2 weeks did not improve pulmonary haemodynamics. No effects were observed in response to TMS on reversal of RVH in females, yet moderate effects were reported in male rats. Although CYP1B1 inhibition did not significantly reverse pulmonary vascular remodeling, there appeared to be a trend towards an improvement, that may have been uncovered had treatment been prolonged. From a histological perspective, luminal narrowing observed in response to MCT appeared reduced in rats treated with TMS (Figure 3-18). Inhibition of CYP1B1 reduced mortality rates in male rats treated with MCT and completely prevented mortalities in female rats (Figure 3-21). Perhaps, it is not surprising that CYP1B1 inhibition was unable to successfully reverse RVH and RVSP in a two-week dosing regimen, given the severity of the induced phenotype, especially when the manifested disease is already far advanced. However, this is challenged by numerous reports that have shown successful attenuation of MCT-PH with various estrogenic drugs, including genistein (a soy phytoestrogen) (Matori *et al.*, 2012) and 17 $\beta$ -E2 (Umar *et al.*, 2011). However, the applicability of this model as a pre-clinical model of PAH has been challenged by the lack of similarity with the arteriopathy that is the hallmark human PAH, even at the end-stages of MCT-PH (reviewed by Gomez-Arroyo *et al.*, 2012a).

Numerous studies have highlighted beneficial effects of circulating 17 $\beta$ -E2 in the hypoxic and MCT models of PAH (Lahm *et al.*, 2012; Umar *et al.*, 2011; White *et al.*, 2011b; Xu *et al.*, 2010; Yuan *et al.*, 2013). In contrast, in models that display heightened activity of the SERT, circulating 17 $\beta$ -E2 exacerbates disease phenotypes (White *et al.*, 2011b; Dempsie *et al.*, 2011). This suggests that SERT may mediate the pathogenic effects of 17 $\beta$ -E2. One hypothesis is that SERT mediates the damaging effects of 17 $\beta$ -E2 by up-regulating the expression of CYP1B1, thereby altering estrogen metabolism towards the formation of pathogenic metabolites (White *et al.*, 2011a). We therefore next investigated the effects of CYP1B1 inhibition with TMS in the female susceptible SERT+ model of PH. In this study, we provide evidence that the estrogen metabolic axis is dysregulated in female SERT+ mice at 5-6 months of age by increased expression of aromatase and CYP1B1 (Figure 3-22 - Figure 3-23). At 5-6 months of age female SERT+ mice present with a PH phenotype - increased PAPs and pulmonary vascular remodeling compared to wild-type mice. Inhibition of CYP1B1 with TMS reverses both the increased PAPs and pulmonary vascular remodeling to pressures akin to wild-type mice, suggesting that the SERT is mediating its effects via increasing CYP1B1 activity (Figure 3-24 - Figure 3-25, Figure 3-27 - Figure 3-28). Despite elevated RVSP and pulmonary vascular remodeling, female SERT+ mice

do not develop compensatory RVH. This supports previous findings where a dissociate mechanism appears to contribute to ventricular remodeling and vascular pressures in this model of PAH (White *et al.*, 2011b). In ovariectomized SERT+ mice, exogenous 17 $\beta$ -E2 reduces RVH (White *et al.*, 2011b) suggesting that 17 $\beta$ -E2 mediates cardioprotective effects in this model, despite exerting pathogenic effects within the pulmonary vasculature. Thus we propose that the underlying genetic transformations occurring specifically in the lung may contribute to vascular remodeling and increased pressures. RVH is an adaptive response to increased PAP, which appears absent in mice with a global over-expression of the SERT, suggesting that SERT may be mediating direct effects in the heart. This is supported by studies that have reported the development of RVH in mice that overexpress SERT specifically in smooth muscle cells driven by the SM22 promoter (Guignabert *et al.*, 2006). To challenge this, it would be of interest to investigate the effects of pulmonary artery banding on RVH in female SERT+ mice. Pulmonary artery banding is a surgical technique that mimics right ventricular pressure overload by ligation of the pulmonary artery. Despite the absence of RVH under normoxic conditions, when exposed to hypoxia, female SERT+ mice develop exaggerated RVH in comparison to wild-type mice exposed to hypoxia, as previously reported (White *et al.*, 2011b). CYP1B1 inhibition failed to attenuate the development of hypoxia-induced RVH in these mice, which contradicts the beneficial effects of CYP1B1 inhibition on reducing RVH in the hypoxic murine models of PH. Thus the absence of a therapeutic effect of CYP1B1 inhibition on hypoxia-induced RVH in female SERT+ may be attributable to an effect mediated directly by SERT over-expression in the right ventricle.

Our present *in vivo* findings highlight a critical role for CYP1B1 in the development and pathogenesis of PAH. CYP1B1 is an extra-hepatic estrogen, xenobiotic and fatty acid metabolizing enzyme. CYP1B1 metabolizes estrogens (17 $\beta$ -E2 and E1) by hydroxylation at the C2, C4 and C16 positions within the carbon ring structure resulting in the formation of 2-, 4, 16-hydroxylated estrogens. The biological effects of estrogens will depend on the profile of metabolites formed within a target tissue. Increased activity of CYP1B1 will therefore alter estrogen metabolism. Proliferative screens of CYP1B1 estrogen metabolites suggest that the 16 $\alpha$ -hydroxylated estrogens are potent inducers of cellular proliferation in hPASCs (White *et al.*, 2012). Recent evidence has suggested that altered estrogen metabolism by CYP1B1 may underlie the development of PAH in patients with BMPR-2 mutations (Austin *et al.*, 2009). Females harboring a BMPR-2 mutation without any evidence of PAH were more likely to present with a polymorphism in CYP1B1 associated with an increased degradation of CYP1B1. In PAH patients with a BMPR-2 mutation and

the wild-type CYP1B1, the 2-OHE/16 $\alpha$ -OHE1 ratio was 2.3 fold lower compared to unaffected mutation carriers (Austin *et al.*, 2009), suggesting that CYP1B1 activity is associated with the formation of 16 $\alpha$ -OHE1. It is therefore likely that the beneficial effects of CYP1B1 inhibition observed in our studies are related to a reduction in the metabolism of 17 $\beta$ -E2 and E1 towards the formation of 16 $\alpha$ -OHE1 (17 $\beta$ -E2 can be converted to E1 which can then be metabolized to 16 $\alpha$ -OHE1 or 16 $\alpha$ -OHE2 can be converted to 16 $\alpha$ -OHE1 by the activity of HSD enzymes). However, the 4-hydroxylation of estrogens is recognized as the predominant metabolic pathway mediated by CYP1B1 activity (Badawi *et al.*, 2001;Hanna *et al.*, 2000;Lee *et al.*, 2003). In addition, in the murine lung, normal CYP1B1 activity is associated with the formation of 4-OHE1 (Peng *et al.*, 2013). The metabolic conversion of 17 $\beta$ -E2 by the 4-hydroxylation pathway is recognized to contribute to DNA damage by superoxide production (Acharya *et al.*, 2010). We have recently provided evidence that 4-hydroxylation induces profound superoxide production in hPASCs (up to 6 fold higher after incubations for 5 minutes compared to control) (unpublished data). Thus, CYP1B1 may be inducing its pathogenic effects via increased superoxide production.

The beneficial effects of CYP1B1 inhibition *in vivo* may also be attributable to subsequent increases in estrogens available to mediate effects via estrogen receptors through genomic and non-genomic signaling or other metabolic pathways. Numerous studies have provided evidence that estrogens mediate protective effects in both acute and chronic vascular injury. 17 $\beta$ -E2 increases eNOS expression and NO synthesis in pulmonary vascular cells via genomic and non-genomic mechanisms through ER $\alpha$  and ER $\beta$  (Austin *et al.*, 2013). Both endogenous and exogenous estrogens mediate rapid vasodilatory effects of isolated pulmonary arterial rings by non-genomic mechanisms (Lahm *et al.*, 2008a). *In vivo*, exogenous 17 $\beta$ -E2 can prevent the onset of hypoxia-induced PH (Lahm *et al.*, 2012) and reverse severe PH in the MCT model (Umar *et al.*, 2011). In contrast, in models that display female susceptibility, including the SERT+ model, the mts100/A4 overexpressing mouse and dexfenfluramine-treated mice, where a PH phenotype is only evident in female mice, 17 $\beta$ -E2 is a critical disease mediator (Dempsie *et al.*, 2011;Dempsie *et al.*, 2013;White *et al.*, 2011b). More recently, we have provided evidence that locally produced estrogens via activity of aromatase are associated with the development and progression of both hypoxia and SU-hypoxia induced PH (Mair *et al.*, 2013). These conflicting results may be attributable to altered estrogen receptor profiles or metabolic enzymes in the different models studied.

CYP1B1 is also an important enzyme in the metabolism of arachidonic acid into EETs and HETEs (Choudhary *et al.*, 2004). Arachidonic acid metabolism results in the formation of eicosanoids which have been implicated in both cancers and cardiovascular diseases (Capdevila & Falck, 2001). In systemic vascular smooth muscle cells, Ang II and arachidonic acid cause migration, proliferation and hypertrophy which is attenuated by CYP1B1 inhibition with TMS (Yaghini *et al.*, 2010). This is associated with a reduced formation of ROS and its downstream signaling molecules ERK1/2 and p38MAPK (Yaghini *et al.*, 2010). In the rabbit pulmonary arteries, arachidonic acid stimulates endothelium-dependent vasoconstriction and these effects are greater in female pulmonary arteries compared to male pulmonary arteries (Pfister, 2011). 15-HETE is a metabolite formed by the metabolism of arachidonic acid by CYP1B1 and 15-lipoxygenase. 15-lipoxygenase expression and 15-HETE synthesis is greater in female rabbit pulmonary arteries compared with males and stimulates vasoconstriction (Pfister, 2011). Taken together, the therapeutic effects observed with CYP1B1 inhibition may be via a reduced formation of the pulmonary vasoconstrictors, EETs and HETEs.

Arachidonic acid is also the precursor to prostaglandins by the COX pathway. Prostacyclin is a member of the prostanoid family and is a potent vasodilator, with anti-inflammatory and anti-mitogenic properties. PAH is associated with increased pulmonary vasoconstriction, inflammation and remodeling and prostacyclin analogues are therefore used in the management of PAH. Prostacyclin is the principle arachidonic acid metabolite (Alhencgelas *et al.*, 1982) and prostacyclin synthase levels are decreased in PAH (Tuder *et al.*, 1999). CYP1B1 inhibition may therefore also increase the availability of arachidonic acid for subsequent prostacyclin synthesis.

Arachidonic acid and estrogen metabolism by CYP1B1 are associated with increased ROS formation (Yaghini *et al.*, 2010;Chen *et al.*, 2004), which is associated with the pathogenesis of PAH (Bowers *et al.*, 2004;Fessel *et al.*, 2013b;Hemnes *et al.*, 2011). Thus multiple pathways may interplay to cause injurious ROS production and cellular proliferation via CYP1B1 activity, resulting in a pathogenic environment in the pulmonary vasculature that can be reversed by CYP1B1 inhibition. The benefits of CYP1B1 inhibition may therefore be pertinent to a greater cohort of patients and have further beneficial effects that target several conjoined pathways that are associated with the pathology of PAH. CYP1B1 expression is increased in hPASMCs by 17 $\beta$ -E2 (White *et al.*, 2011b). Increased aromatase activity is associated with the pathogenesis of PAH (Mair *et al.*, 2013) suggesting that increased production of estrogens within the pulmonary vasculature may

increase CYP1B1 expression therefore driving pathological estrogen and arachidonic acid metabolism whilst reducing levels of estrogens and prostacyclins.

CYP1B1 is a putative pro-carcinogen marker and the results presented here support a role for CYP1B1 in PAH. Inhibition of CYP1B1 is currently under phase II clinical trials for the treatment of cancer (Luby, 2008) and our data indicates that CYP1B1 inhibition may be a promising therapeutic target to restore dysfunctional estrogenic metabolism in PAH. Comprehensive analyses of the estrogen metabolic pathway in PAH are merited to provide a better understanding of estrogen metabolism in PAH. It is imperative that estrogen-related therapies are considered in the management of PAH, given the drastic gender disparity that is observed in clinic. Perhaps we can learn from our colleagues in oncology, whom now effectively treat cancers depending on estrogen status.

## **Chapter 4**

# **Dynamic Alterations in the Estrogen Metabolic Axis in Pulmonary Hypertension**

## 4.1 Introduction

Estrogen and its metabolites are emerging as highly pathogenic mediators in various diseases. Among these, the debilitating and fatal cardiovascular disease PH appears to be affected by abnormal activity of the estrogen pathway to adversely affect pulmonary vascular cell survival and function. PAH is the most fatal subtype of PH and predominantly affects women. For example, in the largest PH registry in the World, the Registry to Evaluate Early and Long-Term PAH Disease Management (REVEAL), more than 80% of patients diagnosed were females (Badesch *et al.*, 2010). Altered estrogen synthesis (Mair *et al.*, 2013) and metabolism (Chapter 3 and White *et al.*, 2012) contributes to the pathogenesis of PAH. We have recently provided evidence that the estrogen metabolic axis is dysregulated in PAH in part via the activity of the putatively pathogenic CYP enzyme CYP1B1 (Chapter 3 and White *et al.*, 2012). PAH is characterised by obstructive vascular lesions in the distal vasculature by excessive PASMC proliferation (Archer *et al.*, 2010; Schermuly *et al.*, 2011), suggesting that anti-proliferative therapies are needed. Estrogen and its metabolites elicit potent biological effects within target cells (Zhu & Conney, 1998), yet the dynamic regulation of estrogen metabolism in PAH remains obscure. We hypothesized that estrogen metabolism is pathologically altered in PAH towards the formation of pro-proliferative estrogen metabolites. Modulation of the estrogen metabolic pathway that favours the formation of anti-proliferative metabolites over pro-proliferative metabolites may represent a novel therapeutic strategy in this highly-gender selective disease.

The circulating C19 precursor's testosterone and androstenedione are converted to  $17\beta$ -E2 and E1 respectively by the activity of CYP19A1 (aromatase). Recent evidence highlights a potential for locally synthesized estrogens ( $17\beta$ -E2 and E1) in the distal pulmonary arteries through expression of aromatase (Mair *et al.*, 2013). Tissues can also regulate their own estrogenic milieu through the  $17\beta$ -HSD enzymes.  $17\beta$ -HSD1 converts E1 into  $17\beta$ -E2, whereas  $17\beta$ -HSD2 converts  $17\beta$ -E2 into E1.  $17\beta$ -E2 and E1 undergo oxidative metabolism by the catalytic activity of CYP enzymes in the presence of NADPH to yield the 2-, 4- and 16-hydroxylated estrogens (Figure 4-1). The catechol estrogens (the 2- and 4-hydroxylated estrogens) formed by this transformation can then undergo rapid methylation by the activity of COMT to their less estrogenic methoxyestrogens. Alternatively, CYP enzymes can also further oxidise catechol estrogens, specifically the 4-hydroxyestrogens to quinones and semiquinones that can enter redox cycling and interact with DNA to form DNA adducts, which can generate apurinic sites resulting in DNA

damage. Recently, DNA damage has been shown to be an important mediator in the pathogenesis of PAH and provides a novel therapeutic target (Meloche *et al.*, 2013).

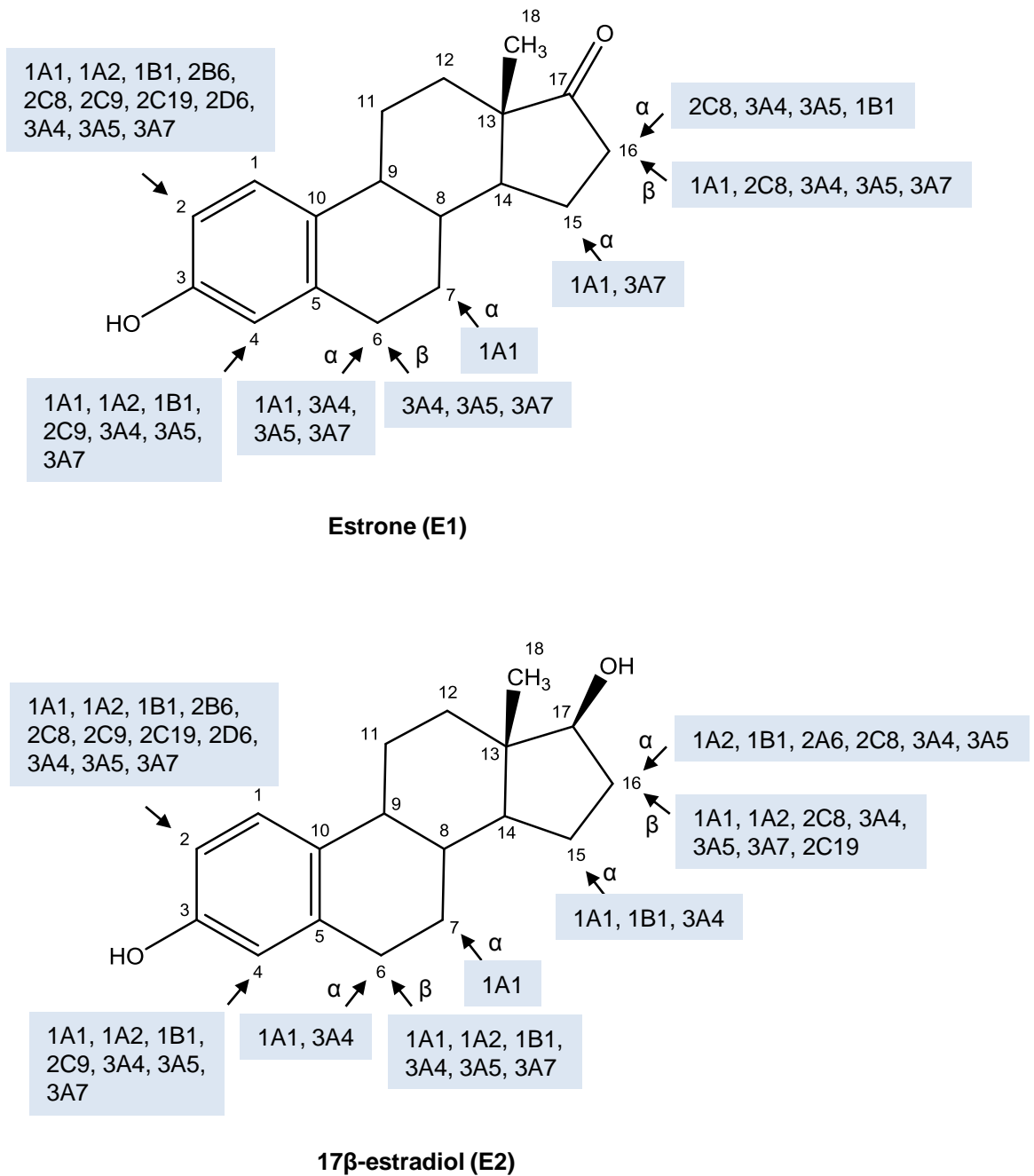


**Figure 4-1 Summary of the hydroxylation of estrone and 17β-estradiol by human cytochrome P450 isoforms**

CYP enzymes that are highlighted in bold have a high activity for the hydroxylation at that specific carbon position. Diagram modified and reproduced with permission from Professor Bao-Ting Zhu (Lee *et al.*, 2003)

Both herein (Chapter 3) and previously (White *et al.*, 2012) we present extensive evidence that estrogen strongly drives PAH onset specifically through pathologic induction of the putative cancer-causing enzyme (Murray *et al.*, 1997) CYP1B1. In effect, this is thought to potently shift estrogen metabolism towards the formation of pathogenic metabolites. 16-hydroxylation and 4-hydroxylation of 17 $\beta$ -E2 represent a pathogenic pathway that may be activated by increased CYP1B1 activity (Chapter 3 and White *et al.*, 2012). 16-hydroxylated estrogens robustly induce proliferation of hPASCs (Chapter 3 and White *et al.*, 2012). The 4-hydroxylated estrogen metabolites are highly associated with tumorigenesis via the formation of ROS that can generate apurinic sites leading to DNA damage (Acharya *et al.*, 2010).

The lung hosts a substantial number of CYP enzymes. The most prominent are CYP1A1, CYP1B1 and CYP2B6 under normal physiological conditions (Bieche *et al.*, 2007) which are predominantly extra-hepatic enzymes. CYP1B1 is also highly expressed in the trachea and to a lesser extent in the bone marrow, kidney, heart, mammary gland, prostate, spleen, thyroid and uterus (Bieche *et al.*, 2007). CYP1A1 is most highly expressed in the lung but is also present within other tissues including the kidney, trachea, liver and mammary gland (Bieche *et al.*, 2007). In contrast, CYP2B6 is less abundantly expressed with similar levels in the liver compared with the lungs as well as the kidney and trachea (Bieche *et al.*, 2007). To date, a comprehensive analysis of estrogen metabolism in PAH has been hampered by challenges in measuring estrogens and its metabolites due to their relatively low abundance, structural similarities and a required high level of expertise in ‘omics analysis. Currently, the most commonly used methodologies include immunoassays, gas chromatography mass spectrometry (GC-MS) and liquid chromatography mass spectrometry (LC-MS) (Gaikwad, 2013). There is a lack of available immunoassays to measure all estrogens of interest and it is impossible to analyse multiple steroids in one single assay. GC-MS and LC-MS are considered the gold standard techniques in steroid analysis yet they carry selective bias and extensive sample preparation for measurement of estrogens. To date, estrogen metabolites have only been preliminarily measured in serum from patients with severe PAH (Chhatwani *et al.*, 2010). Aromatase (Mair *et al.*, 2013) and CYP1B1 (Chapter 3 and White *et al.*, 2012) are expressed within smooth muscle cells of the distal pulmonary vasculature indicating local synthesis and metabolism of estrogens potentially creating a potent estrogenic milieu. It was therefore of importance to examine and quantitatively measure the dynamic profile of estrogen metabolism in a homogenous PASC culture given that an altered estrogen metabolic profile may figure prominently in PAH. Pulmonary vascular smooth muscle cell proliferation is a well-established and

dominant feature of PAH (Archer *et al.*, 2010; Schermuly *et al.*, 2011), suggesting that anti-proliferative therapies are necessary to reverse the extensive vascular obliteration. Thus, we developed a methodology adapting a HPLC approach to quantitatively fate map estrogen metabolism in a homogenous hPASC population to determine the dynamic regulation of estrogen metabolism in PAH and precisely uncover underlying molecular events that contribute to PAH pathogenesis via a dysregulated estrogen metabolic axis.

In this chapter, we investigated the effects of estrogen metabolites on the pulmonary circulation and investigated the metabolism of  $17\beta$ -E2 in hPASCs providing the first direct evidence that estrogen is metabolized by hPASCs. We provide evidence that  $16\alpha$ -OHE1 is a disease-modifying metabolite in female mice only. We demonstrate key differences in estrogen metabolism in control and PAH hPASCs. We provide evidence for prominent, yet variable activity of  $17\beta$ -HSD2 in hPASCs by the formation of E1, considered an inactive reservoir for  $17\beta$ -E2 synthesis. Importantly, we demonstrate that estrogen metabolism is pathologically altered in PAH and highlights a novel treatment paradigm in this highly female-selective disease.

Aims of this chapter:

1. To assess the contribution of estrogen metabolites on pulmonary haemodynamics and cellular function
2. To develop a method to quantitatively measure estrogen metabolism in pulmonary vascular cells
3. To determine the metabolic fate of  $17\beta$ -E2 in hPASCs from naïve cells and PAH-PASCs in both males and females

## 4.2 Results

### 4.2.1 The CYP1B1 metabolite 16 $\alpha$ -hydroxyestrone is increased by hypoxia

We have shown that CYP1B1 expression is increased in human PAH and in murine experimental models of PH (Chapter 3 and White *et al.*, 2012). Furthermore, genetic ablation of CYP1B1 and inhibition of CYP1B1 attenuated the development of hypoxic-induced-PH. We next wished to identify a mechanistic pathway that mediates CYP1B1 pathogenesis. Cellular proliferation screening revealed that 16 $\alpha$ -OHE1 is the predominant CYP1B1 metabolite found to cause significant proliferation in control hPASMCs (White *et al.*, 2012). As an indicative measure of CYP1B1 activity in murine PH, we assessed urinary concentrations of 16 $\alpha$ -OHE1 in response to chronic hypoxia exposure. Urinary concentrations of 16 $\alpha$ -OHE1 were increased in both male and female mice following exposure to chronic hypoxia (Figure 4-2).

### 4.2.2 16 $\alpha$ -hydroxyestrone inflicts a pulmonary hypertensive phenotype in female mice only

To determine whether 16 $\alpha$ -OHE1 is a pulmonary vascular insult that can directly cause a PH phenotype *in vivo*, mice were administered 16 $\alpha$ -OHE1 for 28 days (Figure 4-4). Dr. Kevin White and Ms. Leigh Paton performed the entire female dosing, *in vivo* procedures, pulmonary vascular remodeling and  $\alpha$ -SMA analysis of this study. In female mice, 16 $\alpha$ -OHE1 resulted in increased RVSP, RVH and pulmonary vascular remodeling. In contrast, no effects were observed in male mice in any of the parameters measured. The effects observed were specific to the cardio-pulmonary unit in female mice, as no changes were measured in mSAP. In contrast, 16 $\alpha$ -OHE1 significantly reduced mSAP in male mice (Table 4-1).

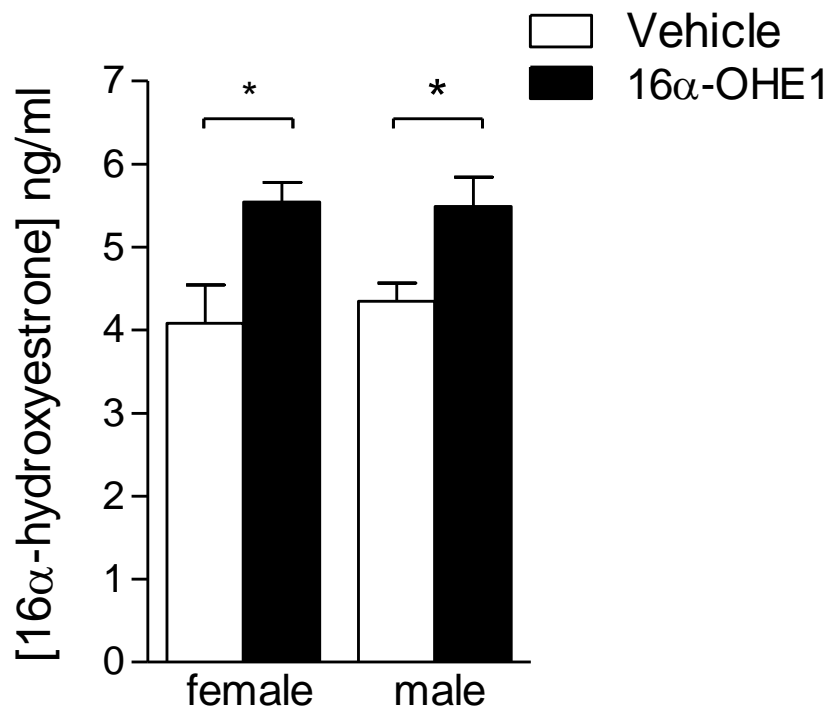


**Figure 4-2 Urinary levels of the 16α-hydroxyestrone is increased by chronic hypoxia in male and female mice**

Urinary levels of 16α-hydroxyestrone (16α-OHE1) were assessed in the urine of mice kept at normoxic conditions or after exposure to 2 weeks hypoxia (10% oxygen) by a competitive immunoassay (ESTRAMET 2/16). n=5, \*P<0.05, t-test, data is expressed as the mean ± SEM.

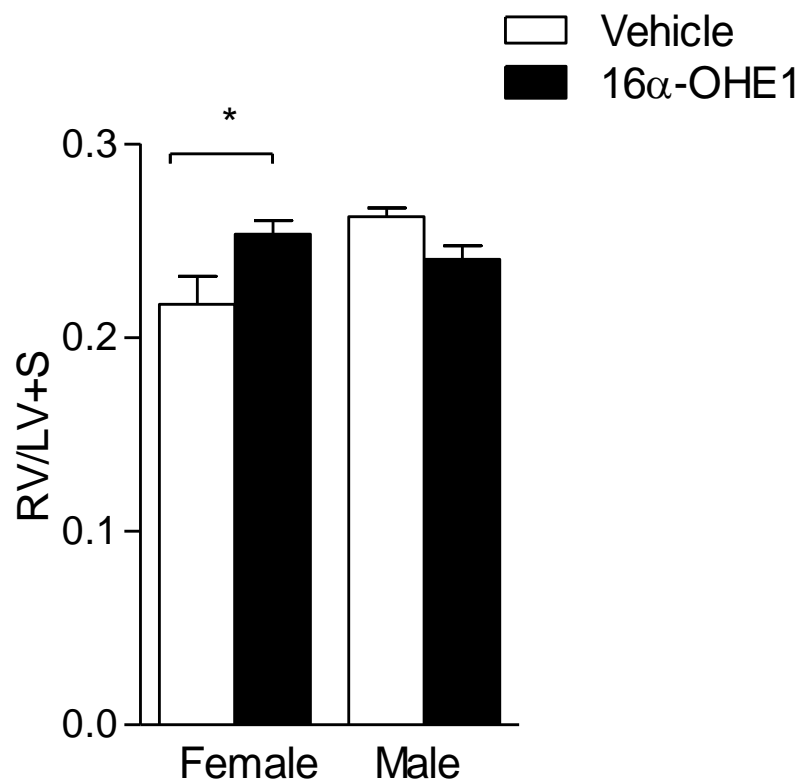


**Figure 4-3 16 $\alpha$ -hydroxyestrone (16 $\alpha$ -OHE1) induces right ventricular hypertrophy in female mice only**

Female and male C57BL/6 mice were dosed with 16 $\alpha$ -OHE1 1.5mg/kg/day or vehicle (~5% ethanol in saline) for 28 days. Right ventricular hypertrophy was assessed by expressing the dry weight of the right ventricle over the left ventricle and septum (RV/LV+S; Fultons index). n=7-10 per group, \*P<0.05, One-way ANOVA with a Bonferroni's post-hoc test. Data is expressed as the mean  $\pm$  SEM.

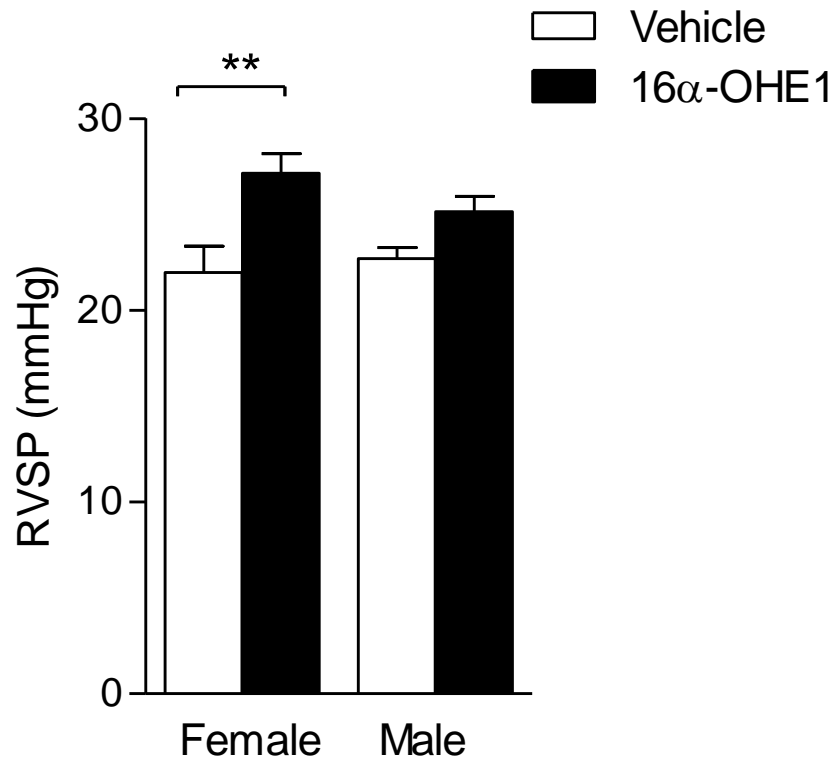


**Figure 4-4 16 $\alpha$ -hydroxyestrone (16 $\alpha$ -OHE1) increases right ventricular systolic pressures in female mice only**

Female and male C57BL/6 mice were dosed with 16 $\alpha$ -OHE1 1.5mg/kg/day or vehicle (~5% ethanol in saline) for 28 days. Right ventricular systolic pressures (RVSP) were measured by right heart catheterisation. n=7-8 per group, \*\*P<0.01 One-way ANOVA with a Bonferroni's post-hoc test. Data is expressed as the mean  $\pm$  SEM.

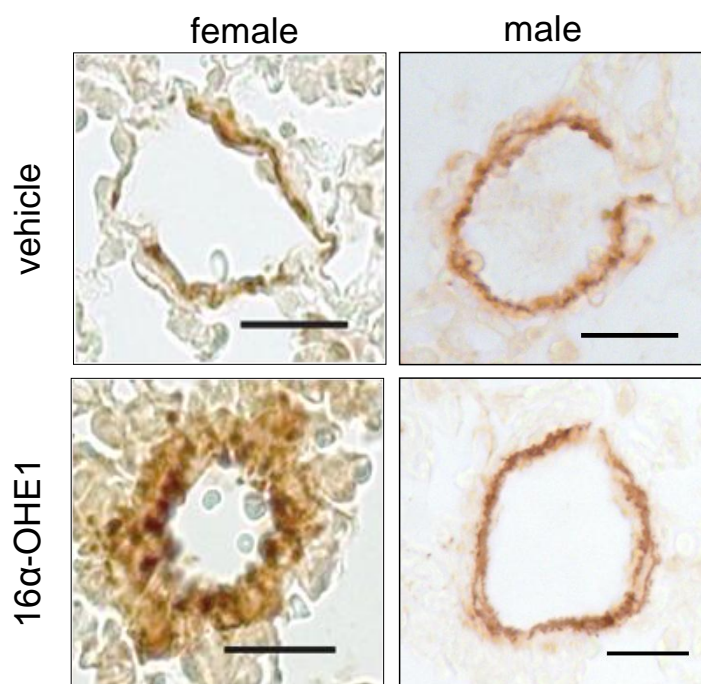


**Figure 4-5 Representative  $\alpha$ -smooth muscle actin-stained pulmonary arteries in 16 $\alpha$ -hydroxyestrone (16 $\alpha$ -OHE1) or vehicle treated C57BL/6 male and female mice**

Female and male C57BL/6 mice were treated with 16 $\alpha$ -hydroxyestrone (16 $\alpha$ -OHE1, 1.5mg/kg/day) or vehicle (~5% ethanol in saline) for 28 days. Muscularisation is visualised by  $\alpha$ -smooth muscle actin staining, which has a brown/orange appearance. Scale bar = 20 $\mu$ m

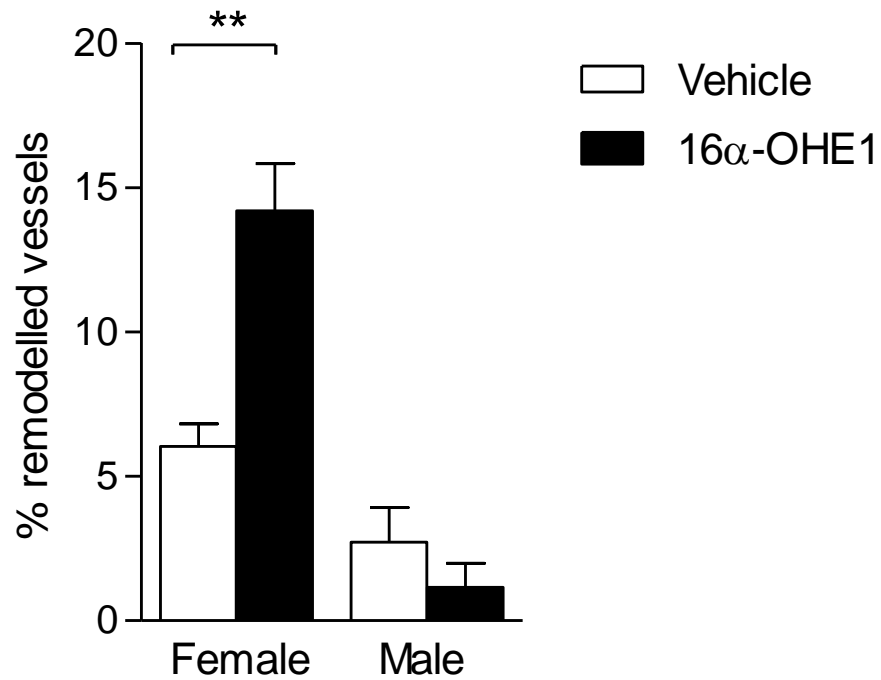


**Figure 4-6 16 $\alpha$ -hydroxyestrone (16 $\alpha$ OHE1) increases pulmonary arterial remodeling in female mice only**

Female and male C57BL/6 mice were treated with 16 $\alpha$ -hydroxyestrone (16 $\alpha$ -OHE1, 1.5mg/kg/day) or vehicle (~5% ethanol in saline) for 28 days. The degree of pulmonary arterial remodeling was assessed by counting the number of remodeled and non-remodeled arteries in a lung section and expressed as the % of remodeled vessels over the total number of vessels. n=4-6 per group, \*\*P<0.05. One-way ANOVA with a Bonferroni's post-hoc test. Data is expressed as the mean  $\pm$  SEM.

**Table 4-1 Phenotypic data from 16 $\alpha$ -hydroxyestrone treated mice**

Animal Group	mSAP (mmHg)	mRVP (mmHg)	Heart Rate (bpm)	Body Weight (g)
Female Vehicle	76.68 $\pm$ 1.97 (5)	12.34 $\pm$ 0.45 (9)	437.1 $\pm$ 19.87 (9)	23.16 $\pm$ 0.56 (10)
Female 16 $\alpha$ -OHE1	86.39 $\pm$ 3.10 (6)	14.95 $\pm$ 0.72* (9)	487.8 $\pm$ 22.40 (9)	23.63 $\pm$ 1.05 (10)
Male Vehicle	91.14 $\pm$ 2.20 (7)	13.58 $\pm$ 0.40 (10)	407.6 $\pm$ 11.72 (10)	23.92 $\pm$ 0.43 (10)
Male 16 $\alpha$ -OHE1	76.87 $\pm$ 2.39** (9)	14.55 $\pm$ 0.89 (8)	434.5 $\pm$ 11.66 (9)	24.01 $\pm$ 0.48 (10)

Female and male C57BL/6 mice were treated with 16 $\alpha$ -hydroxyestrone (16 $\alpha$ -OHE1, 1.5mg/kg/day) or vehicle (~5% ethanol in saline) for 28 days. Mean systemic arterial pressures (mSAP) were measured by cannulation of the carotid artery. Mean right ventricular pressures (mRVP) were calculated from the right ventricular pressure obtained by right heart catheterisation. n numbers are indicated in brackets. \*P<0.05, \*\*P<0.001

### 4.2.3 16 $\alpha$ -hydroxyestrone-induced proliferation is inhibited by a reactive oxygen species scavenger and an inhibitor of extracellular regulated kinase 1/2

We have shown that 16 $\alpha$ -OHE1 induces a PH phenotype in female mice only and that it is a potent inducer of hPASMCs proliferation (White *et al.*, 2012). We were therefore interested in investigating potential mechanisms related to this accelerated rate of proliferation. CYP1B1 is recognised to facilitate production of ROS which mediates phosphorylation of the target gene ERK1/2 (Jennings *et al.*, 2010; Jennings *et al.*, 2012). It was therefore of interest to investigate the effects of a ROS scavenger (tempol) and an inhibitor of ERK1/2 (UO126) on 16 $\alpha$ -OHE1-induced proliferation. hPASMCs did not proliferate to 16 $\alpha$ -OHE1 in the presence of either tempol or UO126, providing evidence that this pathway can also be activated by 16 $\alpha$ -OHE1 (Figure 4-7).

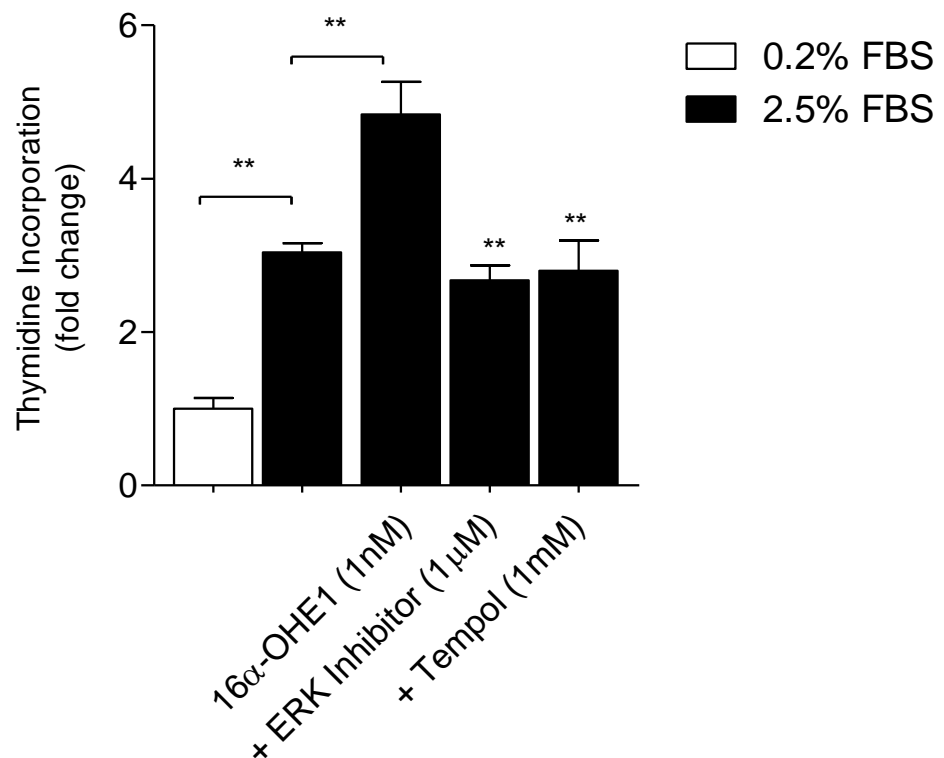


**Figure 4-7 16 $\alpha$ -hydroxyestrone (16 $\alpha$ -OHE1)-induced proliferation in human pulmonary arterial smooth muscle cells (hPASMCs) is mediated by the formation of reactive oxygen species (ROS)**

Female PAH hPASMCs were quiesced for 24 hours in 0.2% charcoal-stripped FBS (estrogen free) phenol red free DMEM. HPASMCs were then pre-incubated with a vehicle (water), an ERK inhibitor (UO126, 1 $\mu$ M) or tempol (ROS scavenger, 1mM) for 45 minutes prior to addition of 16 $\alpha$ -OHE1 (1nM) in the presence of 2.5% charcoal-stripped FBS phenol red free DMEM. Thymidine was added for the last 24 hours (0.1 $\mu$ Ci) and thymidine incorporation was assessed after 72 hours. The effect of inhibitors alone is included in appendix 1. n=1, repeated 4 times, \*\*P<0.01, One-way ANOVA with a Bonferroni's post-hoc test. Data is expressed as the mean  $\pm$  SEM.

#### 4.2.4 4-hydroxyestradiol attenuates serotonin-induced vasoconstriction in the pulmonary arteries

16 $\alpha$ -OHE1 and 16 $\alpha$ OHE2 were the only CYP1B1 metabolite to induce proliferation of hPASCs (White et al., 2012). However, other pathogenic effects beyond smooth muscle cell proliferation may be present. We could therefore not conclude that all effects of CYP1B1 were mediated via formation of 16 $\alpha$ -OHE1. 4-hydroxylation of 17 $\beta$ -E2 is the predominant metabolic pathway of CYP1B1 activity. We therefore wished to determine the effects of 4-OHE2 *in vivo*. No effect was observed in RVSP, RVH (Figure 4-8) or mSAP (Table 4-2). Body weights were significantly reduced in mice dosed with 4-OHE2 (Table 4-2)

Surprisingly, serotonin-induced pulmonary arterial vasoconstriction was significantly reduced in mice that had been treated with 4-OHE2 compared to their vehicle controls Figure 4-10. Given the high estrogenic activity of 4-OHE2 we also monitored potential hypertrophic/growth effects of the reproductive organs. 4-OHE2 significantly increased the dry weight of the uterus and ovaries combined compared to the control-vehicle group (Figure 4-11). Furthermore, this was accompanied by a fluid-filled uterus indicating hydrometrocolpitis.

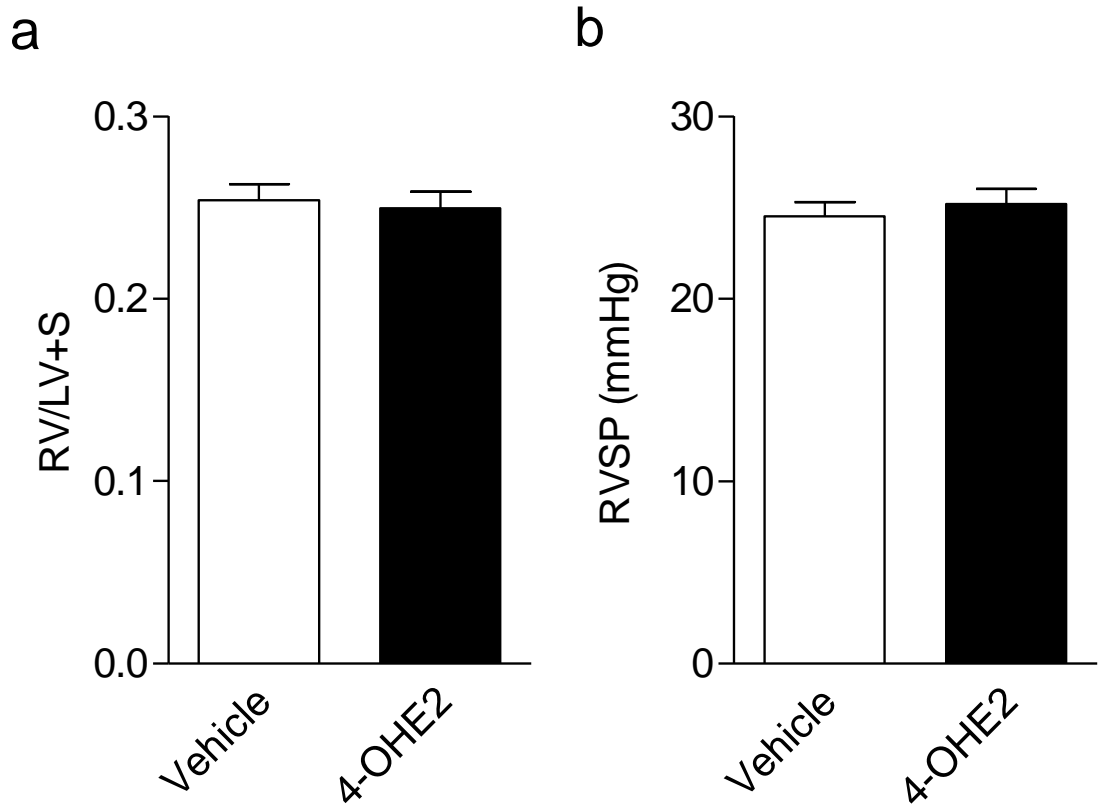


**Figure 4-8 4-hydroxyestradiol (4-OHE2) has no effects on right ventricular hypertrophy or right ventricular systolic pressures**

Female C57BL/6 mice were dosed with 4-OHE2 (1.5mg/kg/day) or vehicle (~5% ethanol in saline) for 28 days. Right ventricular hypertrophy was assessed by expressing the dry weight of the right ventricle over the left ventricle and septum (RV/LV+S; Fultons index) (a). Right ventricular systolic pressures (RVSP) were measured by right heart catheterisation (b). n=6-10. One-way ANOVA with a Bonferroni's post-hoc test. Data is expressed as the mean  $\pm$  SEM

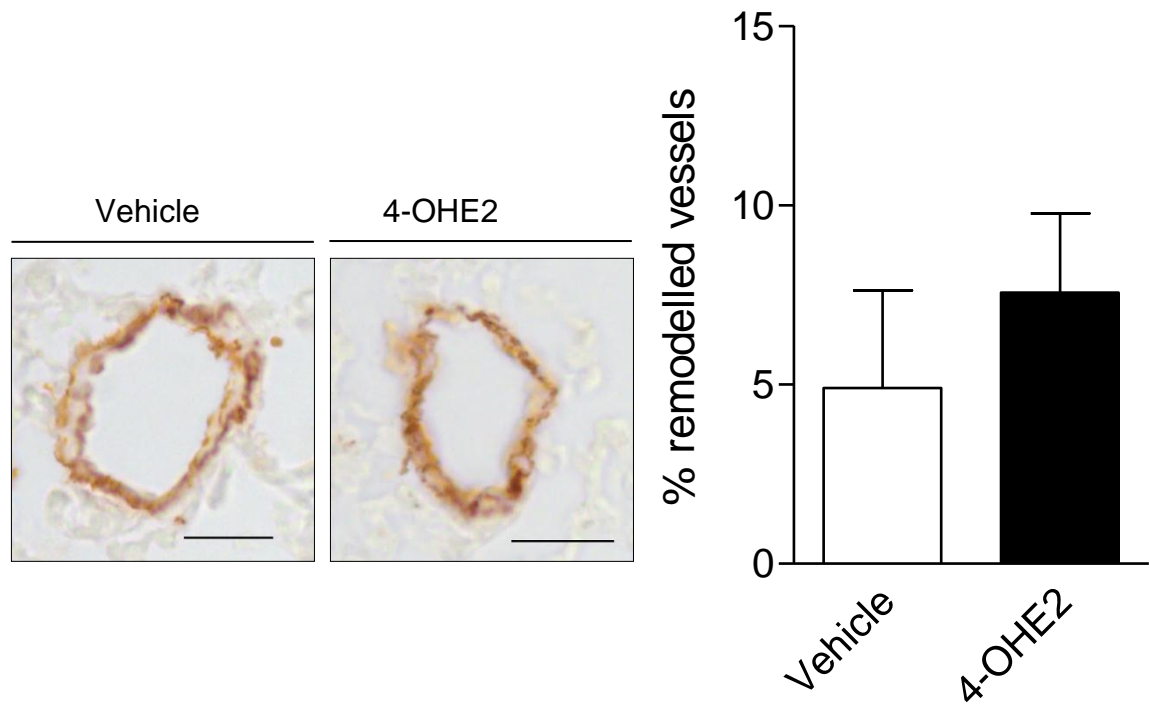


**Figure 4-9 4-hydroxyestradiol had no effects on pulmonary vascular remodeling**

Female C57BL/6 mice were dosed with 4-OHE2 (1.5mg/kg/day) or vehicle (~5% ethanol in saline) for 28 days. Representative  $\alpha$ -smooth muscle actin-stained pulmonary arteries in 4-OHE2 or vehicle treated C57BL/6 female mice and percentage of remodeled pulmonary arteries. The degree of pulmonary arterial remodeling was assessed by counting the number of remodeled and non-remodeled arteries in a lung section and expressed as the % of remodeled vessels over the total number of vessels. n=5-6, One-way ANOVA with a Bonferroni's post-hoc test. Data is expressed as the mean  $\pm$  SEM. Scale bar = 20 $\mu$ m.

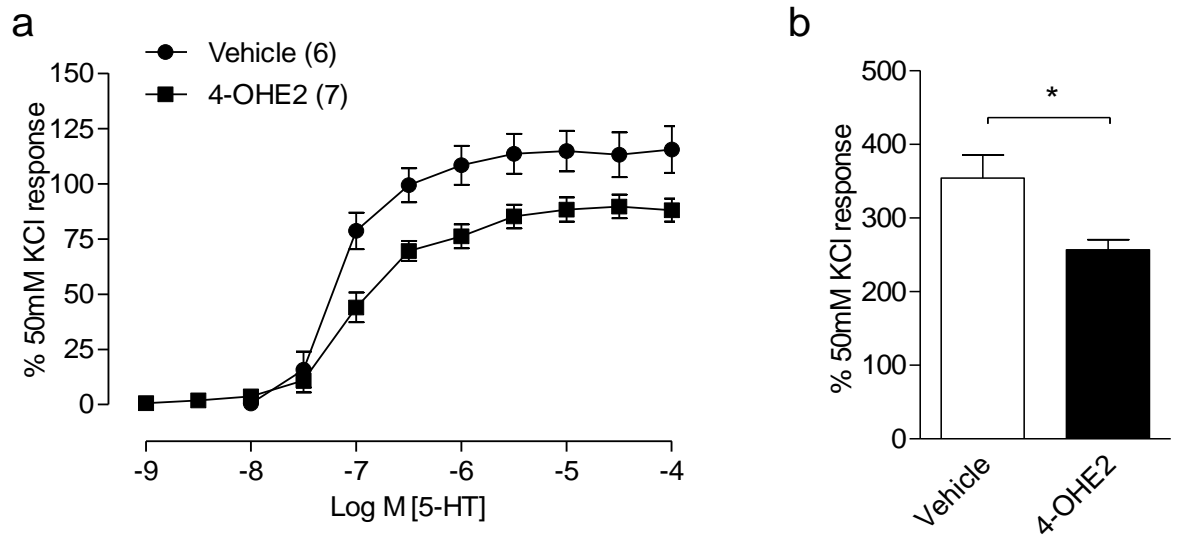


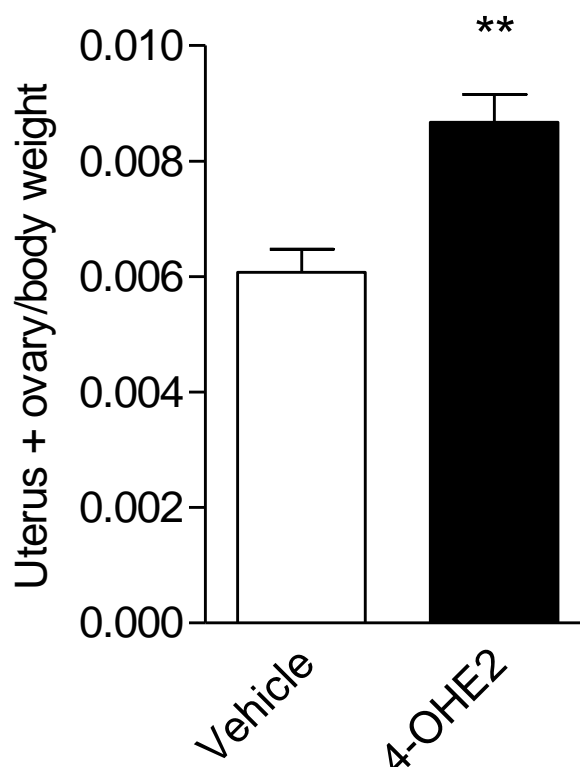
**Figure 4-10 4-hydroxyestradiol reduces serotonin-induced vasoconstriction**

Female C57BL/6 mice were dosed with 4-OHE2 (1.5mg/kg/day) or vehicle (~5% ethanol in saline) for 28 days. The intra-pulmonary arteries were isolated from mice at sacrifice and mounted in a myograph. The arteries were constricted twice by increasing extracellular concentrations to 50mM potassium chloride (KCl). The second response was used as a reference constriction to calculate the % vasoconstriction in response to serotonin. Following a wash-out and re-stabilization, cumulative concentration response curves to serotonin were constructed. Cumulative concentration response curves to serotonin (a). Area under the curve analysis (b). n=6-7, \*P<0.05, t-test. Data is expressed as the mean  $\pm$  SEM.

**Table 4-2 Phenotypic data from 4-hydroxyestradiol treated mice**

Animal Group	mSAP (mmHg)	mRVP (mmHg)	Heart Rate (bpm)	Body Weight (g)
Female Vehicle	84.22 ± 1.51 (4)	11.45 ± 0.42 (6)	366.0 ± 24.20 (6)	18.75 ± 0.56 (6)
Female 4-OHE2	83.31 ± 5.76 (8)	12.60 ± 0.63 (9)	375.6 ± 12.19 (9)	17.61 ± 0.17** (10)

Female C57BL/6 mice were dosed with 4-OHE2 (1.5mg/kg/day) or vehicle (~5% ethanol in saline) for 28 days. Mean systemic arterial pressures (mSAP) were measured by cannulation of the carotid artery. Mean right ventricular pressures (mRVP) were calculated from the right ventricular pressure obtained by right heart catheterisation. n numbers are indicated in brackets \*\*P<0.01.

**Figure 4-11 Effect of 4-hydroxyestradiol on uterus + ovary weights**

Female C57BL/6 mice were dosed with 4-OHE2 (1.5mg/kg/day) or vehicle (~5% ethanol in saline) for 28 days. The dry weight of the uterus and ovaries were expressed over the body weight, n=5-10, \*\*P<0.05, t-test. Data is expressed as the mean ± SEM.

### 4.2.5 Effect of estrogen metabolism by CYP1B1 on cellular function

Recent evidence has highlighted that the predominant CYP1B1 metabolite in the lungs of mice is 4-OHE1 (Peng *et al.*, 2013). Thus, we assessed the functional consequences of increased CYP1B1 activity in hPASMCs from female control patients by exposure to 4-OHE1 (Figure 4-12 - Figure 4-15). 4-OHE1 had no effect on cell viability as assessed by quantification for ATP after 3 and 5 days incubation. In contrast, 4-OHE1 dramatically reduced DNA replication as assessed by a reduction in thymidine incorporation at 3 days (Figure 4-12). Following a 5-day incubation with 4-OHE1, this effect was no longer observed (Figure 4-13).

CYP1B1<sup>-/-</sup> mouse lungs have a higher concentration of 2-MeOHE2 (Peng *et al.*, 2013) suggesting that this is negatively regulated by CYP1B1 activity. We were therefore interested in determining the effects of 2-MeOHE2 on cellular viability and proliferation (Figure 4-12 - Figure 4-15). 2-MeOHE2 caused a dramatic reduction in cell viability and proliferation as assessed by ATP and thymidine incorporation assays, respectively, following incubations for both 3 and 5 days.

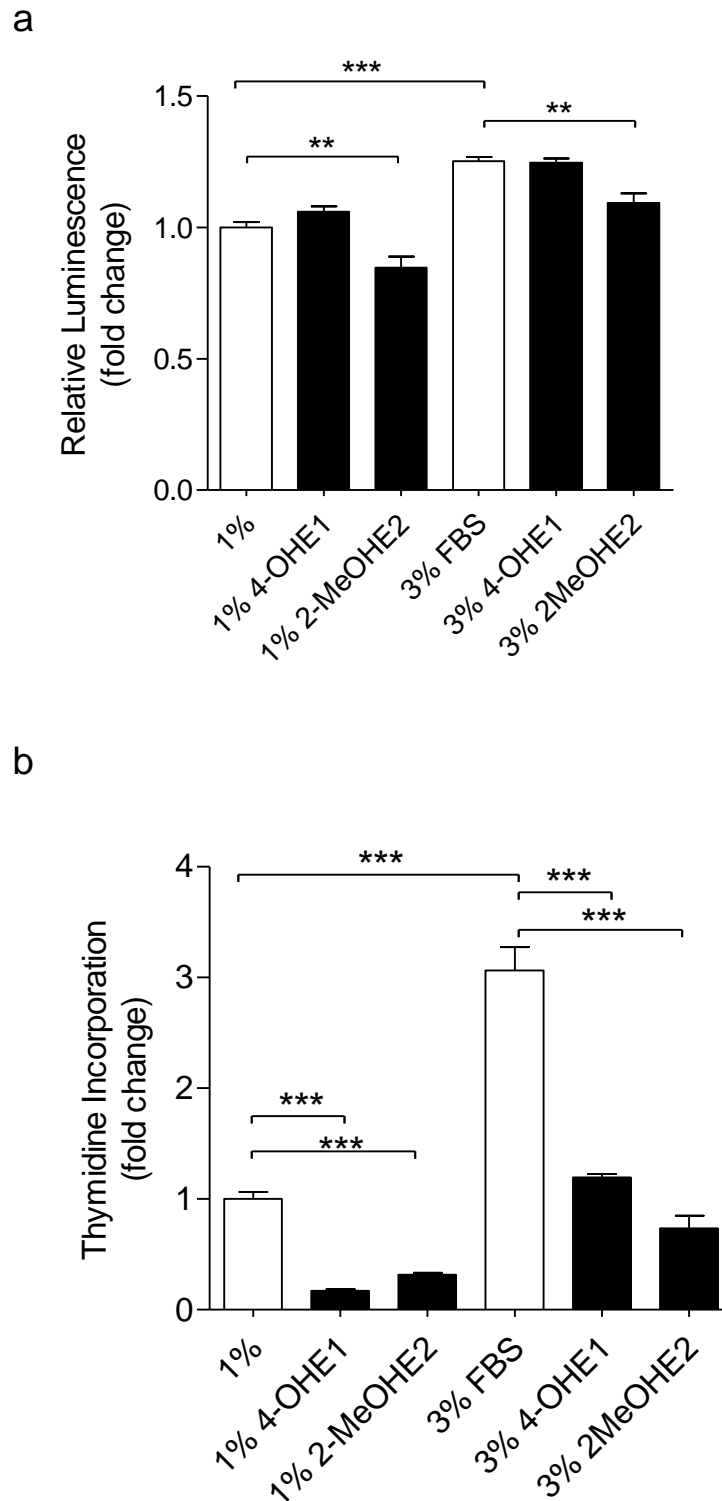


**Figure 4-12 Effect of 4-hydroxyestrone (4-OHE1) and 2-methoxyestradiol (2-MeOHE2) on human pulmonary arterial smooth muscle cell (hPASC) viability and proliferation for 3 days**

Female control hPASCs were quiesced for 24 hours in 0.2% charcoal-stripped FBS (estrogen free) phenol red free DMEM. hPASCs were then incubated with either 4-OHE1 (1 $\mu$ M), 2-MeOHE2 (1 $\mu$ M) or vehicle (0.01% ethanol) for 3 days in 1% or 3% charcoal-stripped FBS phenol red free DMEM and assessed for cell viability with the CellTiter-Glow® luminescence assay (a) and cell proliferation by the thymidine incorporation assay (b) n=1-2, repeated 4 times per cell line. \*\*P<0.01, \*\*\*P<0.001. One-way ANOVA with a Bonferroni's post-hoc test. Data is expressed as the mean  $\pm$  SEM.

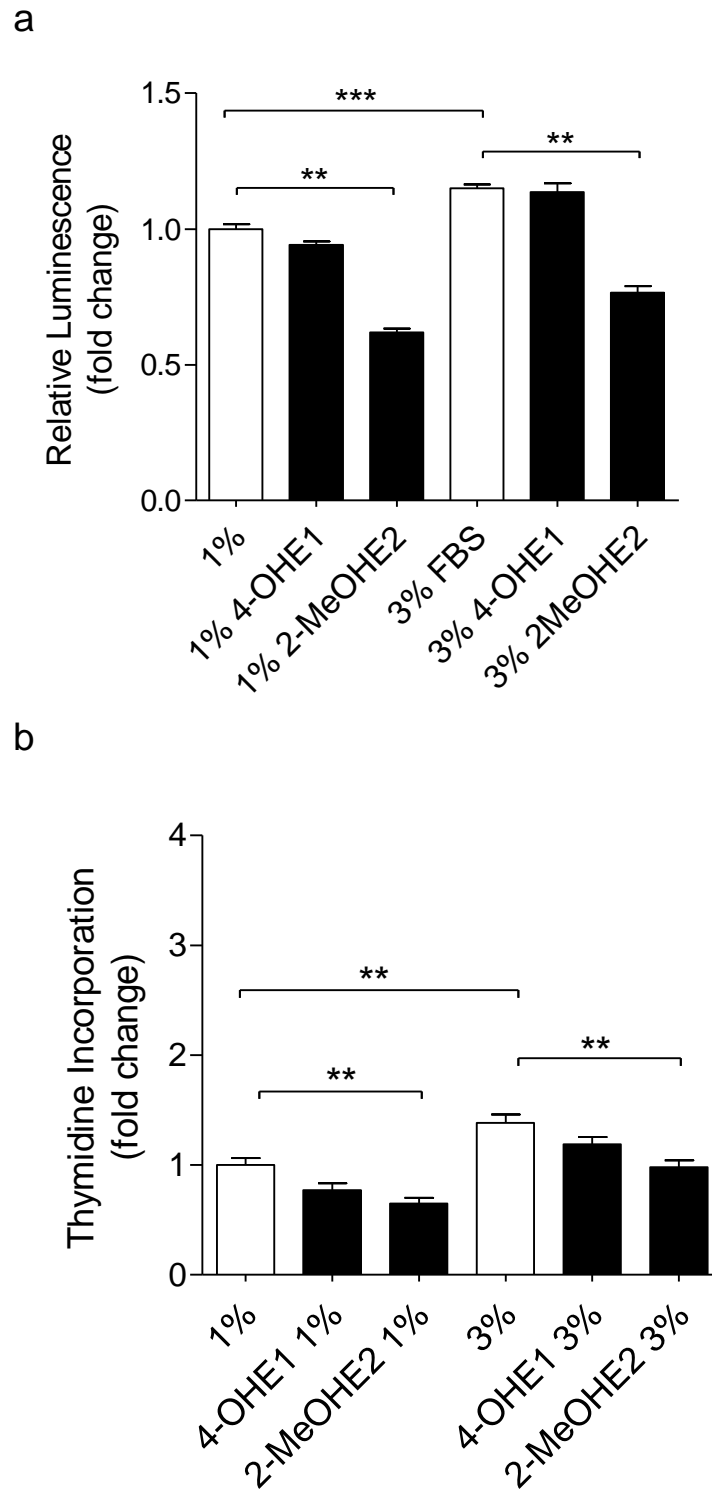


**Figure 4-13 Effect of 4-hydroxyestrone (4-OHE1) and 2-methoxyestradiol (2-MeOHE2) on human pulmonary arterial smooth muscle cell (hPASC) viability and proliferation for 3 days**

Female control hPASCs were quiesced for 24 hours in 0.2% charcoal-stripped FBS (estrogen free) phenol red free DMEM. hPASCs were then incubated with either 4-OHE1 (1 $\mu$ M), 2-MeOHE2 (1 $\mu$ M) or vehicle (0.01% ethanol) for 5 days in 1% or 3% charcoal-stripped FBS phenol red free DMEM and assessed for cell viability with the CellTiter-Glow<sup>®</sup> luminescence assay (a) and cell proliferation by the thymidine incorporation assay (b) n=2, repeated 4 times per cell line. \*\*P<0.01, \*\*\*P<0.001. One-way ANOVA with a Bonferroni's post-hoc test. Data is expressed as the mean  $\pm$  SEM.

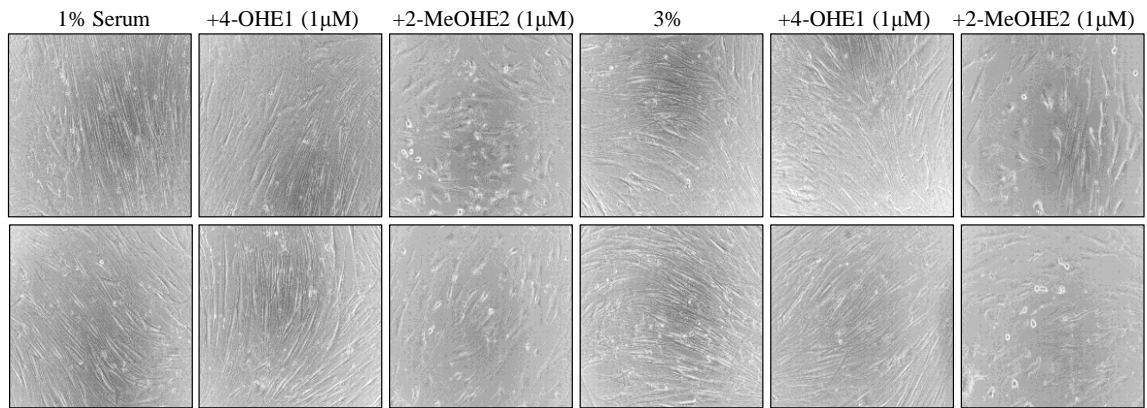


**Figure 4-14 Representative microphotographs of human pulmonary arterial smooth muscle cells (hPASMCs) following incubations with 4-hydroxyestrone (4-OHE1) and 2-methoxyestradiol (2-MeOHE2) for 3 days**

Female control hPASMCs were quiesced for 24 hours in 0.2% charcoal-stripped FBS (estrogen free) phenol red free DMEM. HPASMCs were then incubated with 4-OHE1 (1 $\mu$ M), 2-MeOHE2 (1 $\mu$ M) or vehicle (0.01% ethanol) for 3 days in 1% or 3% charcoal-stripped FBS phenol red free DMEM. Representative images of each condition are shown.

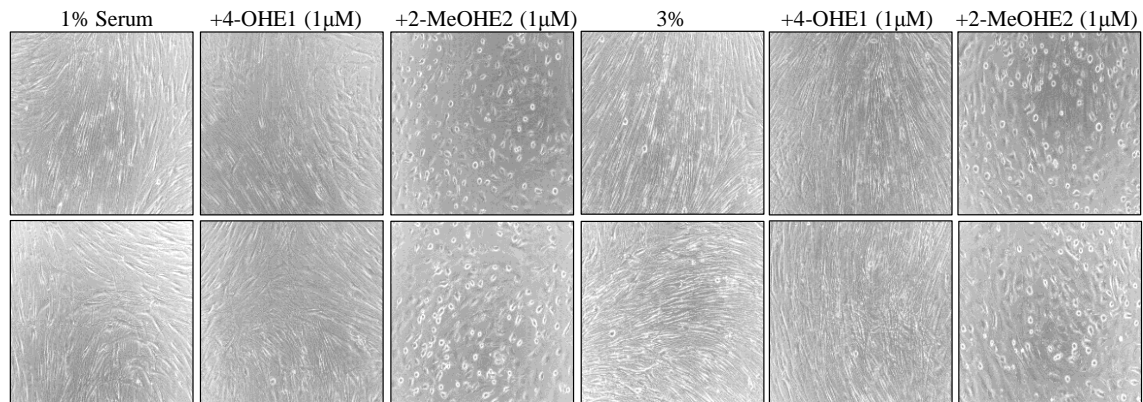


**Figure 4-15 Representative microphotographs of human pulmonary arterial smooth muscle cells (hPASMCs) following incubations with 4-hydroxyestrone (4-OHE1) and 2-methoxyestradiol (2-MeOHE2) for 5 days**

Female control hPASMCs were quiesced for 24 hours in 0.2% charcoal-stripped FBS (estrogen free) phenol red free DMEM. HPASMCs were then incubated with 4-OHE1 (1 $\mu$ M), 2-MeOHE2 (1 $\mu$ M) or vehicle (0.01% ethanol) for 5 days in 1% or 3% charcoal-stripped FBS phenol red free DMEM. Representative images of each condition are shown.

#### **4.2.6 17 $\beta$ -estradiol intracellular levels in human pulmonary arterial smooth muscle cells**

Aromatase is expressed in both murine and human pulmonary arteries, providing evidence for local synthesis of estrogens (Mair *et al.*, 2013). Here, we provide evidence that 17 $\beta$ -E2 is present in abundance in hPASMCs (Figure 4-16). No differences in 17 $\beta$ -E2 levels were observed in patients with PAH compared to control samples. There were also no gender differences. We have recently provided evidence for interactions of the estrogen and serotonin pathways (White *et al.*, 2011b). We were therefore interested in investigating the effects of serotonin on intracellular 17 $\beta$ -E2 concentrations. Serotonin had no effects in any of the groups studied.

#### **4.2.7 Depletion of 17 $\beta$ -estradiol from the extracellular medium in human pulmonary arterial smooth muscle cells**

To directly measure intracellular flux of 17 $\beta$ -E2 in hPASMCs, female control and PAH-hPASMCs were incubated with 17 $\beta$ -E2 and the extracellular medium was collected to analyse the depletion of 17 $\beta$ -E2 at various time-points (Figure 4-17). After ten minutes, there were no differences in the control hPASMCs and the PAH-hPASMCs. After 24 hours, there was substantially less 17 $\beta$ -E2 in the extracellular medium in the PAH hPASMCs in comparison to the control hPASMCs.

#### **4.2.8 Patient characteristics**

Intracellular levels of 17 $\beta$ -E2 was analysed in hPASMCs homogenates from both male and female control and PAH samples. The patients used for these studies are listed in the tables below. We have provided evidence that estrogen metabolism is dysregulated in PH/PAH by increased expression of CYP1B1. We were therefore interested to develop a methodology to quantitatively determine estrogen metabolism in pulmonary vascular cells. Due to the valuable nature of this cell type and time constraints of this project, each experiment was performed in one patient, in duplicate over two separate passages. For clarification, the female control used for this study was a 59 year old female, the male control was a 62 year old male with emphysema, the female PAH patient was a 24 year-old female with IPAH and the male PAH patient was a 43 year-old male with APAH (Eisenmengers syndrome). See Table 4-3 and Table 4-4 for patient characteristics.

**Table 4-3 Patient characteristics of control human pulmonary arterial smooth muscle cells**

<b>Sex</b>	<b>Age</b>	<b>Patient Information</b>	<b>Drug Therapy</b>
F	64	N/A	aspirin
F	58	Mild emphysema	N/A
F	59	N/A	Aspirin, simvastatin, bisoprolol, ramipril, metolazone, wuinine sulphate, loperamide
F	N/A	N/A	N/A
M	72	N/A	N/A
M	62	N/A	N/A
M	76	N/A	N/A
M	N/A	N/A	N/A

**Table 4-4 Patient characteristics of pulmonary arterial hypertension human pulmonary arterial smooth muscle cells**

<b>Sex</b>	<b>Age</b>	<b>Patient Information</b>	<b>mPAP (mmHg)</b>	<b>Drug Therapy</b>
F	24	IPAH	N/A	N/A
F	30	HPAH (R899X mutation)	46	IV prostanoids, warfarin, zopiclone, mebeverine, frusimide
F	33	IPAH	33	IV prostanoids, bosentan, frusemide, adizem
M	43	APAH (Eisenmengers syndrome)	N/A	N/A
M	17	HPAH (W9X mutation)	72	IV prostanoids, warfarin, iloprost

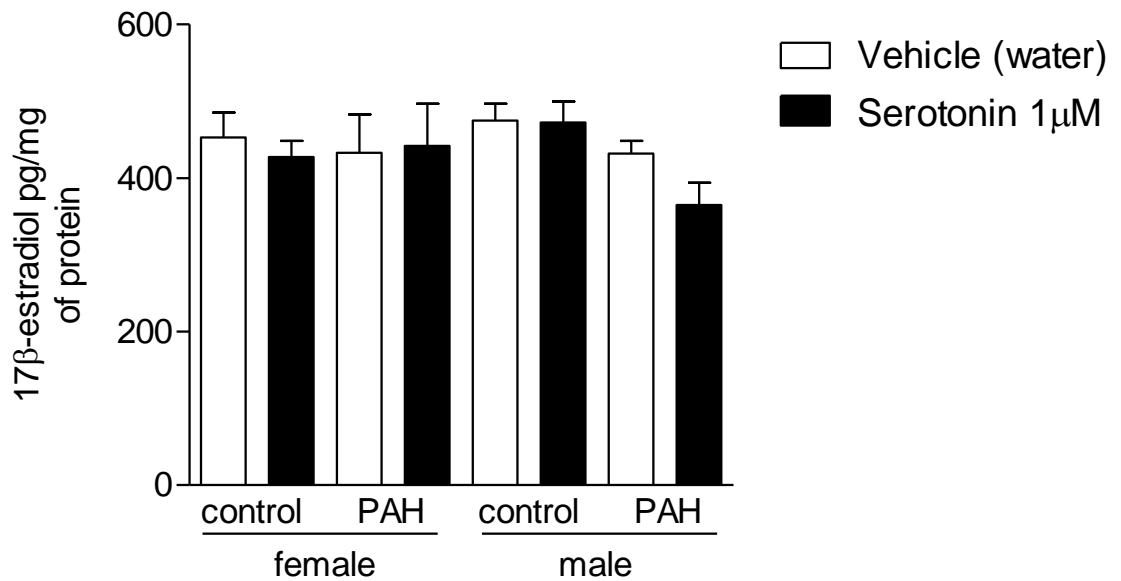


**Figure 4-16 Intracellular 17β-estradiol (17β-E2) concentrations in pulmonary arterial smooth muscle cells (hPASMCs): effect of serotonin**

17β-E2 levels were measured in hPASMCs by ELISA. HPASMCs were grown to 70% confluency and then serum starved in 0.2% charcoal-stripped (estrogen free) DMEM for 24 hours to synchronise the cells. The medium was then changed to 10% charcoal stripped DMEM and maintained under these conditions for 48 hours. The cells were lysed with 1% lauryl maltoside buffer and assayed by ELISA. 50μg of protein was loaded per well. n=2-4 patients per group, assayed in duplicate. One-way ANOVA with a Bonferroni's post-hoc test. Data is expressed as the mean ± SEM.

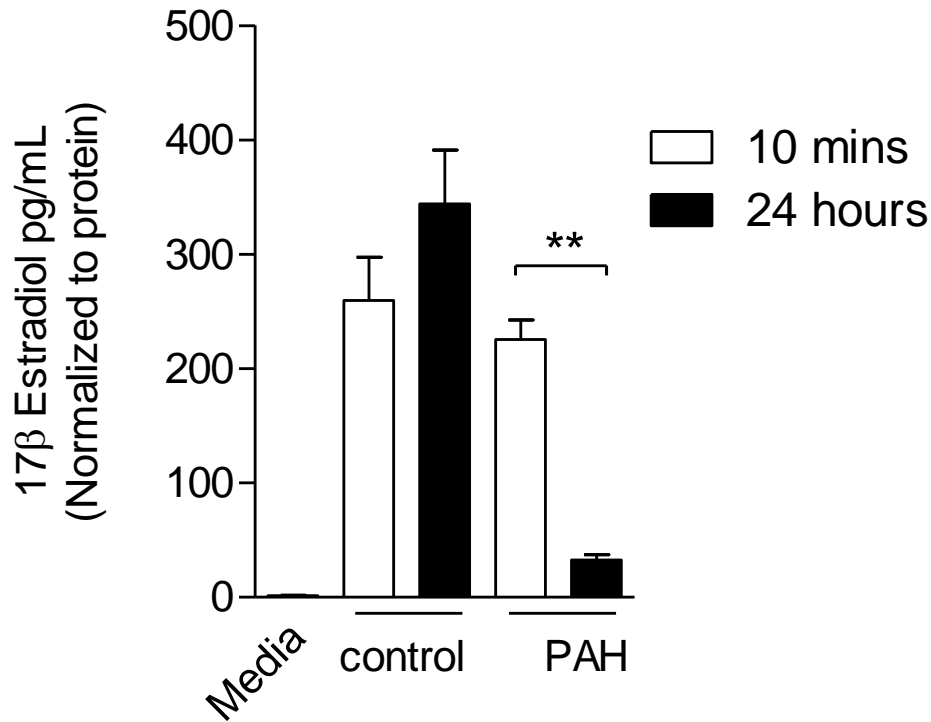


**Figure 4-17 Depletion of 17 $\beta$ -estradiol from the extracellular medium in human pulmonary arterial smooth muscle cells (hPASMCs)**

HPASMCs from a control and PAH patient were incubated with 17 $\beta$ -estradiol (17 $\beta$ E2; 272.38pg/mL) for 10 minutes and 24 hours. Extracellular (medium) levels of 17 $\beta$ -E2 were assayed by ELISA. Basal levels of 17 $\beta$ -E2 in the medium used were almost undetected. The media used for these studies was twice charcoal-stripped (steroid free) phenol-red free DMEM. n=1 patient per group, assayed in duplicate, \*\*P<0.01 t-test comparing the mean  $\pm$ SEM.

### **4.2.9 Absorption profiles of estrogen metabolites by high performance liquid chromatography**

Initially, we identified the unique absorption profiles of the 15 (of the 49 authentic estrogen metabolites of  $17\beta$ -E2 and E1 (Lee *et al.*, 2003)) most prominent estrogen metabolites using an isocratic mobile phase constituted of water (50%), acetonitrile (30%) and methanol (20%) at a flow rate of 1mL per minute at 25°C. Metabolites were separated with a Sunfire C18 5 $\mu$ m, 4.6 x 150mm column (Waters, UK). 100 $\mu$ L of each metabolite at a concentration of 1 $\mu$ g/ml was injected into the HPLC and detected by UV light. Under these conditions, all metabolites were identified within the first 20 minutes (Figure 4-18 - Figure 4-21).

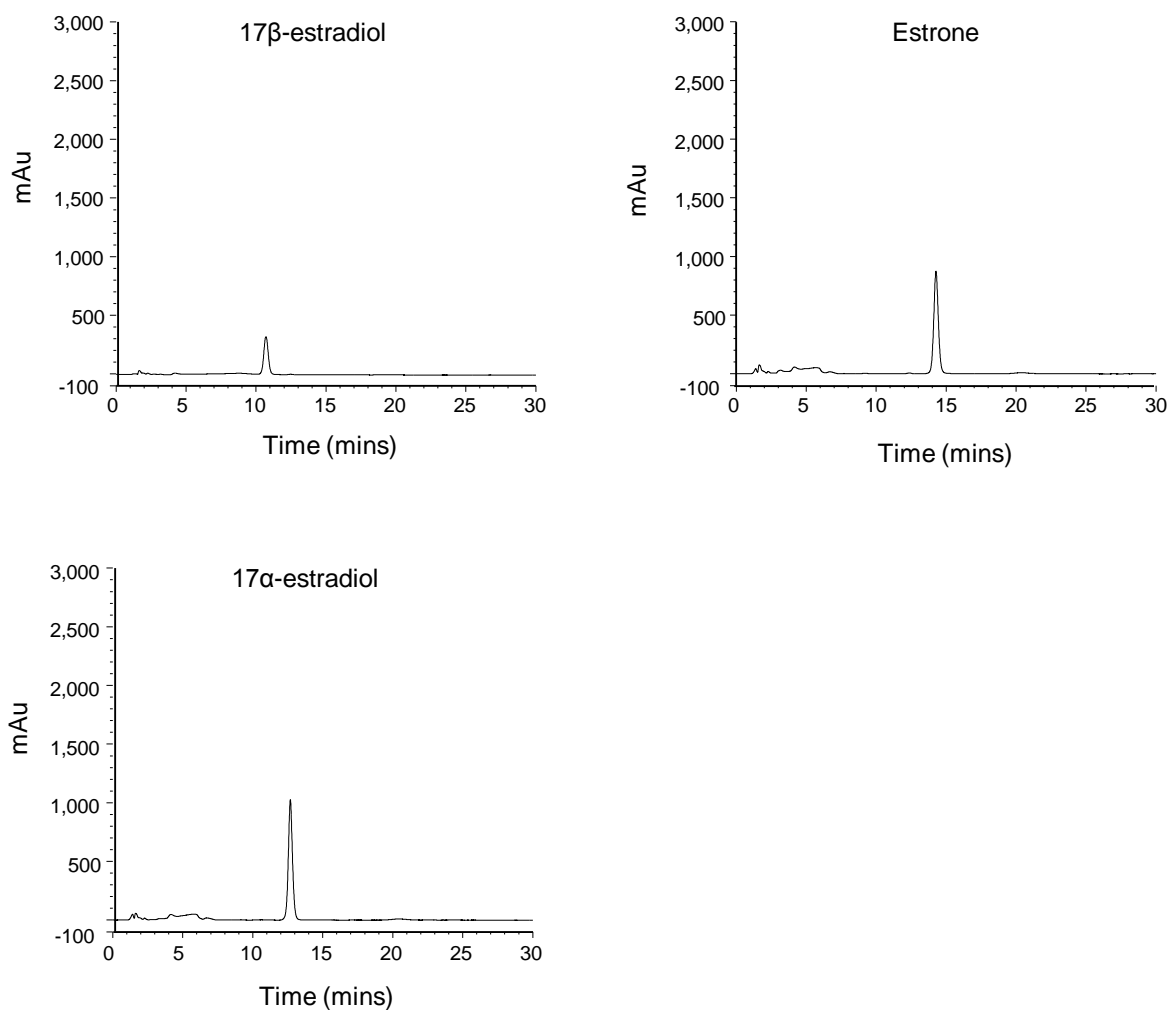


**Figure 4-18 Chromatograms of 17β-estradiol, estrone and 17α-estradiol**

Chromatograms of estrogens following high performance liquid chromatography with ultraviolet absorption ( $\lambda 200\text{nm}$ ). 100 $\mu\text{L}$  of 17β-estradiol, estrone and 17α-estradiol standards at a concentration of 1 $\mu\text{g}/\text{mL}$  was injected onto the Sunfire C18 5 $\mu\text{m}$ , 4.6 x 150mm column and run under isocratic conditions in a mobile phase consisting of water, acetonitrile and methanol in the ratio 50-30-20 at a flow rate of 1mL/min at 25°C. mAu, milli absorbance unit.

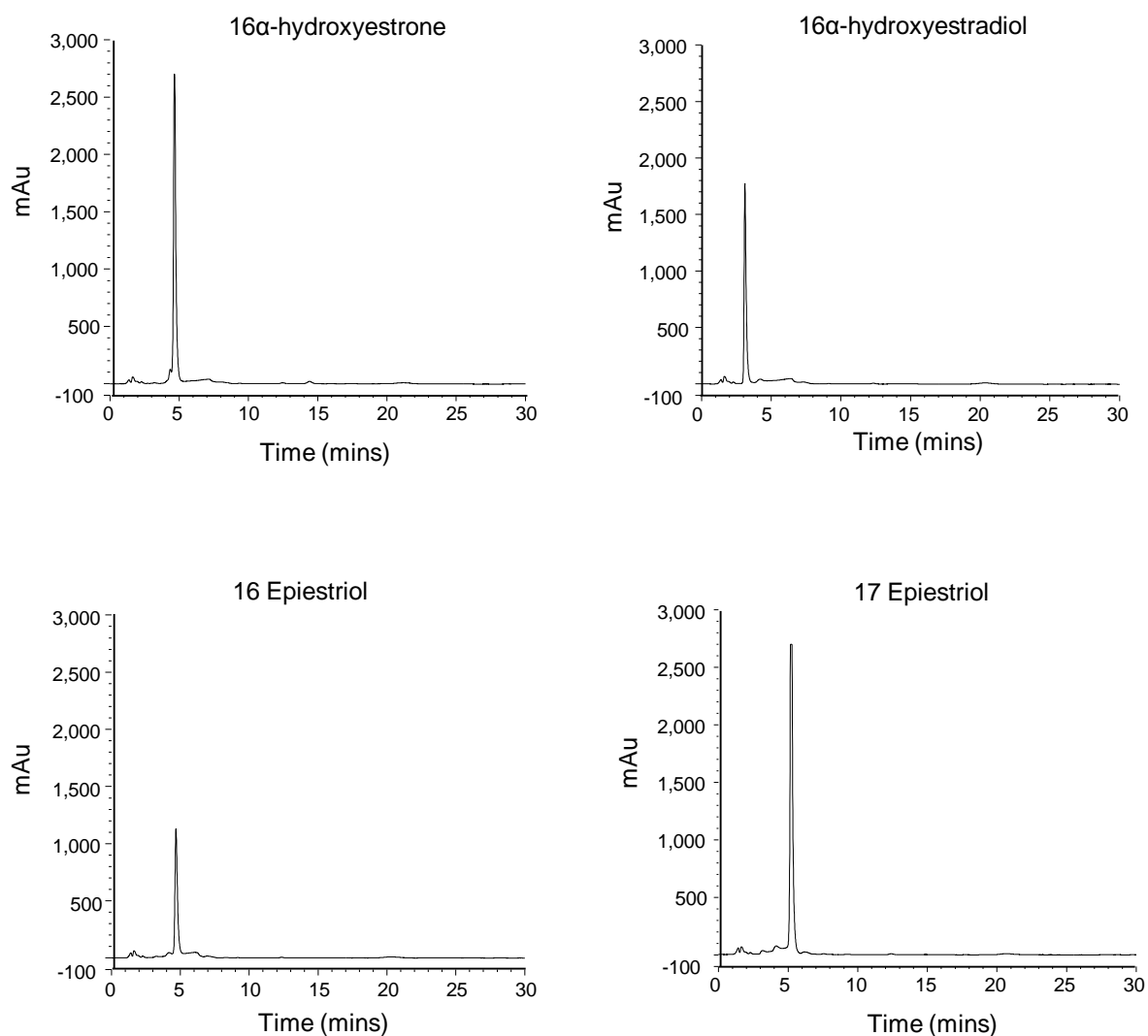


**Figure 4-19 Chromatograms of 16 $\alpha$ -hydroxyestrone, 16 $\alpha$ -hydroxyestradiol, 16 epiestriol and 17 epiestriol**

Chromatograms of estrogens following high performance liquid chromatography with ultraviolet absorption ( $\lambda$ 200nm). 100 $\mu$ L of 16 $\alpha$ -hydroxyestrone, 16 $\alpha$ -hydroxyestradiol, 16 epiestriol and 17 epiestriol standards at a concentration of 1 $\mu$ g/mL was injected onto the Sunfire C18 5 $\mu$ m, 4.6 x 150mm column and run under isocratic conditions in a mobile phase consisting of water, acetonitrile and methanol in the ratio 50-30-20 at a flow rate of 1mL/min at 25 $^{\circ}$ C. mAu, milli absorbance unit.

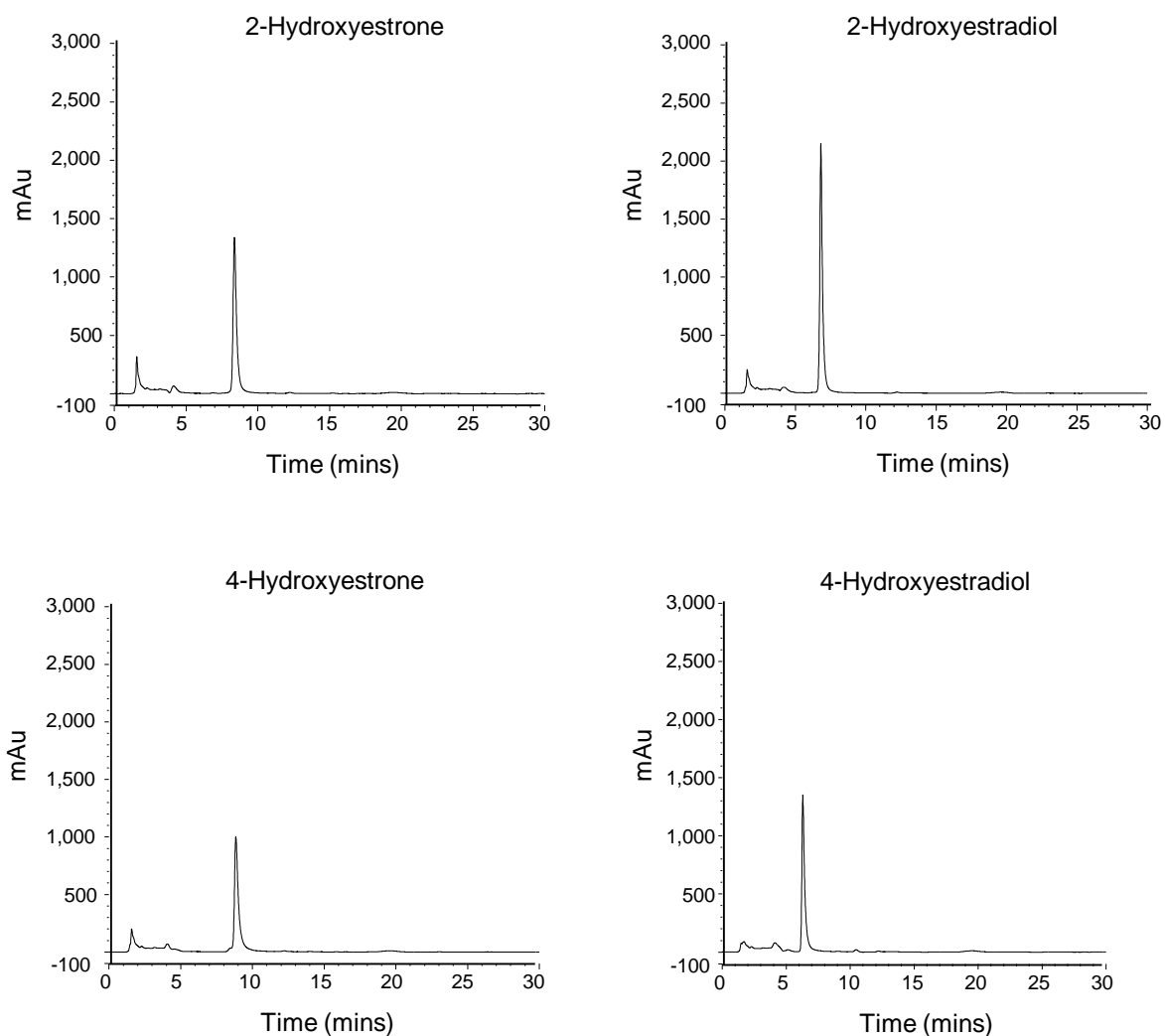


**Figure 4-20 Chromatograms of 2-hydroxyestrone, 2-hydroxyestradiol, 4-hydroxyestrone and 4-hydroxyestradiol**

Chromatograms of estrogens following high performance liquid chromatography with ultraviolet absorption ( $\lambda 200\text{nm}$ ). 100 $\mu\text{L}$  2-hydroxyestrone, 2-hydroxyestradiol, 4-hydroxyestrone and 4-hydroxyestradiol standards at a concentration of 1 $\mu\text{g}/\text{mL}$  was injected onto the Sunfire C18 5 $\mu\text{m}$ , 4.6 x 150mm column and run under isocratic conditions in a mobile phase consisting of water, acetonitrile and methanol in the ratio 50-30-20 at a flow rate of 1mL/min at 25°C. mAu, milli absorbance unit.

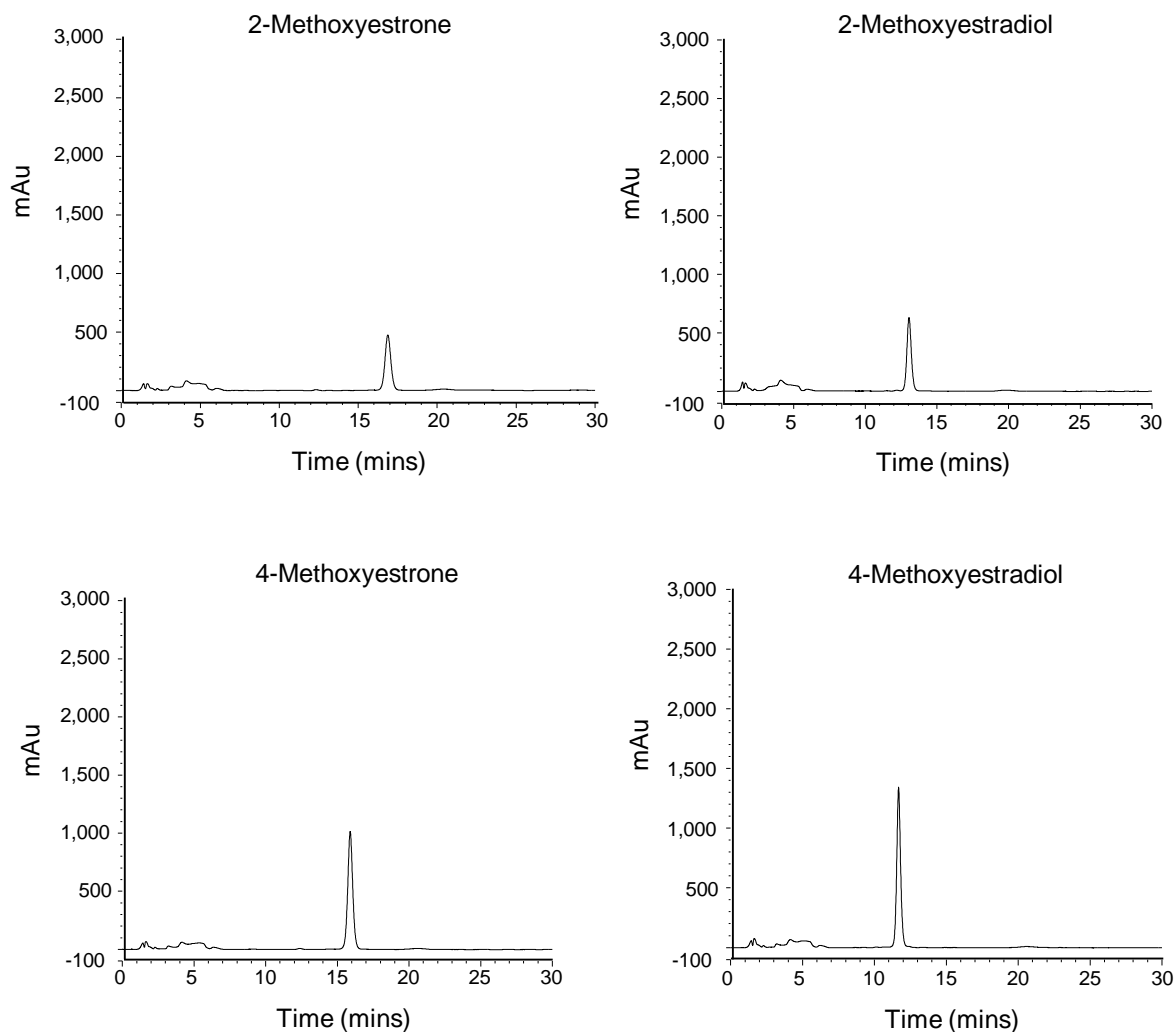


**Figure 4-21 Chromatograms of 2-methoxyestrone, 2-methoxyestradiol, 4-methoxyestrone and 4-methoxyestradiol**

Chromatograms of estrogens following high performance liquid chromatography with ultraviolet absorption ( $\lambda 200\text{nm}$ ).  $100\mu\text{L}$  of 2-methoxyestrone, 2-methoxyestradiol, 4-methoxyestrone and 4-methoxyestradiol standards at a concentration of  $1\mu\text{g/mL}$  was injected onto the Sunfire C18  $5\mu\text{m}$ ,  $4.6 \times 150\text{mm}$  column and run under isocratic conditions in a mobile phase consisting of water, acetonitrile and methanol in the ratio 50-30-20 at a flow rate of  $1\text{mL/min}$  at  $25^\circ\text{C}$ . mAu, milli absorbance unit.

#### 4.2.10 Combined chromatogram of estrogen metabolites

Our goal was to separate all 15 estrogen metabolites in a single chromatographic run to enable comparative analysis. To achieve this, we applied a gradient elution mode (alteration of the mobile phase during the run), which allows for further separation depending on the interaction of the estrogen metabolites with the stationary and mobile phases. This was essential due to the structural similarity of all metabolites.

All estrogen metabolites were successfully separated on gradient elution mode at  $\lambda$ 200nm at 25°C (Figure 4-22). The mobile phase consisted of water, acetonitrile and methanol. The initial mobile phase consisted of 50-10-40 WAM for 1 minute and switched to 55-40-5 over 8 minutes and maintained for 2 minutes in this mobile phase composition. This was changed to 50-30-20 over 1 minute and maintained for 9 minutes. The mobile phase was the reverted back to the initial mobile phase for stabilisation of the UV signal for 10 minutes.

This column allowed for efficient separation for the estrogens with simultaneous detection by the UV system. The programme was initially extremely useful to identify the section of the chromatographic profile where our metabolite peaks formed. However, the widths of the peaks on the radio-labelled HPLC resulted in some difficulties in peak assignment between closely eluting peaks. It was therefore essential to do further method development to suit the different metabolite formation. The samples were therefore also separated with an Allure Biphenyl 5 $\mu$ m, 4.6 x 150mm column (Restek, UK) at 30°C with reverse phase chromatography in isocratic mode using water and methanol in the mobile phase (32% water:78% methanol). All peak integrations for quantification were obtained from the sample run in the Allure Biphenyl column. Peak identification was confirmed using the Sunfire C18 column.

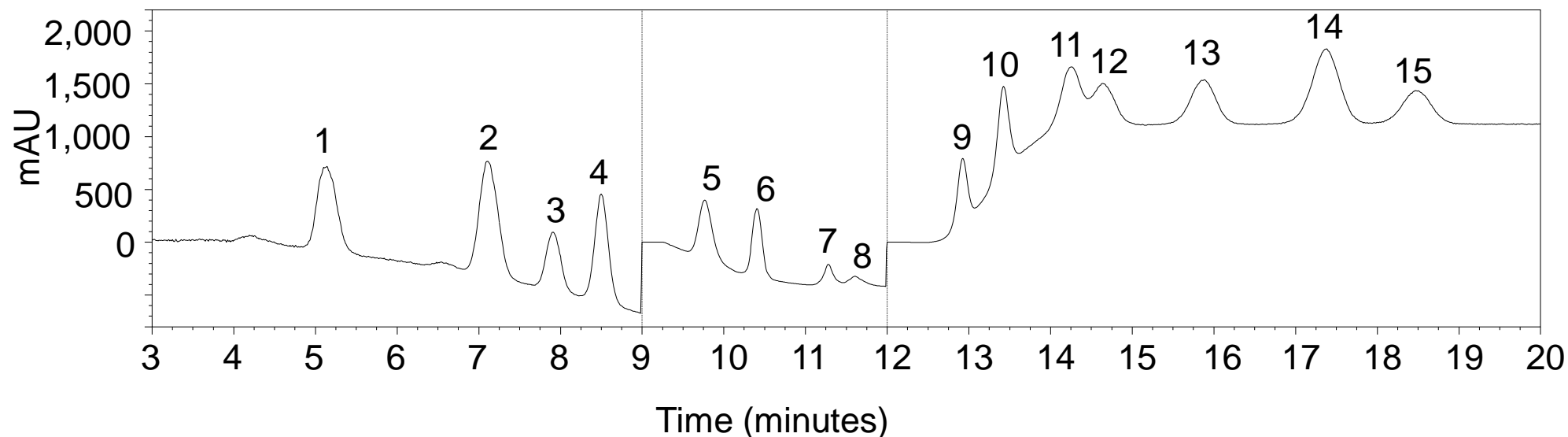


**Figure 4-22 Ultraviolet absorption profiles of the 15 estrogen metabolites with the Sunfire C18 column**

The 15 most prominent estrogen metabolites were separated by high performance liquid chromatography and detected by ultraviolet (UV) absorption in gradient elution mode (the baseline alters due to the variations in absorption during the solvent gradient and was reset at 9 and 12 minutes). The mobile phase consisted of water, acetonitrile and methanol (WAM). The mobile phase was altered to 55-40-4 over a gradient from 1 to 8 minutes and maintained for 2 minutes under these conditions. The mobile phase was then switched to 50-30-20 in a ballistic gradient over 1 minute and maintained in these conditions for a subsequent 9 minutes. The mobile phase was then returned to the initial mobile phase for stabilisation of the UV signal for 10 minutes. (See Table 4-5 for individual peak identification).

**Table 4-5 Estrogen compound retention times on the Sunfire C18 Column**

<b>Peak</b>	<b>Estrogen Compound</b>	<b>Abbreviation</b>	<b>Retention Time (Mins)</b>
1	16 $\alpha$ -Hydroxyestradiol	16 $\alpha$ -OHE2	5.2
2	16 $\alpha$ -Hydroxyestrone	16 $\alpha$ -OHE1	7.2
3	16-Epiestriol	16-epi-E3	8.0
4	17-Epiestriol	17-epi-E3	8.6
5	4-Hydroxyestradiol	4-OHE2	9.8
6	2-Hydroxyestradiol	2-OHE2	10.5
7	2-Hydroxyestrone	2-OHE1	11.4
8	4-Hydroxyestrone	4-OHE1	11.7
9	17 $\beta$ -Estradiol	17 $\beta$ -E2	12.9
10	4-Methoxyestradiol	4-MeOHE2	13.5
11	17 $\alpha$ -Estradiol	17 $\alpha$ -E2	14.3
12	2-Methoxyestradiol	2-MeOHE2	14.8
13	Estrone	E1	16.0
14	4-Methoxyestrone	4-MeOHE1	17.5
15	2-Methoxyestrone	2-MeOHE1	18.6

#### 4.2.11 Extraction of estrogen metabolites-method development

Estrogen metabolites are hydrophobic compounds that require extraction from their sample matrix (to remove non-specific interference) by either SPE or solvent extractions. The goal was to identify the most efficient method to extract all the 15 estrogen metabolites with the best recoveries. For the solvent extractions, we tested ethyl acetate, dichloromethane and ether in the ratios (aqueous: solvent) 1:1, 1:5, 1:10 with the sample medium (not all sample extractions were successful). Extraction recoveries of the 15 standards were assessed by comparisons of extracted samples with samples without an extraction step and samples where the estrogen standards were added after the extraction (See Chapter 2). The recoveries of the estrogens using solvent extractions was inconsistent and relatively poor (Figure 4-23-Figure 4-25; ranging from 0 – 95% recoveries, although only few metabolites were recovered to this level). We tested the application of SPE to extract our samples using Oasis® HLB columns (Waters, UK). This was also an advantage due to the large sample volumes (10ml) that we were working with. The extraction recoveries using the Oasis® HLB columns were consistent across all estrogen metabolites and had excellent recoveries (85 - 100%; Figure 4-26). This was therefore our chosen extraction method for all samples. The extractions were much more consistent in the pre-spiked vs. post-spiked samples compared to the pre-spiked vs. the control samples. The former is however the most representative as both samples contain the sample matrix (the cell culture medium) which may affect the chromatographic profile.

#### 4.2.12 Extraction and recovery of <sup>14</sup>C-17β-estradiol

We had developed a robust methodology for the extraction of the estrogen metabolites. We confirmed that this methodology was equally efficient at extracting radiolabelled 17β-E2 (<sup>14</sup>C-17β-E2; Figure 4-27).

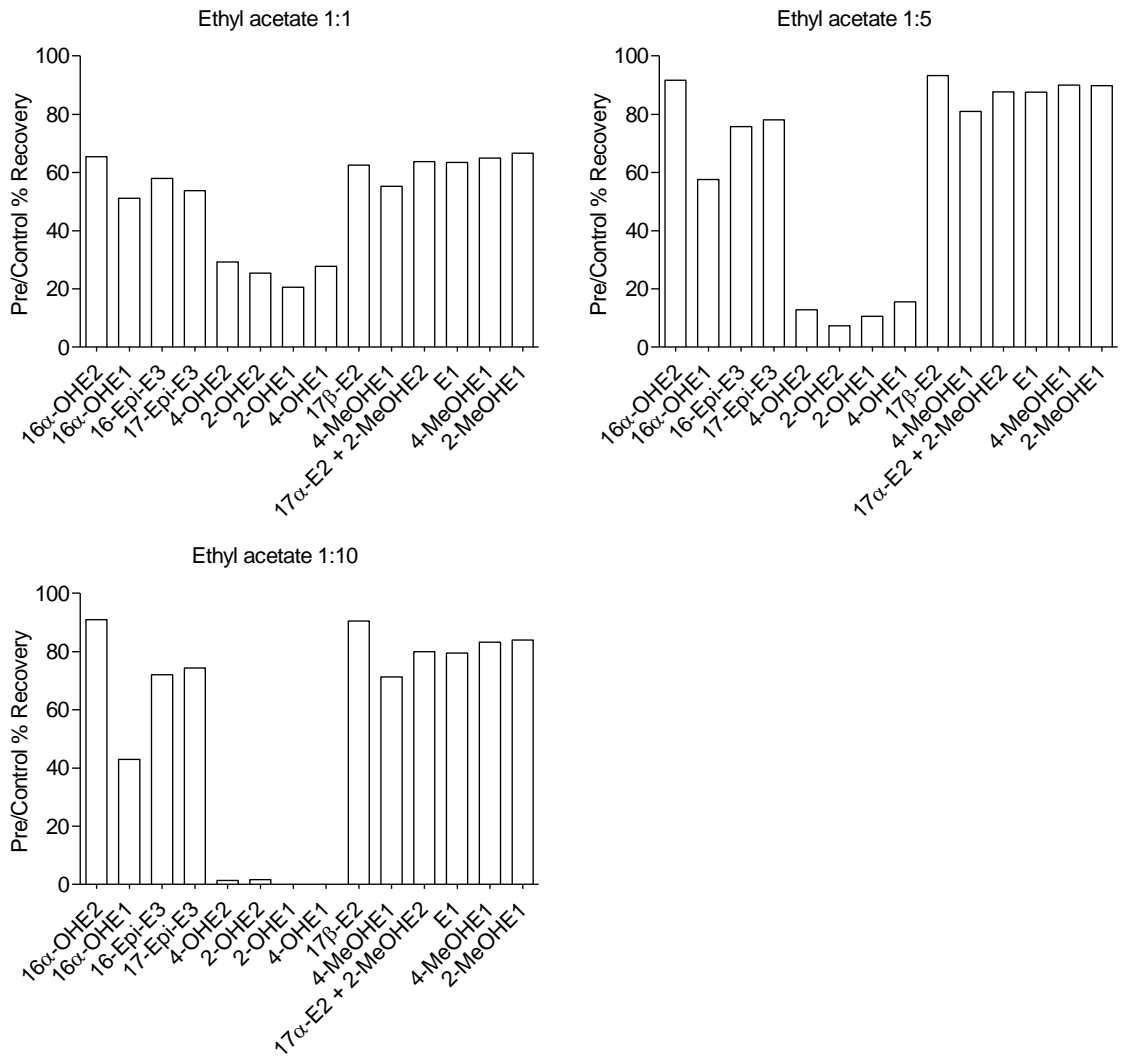


**Figure 4-23 Extraction recoveries of estrogen metabolites with a ethyl acetate solvent extraction**

Estrogen metabolite extractions was assessed with a solvent extraction using ethyl acetate in the ratios 1:1, 1:5 and 1:10 (sample: ethyl acetate) and the percentage extraction recoveries were calculated. Estrogen metabolites (2.5µg of each metabolite) were added to the sample matrix (1% charcoal-stripped phenol red free DMEM) and then extracted using ethyl acetate. Percentage recoveries were calculated by expressing the extracted metabolite over the un-extracted metabolite (control). n=3

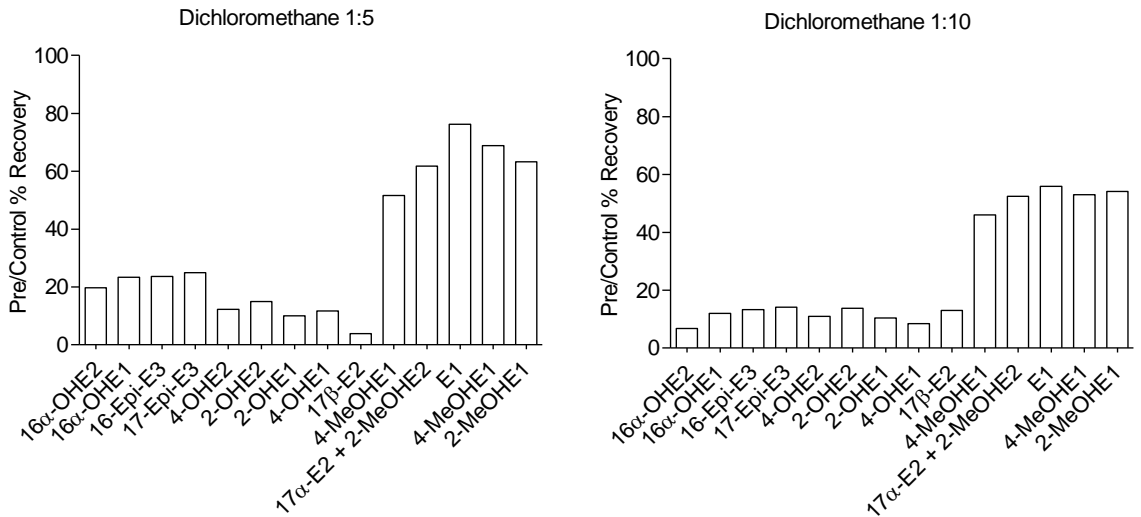


**Figure 4-24 Extraction recoveries of estrogen metabolites with a dichloromethane solvent extraction**

Estrogen metabolite extractions was assessed with a solvent extraction using dichloromethane in the ratios 1:5 and 1:10 (sample: dichloromethane) and the percentage extraction recoveries were calculated. Estrogen metabolites (2.5 $\mu$ g of each metabolite) were added to the sample matrix (1% charcoal-stripped phenol red free DMEM) and then extracted using dichloromethane. Percentage recoveries were calculated by expressing the extracted metabolite over the un-extracted metabolite (control). n=3

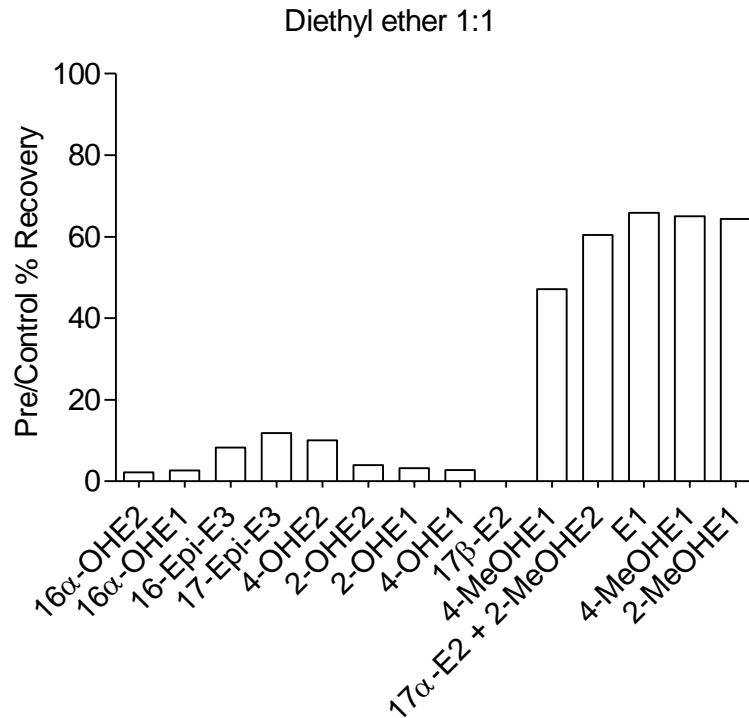


**Figure 4-25 Extraction recoveries of estrogen metabolites with a diethyl ether solvent extraction**

Estrogen metabolite extractions was assessed with a solvent extraction using diethyl ether in the ratios 1:1, 1:5 and 1:10 (sample: diethyl ether) and the percentage extraction recoveries were calculated. Estrogen metabolites (2.5µg of each metabolite) were added to the sample matrix (1% charcoal-stripped phenol red free DMEM) and then extracted using diethyl ether. Percentage recoveries were calculated by expressing the extracted metabolite over the un-extracted metabolite (control). n=3

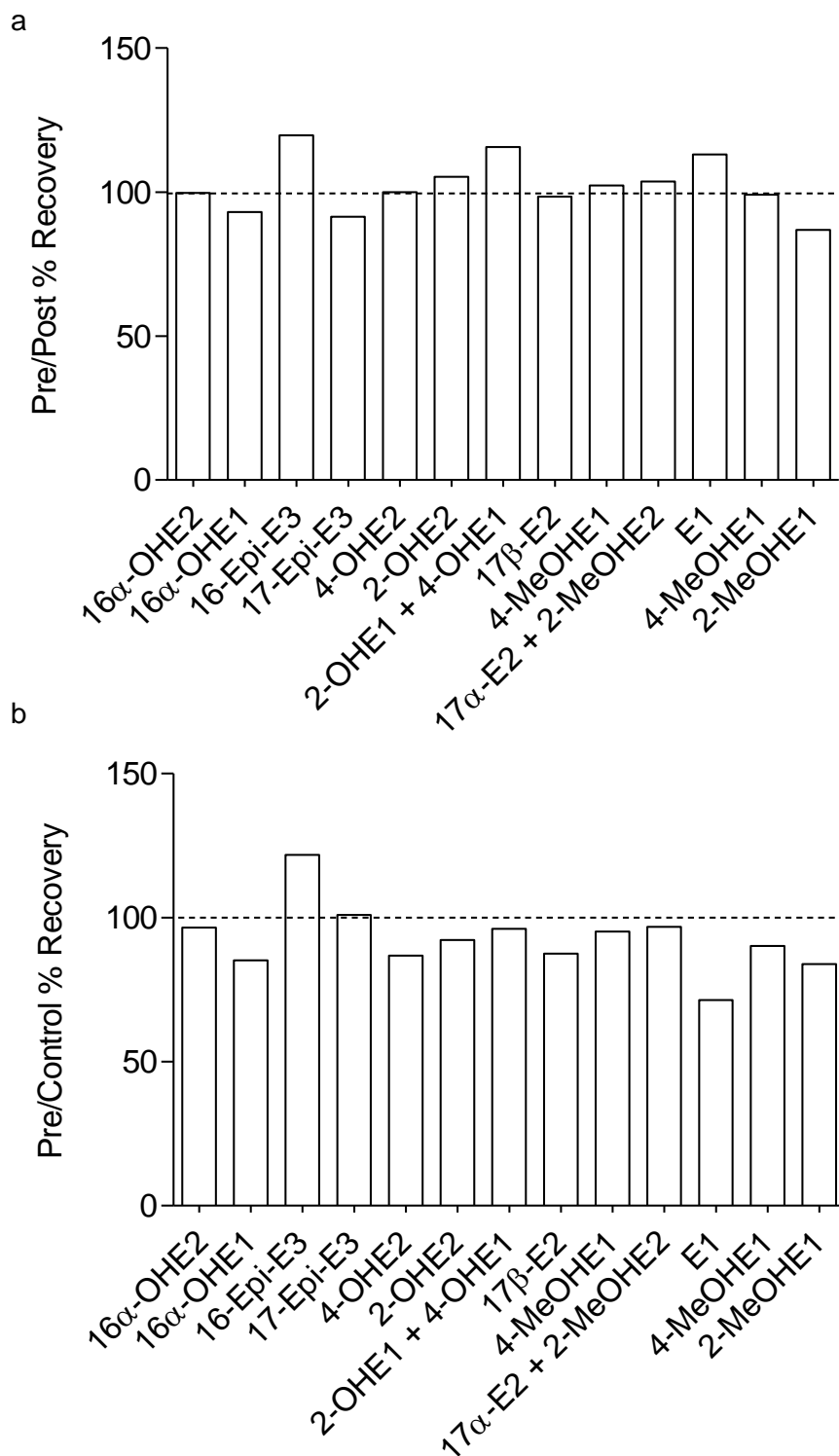


**Figure 4-26 Extraction recovery of estrogen metabolites using Oasis® HLB columns**

Estrogen metabolite extractions were assessed by solid phase extraction using the Oasis® HLB columns and the percentage extraction recoveries were calculated. Estrogen metabolites (2.5 $\mu$ g of each metabolite) were added to the sample matrix (1% charcoal-stripped phenol red free DMEM) either before (pre-spiked) or after the extraction (post-spiked). Percentage recoveries were calculated by expressing the extracted metabolite over the un-extracted metabolite (control) or the post-spiked sample. Extraction recoveries of estrogen metabolites in pre-spiked samples vs. post-spiked samples (a). Extraction recoveries in pre-spiked samples vs. control samples (b). A few peaks merged together making it more suitable to analyze the peaks together. Each extraction was performed in duplicate.

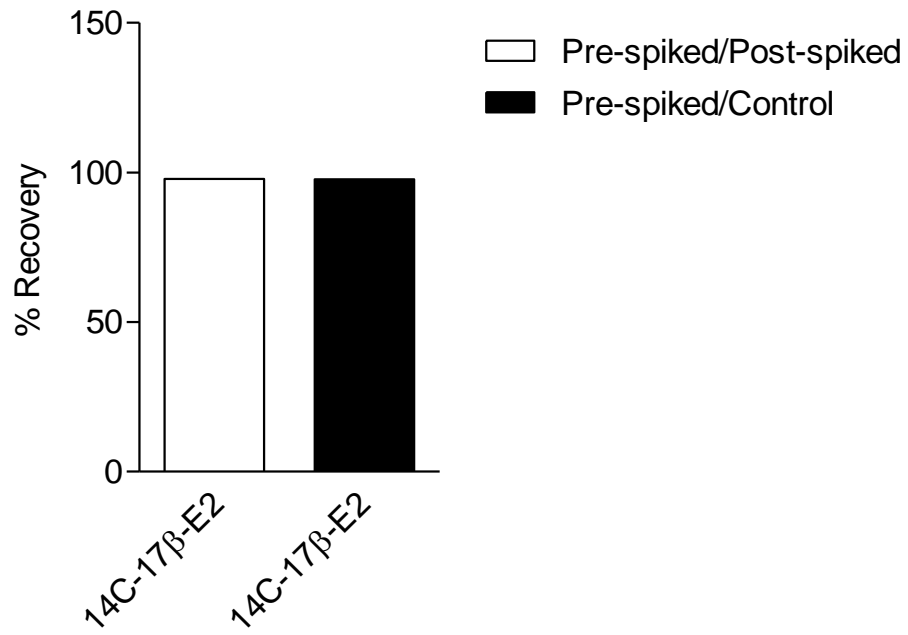


**Figure 4-27 Percentage extraction recovery of radiolabelled 17β-estradiol**

Extraction recovery of radiolabelled 17β-estradiol (14C-17β-E2) using Oasis® HLB columns. Pre-spiked samples represent samples where the estrogen metabolites were added prior to extraction. In the post-spiked samples, the estrogen metabolites were added after the extraction and in the control sample, there was no extraction. Each extraction was performed in triplicate.

### 4.2.13 Estrogen metabolism over time in human pulmonary arterial smooth muscle cells

For clarity, this data is presented in two ways. Firstly, the data is represented as the depletion of  $17\beta$ -E2 and metabolite formation over time in individual cell lines and secondly, the data is represented as comparisons across female and male, control and PAH hPASCs within each time-point.

In female control hPASCs (Figure 4-28) there was no evidence of enzymatic activity between 10 minutes and 1 hour. After 2 hours, there was a small amount of E1 present within the sample. This implicates activity of  $17\beta$ -HSD2, which converts  $17\beta$ -E2 to E1. This gradually increased over time until 48 hours where ~50% of the  $17\beta$ -E2 had been converted to E1. This was the only metabolite that appeared in female control hPASCs.

In male control hPASCs (Figure 4-29) there was substantially more enzymatic activity in comparison to female control hPASCs. After 10 minutes, E1 and the 2 and 4-methoxylated estrogens were present within the samples. This indicates activity of  $17\beta$ -HSD2, CYP and COMT. Whilst there were no hydroxylated metabolites present within the sample, the presence of methoxylated estrogens provides evidence that hydroxylated estrogens had been formed prior to the sample collection. Over time, there was direct evidence of  $17\beta$ -HSD2, CYP and COMT activities with the most abundant metabolite formed being E1. After 1 hour incubation, ~50% of the parent  $17\beta$ -E2 had been metabolised (predominantly to E1). After 48 hours, there was no  $17\beta$ -E2 left within the sample. Interestingly, formation of 17-Epi-E3 was observed at 30 minutes, yet was undetected at any other time-point.

In female PAH hPASCs (Figure 4-30), there was evidence of 2-hydroxylation and methylation as well as  $17\beta$ -HSD2 activity between the time-points 10 minutes and 2 hours. At 4 hours, ~50% of the  $17\beta$ -E2 had been metabolized and there was evidence of 4-hydroxylation and methylation activities. Again, the most predominant metabolite was E1. Interestingly at 24 hours and 48 hours, 16-hydroxylated estrogens, predominantly  $16\alpha$ -OHE1 appeared within the sample, increasing with time.

In male PAH-hPASCs (Figure 4-31),  $17\beta$ -E2 was converted to E1 and  $4$ -OHE1 between 10 minutes and 4 hours. At 24 hours, ~50% of the parent  $17\beta$ -E2 had been metabolized. Here there was a small formation of  $16\alpha$ -OHE2 which increased at 48 hours. At 48 hours, there was also a small formation of  $16\alpha$ -OHE1. In this cell line, there was no evidence of

COMT activity as no methylated metabolites were observed. As with the other cell lines, the predominant metabolite formation was E1.

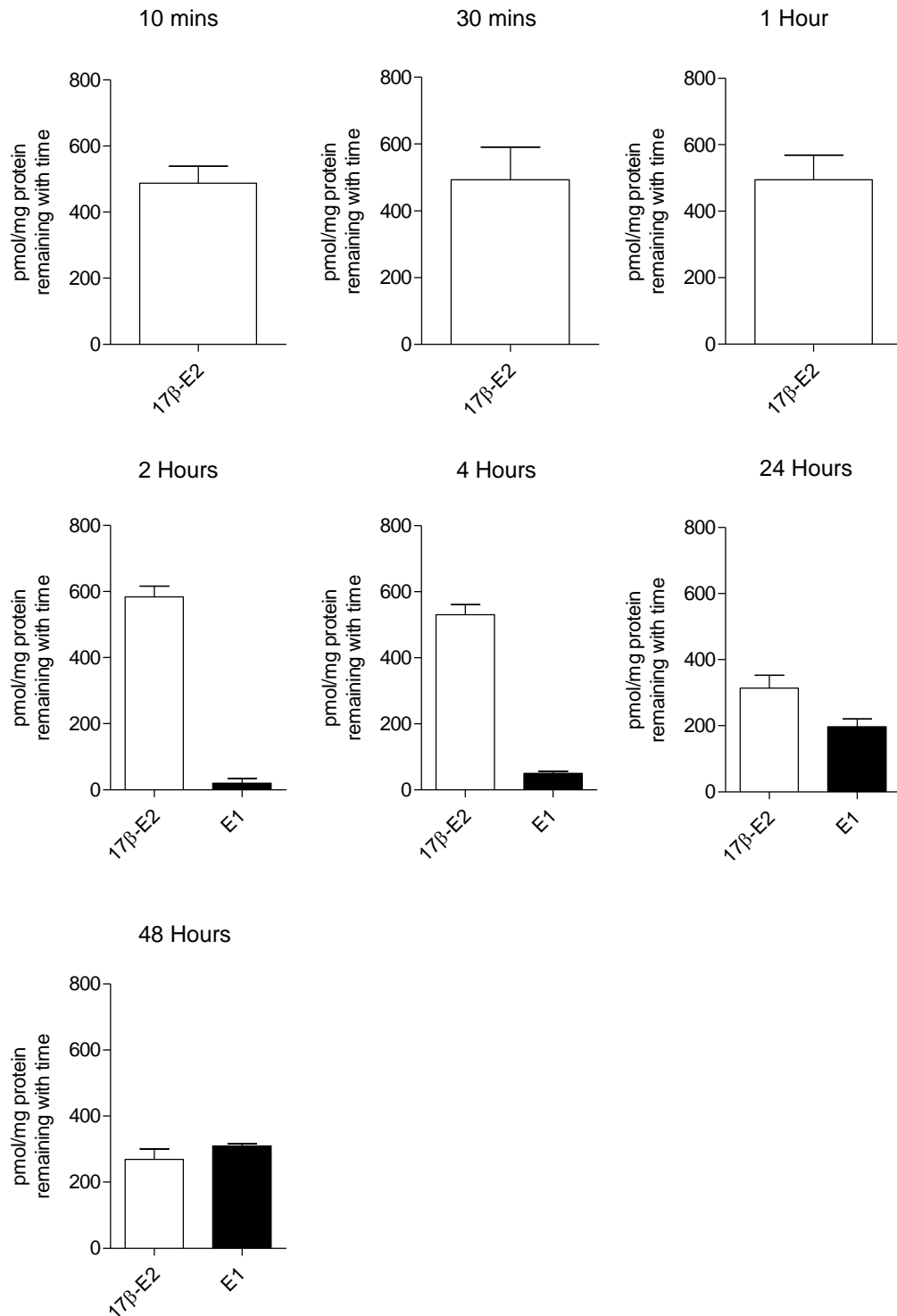


**Figure 4-28 Metabolism of 17β-estradiol over time in control female human pulmonary arterial smooth muscle cells (PASCs)**

Female control (59 year-old) PASCs were incubated with 17β-estradiol (17β-E2; 50nM, 136.19ng) for various time-points in 1% charcoal-stripped (estrogen-free) phenol red free DMEM. Samples were extracted by solid phase extraction with Oasis® HLB cartridges and analyzed by HPLC with ultra-violet and radiolabeled detection. n=1 patient, repeated twice in different passages.

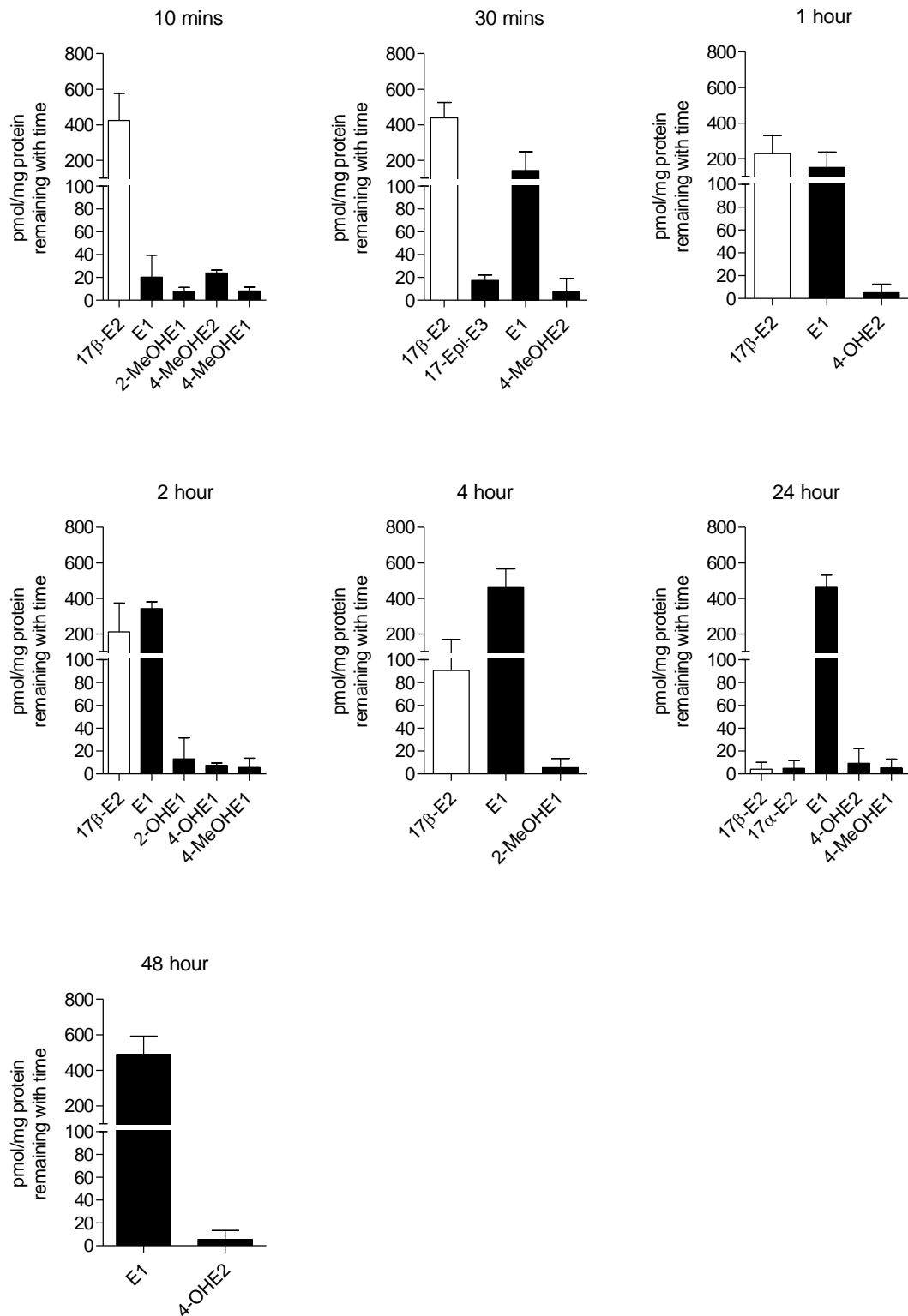


**Figure 4-29 Metabolism of 17β-estradiol over time in control male human pulmonary arterial smooth muscle cells (PASMCs)**

Male control (62 year-old) PASMCs were incubated with 17β-estradiol (17β-E2; 50nM, 136.19ng) for various time-points in 1% charcoal-stripped (estrogen-free) phenol red free DMEM. Samples were extracted by solid phase extraction with Oasis® HLB cartridges and analyzed by HPLC with ultra-violet and radiolabeled detection. n=1 patient, repeated twice in different passages.

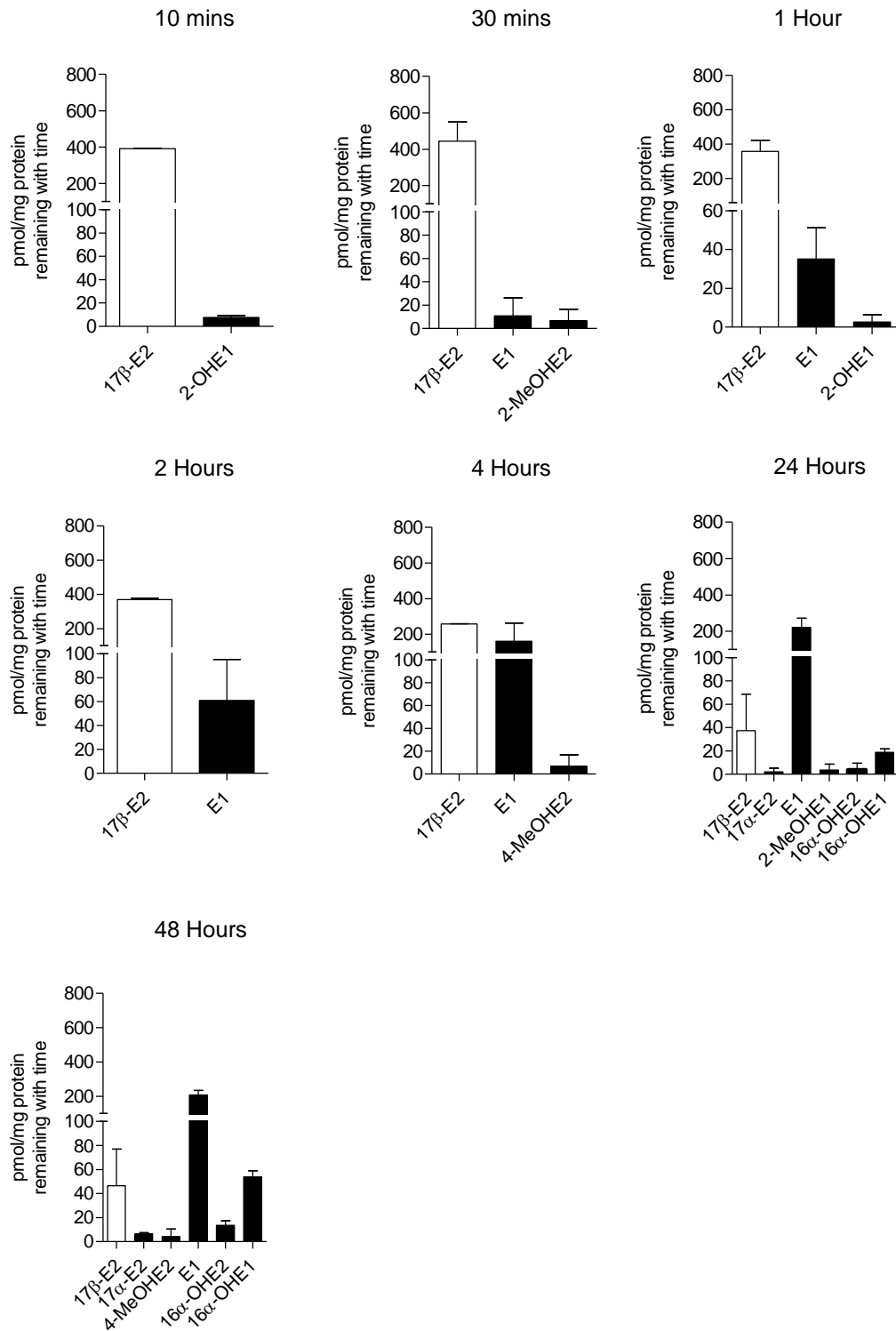


**Figure 4-30 Metabolism of 17β-estradiol over time in PAH female human pulmonary arterial smooth muscle cells (PASMCs)**

Female PAH (24 year-old with IPAH) PASMCs were incubated with 17β-estradiol (17β-E2; 50nM, 136.19ng) for various time-points in 1% charcoal-stripped (estrogen-free) phenol red free DMEM. Samples were extracted by solid phase extraction with Oasis® HLB cartridges and analyzed by HPLC with ultra-violet and radiolabeled detection. n=1 patient, repeated twice in different passages.

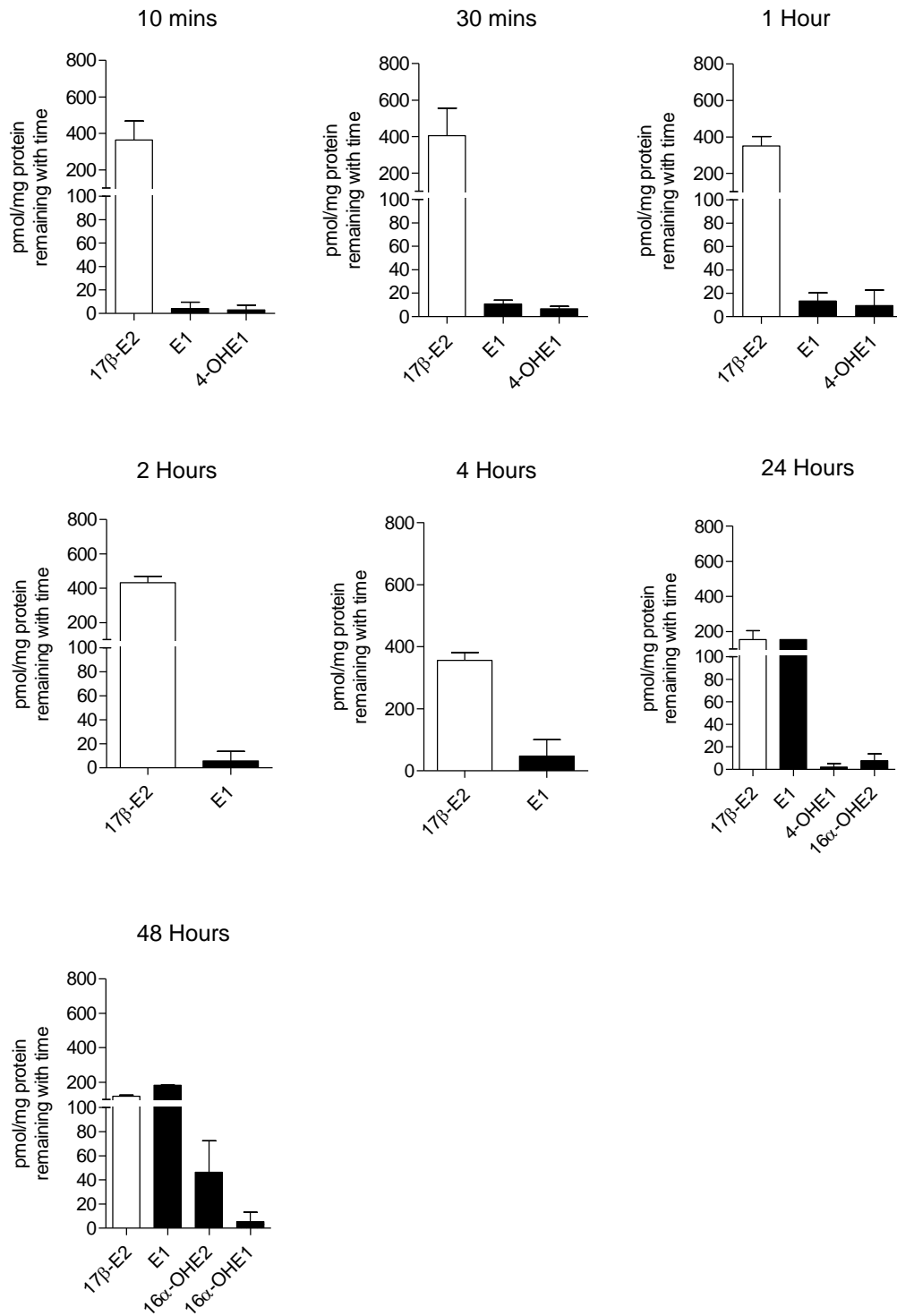


**Figure 4-31 Metabolism of 17β-estradiol over time in PAH male human pulmonary arterial smooth muscle cells (PASCs)**

Male PAH (43 year-old with APAH) PASCs were incubated with 17β-estradiol (17β-E2; 50nM, 136.19ng) for various time-points in 1% charcoal-stripped (estrogen-free) phenol red free DMEM. Samples were extracted by solid phase extraction with Oasis® HLB cartridges and analyzed by HPLC with ultra-violet and radiolabeled detection. n=1 patient, repeated twice in different passages.

#### 4.2.14 Evidence for an altered estrogen metabolic profile in pulmonary arterial hypertension

HPASMCs from both female and male, control and PAH (Figure 4-32 - Figure 4-38) actively metabolize  $17\beta$ -E2, with key differences in rates and product formation. In all the groups studied the metabolic screen indicates a prominent role for  $17\beta$ -HSD2. Interestingly, the rate at which E1 was formed was highly variable with the highest rate in male control hPASMCs followed by female PAH-PASMCs and then male PAH hPASMCs. The lowest rate of conversion was evident in female control hPASMCs.

Whilst male control, female PAH and male PAH hPASMCs displayed evidence for CYP activity, there was no measurable CYP activity in female control hPASMCs. In fact, there was no observable enzymatic activity in female controls apart from the formation of E1. Both male control and female PAH hPASMCs demonstrated COMT activity; this was undetected in male PAH hPASMCs. Male control hPASMCs metabolised  $17\beta$ -E2 to both the 2- and 4-hydroxyestrogens and methoxyestrogens. In female PAH hPASMCs,  $17\beta$ -E2 was also metabolized to the 2- and 4-hydroxyestrogens. However, the metabolic profile after 24 and 48 hours revealed a clear formation of the pathogenic CYP metabolite,  $16\alpha$ -OHE1 (7% at 24 hours and 16% at 48 hours). In addition, there was a small formation of  $16\alpha$ -OHE2 (1% at 24 hours and 4% at 24 hours). In male PAH hPASMCs, there was no evidence for 2-hydroxy/methylation. However, there was evidence of 4-hydroxylation and the predominant CYP metabolite formed at 24 and 48 hours was  $16\alpha$ -OHE2 (2% and 13% respectively). Key enzymatic activities within each cell line have been summarized in Table 4-6.

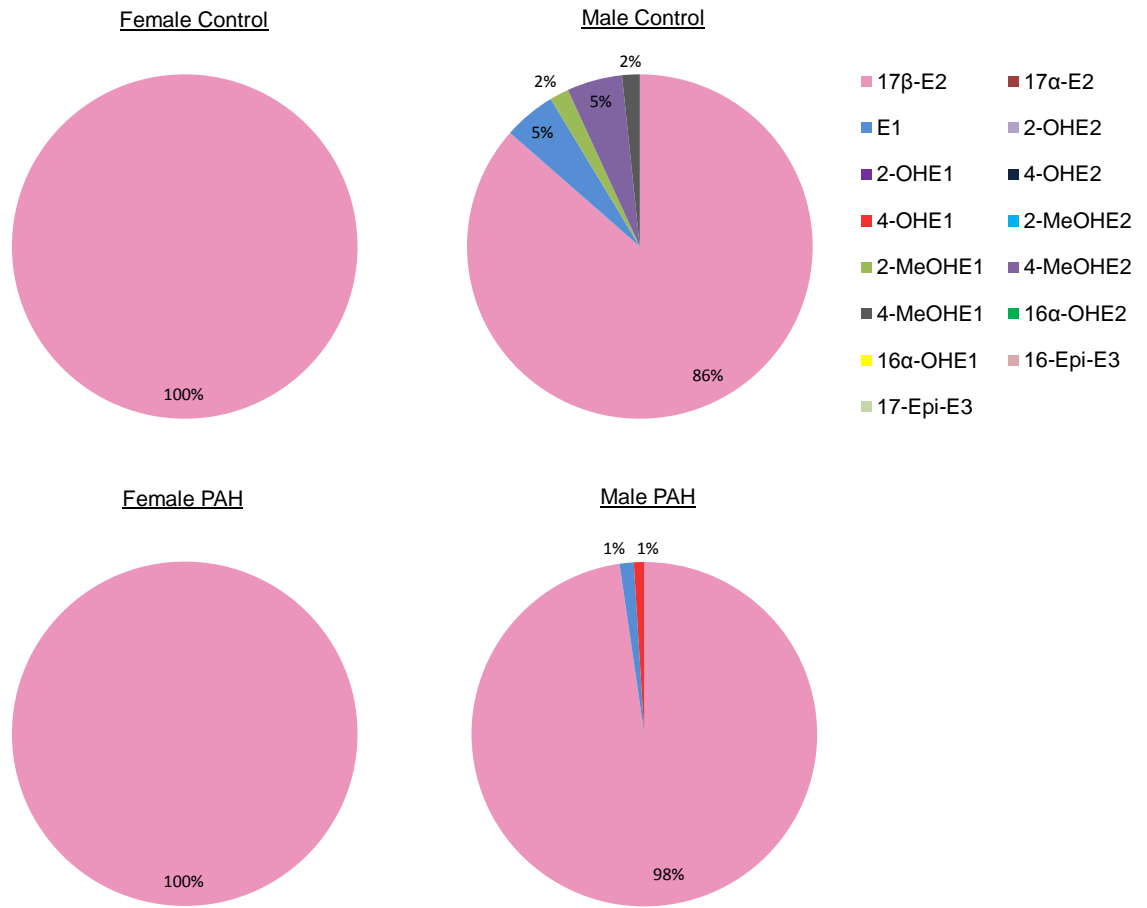


**Figure 4-32 Estrogen metabolic profile in control- and pulmonary arterial hypertension-pulmonary arterial smooth muscle (PASCs) cells after 10 minutes**

Female and male, control and PAH PASCs were incubated with 17β-estradiol (17β-E2; 50nM, 136.19ng) for 10 minutes in 1% charcoal-stripped (estrogen-free) phenol red free DMEM. Samples were extracted by solid phase extraction with Oasis® HLB cartridges and analyzed by HPLC with ultra-violet and radiolabeled detection. n=1 patient per group, repeated twice in different passages.

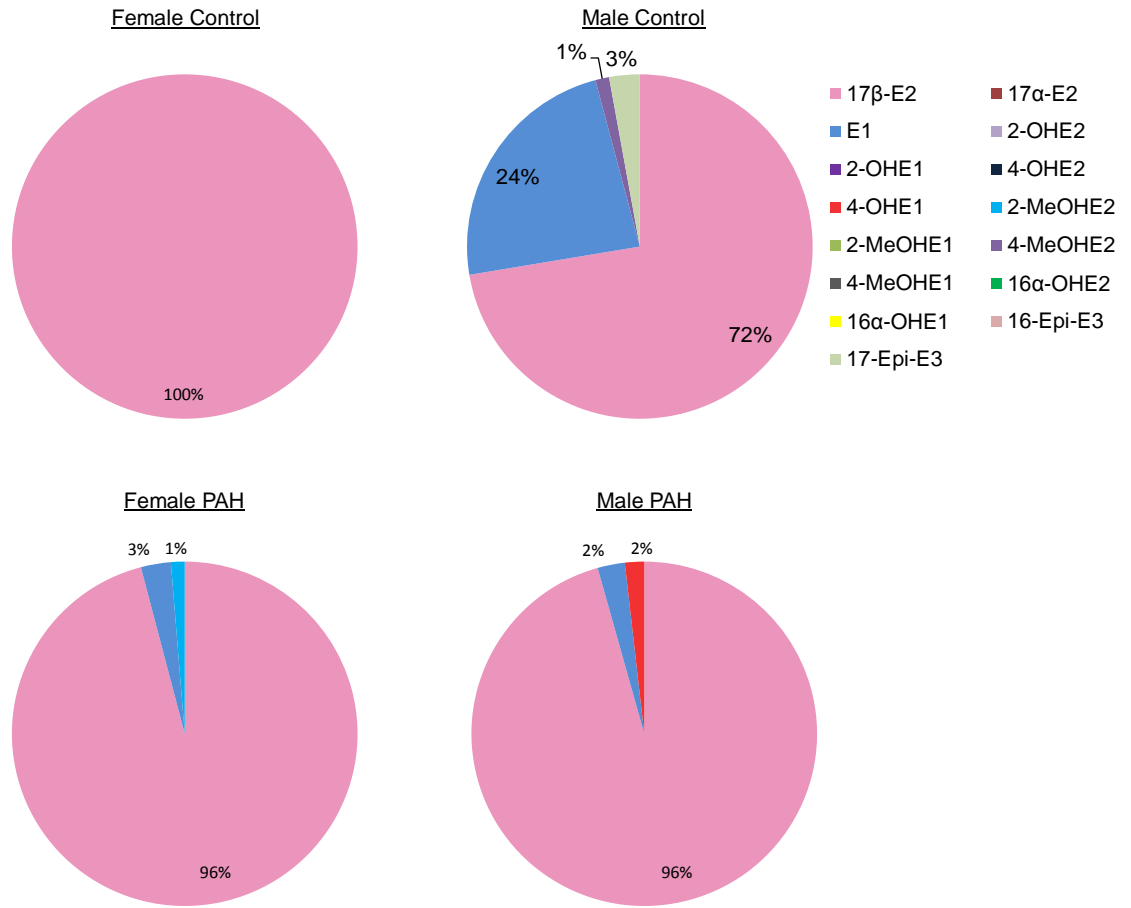


**Figure 4-33 Estrogen metabolic profile in control- and pulmonary arterial hypertension-pulmonary arterial smooth muscle cells (PASMCs) after 30 minutes**

Female and male, control and PAH PASMCs were incubated with 17β-estradiol (17β-E2; 50nM, 136.19ng) for 30 minutes in 1% charcoal-stripped (estrogen-free) phenol red free DMEM. Samples were extracted by solid phase extraction with Oasis® HLB cartridges and analyzed by HPLC with ultra-violet and radiolabeled detection. n=1 patient per group, repeated twice in different passages.

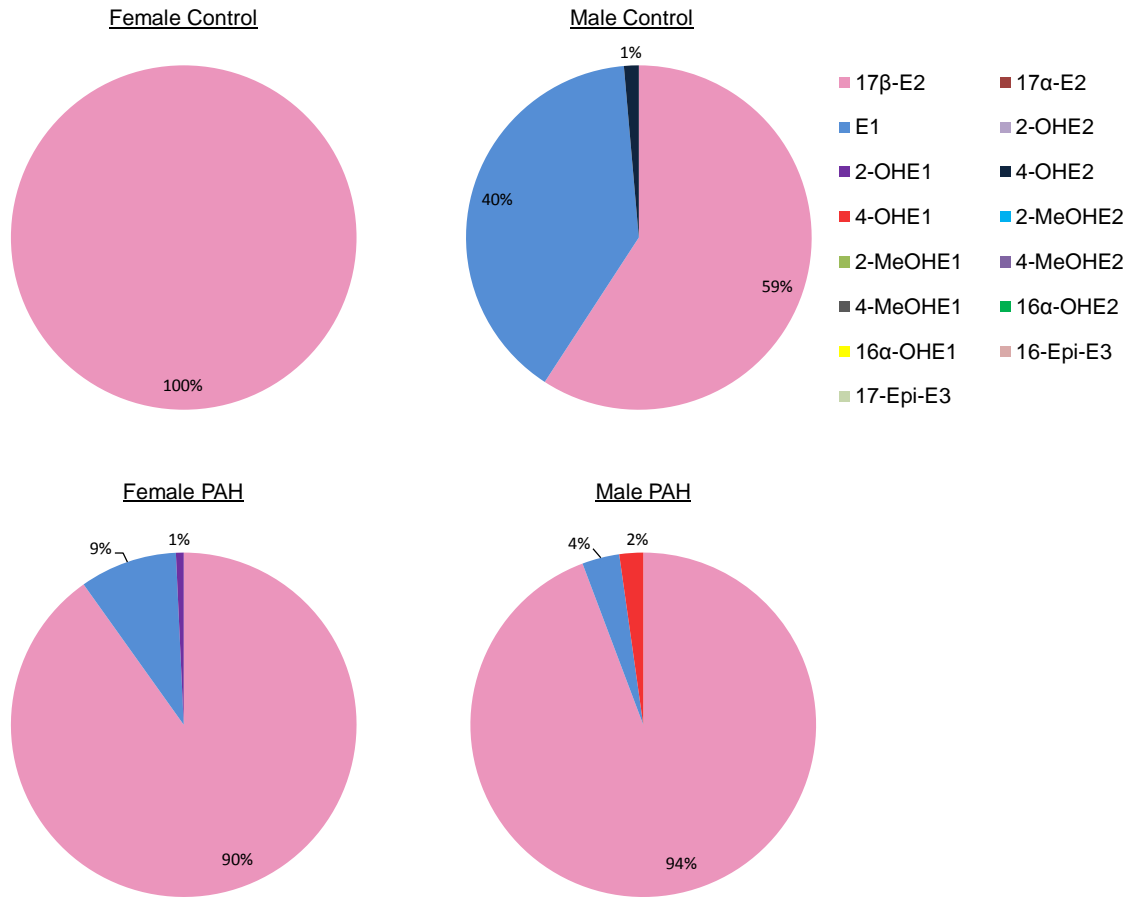


**Figure 4-34 Estrogen metabolic profile in control- and pulmonary arterial hypertension-pulmonary arterial smooth muscle cells (PASMCs) after 1 hour**

Female and male, control and PAH PASMCs were incubated with 17β-estradiol (17β-E2; 50nM, 136.19ng) for 1 hour in 1% charcoal-stripped (estrogen-free) phenol red free DMEM. Samples were extracted by solid phase extraction with Oasis® HLB cartridges and analyzed by HPLC with ultra-violet and radiolabeled detection. n=1 patient per group, repeated twice in different passages.

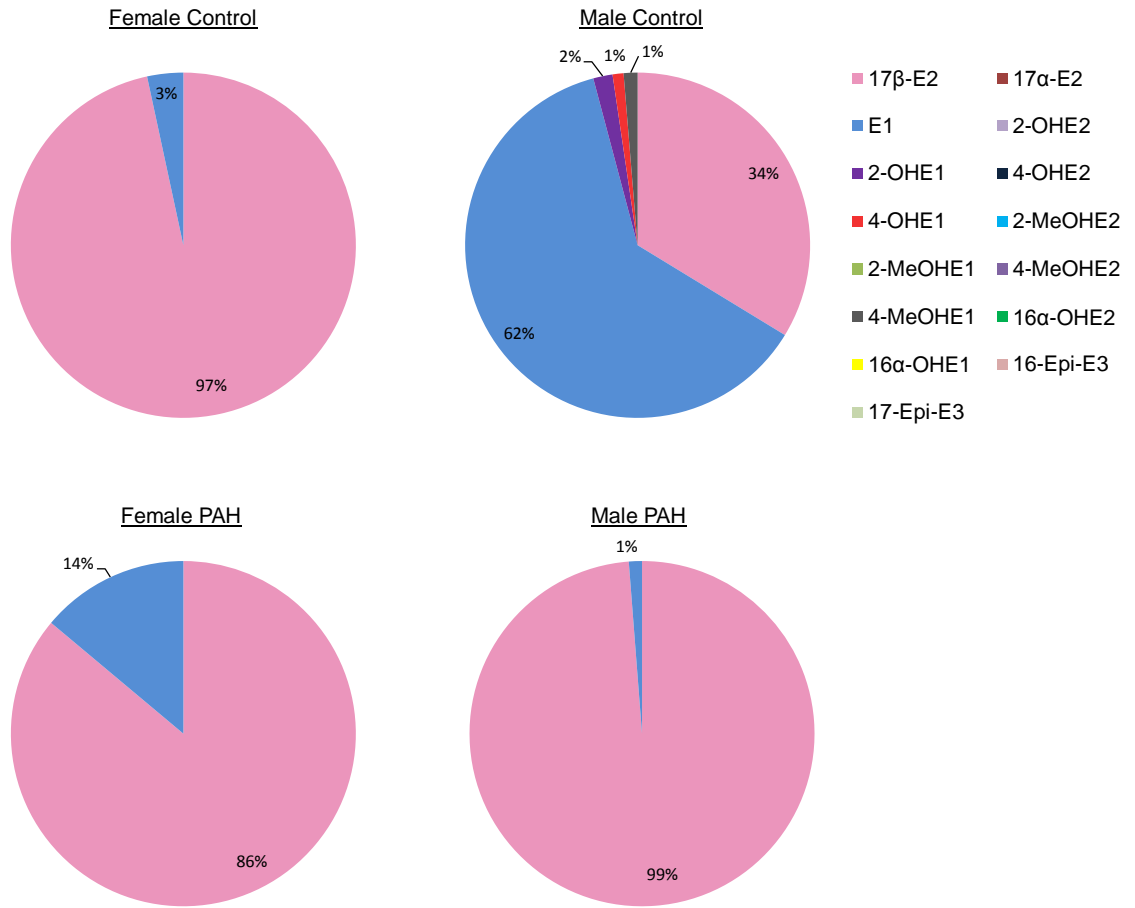


**Figure 4-35 Estrogen metabolic profile in control- and pulmonary arterial hypertension-pulmonary arterial smooth muscle cells (PASMCs) after 2 hours**

Female and male, control and PAH PASMCs were incubated with 17β-estradiol (17β-E2; 50nM, 136.19ng) for 2 hours in 1% charcoal-stripped (estrogen-free) phenol red free DMEM. Samples were extracted by solid phase extraction with Oasis® HLB cartridges and analyzed by HPLC with ultra-violet and radiolabeled detection. n=1 patient per group, repeated twice in different passages.

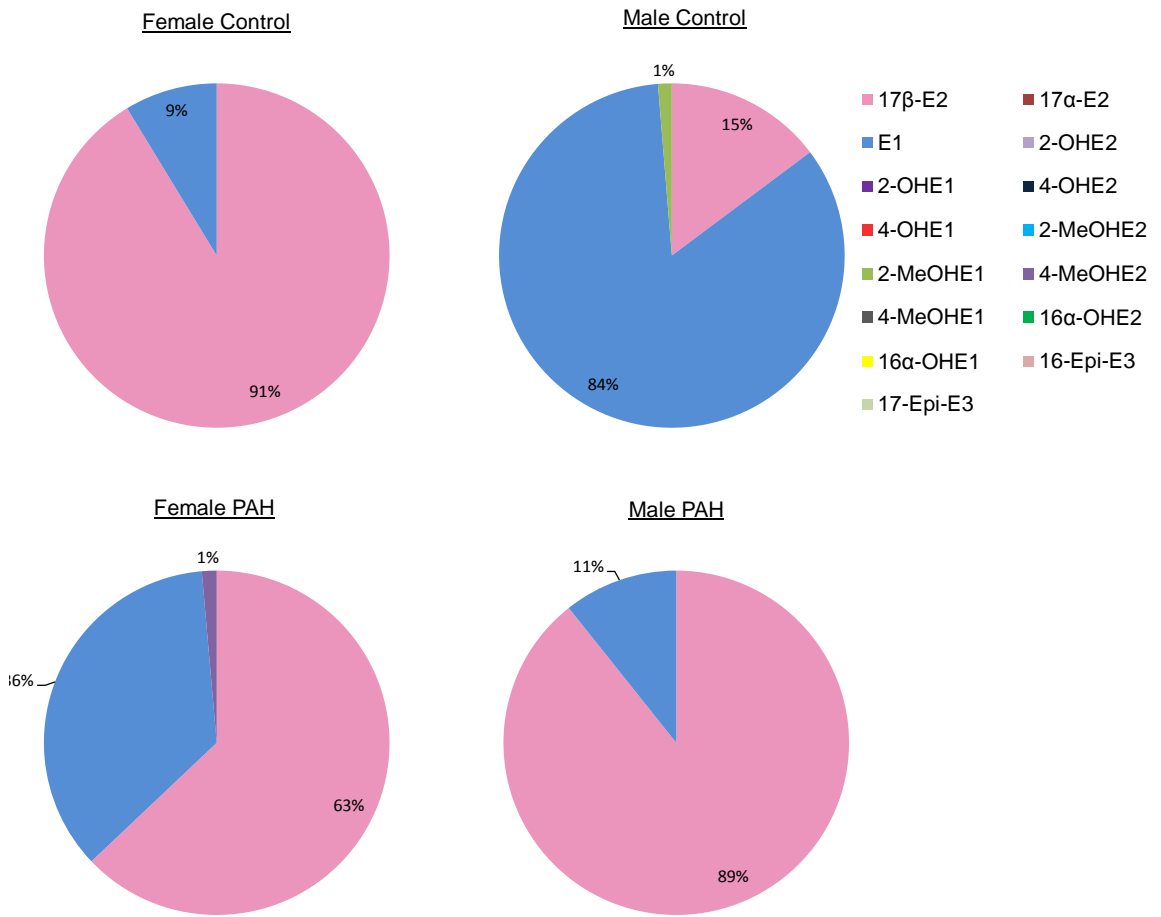


**Figure 4-36 Estrogen metabolic profile in control- and pulmonary arterial hypertension-pulmonary arterial smooth muscle cells (PASMCs) after 4 hours**

Female and male, control and PAH PASMCs were incubated with 17β-estradiol (17β-E2; 50nM, 136.19ng) for 4 hours in 1% charcoal-stripped (estrogen-free) phenol red free DMEM. Samples were extracted by solid phase extraction with Oasis® HLB cartridges and analyzed by HPLC with ultra-violet and radiolabeled detection. n=1 patient per group, repeated twice in different passages.

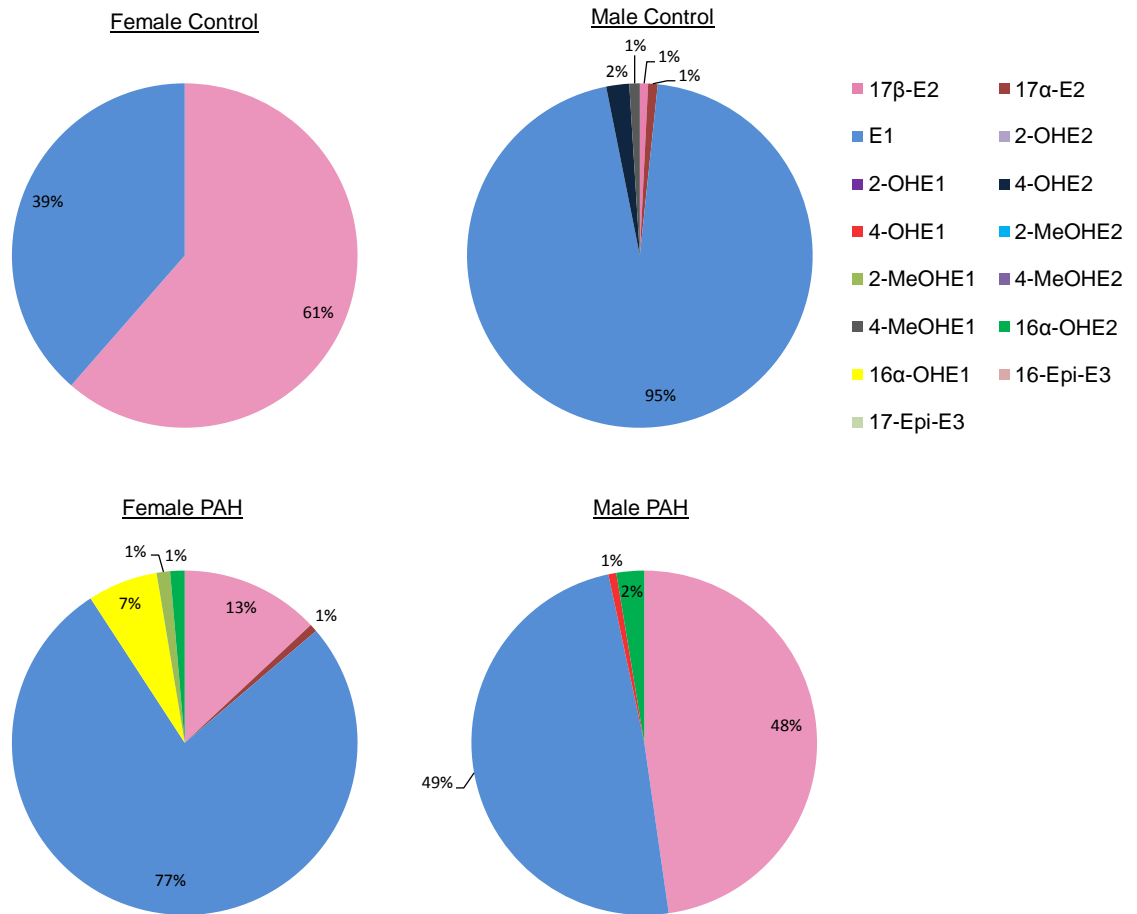


**Figure 4-37 Estrogen metabolic profile in control- and pulmonary arterial hypertension-pulmonary arterial smooth muscle cells (PAMCs) after 24 hours**

Female and male, control and PAH PAMCs were incubated with 17β-estradiol (17β-E2; 50nM, 136.19ng) for 24 hours in 1% charcoal-stripped (estrogen-free) phenol red free DMEM. Samples were extracted by solid phase extraction with Oasis® HLB cartridges and analyzed by HPLC with ultra-violet and radiolabeled detection. n=1 patient per group, repeated twice in different passages.

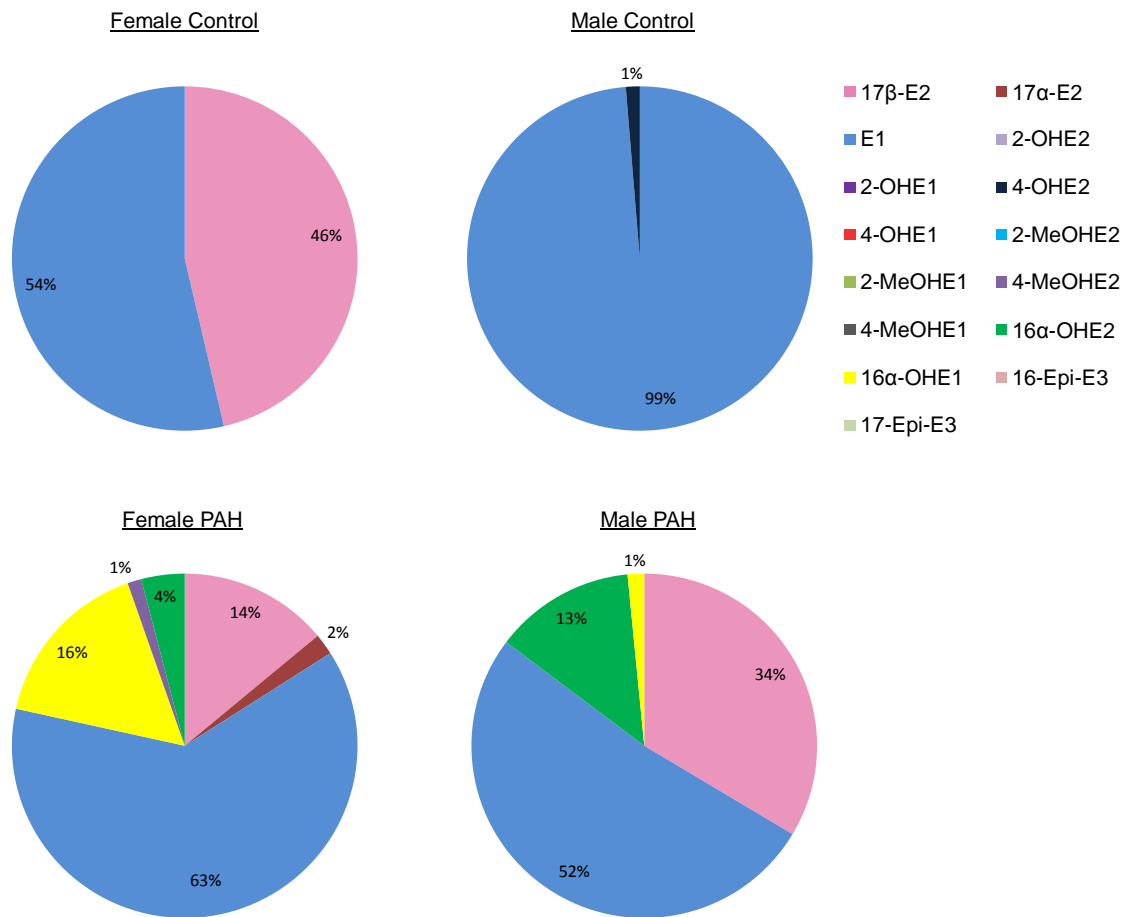


**Figure 4-38 Estrogen metabolic profile in control- and pulmonary arterial hypertension-pulmonary arterial smooth muscle cells (PASCs) after 48 hours**

Female and male, control and PAH PASCs were incubated with 17β-estradiol (17β-E2; 50nM, 136.19ng) for 48 hours in 1% charcoal-stripped (estrogen-free) phenol red free DMEM. Samples were extracted by solid phase extraction with Oasis® HLB cartridges and analyzed by HPLC with ultra-violet and radiolabeled detection. n=1 patient per group, repeated twice in different passages.

**Table 4-6 Summary of metabolite formation in human pulmonary arterial smooth muscle cells**

hPASCs	17 $\beta$ -HSD2	CYP Enzymes	COMT	Dehydrogenases
<b>Female Control</b>	E1			
<b>Female PAH</b>	E1	2-OHE1 16 $\alpha$ -OHE2 16 $\alpha$ -OHE1	2-MeOHE2 4-MeOHE2	17 $\alpha$ -E2
<b>Male Control</b>	E1	2-OHE1 2-OHE2 4-OHE1 4-OHE2	2-MeOHE1 4-MeOHE1 4-MeOHE2	17 $\alpha$ -E2 17-Epi-E3
<b>Male PAH</b>	E1	4-OHE1 16 $\alpha$ -OHE2 16 $\alpha$ -OHE1		

Overall summary of metabolites formed in human pulmonary arterial smooth muscle cells (hPASCs). Metabolites highlighted in blue were specific to pulmonary arterial hypertension (PAH) samples whereas metabolites highlighted in red were specific to male control hPASCs. (E1, estrone; 2-OHE2, 2-hydroxyestradiol; 2-OHE1, 2-hydroxyestrone; 4-OHE2, 4-hydroxyestradiol; 4-OHE1, 4-hydroxyestrone; 16 $\alpha$ -OHE2, 16 $\alpha$ -hydroxyestradiol; 16 $\alpha$ -OHE1, 16 $\alpha$ -hydroxyestrone; 2-MeOHE2, 2-methoxyestradiol; 2-MeOHE1, 2-methoxyestrone; 2-MeOHE2, 2-methoxyestradiol; 4-MeOHE2, 4-methoxyestradiol; 4-MeOHE1, 4-methoxyestrone; 17 $\alpha$ -E2, 17 $\alpha$ -estradiol; 17-Epi-E3, 17-epiestriol.)

### 4.3 Discussion

PAH is predominantly observed in females but the molecular events that govern this effect remain obscure. Understanding the biological basis of this sex difference would offer a new treatment paradigm in this devastating cardiovascular disorder that currently has no cure with a pressing need for more effective therapies (Archer *et al.*, 2010). We have provided evidence that dysregulated estrogen metabolism may underlie this (Chapter 3). We therefore investigated the effects of estrogen metabolites *in vitro* and *in vivo*, providing evidence that the smooth muscle cell mitogen 16 $\alpha$ -OHE1 is associated with the pathogenesis of PAH. Yet the dynamic estrogen metabolic profile in PAH remained undetermined. It was therefore of importance to examine and measure estrogen metabolism in hPASMCs. We challenged the concept that estrogen metabolism is pathologically altered in PAH. To address these challenges, we developed a high-fidelity quantitative technique to measure estrogen metabolism by HPLC, which can be used as a platform to investigate effects of PH insults and therapies on the fate of estrogen in the lung vasculature. We provide the first direct evidence that estrogen metabolism is pathologically altered in PAH and this highlights a novel therapeutic paradigm that can be targeted in the management of this devastating disease.

17 $\beta$ -E2 is metabolised to both pro- and anti-proliferative metabolites by CYP1B1. TMS inhibits 17 $\beta$ -E2-induced proliferation of hPASMCs, suggesting that CYP1B1 metabolism mediates the proliferative effects of 17 $\beta$ -E2 (White *et al.*, 2012). The 16 $\alpha$ -hydroxylated CYP1B1 metabolites induce proliferation of hPASMCs, with the most profound proliferation observed with 16 $\alpha$ -OHE1. Furthermore, the proliferative effects of this mitogen were exaggerated in PAH-PASMC (White *et al.*, 2012). In line with this, urinary levels of 16 $\alpha$ -OHE1 were increased in mice exposed to chronic hypoxia (Figure 4-2). Importantly, increased urinary 16 $\alpha$ -OHE1 has also been reported in patients with HPAH associated with a BMPR-2 mutation (Austin *et al.*, 2009), supporting a functional role of this metabolite in PAH pathogenesis. Moreover, we provide direct evidence that both female and male hPASMCs metabolize 17 $\beta$ -E2 to the 16-hydroxylated estrogens (Figure 4-38). Whether this metabolite is a candidate biomarker is yet to be ascertained. To establish a direct pathological link with 16 $\alpha$ -OHE1 and PAH, both male and female mice were dosed with 16 $\alpha$ -OHE1 (Figure 4-4). Whilst 16 $\alpha$ -OHE1 had no effects on the pulmonary haemodynamics measured in male mice, increased RVSP and RVH was observed in female mice. In a recent report by Fessel and colleagues (Fessel *et al.*, 2013a), 16 $\alpha$ -OHE1 induced a PAH phenotype in male BMPR-2 deficient transgenic mice, whilst

no effect was observed in their respective male wild-type mice. Thus, it appears that 16 $\alpha$ -OHE1 is a PAH insult in genetically-susceptible and female mice. Interestingly, male mice dosed with 16 $\alpha$ -OHE1 had significantly reduced mSAP, highlighting a gender-specific and divergent effect of this metabolite in the systemic vasculature.

The precise mechanism by which 16 $\alpha$ -OHE1 contributes to PAH pathogenesis is yet to be fully investigated. Here we provide evidence that 16 $\alpha$ -OHE1 induced proliferation is attenuated with a ROS scavenger and an ERK inhibitor (Figure 4-7). Unpublished data from our lab have provided evidence that 16 $\alpha$ -OHE1 increases superoxide production in hPASCs. Elevated oxidative stress is associated with PAH pathogenesis, yet the mechanisms that precede this remain uncertain (Bowers *et al.*, 2004; Fessel *et al.*, 2013b; Hemnes *et al.*, 2011). Increased metabolism of 17 $\beta$ -E2 to 16 $\alpha$ -OHE1 by increased CYP1B1 activity may be one mechanism of elevated ROS in PAH. In other studies, 16 $\alpha$ -OHE1 has been shown to have a high binding affinity for ER $\beta$  (Zhu *et al.*, 2006) which is increased following hypoxic exposure (Lahm *et al.*, 2012). However, in pre-clinical models, ER $\beta$  agonists have proven effective in alleviating PH-phenotypes (Umar *et al.*, 2011). Additionally, the protective effects of 17 $\beta$ -E2 in hypoxic-induced PH are attenuated with an ER $\beta$  antagonist (Lahm *et al.*, 2012). Independent of estrogen receptor binding, 16 $\alpha$ -OHE1 in MCF-7 cells has been shown to induce cell proliferation via increased expression of the cell cycle regulator, cyclin D1 (Lewis *et al.*, 2005). This may be relevant to the pathological effects of 16 $\alpha$ -OHE1 in PAH as cyclin D1 is an important mediator in PAH pathogenesis, where it promotes proliferation and vascular remodeling (Zeng *et al.*, 2013)

CYP1B1 is a putative pathological mediator in cancer. Divergent insults such as serotonin (White *et al.*, 2011a), hypoxia (White *et al.*, 2012), shear stress (Conway *et al.*, 2009) and the dioxin, TCDD robustly alter the expression of CYP1B1. The enzymatic activity of CYP1B1 favours the hydroxylation at the C4 position of estrogens (Lee *et al.*, 2003). Furthermore, co-treatment with TCDD (a potent CYP1B1 inducer) and 17 $\beta$ -E2 in human lung cells leads to an accumulation of 4-MeOHE2 (Cheng *et al.*, 2007), further supporting activity of 4-hydroxylation by CYP1B1. Although the 4-hydroxylated estrogens do not stimulate proliferation of hPASCs (White *et al.*, 2012), we wished to investigate its function *in vivo* due to its vast role in cancer (Liehr & Ricci, 1996) and its potential influence on redox signaling. Perhaps surprisingly, 4-OHE2 had no effect of RVSP or RVH. Interestingly, chronic dosing with 4-OHE2 attenuated serotonin-induced vasoconstriction of the intra-pulmonary arteries, suggesting that it mediates vasodilatory

effects in the pulmonary arteries. This merits further investigation in tandem with the effects of 4-OHE2 in hypoxic conditions. However, there are several experimental limitations that need reviewed. Both estrogen metabolites (16 $\alpha$ -OHE1 and 4-OHE2) were administered by intra-peritoneal injections which has several limitations as a route of administration. Intra-peritoneal injections are primarily absorbed through the portal circulations (Lukas *et al.*, 1971) which suggests that all drugs injected by this route will initially undergo first-pass metabolism by the liver. COMT expression and activity is substantial within the liver of mice (Myöhänen *et al.*, 2010) which would breakdown 4-OHE2 into 4-MeOHE2. Thus the effects observed may not be due to 4-OHE2, but rather 4-MeOHE2, which has growth inhibitory effects on lung epithelial cells (Cheng *et al.*, 2007) and renal cancer cells (Chang *et al.*, 2012). Additionally, the methoxyestrogens have also been reported to exert feedback inhibition on both CYP1B1 and CYP1A1 (Dawling *et al.*, 2003). In contrast, 16 $\alpha$ -OHE1 is less likely to be substantially altered whilst passing through the liver, thus giving a stronger possibility that the parent metabolite is reaching the target tissue (the lung).

In a more recent comprehensive study of estrogen metabolites in the lungs of wild-type and CYP1B1<sup>-/-</sup> mice, 4-OHE1 appeared as the predominant CYP1B1 metabolite (Peng *et al.*, 2013). Our previous screen that identified 16 $\alpha$ -OHE1 as a disease-modifying metabolite was limited to thymidine incorporation and did not address other effects that metabolites of 17 $\beta$ -E2 may have on cellular function (White *et al.*, 2012). Thus, we sought to investigate the functional consequence of increased CYP1B1 hydroxylation activity by stimulating naïve hPASCs with 4-OHE1 and measuring DNA replication and cell viability (Figure 4-12 - Figure 4-15). In line with our previous findings, 4-OHE1 did not increase proliferation, but actually inhibited DNA replication, whilst having no effect on cell viability. Following longer incubations (5 days), 4-OHE1 had no significant effects on DNA replication, suggesting that these effects were either transient, or had been overcome by a different mechanism.

In the CYP1B1<sup>-/-</sup> mouse, levels of 2-MeOHE2 in the lungs are increased compared to wild-type mice, suggesting that CYP1B1 may be counteracting COMT activity (Peng *et al.*, 2013). 2-MeOHE2 is a putative protective estrogen metabolite. Thus, the protective effects observed on CYP1B1 inhibition may be mediated via increased formation of 2-MeOHE2. 2-MeOHE2 has previously been reported to have strong anti-mitogenic effects in lung fibroblasts and hPASCs (Tofovic *et al.*, 2009b) and can attenuate bleomycin (Tofovic *et al.*, 2009b), monocrotaline (Tofovic *et al.*, 2005; Tofovic *et al.*, 2006) and SU-

hypoxic (Tofovic & Rafikova, 2009) induced PH. Our findings are consistent with these reports, with 2-MeOHE2 having an inhibitory effect on DNA replication and reducing cell viability (Figure 4-12 - Figure 4-15). Whilst 2-MeOHE2 has proven to be beneficial in this setting and appears to represent a promising therapeutic strategy in PAH, this has been compromised by phase I clinical trials in cancer that were prematurely stopped due to the very low bioavailability of this metabolite (Dahut *et al.*, 2006). To circumvent this, 2-MeOHE2 levels may be increased by CYP1B1 inhibition.

The metabolic conversion of  $17\beta$ -E2 by the 4-hydroxylation pathway is recognized to contribute to DNA damage by superoxide production (Acharya *et al.*, 2010). We have recently provided evidence that 4-hydroxylation induces profound superoxide production in hPASMCs (up to 6 fold higher after incubations for 5 minutes compared to control) (unpublished data). Thus, CYP1B1 may be inducing its pathogenic effects via increased superoxide production. Others have identified a role for serotonin (Lee *et al.*, 1998) and endothelin-1 (Wedgwood *et al.*, 2001) in superoxide production in hPASMCs. Additionally, other metabolic pathways of CYP1B1 may alter redox cycling. For example, arachidonic can be metabolized by CYP1B1 to HETEs (Choudhary *et al.*, 2004). 20-HETE increases superoxide production in human pulmonary arterial endothelial cells (Medhora *et al.*, 2008). Also, angiotensin-II can increase superoxide production via CYP1B1 (Yaghini *et al.*, 2010). Thus multiple pathways may interplay to cause injurious ROS production via CYP1B1 activity. In tandem, increased  $16\alpha$ -hydroxylation activity results in increased hPASMC proliferation (White *et al.*, 2012), leading to a pathogenic environment in the lung. Overall, these pathogenic effects may be reversed by CYP1B1 inhibition.

Others have provided evidence for  $17\beta$ -E2 and E1 within the lung (Meireles *et al.*, 2010; Peng *et al.*, 2013). Here, we provide the first evidence for high intracellular  $17\beta$ -E2 concentrations within hPASMCs ranging from ~25nM to 30nM per mg of protein (Figure 4-16). Patients with PAH did not have significantly different  $17\beta$ -E2 levels compared to control hPASMCs, nor was there any effect on gender. An increased risk of PPHTN is associated with increased plasma  $17\beta$ -E2 as a consequence of a polymorphism in the gene encoding for aromatase (Roberts *et al.*, 2009). Recent studies have confirmed that aromatase inhibition can reverse severe experimental PAH in females, but not in males (Mair *et al.*, 2013). In the absence of changes in  $17\beta$ -E2 levels within hPASMCs, this suggests that it is the metabolic route of  $17\beta$ -E2 and/or altered signaling through estrogen receptors that is adversely affecting the pathogenesis of PAH. Thus the beneficial effects of aromatase inhibition may be attributable to a lack of substrate for subsequent metabolism

by pathogenic CYP enzymes, such as CYP1B1. We have previously reported interactions of the estrogen and serotonin pathways in PH (White *et al.*, 2011b). It was therefore of interest to investigate whether serotonin could alter estrogen levels within hPASMCs. Serotonin had no effect on intracellular  $17\beta$ -E2 levels after 48-hour incubation (Figure 4-16). This supports our patient data, where no changes were observed in  $17\beta$ -E2 levels.

There is evidence that estrogen metabolism is dysregulated in PH and that certain estrogen metabolites provide protective effects *in vivo* and *in vitro*, such as the 2-methoxyestradiol (Tofovic *et al.*, 2009b;Tofovic *et al.*, 2006). In contrast, other estrogen metabolites exert pathogenic effects *in vivo* and *in vitro*, such as the potent smooth muscle cell mitogen,  $16\alpha$ -OHE1 (White *et al.*, 2012). However, the *in vivo* effects of  $16\alpha$ -OHE1 on the pulmonary hypertensive phenotype was only evident in female mice and genetically susceptible mouse models (Fessel *et al.*, 2013a;White *et al.*, 2012). Thus, it is clear that the metabolic fate of  $17\beta$ -E2 can have dramatic consequences on vascular cell fates and one may hypothesize that  $17\beta$ -E2 is differentially metabolized in the severest forms of PH such as PAH. Abnormal PASMC proliferation is a key event that drives PAH-pathobiology (Archer *et al.*, 2010;Schermuly *et al.*, 2011) and was therefore our chosen vascular cell type to study. We initially measured estrogen depletion from the extracellular medium by hPASMCs to ascertain if  $17\beta$ -E2 is differentially metabolized in female control and PAH hPASMCs (Figure 4-17). After 24 hours, it was evident that female PAH hPASMCs rapidly depleted extracellular levels of  $17\beta$ -E2 suggesting a greater metabolic rate compared to control hPASMCs. This provided preliminary evidence for altered  $17\beta$ -E2 metabolism in PAH, but to what effect was still unknown. To answer this question, we determined the metabolic fate of  $17\beta$ -E2 in hPASMCs using the principles of metabolomics and metabolic flux analysis. A homogenous population of PASMCs were exposed to radiolabelled  $17\beta$ -E2 to quantitatively measure their unique metabolic profiles. 50nM (136.19ng) of  $17\beta$ -E2 was selected as the optimal concentration for three primary reasons. First, the concentration was identified as the optimal concentration to sufficiently detect  $17\beta$ -E2 metabolism in the cells. Second, we have provide evidence that intracellular levels of  $17\beta$ -E2 in hPASMCs is predictably higher than circulating levels, which are approximately in the range of 0.4nM to 2.2nM (Mendelsohn & Karas, 1999). Third, we have reported that there are no differences in  $17\beta$ -E2 concentrations between females and males providing rationale to utilize the same concentration in both sexes.

The enzymatic kinetics of CYP enzymes in the lung is largely unknown and it therefore remains essential to perform a time-point analysis to get a broad window of estrogen

metabolism within hPASMCs. This was an extremely fruitful exercise as there appeared to be key differences in rates of metabolism across both males and females and controls and PAH (Figure 4-32-Figure 4-38). To the best of our knowledge, this is the first study to provide direct evidence that hPASMCs actively metabolize  $17\beta$ -E<sub>2</sub>. In addition, it revealed a prominent role for  $17\beta$ -HSD2, the enzymatic isoform that converts  $17\beta$ -E<sub>2</sub> into E<sub>1</sub>.  $17\beta$ -HSD enzymes play an important role in the regulation of 'active' estrogens within tissues.  $17\beta$ -HSD1 converts E<sub>1</sub> into  $17\beta$ -E<sub>2</sub> and therefore plays a role in determining the availability of  $17\beta$ -E<sub>2</sub> and E<sub>1</sub> within specific cell types.  $17\beta$ -HSD2 also catalyses the formation of androstenedione from testosterone. Androstenedione can then be converted to E<sub>1</sub> by the activity of aromatase. Increased activity of  $17\beta$ -HSD1 is associated with increased levels of  $17\beta$ -E<sub>2</sub> and the pathogenesis of breast cancer (Gunnarsson *et al.*, 2008; Oduwole *et al.*, 2004) and lung cancer (Verma *et al.*, 2013). Interestingly, it appeared that female PAH PASMCs had a higher activity of  $17\beta$ -HSD2 compared to control hPASMCs. In contrast, male PAH-PASMCs had reduced activity of  $17\beta$ -HSD2 compared to non-PAH cells. Thus, E<sub>1</sub> (and androstenedione) may play a prominent role in PAH pathogenesis in females whereas  $17\beta$ -E<sub>2</sub> (and testosterone) may play a prominent role in male PAH. E<sub>1</sub> has thus far been assumed to have less estrogenic activity that serves as a reservoir for  $17\beta$ -E<sub>2</sub> within tissues and few studies have addressed its cellular effects in hPASMCs. In male control hPASMCs E<sub>1</sub> has no effects on cell proliferation (White *et al.*, 2011), yet its effects in female hPASMCs remains to be determined. Whilst E<sub>1</sub> itself may be a less active estrogen, its hydroxylated products by activity of CYP enzymes can have profound effects on cellular fates. For example, the formation of the  $16\alpha$ -OHE<sub>1</sub> from the hydroxylation of E<sub>1</sub> would promote PASMC proliferation (White *et al.*, 2012).

Whilst male control, female PAH and male PAH hPASMCs displayed evidence for CYP activity, there was no measurable CYP activity in female control hPASMCs (Figure 4-28). Interestingly, the highest CYP activity was evident in both male and female PAH hPASMCs at 24 and 48 hours and curiously,  $16\alpha$ -hydroxylation was only evident in PAH hPASMCs (Figure 4-32-Figure 4-38). The most prominent isoform in female PAH was  $16\alpha$ -OHE<sub>1</sub> and the most prominent isoform in male hPASMCs was  $16\alpha$ -OHE<sub>2</sub>.  $16\alpha$ -OHE<sub>1</sub> levels are increased in the urine of mice exposed to hypoxia and clinically, the ratio of  $16\alpha$ -OHE<sub>1</sub> to 2-OHE<sub>1</sub> is increased in female patients with heritable PAH associated with a mutation in the BMPR-2 (Austin *et al.*, 2009). Cellular proliferation screens have provided evidence that  $16\alpha$ -OHE<sub>1</sub> is a potent inducer of PASMC proliferation (White *et al.*, 2012). In vivo,  $16\alpha$ -OHE<sub>1</sub> induces a PH phenotype in female mice only and

genetically susceptible mice (BMPR-2 mutant mice), providing direct evidence that 16 $\alpha$ -OHE1 may contribute to PAH pathogenesis (Fessel *et al.*, 2013a; White *et al.*, 2012).

The activity of COMT represents a key deactivation process of hydroxylated estrogens, in particular by reducing the ability of 4-hydroxylated estrogens to generate quinones and semiquinones that can lead to DNA damage, which contributes to the pathogenesis of PAH (Meloche *et al.*, 2013). In female control hPASCs, there was no evidence for COMT activity (Figure 4-28) as measured by the absence of methylated metabolites (albeit CYP activity would have been necessary to determine COMT activity). COMT activity was present in both male control (Figure 4-29) and female PAH hPASCs (Figure 4-30) whilst no activity was detected in male PAH hPASCs (Figure 4-31). However, the activity of CYP enzymes can also interconvert methoxyestrogens back into their hydroxylated estrogens (Dawling *et al.*, 2003). We can therefore not entirely conclude that there was no COMT activity within male PAH hPASCs.

We have previously provided evidence that estrogen metabolism is dysregulated in PAH by numerous studies highlighting increased CYP1B1 expression in pulmonary arteries of patients with severe PAH and inhibition studies in various experimental models (Chapter 3, 4 and White *et al.*, 2012). Furthermore, there is now evidence that aromatase inhibition (the estrogen-synthesizing enzyme) can reverse severe experimental PH (Mair *et al.*, 2013). In contrast, in both the hypoxic and MCT models of PH, exogenous estrogens have protective effects mediated via ER $\alpha$  (Lahm *et al.*, 2012) in the hypoxic model and via ER $\beta$  in the MCT model of PH (Umar *et al.*, 2011). Furthermore, ER $\alpha$  mediates the protective effects of 17 $\beta$ -E2 on right ventricular function in hypoxia-induced PH, evident by a reduced cardiac output in animals co-treated with the ER $\alpha$  antagonist, 1-methyl-4-phenyl pyridinium (MPP) (Lahm *et al.*, 2012). The cardioprotective effects of 17 $\beta$ -E2 may contribute to the improved survival in female patients compared to males. Indeed, improved right ventricular systolic function is superior in both healthy and PAH-affected women compared to men and is associated with higher circulating levels of 17 $\beta$ -E2 (Kawut *et al.*, 2009; Ventetulo *et al.*, 2011). In a small cohort of PAH patients, increased expression of ESR1, the gene encoding ER $\alpha$ , is reported in lungs derived from both male and female PAH patients (Rajkumar *et al.*, 2010). A conserved evolutionary binding site for ER $\alpha$  is present within the BMPR-2 promoter and can thereby alter its expression profile (Austin *et al.*, 2012). In support of this, 17 $\beta$ -E2 (1 $\mu$ M) can reduce the expression of BMPR-2 in human pulmonary arterial endothelial cells (Austin *et al.*, 2012) where it is predominantly expressed (Atkinson *et al.*, 2002). This supports the gender differences in

HPAH associated with BMPR-2 mutations, whereby there is incomplete penetrance (27%) with females much more likely to present with PAH (42% females compared with 14% males) (Larkin *et al.*, 2012). Whilst protective effects of exogenous estrogens have been reported in both the hypoxic and MCT-models of PH (Lahm *et al.*, 2012;Umar *et al.*, 2011), in models that display heightened activity of the serotonergic system (Dempsie *et al.*, 2013;White *et al.*, 2011b), endogenous estrogen is associated with the development of PH. In the female mouse model that over-expresses the serotonin transporter (SERT+ mice) the ER $\alpha$  inhibitor can reverse its spontaneous PH phenotype (Wright *et al.* 2013, unpublished).

Interestingly, whilst estrogen metabolites can mediate receptor-independent effects on cellular functions, they retain strong binding affinities at the estrogen receptors. Thus, the differential effects of 17 $\beta$ -E2 in the hypoxic-, MCT and SERT+ models may be attributable to differential metabolism of 17 $\beta$ -E2 (as well as differences in estrogen concentrations, gender and species used). Whilst inhibition of CYP1B1 can attenuate both hypoxic (Chapter 3 and White *et al.*, 2012) and SERT+ - PH (Chapter 4), it has a much less pronounced effect in MCT-induced PH despite dramatically improving survival (Chapter 3). A comprehensive analysis of the binding affinities of estrogen metabolites to estrogen receptors revealed striking differences suggesting that the unique physiological function of 17 $\beta$ -E2 may be dependent on its metabolism. Whilst 17 $\beta$ -E2, 4-OHE2, 4-OHE1 and 2-OHE2 have an equal binding affinity for both ER $\alpha$  and ER $\beta$ , E1 and 2-OHE1 have a preferential binding affinity for ER $\alpha$  (Zhu *et al.*, 2006). In contrast, the 16-hydroxylated estrogens (16 $\alpha$ -OHE1 and 16 $\alpha$ -OHE2) have a preferential binding affinity for ER $\beta$  (Zhu *et al.*, 2006). Interestingly, ER $\alpha$  lung expression is unchanged in the hypoxic-rat model of PH, whilst ER $\beta$  expression is increased (Lahm *et al.*, 2012). In contrast, in the SERT+ model of PH, ER $\alpha$  levels are increased (Wright *et al.* 2013, unpublished). Thus, there appears to be a two-tiered process by which estrogen signaling may contribute to PAH pathology. First, the route by which it is metabolized by aberrant CYP/COMT activity. Second, the effects mediated by the metabolite formation will depend, in part, on the tissue specific expression of ERs. Overall, this highlights a multi-level complex axis and may explain the controversies within the field that report both protective and pathogenic effects of estrogens. This is challenged by the study by Lahm and colleagues providing evidence that the protective effects of 17 $\beta$ -E2 in the hypoxic-rat model of PH are not mediated via metabolite formation as the general CYP inhibitor, ABT does not attenuate the protective effects of 17 $\beta$ -E2 (Lahm *et al.*, 2012). This suggests that the protective effects of 17 $\beta$ -E2 in this model are not mediated via the formation of protective

17 $\beta$ -E2 metabolites. However, in models where 17 $\beta$ -E2 is causative, 17 $\beta$ -E2 metabolism may figure prominently by the formation of 16 $\alpha$ -hydroxylated estrogens.

Here, we developed a method to measure the dynamic metabolism of 17 $\beta$ -E2 in hPASCs. This methodology can be easily applied to other cell types of interest. Beyond this study, we can utilize *in silico* analysis to identify specific CYP enzymes that may underlie the altered estrogen metabolic phenotype in patients with PAH. For example, at 48 hours, the key metabolite formed in female PAH hPASCs was 16 $\alpha$ -OHE1. This implicates potential activity of CYP1A1, CYP1A2, CYP1B1, CYP2C8, CYP3A4, CYP3A5 and CYP3A7 (Badawi *et al.*, 2001; Hanna *et al.*, 2000; Lee *et al.*, 2003). We can then use this as a platform to investigate potential therapeutic targets that may rescue the estrogen metabolic phenotype. For example, we can utilize highly selective inhibitors and siRNA to CYP1A1 and CYP1B1 to see if this can prevent the metabolism of 17 $\beta$ -E2 to 16 $\alpha$ -OHE1. Successful CYP candidates can then be investigated for their therapeutic potential *in vivo*. Whilst microarray screens are useful in detecting aberrant gene expression, the activities of CYP enzymes do not always correlate with their expression. Thus, the sensitivity of such screens in detecting potentially pathological estrogen metabolic pathways is limited. We are therefore hopeful that this metabolite screen may be useful in identification of novel therapeutic targets for the treatment of PAH.

The enzymes that are involved in the catalytic metabolism of 17 $\beta$ -E2 have variable kinetics in terms of the maximum velocity of the reaction ( $V_{max}$ ) and the affinity of the enzyme for the substrate ( $K_m$ ). High catalytic activity is reflective of a high  $V_{max}$  and a low  $K_m$ . The enzymes that are predominantly involved in 17 $\beta$ -E2 metabolism are CYP1A1, CYP1A2, CYP3A4 and CYP1B1. CYP1A1 and CYP1A2 have high catalytic activities for 2-hydroxylation of 17 $\beta$ -E2 (Badawi *et al.*, 2001; Lee *et al.*, 2003). Our results implicate that the activity and expression of these enzymes in hPASCs from both control and PAH samples are negligible as only a small percentage of 2-hydroxylated estrogens was detected. However, in contradiction it has recently been found that CYP1A1 is a highly up-regulated gene in the SU-hypoxic rat model of PAH (unpublished data from Novartis Pharmaceuticals, Horsham). Although all estrogen metabolizing enzymes have low catalytic activities for 16 $\alpha$ -hydroxylation, CYP1A1, CYP1A2 and CYP3A5 are the principle source of this metabolite, with a minor contribution by CYP1B1 (Badawi *et al.*, 2001). CYP1B1 has an overall lower catalytic activity for 17 $\beta$ -E2 than CYP1A1 and CYP1A2, but has the highest activity for 4-hydroxylation with a low  $K_m$  and a high  $V_{max}$  (Badawi *et al.*, 2001). Evidence for CYP1B1 was detected in all samples except for female

control hPASCs.  $17\beta$ -HSD1 (which interconverts E1 into  $17\beta$ -E2) has a very low  $K_m$  and uses NADPH as a cofactor. On the other hand,  $17\beta$ -HSD2 utilises NAD as a co-factor and has a higher  $K_m$  although its catalytic activity is still high. Thus, the tissue-specific expression of  $17\beta$ -HSD and the availability of co-factors are crucial in regulating the balance between  $17\beta$ -E2 and E1. Here, we provided evidence for variable activity of  $17\beta$ -HSD2 by the formation of E1. However, the activity of  $17\beta$ -HSD2 may be counteracting the effects of  $17\beta$ -HSD1, thus we cannot entirely conclude that its activity is the highest in male control hPASCs, as appears to be the case. Future studies investigating the role of  $17\beta$ -HSD enzymes in PAH are merited.

The purpose of this project was to develop a method to track estrogen metabolism in pulmonary vascular cells and to determine the optimal time-point to assess estrogen metabolism. One key limitation of the data obtained from this study is that the metabolic profile generated was only obtained from one patient in each category. It would be essential to assess estrogen metabolism in a larger cohort of patients to ascertain whether estrogen metabolic profiles are consistently altered in PAH. This is hampered by a general lack of available samples due to the low prevalence of PAH. To overcome this, control PASCs could be stimulated with a known PAH insult (such as knockdown of BMPR-2, endothelin-1, serotonin) to assess if this can alter the estrogen metabolic profile. PAH PASCs are generally end-stage disease as they are obtained from patients either undergoing transplant or post-mortem. These samples may therefore not be reflective of on-going PAH pathogenesis and molecular pathways may have been altered by the therapies that the patient would have been receiving. This variable would also be overcome by studying control PASCs with a PAH insult. However, it would be challenging to truly mimic a PAH profile *in vitro* as it is likely that numerous pathways contribute to PAH pathogenesis. Age may also be an important contributor to extra-gonadal estrogen metabolism and as the control samples used in this study were from older patients whereas the PAH samples were from younger patients, we cannot disregard that the results obtained may be attributable to the different age groups studied.

The data shown here is the first study to measure the dynamic metabolism of estrogen in PAH specifically in the PASCs. To date, estrogen metabolites have only been preliminarily measured by mass spectrometry in serum from post-menopausal patients with severe PAH (Chhatwani *et al.*, 2010). In this study, E1 and the E1+ $17\beta$ E2/total estrogen metabolites were significantly decreased in post-menopausal PAH patients compared to controls. PAH patients also had greater plasma levels of 2-methoxyestrogens. This study

did not report detections of the 4- or the 16 $\alpha$ -hydroxyestrogens suggesting that they did not measure them. Mass spectrometry is considered the gold-standard analytical technique, yet it carries selective bias as you have to specify what compounds you are interested in detecting. The methodology described here is a sensitive and quantitative technique that can measure estrogen metabolism in vascular cells. Furthermore, all metabolites that are formed by the reaction will be radio-labelled and will therefore be detected. Furthermore, this assay allows for absolute quantification as the percentage of radioactive product formed directly correlates with the amount of metabolite formation. In LC-MS, absolute quantification would require pure authentic standards for each analyte, which are currently unavailable. It is challenging to correlate the sensitivity of this assay in comparison to other assays available as it employs radioactivity to measure metabolism whereas other assays measure relative abundance of unlabelled metabolites. In other assays, estrogens are often derivitised in order to improve their detection. This is not necessary in our assay as we have incorporated a radioactive label which can be measured in counts per million and is extremely sensitive. However, this methodology requires the undesired use of radioactive compounds. Furthermore, it restricts future experimental procedures that involve tracking of 17 $\beta$ -E2 *in vivo* and endogenous tissue sample concentrations of estrogen metabolites. Additionally, all estrogen metabolites identified by radio-labelled HPLC need to be validated by LC-MS to confirm metabolite identity. Ultimately, we will develop a LC-MS approach to address these questions and a general metabolomics approach to identify all substrates and metabolites within the steroidogenic pathway. Together, this will identify the unique steroidogenic profile that is associated with PAH.

Estrogen metabolism may be integral to a wide span of diseases and may offer targets for therapeutic intervention in the management of PAH. We have provided direct evidence that estrogen metabolism is dysregulated in PAH, in particular by increased 16 $\alpha$ -hydroxylation. This pathway has already been associated with the development of PAH (Austin *et al.*, 2009; White *et al.*, 2012). Current PAH therapies do not encompass this well-defined gender disparity that occurs in PAH, or the potential divergent response to current therapies that may be affected by gender. Future therapies that target dysregulated estrogen metabolism may have a favourable outcome in this highly neglected, devastating disease.

# **Chapter 5**

## **General Discussion**

## 5.1 General Discussion

In general, females are less likely to develop cardiovascular diseases compared to males. However, the risk for cardiovascular diseases increases after menopause, when estrogens are ~20-fold lower (Mendelsohn & Karas, 1999). In contrast, in several lung diseases, estrogens are associated with the development and disease progression. Female gender is now the most established risk factor in PAH. Although long recognised (Dresdale *et al.*, 1951), it is only in the last decade that we have started to appreciate the potential impact of steroid hormones in PAH. There are currently no treatments available that target the steroidogenic pathway nor do any treatments encompass any gender-related effect on treatment response. A recent study highlighted the importance of the latter, where they reported that females had much greater responses to endothelin receptor antagonists than males (Gabler *et al.*, 2012). Furthermore, the REVEAL registry recently reported sex differences in the diagnosis, treatment response and outcome in patients with PAH (Shapiro *et al.*, 2012). This highlights the importance of understanding the role of the steroidogenic pathway in PAH.

Although the incidence of PAH is more common in women than in men, in older patients (>60 years old) the estimated 2-year survival in males is significantly less than female patients (Shapiro *et al.*, 2012). In patients younger than 60 years, there are no sex differences in the estimated 2-year survival rates (Shapiro *et al.*, 2012). However, there are sex differences in haemodynamics between young (<45 years) female and male patients, with male patients presenting with higher mean PAPs and pulmonary vascular resistance compared with females, whilst these differences are attenuated in older patients (Ventetuolo *et al.*, 2014). Interestingly, in older patients (>45 years) with IPAH, mean PAPs and pulmonary vascular resistance are lower than younger patients in both sexes (Ventetuolo *et al.*, 2014) despite having worse survival rates (Shapiro *et al.*, 2012). These sexual dimorphisms suggest that both estrogens and androgens may influence the pathogenesis of PAH.

The fact that PAH is more common in women than in men has led to the hypothesis that estrogens, in particular  $17\beta$ -E<sub>2</sub>, the main pre-menopausal hormone, may be facilitating the development and pathogenesis of PAH. Despite this, numerous pre-clinical studies have provided evidence for a protective role for  $17\beta$ -E<sub>2</sub> in the pulmonary vasculature (Lahm *et al.*, 2007; Lahm *et al.*, 2008b; Lahm *et al.*, 2012; Umar *et al.*, 2011; White *et al.*, 2011b; Yuan *et al.*, 2013). Furthermore, female rats have been shown to develop less severe PH

compared to male rats (Rabinovitch *et al.*, 1981).  $17\beta$ -E2 is a potent vasodilator of the pulmonary vascular bed (English *et al.*, 2001) and physiological increases in circulating estrogens can attenuate pulmonary arterial vasoconstriction under both normoxic and hypoxic conditions (Lahm *et al.*, 2007).

However, there is controversial data that indicates a pathogenic function of estrogen that suggests it may contribute to the pathogenesis of PAH.  $17\beta$ -E2 can induce proliferation in a variety of cell types including PASMCs and may therefore contribute to pulmonary vascular remodeling (White *et al.*, 2011b; White *et al.*, 2012). We have recently characterised novel murine models of PH that show female susceptibility to the development of PH, including SERT+ mice, mts100/A4 overexpressing mice and mice treated with dexfenfluramine (Dempsey *et al.*, 2010; Dempsey *et al.*, 2013; White *et al.*, 2011b). In these models, only females develop a PH phenotype and this is dependent on circulating (gonadal) estrogens. More recently, we and others have provided unique evidence that suggests that locally produced estrogens within the lung are associated with the pathogenesis of PAH (Mair *et al.*, 2013; Tofovic *et al.*, 2012). Certain tissues can modulate their own estrogenic milieu by the local conversion of testosterone or androstenedione to  $17\beta$ -E2 and E1 respectively by the activity of aromatase (Harada *et al.*, 1999). Aromatase synthesizes estrogens from testosterone and androstenedione and is expressed within the pulmonary arteries (Mair *et al.*, 2013). Furthermore, inhibition of aromatase attenuates hypoxia-induced and SU-hypoxia-induced PH (Mair *et al.*, 2013). Interestingly, aromatase expression is unchanged in pre-clinical models of PAH, suggesting that the protective effects are either mediated by an increase in testosterone or a decrease in subsequent metabolism. Recently, we have shown that testosterone levels are unchanged following aromatase inhibition (Mair *et al.* unpublished), suggesting that estrogen metabolism may be altered in PAH.

$17\beta$ -E2 is metabolised by various CYP enzymes to both pro- and anti-proliferative metabolites. Others have previously provided evidence that alterations in estrogen metabolism by aberrant CYP1B1 expression may contribute to the development of HPAH (Austin *et al.*, 2009). Furthermore, in the female susceptible SERT+ model of PH and in IPAH, CYP1B1 expression is increased (White *et al.*, 2011a). This led us to hypothesize that the effects of estrogens in the pulmonary vasculature may be mediated by altered estrogen metabolism by increased activity of CYP1B1. Increased activity and expression of CYP1B1 had already been reported in many diseases including breast cancer (McKay *et al.*, 1995), lung cancer (Murray *et al.*, 1997), ovarian cancer (McFadyen *et al.*, 2001), and

systemic hypertension (Jennings *et al.*, 2010). It was therefore the aim of this project to investigate the contribution of CYP1B1 and estrogen metabolism in PH/PAH.

Here, we provide evidence that a dysregulated estrogen metabolic axis via elevated CYP1B1 activity may contribute to the pathogenesis of PAH and represents an attractive novel therapeutic strategy (Chapter 3). Pulmonary arterial CYP1B1 expression was increased in both experimental models and in human PAH. CYP1B1<sup>-/-</sup> mice and CYP1B1 inhibition attenuated the development of hypoxia-induced PH. This provided the first evidence that dysregulated estrogen metabolism by up-regulation of CYP1B1 contributed to the pathogenesis of PH/PAH. In the MCT-model of PH, CYP1B1 inhibition had no statistically significant therapeutic effects, although it improved survival in both male and female rats and appeared to reduce pulmonary arterial neointimal formation. The classical models of PH do not show female selectivity. One animal model that displays a unique female susceptibility is the mouse model that overexpresses the human SERT gene (White *et al.*, 2011b). Recent evidence has highlighted that 17 $\beta$ -E2 is a critical steroid hormone in the development of PH in this model (White *et al.*, 2011b). CYP1B1 expression is increased in the pulmonary arteries from these mice (White *et al.*, 2011a), suggesting that altered estrogen metabolism may underlie this phenotype in these mice. Here, we established that aromatase and CYP1B1 expression was heightened in the lungs of these mice compared to wild-type mice. 17 $\beta$ -E2 levels in the lungs were however unaffected. CYP1B1 inhibition in these mice reverses the elevated RVSP and pulmonary vascular remodeling under both normoxic and hypoxic conditions. Female SERT<sup>+</sup> mice fail to develop compensatory RVH in response to the increased remodeling in the pulmonary vasculature and this was unaffected by CYP1B1 inhibition.

CYP1B1 activity is recognised to contribute to the pathogenic effects of estrogens by altering estrogen metabolism towards the formation of pro-proliferative, pro-oxidative metabolites capable of inducing DNA damage. However, the beneficial effects of CYP1B1 inhibition *in vivo* may also be mediated by subsequent increases in estrogen that can signal through genomic and non-genomic pathways. Estrogens have been shown to mediate protective effects via estrogen receptors in both acute and chronic vascular injury. The relative expression profile of estrogen receptors may vary in a clinical setting and determine the effects of estrogens. For example, 17 $\beta$ -E2 exerts differential effects in normoxic and hypoxic (1% oxygen) rat pulmonary arterial endothelial cells (Lahm *et al.*, 2012). In hypoxic but not normoxic cells, 17 $\beta$ -E2 decreases ERK1/2 activation and increases the expression of the cell cycle inhibitor p27<sup>kip1</sup>. 17 $\beta$ -E2 has been shown to

induce eNOS expression in pulmonary vascular cells by non-genomic mechanisms through ER $\alpha$  and ER $\beta$  (Austin *et al.*, 2013). In the fetal pulmonary endothelium, 17 $\beta$ -E2 rapidly stimulates NO production via a non-genomic mechanism that is dependent on calcium (Lantin Hermoso *et al.*, 1997) and MAP kinases (Chen *et al.*, 1999). In fetal pulmonary arterial endothelial cells, 17 $\beta$ -E2 rapidly and dramatically increases prostacyclin synthesis via ER $\beta$  and is dependent on calcium and independent on MAP kinase signaling (Sherman *et al.*, 2002). In isolated pulmonary arterial rings, both endogenous and exogenous estrogens mediate vasodilation and selective activation of either ER $\alpha$  or ER $\beta$  can also attenuate pulmonary vasoconstriction via increased NO (Lahm *et al.*, 2008a). These vasodilatory effects are rapid and are therefore presumed to be mediated via a non-genomic mechanism. *In vivo*, 17 $\beta$ -E2 rescues established PH induced by MCT and completely abolishes mortalities in male rats (Umar *et al.*, 2011). In this study, 17 $\beta$ -E2 had angiogenic effects restoring the loss of blood vessels in the lungs and the right ventricle. Furthermore, these effects were inhibited by an ER $\beta$  antagonist and mimicked by an ER $\beta$  agonist suggesting that ER $\beta$  is a critical mediator in the protective effects of 17 $\beta$ -E2 in this model (Umar *et al.*, 2011). In contrast, in the hypoxic model of PH, exogenous 17 $\beta$ -E2 mediates protective effects, and these effects can be blocked by ER $\alpha$  antagonism (Lahm *et al.*, 2012). Taken together, the beneficial effects observed by CYP1B1 inhibition may be related to increases in 17 $\beta$ -E2. However, we also provided evidence for a protective role for CYP1B1 inhibition in the female susceptible SERT+ model of PH, where 17 $\beta$ -E2 has been shown to mediate pathogenic effects (White *et al.*, 2011b). This suggests that the protective effects observed by CYP1B1 inhibition may not be mediated via increases in 17 $\beta$ -E2 within this model. Future studies addressing the effects of CYP1B1 inhibition on levels of 17 $\beta$ -E2 are merited for further clarification.

CYP1B1 also catalyses the metabolic conversion of arachidonic acid into EETs and HETEs (Choudhary *et al.*, 2004). The metabolism of arachidonic acid results in the formation of eicosanoids that have been associated with the pathogenesis of both cancers and cardiovascular diseases, including PAH (Capdevila & Falck, 2001). Arachidonic acid stimulates endothelium-dependent contractions in both male and female pulmonary arteries from rabbits and these effects are potentiated in females and are mediated by 17 $\beta$ -E2 (Pfister, 2011). Arachidonic acid is metabolized by CYP450 mediated oxidation, lipoxygenases, cyclooxygenases, epoxygenases and hydroxylases. Lipoxygenases metabolise arachidonic acid into the leukotrienes and cyclooxygenases metabolize arachidonic acid into the prostaglandins. The formation of 15-HETE by upregulation of 15-lipoxygenase has been associated with pulmonary arterial contraction and cell

proliferation (as reviewed by Zhu & Ran, 2012). 15-HETE is a metabolite of both CYP1B1 metabolism and the lipoxygenase pathway. The expression of 15- and 5-lipoxygenase is greater in female rabbit pulmonary arteries and 15-HETE synthesis is increased in female rabbit pulmonary arteries and stimulates vascular contraction (Pfister, 2011). Furthermore, a specific 15-lipoxygenase inhibitor can attenuate the vasoconstrictor response to arachidonic acid in pulmonary arteries (Pfister, 2011). In male rabbit pulmonary arteries, incubations with 17 $\beta$ -E2 increases 15-lipoxygenase expression and 15-HETE production (Pfister, 2011). In the systemic vasculature, EETs are associated with their vasodilatory and anti-inflammatory properties. However, in the pulmonary circulation, EETs potentiate vasoconstriction (Loot & Fleming, 2011). Thus, the therapeutic effects associated with CYP1B1 inhibition may also be via a reduced formation of HETEs and EETs that mediate pulmonary arterial vasoconstriction.

In the vasculature, CYP1B1 is predominantly expressed within smooth muscle cells, yet its expression is increased by shear stress within the vascular endothelium (Conway *et al.*, 2009). In vascular smooth muscle cells, Ang II and arachidonic acid cause migration, proliferation and hypertrophy which is inhibited with TMS (Yaghini *et al.*, 2010). This is associated with a reduced formation of ROS and its downstream signaling molecules ERK1/2 and p38MAPK (Yaghini *et al.*, 2010). Moreover, the therapeutic effects associated with CYP1B1 inhibition may be mediated by subsequent increases in prostacyclin synthesis from arachidonic acid by the COX pathway. Prostacyclin is a potent vasodilator of the pulmonary vasculature and prostacyclin analogues are widely used in the management of PAH.

Taken together, CYP1B1 may be considered a hub for the formation of pathogenic metabolites and inhibition may provide multiple therapeutic effects by increasing levels of 17 $\beta$ -E2, arachidonic acid availability for prostacyclin synthesis whilst preventing the formation of genotoxic and proliferative estrogen metabolites, EETs, and HETEs. Future studies comparing the concentrations of pre-cursors within the pulmonary vasculature together with the catalytic activity ( $K_m$  and  $V_{max}$ ) of CYP1B1 for each substrate would provide insight in to which pathway predominates.

CYP1B1 is also a key enzyme in the metabolism of polyaromatic hydrocarbons (atmospheric pollutants). Polycyclic aromatic hydrocarbons are activated by the activity of CYP1B1 (and CYP1A1) into highly toxic compounds that have tumorigenic properties by inducing DNA damage. Whilst polyaromatic hydrocarbons may contribute to the

pathogenesis of PAH (although such data is lacking), in our experimental models, animals were not exposed to environmental toxins suggesting that the therapeutic effects of CYP1B1 inhibition were not related to this metabolic pathway.

Cell proliferation screens of the CYP1B1 estrogen metabolites revealed that the 16 $\alpha$ -hydroxylated estrogens (16 $\alpha$ -OHE1 and 16 $\alpha$ -OHE2) are potent hPASMC mitogens (White *et al.*, 2012). In chapter 4, we showed that urinary concentrations of 16 $\alpha$ -OHE1 were increased following exposure to chronic hypoxia. Interestingly, chronic dosing with 16 $\alpha$ -OHE1 in mice resulted in the development of a PH phenotype in female mice only. A recent study supported these findings, where 16 $\alpha$ -OHE1 induced a PH phenotype in male BMPR-2 mutant mice but not in wild-type mice (Fessel *et al.*, 2013a). This suggests that in females and genetically-susceptible mouse models, 16 $\alpha$ -OHE1 mediates pathogenic effects. In BMPR-2 mice with a R899X mutation, 16 $\alpha$ -OHE1 suppressed cytokine and inflammatory pathways whilst promoting platelet adhesion gene expression and genes associated with insulin resistance and angiogenesis (Fessel *et al.*, 2013a). The authors concluded that the latter effect may be the mechanism by which 16 $\alpha$ -OHE1 may be promoting vascular injury.

CYP1B1 has the highest catalytic activity for the 4-hydroxylation of 17 $\beta$ -E2 (Badawi *et al.*, 2001; Lee *et al.*, 2003) and 4-hydroxylated estrogens are associated with the generation of semi-quinones and quinones which are associated with the initiation of tumorigenesis. We were therefore interested in investigating the effects of 4-OHE2 *in vivo*. Cellular proliferation screens have indicated that 4-OHE2 does not induce cell proliferation (White *et al.*, 2012). However, unpublished data from our lab indicate that 4-OHE2 induces oxidative damage by increased superoxide production in hPASMCs. 4-OHE2 had no effects on RVSP, RVH and pulmonary vascular remodeling. In contrast, 4-OHE2 reduced serotonin-induced vasoconstriction of the intra-pulmonary arteries, suggesting that it may be mediating a protective effect. This is supported by a more recent study that provides evidence for beneficial effects of 4-OHE2 in the SU-hypoxic rat model of PH (Tofovic *et al.*, 2013). This data suggests that the CYP1B1 mediates its pathogenic effects via the formation of the 16 $\alpha$ -hydroxylated estrogens.

A recent study examined estrogen metabolite levels in wild-type and CYP1B1<sup>-/-</sup> mice. The two metabolites that were most profoundly affected by CYP1B1 deletion were 4-OHE1 and 2-MeOHE2 (Peng *et al.*, 2013). 4-OHE1 was decreased and 2-MeOHE2 was increased. Hence we were interested in investigating the effects of these two metabolites

on cellular proliferation and viability in hPASMCs. Both 4-OHE1 and 2-MeOHE2 reduced cellular proliferation, but only 2-MeOHE2 reduced cell viability at 3 days. Following longer incubations (5 days), the proliferative effects were reduced and 4-OHE1 no longer caused a significant inhibition of proliferation. Further studies examining the role of these two metabolites in human vascular cells require further investigation. Studies on-going in our lab have highlighted a potential for ROS species derived from 4-OHE1, which may contribute to CYP1B1-induced pathogenesis.

### **5.1.1 The therapeutic potential of CYP1B1 inhibition in the management of PAH**

The therapeutic strategy in PAH is aimed at developing pulmonary specific therapies to prevent off-target effects whilst inhibiting vascular cell proliferation and promoting regeneration of the lost distal pulmonary arteries. We have provided evidence that estrogen metabolism is dysregulated in PAH by up-regulation of CYP1B1 and that inhibition of this pathway can prevent the onset of experimental PH (Chapter 3 and Chapter 4). Moreover, we have shown that CYP1B1 inhibition with TMS attenuates 17 $\beta$ -E2 induced-proliferation in hPASMCs and this inhibitory effect is ~100 fold more potent in hPASMCs isolated from PAH patients (White *et al.*, 2012).

Increased activity and expression of CYP1B1 has already been reported in many diseases including breast cancer (McKay *et al.*, 1995), lung cancer (Murray *et al.*, 1997), ovarian cancer (McFadyen *et al.*, 2001) and systemic hypertension (Jennings *et al.*, 2010). From a therapeutic perspective, CYP1B1 is highly expressed within most cancers with only minimal expression in non-cancerous, healthy tissues (Maecker *et al.*, 2003; Murray *et al.*, 1997) providing a basis for selective targeting. However, of some concern is the presence of positive CYP1B1 cells within healthy fallopian tubes, breast, uterine and ureter specimens (Maecker *et al.*, 2003). CYP1B1 is also commonly expressed in the human lung (Spivack *et al.*, 2001), where it is an important enzyme in the metabolism of xenobiotics, such as polycyclic aromatic hydrocarbons. Paradoxically, the metabolism of xenobiotics results in the activation of these compounds by formation of epoxides that generate DNA adducts - an early step in tumorigenesis. Inhibition of this pathway in the lung, where CYP1B1 is expressed, would therefore be considered advantageous.

A phase I clinical trial assessing the feasibility, safety, tolerability and the generation of CYP1B1 immunity in patients with breast, ovarian, prostate, colon and renal cancer using ZYC300 has been evaluated with promising results (Gribben *et al.*, 2005; Luby, 2008).

ZYC300 is a plasmid DNA encoding an inactivated form of CYP1B1 that was developed as a vaccination to stimulate the immune system to elicit a cytotoxic T lymphocyte mediated response against CYP1B1, resulting in the lysis of CYP1B1 positive cells (Gribben *et al.*, 2005;Luby, 2008). Importantly, vaccination with ZYC300 in patients with advanced stage cancer has been reported to be well tolerated, safe and patients that developed anti-CYP1B1-immunity responded better to therapy and appeared to have a clinical benefit (Gribben *et al.*, 2005). The application of ZYC300 in the management of PAH is appealing and should be considered as adjunct therapy, given the high pulmonary arterial expression of CYP1B1. In addition, others have provided evidence that CYP1B1 inhibition can attenuate Ang II and DOCA-salt induced hypertension, cardiac hypertrophy and fibrosis (Jennings *et al.*, 2010;Sahan-Firat *et al.*, 2010). The increased vascular reactivity associated with Ang II and DOCA-salt induced hypertension in aortic, mesenteric and femoral arteries is inhibited in CYP1B1<sup>-/-</sup> mice and by TMS treatment (Jennings *et al.*, 2010;Sahan-Firat *et al.*, 2010). Ang II induces aortic endothelial dysfunction as assessed by an impairment in the vasorelaxant response to acetylcholine and this is prevented with TMS (Jennings *et al.*, 2010). This provides evidence that CYP1B1 inhibition may be beneficial in numerous cancers and cardiovascular diseases.

Of caution is the importance of CYP1B1 in normal eye functions and reduced CYP1B1 activity has been associated with the development of glaucoma (Vasiliou & Gonzalez, 2008). Thus, in the development of drugs that target CYP1B1, it is important to determine the ability of the drug/vaccine to cross the blood brain barrier, so as to prevent off-target effects in the ocular region.

The therapeutic potential of the CYP1B1 inhibitor TMS has yet to be clinically evaluated. TMS is a synthetic derivative of a stilbene which was created as an anti-cancer agent with a high inhibitory potency for CYP1B1 to prevent the formation of highly genotoxic estrogen metabolites (Chun *et al.*, 2001). TMS is a potent and selective CYP1B1 inhibitor, with an IC<sub>50</sub> value of 6nM and displays 50-fold selectivity over CYP1A1 and 500-fold selectivity over CYP1A2 (Chun *et al.*, 2001). TMS was originally developed as an inhibitor of the 4-hydroxylation of 17β-E2, and ultimately tumour formation. However, TMS has also been shown to induce cell apoptosis and inhibition of microtubule polymerisation (Park *et al.*, 2007). It appears to have relatively low toxicity *in vivo* whilst displaying potent anti-tumour and anti-hypertensive effects, making this a good therapeutic candidate in cancers and cardiovascular diseases, including PAH that merits consideration.

TMS is a derivative of trans-resveratrol which is abundant in grapes and other berries. Resveratrol is proposed to be a major factor contributing to the ‘French Paradox’, which is the observation that despite having diets high in saturated fats, the French have a relatively low incidence of cardiovascular disease (Zern & Fernandez, 2005). Resveratrol is a potent inhibitor of CYP1B1, CYP1A1 and CYP1A2 activities with  $K_i$  values of  $\sim 0.8\mu\text{M}$ ,  $1.2\mu\text{M}$  and  $15.5\mu\text{M}$ , respectively (Chang *et al.*, 2001). Resveratrol is well tolerated and safe in humans and has been tested in numerous clinical trials. The therapeutic potential of resveratrol in PAH has been assessed in the MCT model of PAH with remarkable efficacy in attenuating increased RVSP and pulmonary vascular remodeling (Csiszar *et al.*, 2009). Furthermore, it decreased the expression of inflammatory cytokines, exerted anti-oxidant and anti-proliferative effects (Csiszar *et al.*, 2009). The extent to which these effects are mediated by CYP1B1 activity are yet to be evaluated, but it certainly highlights an attractive therapeutic avenue in PAH that has already been successfully applied in other cardiovascular diseases and cancers.

### 5.1.2 Targeting estrogen metabolism in the management of PAH

We have provided evidence that estrogen metabolism is dysregulated in PAH by increased activity of CYP1B1. Yet the dynamic estrogen metabolic profile in pulmonary vascular cells remained undetermined. Whilst gene and protein expression are powerful tools in understanding molecular pathways that are altered in disease, they are often just a small component of a more complex cellular process. Furthermore, the availability of co-factors that are required for the activities of enzymes, the possibility of epigenetic alterations and polymorphisms are not taken into consideration. We were therefore interested in adopting a metabolomics approach to provide the unique estrogen metabolic profile that is the final product of the many complex cellular processes that may be occurring within a given cell. We utilized a quantitative HPLC approach to ‘fate-map’ estrogen metabolism in hPASMCs (Chapter 4). We report high intracellular concentration of  $17\beta\text{-E}_2$  within both male and female hPASMCs and this is unaffected by PAH status. We provide the first direct evidence that male and female, non-PAH and PAH hPASMCs actively metabolize  $17\beta\text{-E}_2$ . In all groups studied, the predominant metabolite formation was E1 indicating the activity of  $17\beta\text{-HSD}_2$ . E1 is less estrogenic and is considered a reservoir for the synthesis of  $17\beta\text{-E}_2$ . Thus, the activity of  $17\beta\text{-HSD}_2$  could be considered as a deactivation process of the highly estrogenic  $17\beta\text{-E}_2$ . Of importance, only PAH hPASMCs (from both male and female samples) metabolized  $17\beta\text{-E}_2$  to the potent mitogens  $16\alpha\text{-OHE}_1$  and  $16\alpha\text{-OHE}_2$ .

Although these findings are preliminary and require validation in a larger cohort of PAH patients, these studies fit closely with already published data. We have provided evidence that urinary levels of 16 $\alpha$ -OHE1 are increased in mice exposed to chronic hypobaric hypoxia (Chapter 4 and White *et al.*, 2012) and Austin *et al.* reported a 2.3 fold lower 2-OHE/16 $\alpha$ OHE1 ratio in PAH patients with a BMPR-2 mutation compared to patients without any evidence of PAH (Austin *et al.*, 2009). In addition, 16 $\alpha$ -OHE1 is a potent inducer of PASMC proliferation and is associated with the development of a PAH phenotype in murine models (Fessel *et al.*, 2013a;White *et al.*, 2012). The formation of 16 $\alpha$ -hydroxylated metabolites may be associated with increased CYP1B1 expression and/or CYP1B1 polymorphisms (Badawi *et al.*, 2001;Hanna *et al.*, 2000). However, we cannot exclude the activities of other enzymes that have been reported to metabolize 17 $\beta$ -E2 and E1 to 16 $\alpha$ -OHE2 and 16 $\alpha$ -OHE1, respectively. In particular, CYP1A2 has been shown to have a prominent role for 16 $\alpha$ -hydroxylation (Badawi *et al.*, 2001). With the application of selective inhibitors of these enzymes, including TMS, we will be able to determine the prominent enzyme/s that is associated with this unique ‘finger-print’ in PAH PASMCs. This discovery would highlight a novel therapeutic target that merits investigation *in vivo*.

16 $\alpha$ -hydroxylated estrogens have also been postulated to be important in carcinogenesis. Low urinary 2-OHE: 16 $\alpha$ -OHE1 levels are associated with a high risk of breast cancer (Im *et al.*, 2009;Kabat *et al.*, 1997;Kabat *et al.*, 2006). Furthermore, 16-hydroxylated metabolites stimulate proliferation of breast cancer cells (Seeger *et al.*, 2006;Lippert *et al.*, 2003). 16 $\alpha$ -OHE1 has previously been shown to induce cell proliferation by upregulating cyclin D1 expression in breast cancer cells (Lewis *et al.*, 2005). This may be relevant to the pathological effects of 16 $\alpha$ -OHE1 in PAH as cyclin D1 is an important mediator in PAH pathogenesis, where it promotes proliferation and vascular remodeling (Zeng *et al.*, 2013). A successful candidate that attenuates the metabolic conversion of 17 $\beta$ -E2 into the 16 $\alpha$ -hydroxylated estrogens may therefore be applicable to a wider span of disease states, including PAH.

### 5.1.3 Concluding remarks

In summary of these findings, we have provided evidence for a dysregulated estrogen metabolic axis, particularly via increased CYP1B1 activity, in both pre-clinical models of PH and human PAH. CYP1B1 expression was increased in the pulmonary arteries of both IPAH and HPAH, independent of sex. 17 $\beta$ -E2 is historically regarded as a female gonadal

hormone. However, we have provided evidence for local production of  $17\beta$ -E2 in both male and female hPASMC creating a local estrogenic milieu (Chapter 4). In healthy blood vessels,  $17\beta$ -E2 promotes vasodilation and provides atherogenic protection. Cellular insults, such as hypoxia, that dysregulate estrogen signaling by altering estrogen receptor profiles and estrogen metabolism may perturb the beneficial effects of  $17\beta$ -E2 promoting a pathogenic environment. Here we provide the first direct evidence that  $17\beta$ -E2 is metabolized by hPASMCs. Importantly, we noticed a unique metabolic profile in both male and female PAH hPASMCs. Specifically, the smooth muscle cell mitogens, the  $16\alpha$ -hydroxylated estrogens were only formed in PAH samples, independent of sex, highlighting that altered estrogen metabolism may be a crucial mediator in the pathogenesis of PAH.

Inhibition of CYP1B1 with the highly potent and selective CYP1B1 inhibitor displayed impressive results in preventing PH onset in both the hypoxic and SU-hypoxic murine models of PH. This highlights CYP1B1 as a disease modifying enzyme that can be pharmacologically inhibited with TMS. TMS appears to have relatively low toxicity *in vivo* whilst displaying potent anti-tumour and anti-hypertensive effects, making this a good therapeutic candidate in cancers and cardiovascular diseases, including PAH that merits consideration.

PAH is a disease of women that currently has no cure. Altered estrogen metabolism may be a key disease driver in females (and males) by shifting the protective effects of estrogens to pathogenic effects by altered enzymatic profiles. We have reinforced a pathogenic role for estrogen metabolism in the genesis and pathogenesis of PAH and we propose that clinical trials investigating the safety, tolerability and effectiveness of TMS in cancer and cardiovascular diseases including PAH are strongly encouraged.

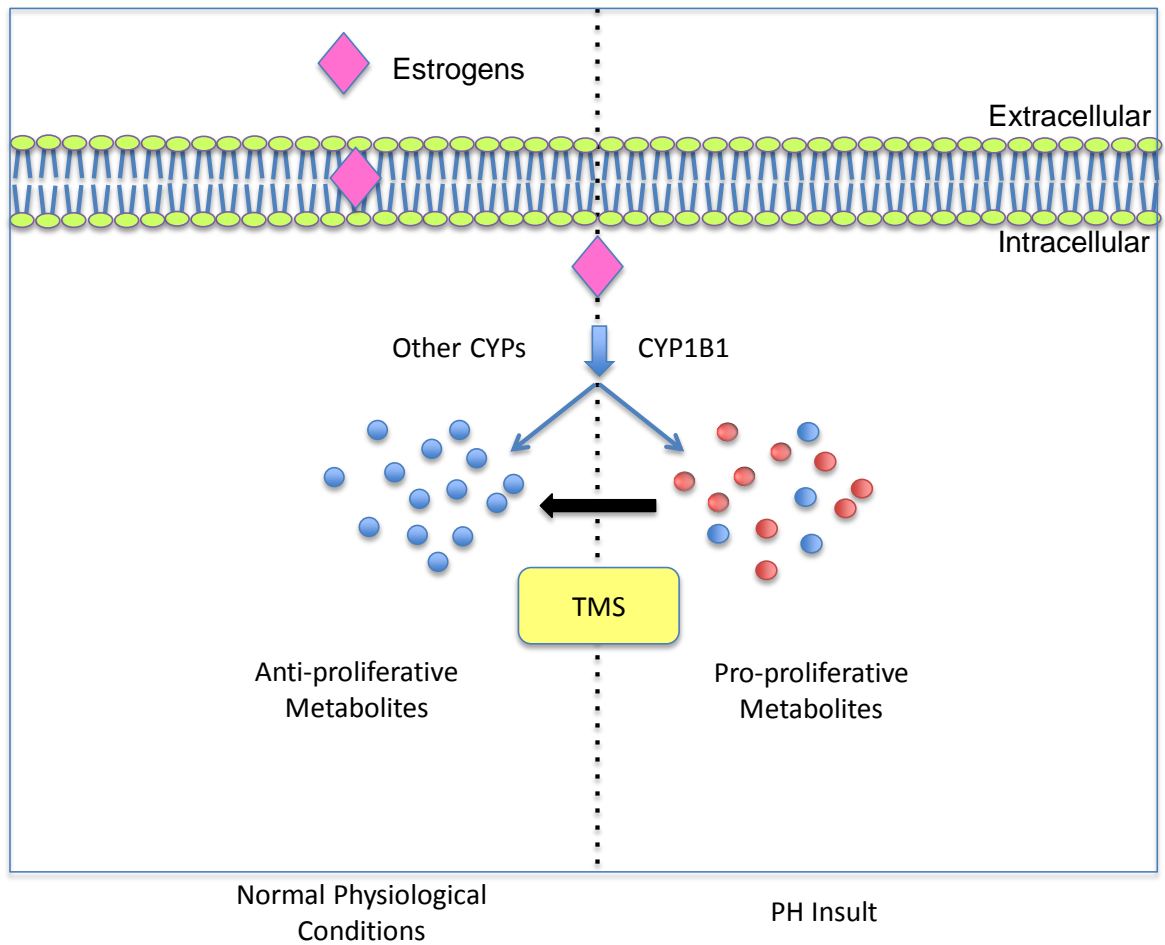


**Figure 5-1 Summary diagram**

Under normal physiological conditions, estrogens are metabolized towards the formation of anti-proliferative metabolites. Up-regulation of CYP1B1 results in the formation of pro-proliferative metabolites which represent a pulmonary hypertensive (PH) insult, which can be rescued by CYP1B1 inhibition with 2,3',4,5'-Tetramethoxystilbene (TMS).

## 5.2 Future Perspective

Future studies investigating the safety, tolerability and effectiveness of TMS in cancer and cardiovascular diseases including PAH strongly encouraged. Understanding the molecular basis of the therapeutic effects of CYP1B1 inhibition is critical. Multiple pathogenic pathways are activated by CYP1B1 activity – the formation of genotoxic estrogen metabolites, pathogenic eicosanoids and ROS. Furthermore, the inhibition of CYP1B1 may increase levels of 17 $\beta$ -E2 and arachidonic acid that may signal by protective or pathogenic mechanisms depending on the cellular composition of enzymes and receptors. Delineating these effects is crucial in our understanding of the therapeutic effects and potential of CYP1B1 inhibition in cancers and cardiovascular diseases.

We have developed a platform to investigate estrogen metabolism in pulmonary vascular cells. This can now be utilized to investigate estrogen metabolism in other cell types and the effect of PAH insults on metabolism in control cells. Furthermore, using *in silico* analysis we can predict potential enzymes that may be responsible for the altered estrogen metabolism in PAH. We can then target these enzymes *in vitro* to assess if we can reverse this metabolic phenotype. Effectively, this can be utilized as a screening method to identify novel therapeutic targets that can beneficially rescue the altered metabolic profile. Ultimately, we need to validate our results with the gold standard analytical technique, LC-MS.

We have highlighted a key role for CYP1B1 in PAH pathogenesis and future studies will examine the contribution of CYP1B1 to the formation of 16 $\alpha$ -hydroxylated estrogens in hPASMCs. Future studies will also address the molecular mechanisms associated with CYP1B1 pathogenesis and specifically the effects of 16 $\alpha$ -OHE1 and 16 $\alpha$ -OHE2 on cellular signalling pathways.

We anticipate that future therapies that target the estrogen pathway in PAH will show promising therapeutic effects on the basis of the evidence that we have provided here and that have been shown by other researchers within the field. We strongly encourage the development of therapies that target estrogen and its metabolism in this devastating cardiovascular disease.

## 6.1 References

- Abe, K, Toba, M, Alzoubi, A, Ito, M, Fagan, KA, Cool, CD, Voelkel, NF, McMurtry, IF & Oka, M. (2010). Formation of plexiform lesions in experimental severe pulmonary arterial hypertension. *Circulation*, **121**, 2747-2754.
- Abenhaim, L, Moride, Y, Brenot, F, Rich, S, Benichou, J, Kurz, X, Higenbottam, T, Oakley, C, Wouters, E & Aubier, M. (1996). Appetite-suppressant drugs and the risk of primary pulmonary hypertension. International primary pulmonary hypertension study group. *N Engl J Med*, **335**, 609-616.
- Abid, S, Houssaini, A, Chevarin, C, Marcos, E, Tissot, CM, Gary-Bobo, G, Wan, F, Mouraret, N, Amsellem, V, Dubois-Rande, JL, Hamon, M & Adnot, S. (2012). Inhibition of gut- and lung-derived serotonin attenuates pulmonary hypertension in mice. *Am J Physiol Lung Cell Mol Physiol*, **303**, L500-L509.
- Acharya, A, Das, I, Chandhok, D & Saha, T. (2010). Redox regulation in cancer: a double-edged sword with therapeutic potential. *Oxidative Medicine and Cellular Longevity*, **3**, 23-34.
- Agarwal, VR, Bulun, SE, Leitch, M, Rohrich, R & Simpson, ER. (1996). Use of alternative promoters to express the aromatase cytochrome P450 (CYP19) gene in breast adipose tissues of cancer-free and breast cancer patients. *Journal of Clinical Endocrinology & Metabolism*, **81**, 3843-3849.
- Ahn, BH, Park, HK, Cho, HG, Lee, HA, Lee, YM, Yang, EK & Lee, WJ. (2003). Estrogen and enalapril attenuate the development of right ventricular hypertrophy induced by monocrotaline in ovariectomized rats. *Journal of Korean Medical Science*, **18**, 641-648.
- Aka, JA, Mazumdar, M, Chen, CQ, Poirier, D & Lin, SX. (2010). 17beta-hydroxysteroid dehydrogenase type 1 stimulates breast cancer by dihydrotestosterone inactivation in addition to estradiol production. *Mol Endocrinol*, **24**, 832-845.
- Akishita, M, Ouchi, Y, Miyoshi, H, Orimo, A, Kozaki, K, Eto, M, Ishikawa, M, Kim, S, Toba, K & Orimo, H. (1996). Estrogen inhibits endothelin-1 production and c-fos gene expression in rat aorta. *Atherosclerosis*, **125**, 27-38.
- Aldashev, AA, Sarybaev, AS, Sydykov, AS, Kalmyrzaev, BB, Kim, EV, Mamanova, LB, Maripov, R, Kojonazarov, BK, Mirrakhimov, MM, Wilkins, MR & Morrell, NW. (2002). Characterization of high-altitude pulmonary hypertension in the Kyrgyz. *Am J Respir Crit Care Med*, **166**, 1396-1402.
- Alexander, AF & Jensen, R. (1959). Gross cardiac changes in cattle with high mountain (brisket) disease and in experimental cattle maintained at high altitudes. *American Journal of Veterinary Research*, **20**, 680-689.
- Alhencgelas, F, Tsai, SJ, Callahan, KS, Campbell, WB & Johnson, AR. (1982). Stimulation of prostaglandin formation by vasoactive mediators in cultured human-endothelial cells. *Prostaglandins*, **24**, 723-742.
- Alzoubi, A, Toba, M, Abe, K, O'Neill, KD, Rocic, P, Fagan, KA, McMurtry, IF & Oka, M. (2013). Dehydroepiandrosterone restores right ventricular structure and function in rats with severe pulmonary arterial hypertension. *American Journal of Physiology-Heart and Circulatory Physiology*, **304**, H1708-H1718.

- Archer, SL, Weir, EK & Wilkins, MR. (2010). Basic science of pulmonary arterial hypertension for clinicians: new concepts and experimental therapies. *Circulation*, **121**, 2045-2066.
- Atkinson, C, Stewart, S, Upton, PD, Machado, R, Thomson, JR, Trembath, RC & Morrell, NW. (2002). Primary pulmonary hypertension is associated with reduced pulmonary vascular expression of type II bone morphogenetic protein receptor. *Circulation*, **105**, 1672-1678.
- Austin, ED, Cogan, JD, West, JD, Hedges, LK, Hamid, R, Dawson, EP, Wheeler, LA, Parl, FF, Loyd, JE & Phillips, JA. (2009). Alterations in oestrogen metabolism: implications for higher penetrance of familial pulmonary arterial hypertension in females. *Eur Respir J*, **34**, 1093-1099.
- Austin, ED, Lahm, T, West, J, Tofovic, SP, Johansen, AK, MacLean, MR, Alzoubi, A & Oka, M. (2013). Gender, sex hormones and pulmonary hypertension. *Pulm Circ*, **3**, 294-314.
- Austin, E, Hamid, R, Hemnes, A, Loyd, J, Blackwell, T, Yu, C, Phillips III, J, Gaddipati, R, Gladson, S, Gu, E, West, J & Lane, K. (2012). BMPR2 expression is suppressed by signaling through the estrogen receptor. *Biology of Sex Differences*, **3**, 6.
- Badawi, AF, Cavalieri, EL & Rogan, EG. (2001). Role of human cytochrome P450 1A1, 1A2, 1B1, and 3A4 in the 2-, 4-, and 16 $\alpha$ -hydroxylation of 17 $\beta$ -estradiol. *Metabolism*, **50**, 1001-1003.
- Badesch, DB, Champion, HC, Sanchez, MAG, Hoepfer, MM, Loyd, JE, Manes, A, McGoon, M, Naeije, R, Olschewski, H, Oudiz, RJ & Torbicki, A. (2009). Diagnosis and assessment of pulmonary arterial hypertension. *Journal of the American College of Cardiology*, **54**, S55-S66.
- Badesch, DB, Raskob, GE, Elliott, CG, Krichman, AM, Farber, HW, Frost, AE, Barst, RJ, Benza, RL, Liou, TG, Turner, M, Giles, S, Feldkircher, K, Miller, DP & McGoon, MD. (2010). Pulmonary arterial hypertension: baseline characteristics from the REVEAL Registry. *Chest*, **137**, 376-387.
- Badesch, DB, Orton, EC, Zapp, LM, Westcott, JY, Hester, J, Voelkel, NF & Stenmark, KR. (1989). Decreased arterial wall prostaglandin production in neonatal calves with severe chronic pulmonary hypertension. *American Journal of Respiratory Cell and Molecular Biology*, **1**, 489-498.
- Ball, P, Emons, G, Kayser, H & Teichmann, J. (1983). Metabolic-Clearance Rates of Catechol Estrogens in Rats. *Endocrinology*, **113**, 1781-1783.
- Baloira, A, Nunez, M, Cifrian, J, Vilarino, C, Ojeda, M & Valverde, D. (2012). Polymorphisms in the Serotonin Transporter Protein (SERT) Gene in Patients With Pulmonary Arterial Hypertension. *Archivos de Bronconeumologia*, **48**, 77-80.
- Bandiera, S, Weidlich, S, Harth, V, Broede, P, Ko, Y & Friedberg, T. (2005). Proteasomal degradation of human CYP1B1: effect of the Asn453Ser polymorphism on the post-translational regulation of CYP1B1 expression. *Molecular Pharmacology*, **67**, 435-443.

- Barberis, MCP, Veronese, S, Bauer, D, DeJuli, E & Harari, S. (1995). Immunocytochemical detection of progesterone receptors - A study in a patient with primary pulmonary-hypertension. *Chest*, **107**, 869-872.
- Barros, R & Gustafsson, JÅ. (2011). Estrogen Receptors and the Metabolic Network. *Cell Metabolism*, **14**, 289-299.
- Benza, RL, Miller, DP, Barst, RJ, Badesch, DB, Frost, AE & McGoon, MD. (2012). An evaluation of long-term survival from time of diagnosis in pulmonary arterial hypertension from the REVEAL Registry.(Report). *Chest*, **142**, 448-456.
- Benza, RL, Miller, DP, Gomberg-Maitland, M, Frantz, RP, Foreman, AJ, Coffey, CS, Frost, A, Barst, RJ, Badesch, DB, Elliott, CG, Liou, TG & McGoon, MD. (2010). Predicting survival in pulmonary arterial hypertension: insights from the registry to evaluate early and long-term pulmonary arterial hypertension disease management (REVEAL). *Circulation*, **122**, 164-172.
- Beretta, L, Caronni, M, Origgi, L, Ponti, A, Santaniello, A & Scorza, R. (2006). Hormone replacement therapy may prevent the development of isolated pulmonary hypertension in patients with systemic sclerosis and limited cutaneous involvement. *Scandinavian Journal of Rheumatology*, **35**, 468-471.
- Bieche, I, Narjoz, C, Asselah, T, Vacher, S, Marcellin, P, Lidereau, R, Beaune, P & de Wazières, I. (2007). Reverse transcriptase-PCR quantification of mRNA levels from cytochrome (CYP)1, CYP2 and CYP3 families in 22 different human tissues. *Pharmacogenetics and Genomics*, **17**, 731-742.
- Blalock, SE, Matulevicius, S, Mitchell, LC, Reimold, S, Warner, J, Peshock, R, Torres, F & Chin, KM. (2010). Long-term outcomes with ambrisentan monotherapy in pulmonary arterial hypertension. *Journal of Cardiac Failure*, **16**, 121-127.
- Bonnet, S, Dumas-de-La-Roque, E, Begueret, H, Marthan, R, Fayon, M, Dos Santos, P, Savineau, JP & Baulieu, EE. (2003). Dehydroepiandrosterone (DHEA) prevents and reverses chronic hypoxic pulmonary hypertension. *Proceedings of the National Academy of Sciences of the United States of America*, **100**, 9488-9493.
- Bowers, R, Cool, C, Murphy, RC, Tuder, RM, Hopken, MW, Flores, SC & Voelkel, NF. (2004). Oxidative stress in severe pulmonary hypertension. *Am J Respir Crit Care Med*, **169**, 764-769.
- Bui, QD & Weisz, J. (1989). Monooxygenase mediating catecholesterogen formation by rat anterior-pituitary is an estrogen-4-hydroxylase. *Endocrinology*, **124**, 1085-1087.
- Burton, RR, Besch, EL & Smith, AH. (1968). Effect of chronic hypoxia on the pulmonary arterial blood pressure of the chicken. *American Journal of Physiology -- Legacy Content*, **214**, 1438-1442.
- Buters, JTM, Sakai, S, Richter, T, Pineau, T, Alexander, DL, Savas, U, Doehmer, J, Ward, JM, Jefcoate, CR & Gonzalez, FJ. (1999). Cytochrome P450 CYP1B1 determines susceptibility to 7,12-dimethylbenz[a]anthracene-induced lymphomas. *Proceedings of the National Academy of Sciences*, **96**, 1977-1982.
- Capdevila, JH & Falck, JR. (2001). The CYP P450 arachidonic acid monooxygenases: from cell signaling to blood pressure regulation. *Biochemical and Biophysical Research Communications*, **285**, 571-576.

Carey, MA, Card, JW, Voltz, JW, Germolec, DR, Korach, KS & Zeldin, DC. (2007). The impact of sex and sex hormones on lung physiology and disease: lessons from animal studies. *American Journal of Physiology - Lung Cellular and Molecular Physiology*, **293**, L272-L278.

Cauley, JA, Zmuda, JM, Danielson, ME, Ljung, BM, Bauer, DC, Cummings, SR & Kuller, LH. (2003). Estrogen metabolites and the risk of breast cancer in older women. *Epidemiology*, **14**, 740-744.

Cavalieri, EL, Stack, DE, Devanesan, PD, Todorovic, R, Dwivedy, I, Higginbotham, S, Johansson, SL, Patil, KD, Gross, ML, Gooden, JK, Ramanathan, R, Cerny, RL & Rogan, EG. (1997). Molecular origin of cancer: Catechol estrogen-3,4-quinones as endogenous tumor initiators. *Proceedings of the National Academy of Sciences of the United States of America*, **94**, 10937-10942.

Cerfolio, RJ, Bryant, AS, Scott, E, Sharma, M, Robert, F, Spencer, SA & Garver, RI. (2006). Women with pathologic stage I, II, and III non-small cell lung cancer have better survival than men. *Chest*, **130**, 1796-1802.

Chang, I, Liu, J, Majid, S, Saini, S, Zaman, MS, Yamamura, S, Shahryari, V, Chiyomaru, T, Deng, G, Dahiya, R & Tanaka, Y. (2012). Catechol-O-methyltransferase-mediated metabolism of 4-hydroxyestradiol inhibits the growth of human renal cancer cells through the apoptotic pathway. *Carcinogenesis*, **33**, 420-426.

Chang, TKH, Chen, J & Lee, WBK. (2001). Differential inhibition and inactivation of human CYP1 enzymes by trans-resveratrol: Evidence for mechanism-based inactivation of CYP1A2. *Journal of Pharmacology and Experimental Therapeutics*, **299**, 874-882.

Chaouat, A, Coulet, F, Favre, C, Simonneau, G, Weitzenblum, E, Soubrier, F & Humbert, M. (2004). Endoglin germline mutation in a patient with hereditary haemorrhagic telangiectasia and dexfenfluramine associated pulmonary arterial hypertension. *Thorax*, **59**, 446-448.

Chen, SJ, Chen, YF, Meng, QC, Durand, J, Dicarlo, VS & Oparil, S. (1995). Endothelin-receptor antagonist bosentan prevents and reverses hypoxic pulmonary hypertension in rats. *Journal of Applied Physiology*, **79**, 2122-2131.

Chen, Z, Yuhanna, IS, Galcheva-Gargova, Z, Karas, RH, Mendelsohn, RE & Shaul, PW. (1999). Estrogen receptor alpha mediates the nongenomic activation of endothelial nitric oxide synthase by estrogen. *Journal of Clinical Investigation*, **103**, 401-406.

Chen, ZH, Hurh, YJ, Na, HK, Kim, JH, Chun, YJ, Kim, DH, Kang, KS, Cho, MH & Surh, YJ. (2004). Resveratrol inhibits TCDD-induced expression of CYP1A1 and CYP1B1 and catechol estrogen-mediated oxidative DNA damage in cultured human mammary epithelial cells. *Carcinogenesis*, **25**, 2005-2013.

Cheng, GJ, Zhang, WH, Makinen, S, Saji, S, Warner, M, Gustafsson, JA & Hovatta, O. (2002). A role for the androgen receptor in follicular atresia of estrogen receptor beta knockout mouse ovary. *Biology of Reproduction*, **66**, 77-84.

Cheng, Y, Chang, LW, Cheng, LC, Tsai, MH & Lin, P. (2007). 4-Methoxyestradiol-induced oxidative injuries in human lung epithelial cells. *Toxicology and Applied Pharmacology*, **220**, 271-277.

- Chhatwani, L, Xu, X, Veenstra, TD, Voelkel, N & Sweeney, LB. (2010). Serum estrogen metabolites in patients with severe pulmonary arterial hypertension. *Am J Respir Crit Care Med*, **181**, A4860.
- Choudhary, D, Jansson, I, Schenkman, JB, Sarfarazi, M & Stoilov, I. (2003). Comparative expression profiling of 40 mouse cytochrome P450 genes in embryonic and adult tissues. *Archives of Biochemistry and Biophysics*, **414**, 91-100.
- Choudhary, D, Jansson, I, Stoilov, I, Sarfarazi, M & Schenkman, JB. (2004). Metabolism of retinoids and arachidonic acid by human and mouse cytochrome P450 1B1. *Drug Metabolism and Disposition*, **32**, 840-847.
- Chun, YJ, Kim, S, Kim, D, Lee, SK & Guengerich, FP. (2001). A new selective and potent inhibitor of human cytochrome P4501B1 and its application to antimutagenesis. *Cancer Research*, **61**, 8164-8170.
- Ciolino, H, MacDonald, C, Memon, O, Dankwah, M & Chao Yeh, G. (2003). Dehydroepiandrosterone inhibits the expression of carcinogen-activating enzymes in vivo. *Int J Cancer*, **105**, 321-325.
- Ciuculan, L, Bonneau, O, Hussey, M, Duggan, N, Holmes, AM, Good, R, Stringer, R, Jones, P, Morrell, NW, Jarai, G, Walker, C, Westwick, J & Thomas, M. (2011). A novel murine model of severe pulmonary arterial hypertension. *Am J Respir Crit Care Med*, **184**, 1171-1182.
- Ciuculan, L, Hussey, MJ, Burton, V, Good, R, Duggan, N, Beach, S, Jones, P, Fox, R, Clay, I, Bonneau, O, Konstantinova, I, Pearce, A, Rowlands, DJ, Jarai, G, Westwick, J, MacLean, MR & Thomas, M. (2012). Imatinib attenuates hypoxia-induced PAH pathology via reduction in 5-HT through inhibition of TPH1 expression. *Am J Respir Crit Care Med*.
- Clifton, KH & Meyer, RK. (1956). Mechanism of anterior pituitary tumor induction by estrogen. *Anatomical Record*, **125**, 65-81.
- Comroe, JH. (1966). The main functions of the pulmonary circulation. *Circulation*, **33**, 146-158.
- Conway, DE, Sakurai, Y, Weiss, D, Vega, JD, Taylor, WR, Jo, H, Eskin, SG, Marcus, CB & McIntire, LV. (2009). Expression of CYP1A1 and CYP1B1 in human endothelial cells: regulation by fluid shear stress. *Cardiovascular Research*, **81**, 669-677.
- Cool, CD, Stewart, JS, Werahera, P, Miller, GJ, Williams, RL, Voelkel, NF & Tuder, RW. (1999). Three-dimensional reconstruction of pulmonary arteries in plexiform pulmonary hypertension using cell-specific markers - Evidence for a dynamic and heterogeneous process of pulmonary endothelial cell growth. *American Journal of Pathology*, **155**, 411-419.
- Corbin, JD, Beasley, A, Blount, MA & Francis, SH. (2005). High lung PDE5: A strong basis for treating pulmonary hypertension with PDE5 inhibitors. *Biochemical and Biophysical Research Communications*, **334**, 930-938.
- Cribb, AE, Knight, MJ, Dryer, D, Guernsey, J, Hender, K, Tesch, M & Saleh, TM. (2006). Role of polymorphic human cytochrome P450 enzymes in estrone oxidation. *Cancer Epidemiology Biomarkers & Prevention*, **15**, 551-558.

Csiszar, A, Labinskyy, N, Olson, S, Pinto, JT, Gupte, S, Wu, JM, Hu, F, Ballabh, P, Podlutzky, A, Losonczy, G, de Cabo, R, Mathew, R, Wolin, MS & Ungvari, Z. (2009). Resveratrol prevents monocrotaline-induced pulmonary hypertension in rats  
122. *Hypertension*, **54**, 668-675.

D'Alonzo, GE, Barst, RJ, Ayres, SM, Bergofsky, EH, Brundage, BH, Detre, KM, Fishman, AP, Goldring, RM, Groves, BM, Kernis, JT, Levy, PS, Pietra, GG, Reid, LM, Reeves, JT, Rich, S, Vreim, CE, Williams, GW & Wu, M. (1991). Survival in patients with primary pulmonary hypertension: results from a national prospective registry. *Annals of Internal Medicine*, **115**, 343-349.

Dahut, WL, Lakhani, NJ, Gulley, JL, Arlen, PM, Kohn, EC, Kotz, H, McNally, D, Parr, A, Nguyen, D, Yang, SX, Steinberg, SM, Venitz, J, Sparreboom, A & Figg, WD. (2006). Phase I clinical trial of oral 2-methoxyestradiol, an antiangiogenic and apoptotic agent, in patients with solid tumors. *Cancer Biology & Therapy*, **5**, 22-27.

Dallal, CM, Tice, JA, Buist, DSM, Bauer, DC, Lacey, JV, Cauley, JA, Hue, TF, LaCroix, A, Falk, RT, Pfeiffer, RM, Fuhrman, BJ, Veenstra, TD, Xu, X, Brinton, LA & for, tB. (2013). Estrogen metabolism and breast cancer risk among postmenopausal women: a case-cohort study within B~FIT. *Carcinogenesis*.

Dawling, S, Roodi, N & Parl, FF. (2003). Methoxyestrogens exert feedback inhibition on cytochrome P450 1A1 and 1B1. *Cancer Research*, **63**, 3127-3132.

de Jesus Perez, VA, Alastalo, TP, Wu, JC, Axelrod, JD, Cooke, JP, Amieva, M & Rabinovitch, M. (2009). Bone morphogenetic protein 2 induces pulmonary angiogenesis via Wnt- $\beta$ -catenin and Wnt-RhoA-Rac1 pathways. *The Journal of Cell Biology*, **184**, 83-99.

de La Roque, ED, Savineau, JP, Metivier, AC, Billes, MA, Kraemer, JP, Doutreleau, S, Jougon, J, Marthan, R, Moore, N, Fayon, M, Baulieu, EE & Dromer, C. (2012). Dehydroepiandrosterone (DHEA) improves pulmonary hypertension in chronic obstructive pulmonary disease (COPD): A pilot study. *Annales D Endocrinologie*, **73**, 20-25.

deMello, DE & Reid, L (1991). Arteries and veins. In *The lung, scientific foundations*. ed. Crystal, RG & West, JB pp. 767-777. Raven Press: New York.

Dempsie, Y, MacRitchie, NA, White, K, Morecroft, I, Wright, AF, Nilsen, M, Loughlin, L, Mair, KM & MacLean, MR. (2013). Dexfenfluramine and the oestrogen metabolizing enzyme CYP1B1 in the development of pulmonary arterial hypertension. *Cardiovascular Research*.

Dempsie, Y, Morecroft, I, Welsh, DJ, MacRitchie, NA, Herold, N, Loughlin, L, Nilsen, M, Peacock, AJ, Harmar, A, Bader, M & MacLean, MR. (2008). Converging evidence in support of the serotonin hypothesis of dexfenfluramine-induced pulmonary hypertension with novel transgenic mice. *Circulation*, **117**, 2928-2937.

Dempsie, Y, Nilsen, M, White, K, Loughlin, L & MacLean, MR. (2010). Effects of gender on the development of pulmonary arterial hypertension in Mice over-expressing S100A4/Mts1. *Am J Respir Crit Care Med*, **181**, A6309.

Dempsie, Y, Nilsen, M, White, K, Mair, K, Loughlin, L, Ambartsumian, N, Rabinovitch, M & MacLean, M. (2011). Development of pulmonary arterial

- hypertension in mice over-expressing S100A4/Mts1 is specific to females. *Respiratory Research*, **12**, 159.
- Deng, Z, Morse, JH, Slager, SL, Cuervo, N, Moore, KJ & Venetos, G. (2000). Familial primary pulmonary hypertension (gene PPH1) is caused by mutations in the bone morphogenetic protein receptor-II gene. *Am J Hum Genet*, **67**, 737-744.
- Dresdale, DT, Schultz, M & Michtom, RJ. (1951). Primary pulmonary hypertension .1. Clinical and hemodynamic study. *American Journal of Medicine*, **11**, 686-705.
- Dubey, RK, Jackson, EK, Keller, PJ, Imthurn, B & Rosselli, M. (2001). Estradiol metabolites inhibit endothelin synthesis by an estrogen receptor-independent mechanism. *Hypertension*, **37**, 640-644.
- Dunn, JF, Nisula, BC & Rodbard, D. (1981). Transport of steroid-hormones - binding of 21 endogenous steroids to both testosterone-binding globulin and corticosteroid-binding globulin in human-plasma. *Journal of Clinical Endocrinology & Metabolism*, **53**, 58-68.
- Earley, S & Resta, TC. (2002). Estradiol attenuates hypoxia-induced pulmonary endothelin-1 gene expression. *American Journal of Physiology-Lung Cellular and Molecular Physiology*, **283**, L86-L93.
- Eddahibi, S, Adnot, S, Frisdal, E, Levame, M, Hamon, M & Raffestin, B. (2001a). Dexfenfluramine-associated changes in 5-hydroxytryptamine transporter expression and development of hypoxic pulmonary hypertension in rats. *J Pharmacol Exp Ther*, **297**, 148-154.
- Eddahibi, S, Fabre, V, Boni, C, Martres, MP, Raffestin, B, Hamon, M & Adnot, S. (1999). Induction of serotonin transporter by hypoxia in pulmonary vascular smooth muscle cells: relationship with the mitogenic action of serotonin. *Circ Res*, **84**, 329-336.
- Eddahibi, S, Hanoun, N, Lanfumey, L, Lesch, KP, Raffestin, B, Hamon, M & Adnot, S. (2000). Attenuated hypoxic pulmonary hypertension in mice lacking the 5-hydroxytryptamine transporter gene. *J Clin Invest*, **105**, 1555-1562.
- Eddahibi, S, Raffestin, B, Clozel, M, Levame, M & Adnot, S. (1995). Protection from pulmonary-hypertension with an orally-active endothelin receptor antagonist in hypoxic rats. *American Journal of Physiology-Heart and Circulatory Physiology*, **268**, H828-H835.
- Eddahibi, S, Humbert, M, Fadel, E, Raffestin, B, Darmon, M, Capron, F, Simonneau, G, Darteville, P, Hamon, M & Adnot, S. (2001b). Serotonin transporter overexpression is responsible for pulmonary artery smooth muscle hyperplasia in primary pulmonary hypertension. *J Clin Invest*, **108**, 1141-1150.
- Eliassen, AH, Missmer, SA, Tworoger, SS & Hankinson, SE. (2008). Circulating 2-hydroxy- and 16 alpha-hydroxy estrone levels and risk of breast cancer among postmenopausal women. *Cancer Epidemiology Biomarkers & Prevention*, **17**, 2029-2035.
- Elliot, FM & Reid, L. (1964). Some new facts about the pulmonary artery and its branching pattern. *Clinical Radiology*, **16**, 193-198.

- English, KM, Jones, RD, Jones, TH, Morice, AH & Channer, KS. (2001). Gender differences in the vasomotor effects of different steroid hormones in rat pulmonary and coronary arteries. *Hormone and Metabolic Research*, **33**, 645-652.
- Euler, US & Liljestrand, G. (1946). Observations on the pulmonary arterial blood pressure in the cat. *Acta Physiologica Scandinavica*, **12**, 301-320.
- Fairweather, D, Frisancho-Kiss, S & Rose, NR. (2008). Sex differences in autoimmune disease from a pathological perspective. *American Journal of Pathology*, **173**, 600-609.
- Farhat, MY, Chen, MF, Bhatti, T, Iqbal, A, Cathapermal, S & Ramwell, PW. (1993). Protection by oestradiol against the development of cardiovascular changes associated with monocrotaline pulmonary hypertension in rats. *Br J Pharmacol*, **110**, 719-723.
- Farhat, MY, Vargas, R, Dingaana, B & Ramwell, PW. (1992). In vitro effect of oestradiol on thymidine uptake in pulmonary vascular smooth muscle cell: role of the endothelium. *Br J Pharmacol*, **107**, 679-683.
- Farkas, L, Farkas, D, Ask, K, Iler, A, Gauldie, J, Margetts, P, Inman, M & Kolb, M. (2009). VEGF ameliorates pulmonary hypertension through inhibition of endothelial apoptosis in experimental lung fibrosis in rats. *J Clin Invest*, **119**, 1298-1311.
- Fessel, JP, Chen, X, Frump, A, Gladson, S, Blackwell, T, Kang, C, Johnson, J, Loyd, JE, Hemnes, A, Austin, E & West, J. (2013a). Interaction between bone morphogenetic protein receptor type 2 and estrogenic compounds in pulmonary arterial hypertension. *Pulm Circ*, **3**, 564-577.
- Fessel, JP, Flynn, CR, Robinson, LJ, Penner, NL, Gladson, S, Kang, C, Wasserman, DH, Hemnes, AR & West, JD. (2013b). Hyperoxia Synergizes with Mutant BMPR2 to Cause Metabolic Stress, Oxidant Injury, and Pulmonary Hypertension. *American Journal of Respiratory Cell and Molecular Biology*.
- Filardo, EJ, Graeber, CT, Quinn, JA, Resnick, MB, Giri, D, DeLellis, RA, Steinhoff, MM & Sabo, E. (2006). Distribution of GPR30, a seven membrane-spanning estrogen receptor, in primary breast cancer and its association with clinicopathologic determinants of tumor progression. *Clinical Cancer Research*, **12**, 6359-6366.
- Filardo, EJ, Quinn, JA, Bland, KI & Frackelton, AR. (2000). Estrogen-Induced Activation of Erk-1 and Erk-2 Requires the G Protein-Coupled Receptor Homolog, GPR30, and Occurs via Trans-Activation of the Epidermal Growth Factor Receptor through Release of HB-EGF. *Molecular Endocrinology*, **14**, 1649-1660.
- Flouriot, G, Brand, H, Denger, S, Metivier, R, Kos, M, Reid, G, Sonntag-Buck, V & Gannon, F. (2000). Identification of a new isoform of the human estrogen receptor-alpha (hER-alpha) that is encoded by distinct transcripts and that is able to repress hER-alpha activation function 1. *Embo Journal*, **19**, 4688-4700.
- Forster, C, Kietz, S, Hultenby, K, Warner, M & Gustafsson, JA. (2004). Characterization of the ER beta(-/-) mouse heart. *Proceedings of the National Academy of Sciences of the United States of America*, **101**, 14234-14239.
- Frid, MG, Kale, VA & Stenmark, KR. (2002). Mature vascular endothelium can give rise to smooth muscle cells via endothelial-mesenchymal transdifferentiation - In vitro analysis. *Circ Res*, **90**, 1189-1196.

Frid, MG, Moiseeva, EP & Stenmark, KR. (1994). Multiple phenotypically distinct smooth-muscle cell-populations exist in the adult and developing bovine pulmonary arterial media in-vivo. *Circ Res*, **75**, 669-681.

Fujita, M, Mason, RJ, Cool, C, Shannon, JM, Hara, N & Fagan, KA. (2002). Pulmonary hypertension in TNF-alpha-overexpressing mice is associated with decreased VEGF gene expression. *Journal of Applied Physiology*, **93**, 2162-2170.

Fulton, RM, Hutchinson, EC & Jones, AM. (1952). Ventricular weight in cardiac hypertrophy. *British Heart Journal*, **14**, 413-420.

Gabler, NB, French, B, Strom, BL, Liu, ZY, Palevsky, HI, Taichman, DB, Kawut, SM & Halpern, SD. (2012). Race and sex differences in response to endothelin receptor antagonists for pulmonary arterial hypertension. *Chest*, **141**, 20-26.

Gaikwad, NW. (2013). Ultra performance liquid chromatography-tandem mass spectrometry method for profiling of steroid metabolome in human tissue. *Anal Chem*, **85**, 4951-4960.

Galie, N, Hoeper, MM, Humbert, M, Torbicki, A, Vachiery, JL, Barbera, JA, Beghetti, M, Corris, P, Gaine, S, Gibbs, JS, Gomez-Sanchez, MA, Jondeau, G, Klepetko, W, Opitz, C, Peacock, A, Rubin, L, Zellweger, M & Simonneau, G. (2009). Guidelines for the diagnosis and treatment of pulmonary hypertension. *European Heart Journal*, **30**, 2493-2537.

Galie, N, Torbicki, A, Barst, R, Darteville, P, Haworth, S, Higenbottam, T, Olschewski, H, Peacock, A, Pietra, G, Rubin, LJ & Simonneau, G. (2004). Guidelines on diagnosis and treatment of pulmonary arterial hypertension - The task force on diagnosis and treatment of pulmonary arterial hypertension of the European society of cardiology. *European Heart Journal*, **25**, 2243-2278.

Galiè, N, Corris, PA, Frost, A, Girgis, RE, Granton, J, Jing, ZC, Klepetko, W, McGoon, MD, McLaughlin, VV, Preston, IR, Rubin, LJ, Sandoval, J, Seeger, W & Keogh, A. (2013). Updated treatment algorithm of pulmonary arterial hypertension. *Journal of the American College of Cardiology*, **62**.

Galié, N, Manes, A & Branzi, A. (2004). The endothelin system in pulmonary arterial hypertension. *Cardiovascular Research*, **61**, 227-237.

Ghodsi, F & Will, JA. (1981). Changes in pulmonary structure and function induced by monocrotaline intoxication. *American Journal of Physiology*, **240**, H149-H155.

Ghofrani, HA, Galie, N, Grimminger, F, Grunig, E, Humbert, M, Jing, ZC, Keogh, AM, Langleben, D, Kilama, MO, Fritsch, A, Neuser, D & Rubin, LJ. (2013). Riociguat for the treatment of pulmonary arterial hypertension. *N Engl J Med*, **369**, 330-340.

Giaid, A, Yanagisawa, M, Langleben, D, Michel, RP, Levy, R, Shennib, H, Kimura, S, Masaki, T, Duguid, WP & Stewart, DJ. (1993). Expression of endothelin-1 in the lungs of patients with pulmonary-hypertension. *N Engl J Med*, **328**, 1732-1739.

Gibson, GG & Skett, P. (2001). *Introduction to drug metabolism*. Nelson Thorne Publishers: Cheltenham.

- Glover, GH & Newsom, LE. (1915). Brisket disease (dropsy of high altitude). *Agr Expt Sta Colorado Agri Coll Bull*, **204**, 3-24.
- Gomez-Arroyo, J, Saleem, SJ, Mizuno, S, Syed, AA, Bogaard, HJ, Abbate, A, Taraseviciene-Stewart, L, Sung, Y, Kraskauskas, D, Farkas, D, Conrad, DH, Nicolls, MR & Voelkel, NF. (2012a). A brief overview of mouse models of pulmonary arterial hypertension: problems and prospects. *American Journal of Physiology - Lung Cellular and Molecular Physiology*, **302**, L977-L991.
- Gomez-Arroyo, JG, Farkas, L, Alhussaini, AA, Farkas, D, Kraskauskas, D, Voelkel, NF & Bogaard, HJ. (2012b). The monocrotaline model of pulmonary hypertension in perspective. *American Journal of Physiology - Lung Cellular and Molecular Physiology*, **302**, L363-L369.
- Graham, BB, Bandeira, AP, Morrell, NW, Butrous, G & Tuder, RM. (2010). Schistosomiasis-associated pulmonary hypertension pulmonary vascular disease: The global perspective. *Chest*, **137**, 20S-29S.
- Greenway, S, van Suylen, RJ, Sarvaas, GD, Kwan, E, Ambartsumian, N, Lukanidin, E & Rabinovitch, M. (2004). S100A4/Mts1 produces murine pulmonary artery changes resembling plexogenic arteriopathy and is increased in human plexogenic arteriopathy. *American Journal of Pathology*, **164**, 253-262.
- Gribben, JG, Ryan, DP, Boyajian, R, Urban, RG, Hedley, ML, Beach, K, Nealon, P, Matulonis, U, Campos, S, Gilligan, TD, Richardson, PG, Marshall, B, Neuberg, D & Nadler, LM. (2005). Unexpected association between induction of immunity to the universal tumor antigen CYP1B1 and response to next therapy. *Clinical Cancer Research*, **11**, 4430-4436.
- Gros, R, Ding, QM, Sklar, LA, Prossnitz, EE, Arterburn, JB, Chorazyczewski, J & Feldman, RD. (2011). GPR30 expression is required for the mineralocorticoid receptor-independent rapid vascular effects of aldosterone. *Hypertension*, **57**, 442-U201.
- Guignabert, C, Izikki, M, Tu, LI, Li, Z, Zadigue, P, Barlier-Mur, AM, Hanoun, Nm, Rodman, D, Hamon, M, Adnot, S & Eddahibi, S. (2006). Transgenic mice overexpressing the 5-hydroxytryptamine transporter gene in smooth muscle develop pulmonary hypertension. *Circ Res*, **98**, 1323-1330.
- Gunnarsson, C, Jerevall, PL, Hammar, K, Olsson, B, Nordenskjöld, B, Jansson, A & Stål, O. (2008). Amplification of HSD17B1 has prognostic significance in postmenopausal breast cancer. *Breast Cancer Res Treat*, **108**, 35-41.
- Haddad, F, Skhiri, M & Michelakis, E (2011). Right ventricular dysfunction in pulmonary hypertension. In *Textbook of pulmonary vascular diseases*. ed. Yuan, JXJ, Garcia, JGN, Hales, CA, Rich, S, Archer, SL & West, JB pp. 1313-1331. Springer: New York.
- Hamid, R, Cogan, JD, Hedges, LK, Austin, E, Phillips, JA, Newman, JH & Loyd, JE. (2009). Penetrance of pulmonary arterial hypertension is modulated by the expression of normal BMPR2 allele. *Hum Mutat*, **30**, 649-654.
- Hammond, DK, Zhu, BT, Wang, MY, Ricci, MJ & Liehr, JG. (1997). Cytochrome P450 metabolism of estradiol in hamster liver and kidney. *Toxicology and Applied Pharmacology*, **145**, 54-60.

- Hanna, IH, Dawling, S, Roodi, N, Guengerich, FP & Parl, FF. (2000). Cytochrome P450 1B1 (CYP1B1) pharmacogenetics: association of polymorphisms with functional differences in estrogen hydroxylation activity. *Cancer Research*, **60**, 3440-3444.
- Harada, N, Sasano, H, Murakami, H, Ohkuma, T, Nagura, H & Takagi, Y. (1999). Localized expression of aromatase in human vascular tissues. *Circulation Research*, **84**, 1285-1291.
- Harrison, RE, Flanagan, JA, Sankelo, M, Abdalla, SA, Rowell, J, Machado, RD, Elliott, CG, Robbins, IM, Olschewski, H, McLaughlin, V, Gruenig, E, Kermeen, F, Laitinen, T, Morrell, NW & Trembath, RC. (2003). Molecular and functional analysis identifies ALK-1 as the predominant cause of pulmonary hypertension related to hereditary haemorrhagic telangiectasia. *Journal of Medical Genetics*, **40**, 865-871.
- Heldring, N, Isaacs, GD, Diehl, AG, Sun, M, Cheung, E, Ranish, JA & Kraus, WL. (2011). Multiple sequence- specific DNA-binding proteins mediate estrogen receptor signaling through a tethering pathway. *Molecular Endocrinology*, **25**, 564-574.
- Heldring, N, Pike, A, Andersson, S, Matthews, J, Cheng, G, Hartman, J, Tujague, M, Ström, A, Treuter, E, Warner, M & Gustafsson, JÅ. (2007). Estrogen receptors: How do they signal and what are their targets. *Physiological Reviews*, **87**, 905-931.
- Hemnes, AR, Maynard, KB, Champion, HC, Gleaves, L, Penner, N, West, J & Newman, J. (2012). Testosterone negatively regulates right ventricular load stress responses in mice. *Pulm Circ*, **2**, 352-358.
- Hemnes, A, Fike, C, Austin, E, West, J, Johnson, J, Fessel, J, Lane, K, Roberts II, L, Robinson, L, Talati, M, Mernaugh, R & Blackwell, T. (2011). Oxidative injury is a common consequence of BMPR2 mutations. *Pulm Circ*, **1**, 72-83.
- Hirata, Y, Emori, T, Eguchi, S, Kanno, K, Imai, T, Ohta, K & Marumo, F. (1993). Endothelin receptor subtype-B mediates synthesis of nitric-oxide by cultured bovine endothelial-cells. *Journal of Clinical Investigation*, **91**, 1367-1373.
- Huang, W, Yen, RT, McLaurine, M & Bledsoe, G. (1996). Morphometry of the human pulmonary vasculature. *Journal of Applied Physiology*, **81**, 2123-2133.
- Humbert, M, Monti, G, Brenot, F, Sitbon, O, Portier, A, Grangeot-Keros, L, Duroux, P, Galanaud, P, Simonneau, G & Emilie, D. (1995). Increased interleukin-1 and interleukin-6 serum concentrations in severe primary pulmonary hypertension. *Am J Respir Crit Care Med*, **151**, 1628-1631.
- Humbert, M, Sitbon, O, Chaouat, A, Bertocchi, M, Habib, G, Gressin, V, Yaici, A, Weitzenblum, E, Cordier, JF, Chabot, F, Dromer, C, Pison, C, Reynaud-Gaubert, M, Haloun, A, Laurent, M, Hachulla, E & Simonneau, G. (2006). Pulmonary arterial hypertension in France: results from a national registry. *Am J Respir Crit Care Med*, **173**, 1023-1030.
- Humbert, M, Sitbon, O, Yaïci, A, Montani, D, O'Callaghan, DS, Jaïs, X, Parent, F, Savale, L, Natali, D, Günther, S, Chaouat, A, Chabot, F, Cordier, JF, Habib, G, Gressin, V, Jing, ZC, Souza, R & Simonneau, G. (2010). Survival in incident and prevalent cohorts of patients with pulmonary arterial hypertension. *European Respiratory Journal*, **36**, 549-555.

Ichimori, H, Kogaki, S, Takahashi, K, Ishida, H, Narita, J, Nawa, N, Baden, H, Uchikawa, T, Okada, Y & Ozono, K. (2013). Drastic shift from positive to negative estrogen effect on bone morphogenetic protein signaling in pulmonary arterial endothelial cells under hypoxia. *Circulation Journal*, **77**, 2118-2126.

Im, A, Vogel, VG, Ahrendt, G, Lloyd, S, Ragin, C, Garte, S & Taioli, E. (2009). Urinary estrogen metabolites in women at high risk for breast cancer. *Carcinogenesis*, **30**, 1532-1535.

Izikki, M, Hanoun, N, Marcos, E, Savale, L, Barlier-Mur, AM, Saurini, F, Eddahibi, S, Hamon, M & Adnot, S. (2007). Tryptophan hydroxylase 1 knockout and tryptophan hydroxylase 2 polymorphism: effects on hypoxic pulmonary hypertension in mice. *American Journal of Physiology - Lung Cellular and Molecular Physiology*, **293**, L1045-L1052.

Jacobs, W, van de Veerdonk, MIC, Trip, P, de Man, F, Heymans, MW, Marcus, JT, Kawut, SM, Bogaard, HJ, Boonstra, A & Vonk Noordegraaf, A. (2013). The right ventricle explains sex differences in survival in idiopathic pulmonary arterial hypertension. *CHEST Journal*.

Jennings, BL, Anderson, LJ, Estes, AM, Yaghini, FA, Fang, XR, Porter, J, Gonzalez, FJ, Campbell, WB & Malik, KU. (2012). Cytochrome P450 1B1 contributes to renal dysfunction and damage caused by angiotensin II in mice. *Hypertension*, **59**, 348-354.

Jennings, BL, Sahan-Firat, S, Estes, AM, Das, K, Farjana, N, Fang, XR, Gonzalez, FJ & Malik, KU. (2010). Cytochrome P450 1B1 contributes to angiotensin II-induced hypertension and associated pathophysiology. *Hypertension*, **56**, 667-674.

Jesmin, S, Mowa, CN, Sultana, SN, Shimojo, N, Togashi, H, Iwashima, Y, Kato, N, Sato, A, Sakuma, I, Hiroe, M, Hattori, Y, Yamaguchi, N & Kobayashi, H. (2010). VEGF signaling is disrupted in the hearts of mice lacking estrogen receptor alpha. *European Journal of Pharmacology*, **641**, 168-178.

Jiang, YF, Miyazaki, T, Honda, A, Hirayama, T, Yoshida, S, Tanaka, N & Matsuzaki, Y. (2005). Apoptosis and inhibition of the phosphatidylinositol 3-kinase/Akt signaling pathway in the anti-proliferative actions of dehydroepiandrosterone. *Journal of Gastroenterology*, **40**, 490-497.

Johnson, SR & Granton, JT. (2011). Pulmonary hypertension in systemic sclerosis and systemic lupus erythematosus. *European Respiratory Review*, **20**, 277-286.

Jones, MEE, Thorburn, AW, Britt, KL, Hewitt, KN, Wreford, NG, Proietto, J, Oz, OK, Leury, BJ, Robertson, KM, Yao, S & Simpson, ER. (2000). Aromatase-deficient (ArKO) mice have a phenotype of increased adiposity. *Proceedings of the National Academy of Sciences*, **97**, 12735-12740.

Jones, RC & Capen, DE (2011). Pulmonary vascular development. In *Textbook of pulmonary vascular diseases*. ed. Yuan, JXJ, Garcia, JGN, Hales, CA, Rich, S, Archer, SL & West, JB pp. 25-60. Springer: New York.

Jones, RD, English, KM, Pugh, PJ, Morice, AH, Jones, TH & Channer, KS. (2002). Pulmonary vasodilatory action of testosterone: Evidence of a calcium antagonistic action. *Journal of Cardiovascular Pharmacology*, **39**, 814-823.

- Jonigk, D, Golpon, H, Bockmeyer, CL, Maegel, L, Hoepfer, MM, Gottlieb, J, Nickel, N, Hussein, K, Maus, U, Lehmann, U, Janciauskiene, S, Welte, T, Haverich, A, Rische, J, Kreipe, H & Laenger, F. (2011). Plexiform lesions in pulmonary arterial hypertension composition, architecture, and microenvironment. *American Journal of Pathology*, **179**, 167-179.
- Kabat, GC, Chang, CJ, Sparano, JA, Sepkovic, DW, Hu, XP, Khalil, A, Rosenblatt, R & Bradlow, HL. (1997). Urinary estrogen metabolites and breast cancer: A case-control study. *Cancer Epidemiology Biomarkers & Prevention*, **6**, 505-509.
- Kabat, GC, O'Leary, ES, Gammon, MD, Sepkovic, DW, Teitelbaum, SL, Britton, JA, Terry, MB, Neugut, AI & Bradlow, HL. (2006). Estrogen metabolism and breast cancer. *Epidemiology*, **17**, 80-88.
- Kajstura, J, Rota, M, Hall, SR, Hosoda, T, D'Amario, D, Sanada, F, Zheng, HQ, Ogorek, B, Rondon-Clavo, C, Ferreira-Martins, J, Matsuda, A, Arranto, C, Goichberg, P, Giordano, G, Haley, KJ, Bardelli, S, Rayatzadeh, H, Liu, XL, Quaini, F, Liao, RL, Leri, A, Perrella, MA, Loscalzo, J & Anversa, P. (2011). Evidence for human lung stem cells. *N Engl J Med*, **364**, 1795-1806.
- Karamsetty, MR, Klinger, JR & Hill, NS. (2001). Phytoestrogens restore nitric oxide-mediated relaxation in isolated pulmonary arteries from chronically hypoxic rats. *Journal of Pharmacology and Experimental Therapeutics*, **297**, 968-974.
- Kato, S, Endoh, H, Masuhiro, Y, Kitamoto, T, Uchiyama, S, Sasaki, H, Masushige, S, Gotoh, Y, Nishida, E, Kawashima, H, Metzger, D & Chambon, P. (1995). Activation of the estrogen-receptor through phosphorylation by mitogen-activated protein-kinase. *Science*, **270**, 1491-1494.
- Kawut, SM, Al-Naamani, N, Agerstrand, C, Rosenzweig, EB, Rowan, C, Barst, RJ, Bergmann, S & Horn, EM. (2009). Determinants of right ventricular ejection fraction in pulmonary arterial hypertension. *Chest*, **135**, 752-759.
- Kay, JM, Harris, P & Heath, D. (1967). Pulmonary hypertension produced in rats by ingestion of crotalaria spectabilis seeds. *Thorax*, **22**, 176-179.
- Kramer, MS & Lane, DA. (1998). Aminorex, dexfenfluramine, and primary pulmonary hypertension. *Journal of Clinical Epidemiology*, **51**, 361-364.
- Lahm, T, Crisostomo, PR, Markel, TA, Wang, MJ, Wang, Y, Tan, JN & Meldrum, DR. (2008a). Selective estrogen receptor-alpha and estrogen receptor-beta agonists rapidly decrease pulmonary artery vasoconstriction by a nitric oxide-dependent mechanism. *American Journal of Physiology-Regulatory Integrative and Comparative Physiology*, **295**, R1486-R1493.
- Lahm, T, Patel, KM, Crisostomo, PR, Markel, TA, Wang, M, Herring, C & Meldrum, DR. (2007). Endogenous estrogen attenuates pulmonary artery vasoreactivity and acute hypoxic pulmonary vasoconstriction: the effects of sex and menstrual cycle. *American Journal of Physiology-Endocrinology and Metabolism*, **293**, E865-E871.
- Lahm, T, Albrecht, M, Fisher, AJ, Selej, M, Patel, NG, Brown, JA, Justice, MJ, Brown, MB, Van Demark, M, Trulock, KM, Dieudonne, D, Reddy, JG, Presson, RG & Petrache, I. (2012). 17 $\beta$ -estradiol attenuates hypoxic pulmonary hypertension via estrogen receptor-mediated effects. *Am J Respir Crit Care Med*, **185**, 965-980.

- Lahm, T, Crisostomo, PR, Markel, TA, Wang, M, Wang, Y, Weil, B & Meldrum, DR. (2008b). Exogenous estrogen rapidly attenuates pulmonary artery vasoreactivity and acute hypoxic pulmonary vasoconstriction. *Shock*, **30**.
- Lakhani, NJ, Sarkar, MA, Venitz, J & Figg, WD. (2003). 2-Methoxyestradiol, a promising anticancer agent. *Pharmacotherapy: The Journal of Human Pharmacology and Drug Therapy*, **23**, 165-172.
- Lane, KB, Machado, RD, Pauciulo, MW, Thomson, JR, Phillips, JA, Loyd, JE, Nichols, WC & Trembath, RC. (2000). Heterozygous germline mutations in BMPR2, encoding a TGF-beta receptor, cause familial primary pulmonary hypertension. The International PPH Consortium. *Nat Genet*, **26**, 81-84.
- Lantin Hermoso, RL, Rosenfeld, CR, Yuhanna, IS, German, Z, Chen, Z & Shaul, PW. (1997). Estrogen acutely stimulates nitric oxide synthase activity in fetal pulmonary artery endothelium. *American Journal of Physiology-Lung Cellular and Molecular Physiology*, **273**, L119-L126.
- Larkin, EK, Newman, JH, Austin, ED, Hemnes, AR, Wheeler, L, Robbins, IM, West, JD, Phillips, JA, Hamid, R & Loyd, JE. (2012). Longitudinal analysis casts doubt on the presence of genetic anticipation in heritable pulmonary arterial hypertension. *American Journal of Respiratory and Critical Care Medicine*, **186**, 892-896.
- Lawrie, A, Spiekerkoetter, E, Martinez, EC, Ambartsumian, N, Sheward, WJ, MacLean, MR, Harmar, AJ, Schmidt, AM, Lukanidin, E & Rabinovitch, M. (2005). Interdependent serotonin transporter and receptor pathways regulate S100A4/Mts1, a gene associated with pulmonary vascular disease. *Circ Res*, **97**, 227-235.
- Lee, AJ, Cai, MX, Thomas, PE, Conney, AH & Zhu, BT. (2003). Characterization of the oxidative metabolites of 17 $\beta$ -estradiol and estrone formed by 15 selectively expressed human cytochrome P450 ssoforms. *Endocrinology*, **144**, 3382-3398.
- Lee, SL, Wang, WW & Fanburg, BL. (1998). Superoxide as an intermediate signal for serotonin-induced mitogenesis. *Free Radical Biology and Medicine*, **24**, 855-858.
- Lemon, HM, Heidel, JW & Rodriguezsierra, JF. (1992). Increased catechol estrogen metabolism as a risk factor for nonfamilial breast-cancer. *Cancer*, **69**, 457-465.
- Lesch, KP, Bengel, D, Heils, A, Sabol, SZ, Greenberg, BD, Petri, S, Benjamin, J, Muller, CR, Hamer, DH & Murphy, DL. (1996). Association of anxiety-related traits with a polymorphism in the serotonin transporter gene regulatory region. *Science*, **274**, 1527-1531.
- Lewis, JS, Thomas, TJ, Pestell, RG, Albanese, C, Gallo, MA & Thomas, T. (2005). Differential effects of 16 $\alpha$ -hydroxyestrone and 2-methoxyestradiol on cyclin D1 involving the transcription factor ATF-2 in MCF-7 breast cancer cells. *Journal of Molecular Endocrinology*, **34**, 91-105.
- Li, HB, Chen, SJ, Chen, YF, Meng, QC, Durand, J, Oparil, S & Elton, TS. (1994). Enhanced endothelin-1 and endothelin receptor gene-expression in chronic hypoxia. *Journal of Applied Physiology*, **77**, 1451-1459.
- Li, HF, Zheng, TZ, Li, W, Qu, SY & Zhang, CL. (2001). Effect of progesterone on the contractile response of isolated pulmonary artery in rabbits. *Canadian Journal of Physiology and Pharmacology*, **79**, 545-550.

- Li, L, Haynes, MP & Bender, JR. (2003). Plasma membrane localization and function of the estrogen receptor alpha variant (ER46) in human endothelial cells. *Proceedings of the National Academy of Sciences of the United States of America*, **100**, 4807-4812.
- Liehr, JG, Avitts, TA, Randerath, E & Randerath, K. (1986). Estrogen-induced endogenous DNA adduction - Possible mechanism of hormonal cancer. *Proceedings of the National Academy of Sciences of the United States of America*, **83**, 5301-5305.
- Liehr, JG & Ricci, MJ. (1996). 4-Hydroxylation of estrogens as marker of human mammary tumors. *Proceedings of the National Academy of Sciences*, **93**, 3294-3296.
- Liehr, JG, Ricci, MJ, Jefcoate, CR, Hannigan, EV, Hokanson, JA & Zhu, BT. (1995). 4-Hydroxylation of estradiol by human uterine myometrium and myoma microsomes - Implications for the mechanism of uterine tumorigenesis. *Proceedings of the National Academy of Sciences of the United States of America*, **92**, 9220-9224.
- Ling, Y, Johnson, MK, Kiely, DG, Condliffe, R, Elliot, CA, Gibbs, JS, Howard, LS, Pepke-Zaba, J, Sheares, KKK, Corris, PA, Fisher, AJ, Lordan, JL, Gaine, S, Coghlan, JG, Wort, SJ, Gatzoulis, MA & Peacock, AJ. (2012). Changing demographics, epidemiology, and survival of incident pulmonary arterial hypertension. *Am J Respir Crit Care Med*, **186**, 790-796.
- Lippert, C, Seeger, H & Mueck, AO. (2003). The effect of endogenous estradiol metabolites on the proliferation of human breast cancer cells. *Life Sciences*, **72**, 877-883.
- Lizotte, E, Grandy, SA, Tremblay, A, Allen, BG & Fiset, C. (2009). Expression, distribution and regulation of sex steroid hormone receptors in mouse heart. *Cellular Physiology and Biochemistry*, **23**, 75-86.
- Loot, AE & Fleming, I. (2011). Cytochrome P450-derived epoxyeicosatrienoic acids and pulmonary hypertension: central role of transient receptor potential C6 channels. *Journal of Cardiovascular Pharmacology*, **57**, 140-147.
- Loyd, JE, Butler, MG, Foroud, TM, Conneally, PM, Phillips, JA & Newman, JH. (1995). Genetic anticipation and abnormal gender ratio at birth in familial primary pulmonary-hypertension. *Am J Respir Crit Care Med*, **152**, 93-97.
- Luby, TM. (2008). Targeting cytochrome P450 CYP1B1 with a therapeutic cancer vaccine. *Expert Rev Vaccines*, **7**, 995-1003.
- Lukas, G, Brindle, SD & Greengard, P. (1971). The route of absorption of intraperitoneally administered compounds. *Journal of Pharmacology and Experimental Therapeutics*, **178**, 562-566.
- Lund, AK, Agbor, LN, Zhang, N, Baker, A, Zhao, H, Fink, GD, Kanagy, NL & Walker, MK. (2008). Loss of the aryl hydrocarbon receptor induces hypoxemia, endothelin-1, and systemic hypertension at modest altitude. *Hypertension*, **51**, 803-809.
- Ma, L, Roman-Campos, D, Austin, ED, Eyries, M, Sampson, KS, Soubrier, F, Germain, M, Trégouët, D, Borczuk, A, Rosenzweig, EB, Girerd, B, Montani, D, Humbert, M, Loyd, JE, Kass, RS & Chung, WK. (2013). A novel channelopathy in pulmonary arterial hypertension. *N Engl J Med*, **369**, 351-361.

Machado, RD, Pauciulo, MW, Thomson, JR, Lane, KB, Morgan, NV, Wheeler, L, Phillips, JA, Newman, J, Williams, D, Galie, N, Manes, A, McNeil, K, Yacoub, M, Mikhail, G, Rogers, P, Corris, P, Humbert, M, Donnai, D, Martensson, G, Tranebjaerg, L, Loyd, JE, Trembath, RC & Nichols, WC. (2001). BMP2 haploinsufficiency as the inherited molecular mechanism for primary pulmonary hypertension. *American Journal of Human Genetics*, **68**, 92-102.

Machado, RD, Trembath, RC & Morrell, NW (2011). Genetics of severe pulmonary hypertension. In *Pulmonary hypertension, the present and future*. ed. Voelkel, N pp. 211-238. People's Medical Publishing House-USA: Shelton.

Machado, RD, Aldred, MA, James, V, Harrison, RE, Patel, B, Schwalbe, EC, Gruenig, E, Janssen, B, Koehler, R, Seeger, W, Eickelberg, O, Olschewski, H, Gregory Elliott, C, Glissmeyer, E, Carlquist, J, Kim, M, Torbicki, A, Fijalkowska, A, Szewczyk, G, Parma, J, Abramowicz, MJ, Galie, N, Morisaki, H, Kyotani, S, Nakanishi, N, Morisaki, T, Humbert, M, Simonneau, G, Sitbon, O, Soubrier, F, Coulet, F, Morrell, NW & Trembath, RC. (2006a). Mutations of the TGF- $\beta$  type II receptor BMP2 in pulmonary arterial hypertension. *Hum Mutat*, **27**, 121-132.

Machado, RD, Koehler, R, Glissmeyer, E, Veal, C, Suntharalingam, J, Kim, M, Carlquist, J, Town, M, Elliott, CG, Hoeper, M, Fijalkowska, A, Kurzyna, M, Thomson, JR, Gibbs, SR, Wilkins, MR, Seeger, W, Morrell, NW, Gruenig, E, Trembath, RC & Janssen, B. (2006b). Genetic association of the serotonin transporter in pulmonary arterial hypertension. *Am J Respir Crit Care Med*, **173**, 793-797.

Maclean, MR, Clayton, RA, Templeton, AGB & Morecroft, I. (1996). Evidence for 5-HT<sub>1</sub>-like receptor-mediated vasoconstriction in human pulmonary artery. *Br J Pharmacol*, **119**, 277-282.

Maclean, MR, Deuchar, GA, Hicks, MN, Morecroft, I, Shen, S, Sheward, J, Colston, J, Loughlin, L, Nilsen, M & Dempsie, Y. (2004). Overexpression of the 5-hydroxytryptamine transporter gene: effect on pulmonary hemodynamics and hypoxia-induced pulmonary hypertension. *Circulation*, **109**, 2150-2155.

Maclean, MR, McCulloch, KM & Baird, M. (1994). Endothelin Et(A)-receptor-mediated and Et(B)-receptor-mediated vasoconstriction in rat pulmonary-arteries and arterioles. *Journal of Cardiovascular Pharmacology*, **23**, 838-845.

MacLean, MR, Deuchar, GA, Hicks, MN, Morecroft, I, Shen, S, Sheward, J, Colston, J, Loughlin, L, Nilsen, M, Dempsie, Y & Harmar, A. (2004). Overexpression of the 5-hydroxytryptamine transporter gene: effect on pulmonary hemodynamics and hypoxia-induced pulmonary hypertension. *Circulation*, **109**, 2150-2155.

Maecker, B, Sherr, DH, Vonderheide, RH, von Bergwelt-Baildon, MS, Hirano, N, Anderson, KS, Xia, Z, Butler, MO, Wucherpfnig, KW, O'Hara, C, Cole, G, Kwak, SS, Ramstedt, U, Tomlinson, AJ, Chiczy, RM, Nadler, LM & Schultze, JL. (2003). The shared tumor-associated antigen cytochrome P450 1B1 is recognized by specific cytotoxic T cells  
120. *Blood*, **102**, 3287-3294.

Mair, KM, Duggan, N, Rowlands, D, Hussey, M, Roberts, S, Fullerton, J, Thomas, M & Maclean, MR. (2013). Beneficial effects of an aromatase inhibitor in two distinct models of established pulmonary arterial hypertension. *Am J Respir Crit Care Med*, **187**, A1030.

- Malik, KU, Jennings, BL, Yaghini, FA, Sahan-Firat, S, Song, CY, Estes, AM & Fang, XR. (2012). Contribution of cytochrome P450 1B1 to hypertension and associated pathophysiology: A novel target for antihypertensive agents. *Prostaglandins & Other Lipid Mediators*, **98**, 69-74.
- Marcos, E, Fadel, E, Sanchez, O, Humbert, M, Dartevelle, P, Simonneau, G, Hamon, M, Adnot, S & Eddahibi, S. (2004). Serotonin-induced smooth muscle hyperplasia in various forms of human pulmonary hypertension. *Circ Res*, **94**, 1263-1270.
- Maron, BA, Opotowsky, AR, Landzberg, MJ, Loscalzo, J, Waxman, AB & Leopold, JA. (2013). Plasma aldosterone levels are elevated in patients with pulmonary arterial hypertension in the absence of left ventricular heart failure: a pilot study. *European Journal of Heart Failure*, **15**, 277-283.
- Marquez-Garban, DC, Chen, HW, Goodglick, L, Fishbein, MC & Pietras, RJ. (2009). Targeting aromatase and estrogen signaling in human non-small cell lung cancer. *Steroid Enzymes and Cancer*, **1155**, 194-205.
- Massague, J. (2003). Integration of Smad and MAPK pathways: a link and a linker revisited. *Genes & Development*, **17**, 2993-2997.
- Matori, H, Umar, S, Nadadur, RD, Sharma, S, Partow-Navid, R, Afkhami, M, Amjadi, M & Eghbali, M. (2012). Genistein, a soy phytoestrogen, reverses severe pulmonary hypertension and prevents right heart failure in rats. *Hypertension*, **60**, 425-430.
- Mcculloch, KM, Docherty, CC, Morecroft, I & Maclean, MR. (1996). Endothelin(B) receptor-mediated contraction in human pulmonary resistance arteries. *Br J Pharmacol*, **119**, 1125-1130.
- McFadyen, MCE, Cruickshank, ME, Miller, ID, Mcleod, HL, Melvin, WT, Haites, NE, Parkin, D & Murray, GI. (2001). Cytochrome P450 CYP1B1 over-expression in primary and metastatic ovarian cancer. *British Journal of Cancer*, **85**, 242-246.
- McKay, JA, Melvin, WT, Ah-See, AK, Ewen, SWB, Greenlee, WF, Marcus, CB, Burke, MD & Murray, GI. (1995). Expression of cytochrome P450 CYP1B1 in breast cancer. *FEBS Letters*, **374**, 270-272.
- McMurtry, IF, Davidson, AB, Reeves, JT & Grover, RF. (1976). Inhibition of hypoxic pulmonary vasoconstriction by calcium antagonists in isolated rat lungs. *Circ Res*, **38**, 99-104.
- McMurtry, IF, Frith, CH & Will, DH. (1973). Cardiopulmonary responses of male and female swine to simulated high-altitude. *Journal of Applied Physiology*, **35**, 459-462.
- Medhora, M, Chen, YM, Gruenloh, S, Harland, D, Bodiga, S, Zielonka, J, Gebremedhin, D, Gao, Y, Falck, JR, Anjaiah, S & Jacobs, ER. (2008). 20-HETE increases superoxide production and activates NADPH oxidase in pulmonary artery endothelial cells. *American Journal of Physiology-Lung Cellular and Molecular Physiology*, **294**, L902-L911.
- Meireles, SI, Esteves, GH, Hirata, R, Peri, S, Devarajan, K, Slifker, M, Mosier, SL, Peng, J, Vadhanam, MV, Hurst, HE, Neves, EJ, Reis, LF, Gairola, CG, Gupta, RC & Clapper, ML. (2010). Early changes in gene expression induced by tobacco smoke: evidence for the importance of estrogen within lung tissue. *Cancer Prevention Research*, **3**, 707-717.

- Meloche, J, Pflieger, A, Vaillancourt, Mn, Paulin, R, Potus, F, Zervopoulos, S, Graydon, C, Courboulin, A, Breuils-Bonnet, S, Tremblay, È, Couture, C, Michelakis, ED, Provencher, S & Bonnet, S. (2013). Role for DNA damage signaling in pulmonary arterial hypertension. *Circulation*, **129**, 786-797.
- Mendelsohn, ME & Karas, RH. (1999). The protective effects of estrogen on the cardiovascular system. *N Engl J Med*, **340**, 1801-1811.
- Merriam, GR, Brandon, DD, Kono, S, Davis, SE, Loriaux, DL & Lipsett, MB. (1980). Rapid metabolic-clearance of the catechol estrogen 2-hydroxyestrone. *Journal of Clinical Endocrinology & Metabolism*, **51**, 1211-1213.
- Meyrick, B & Reid, L. (1980). Hypoxia-induced structural-changes in the media and adventitia of the rat hilar pulmonary-artery and their regression. *American Journal of Pathology*, **100**, 151-178.
- Michelakis, ED, Wilkins, MR & Rabinovitch, M. (2008). Emerging concepts and translational priorities in pulmonary arterial hypertension. *Circulation*, **118**, 1486-1495.
- Mitani, Y, Mutlu, A, Russell, JC, Brindley, DN, DeAlmeida, J & Rabinovitch, M. (2002). Dexfenfluramine protects against pulmonary hypertension in rats. *Journal of Applied Physiology*, **93**, 1770-1778.
- Montani, D, Savale, L, Natali, D, Jais, X, Herve, P, Garcia, G, Humbert, M, Simonneau, G & Sitbon, O. (2010). Long-term response to calcium-channel blockers in non-idiopathic pulmonary arterial hypertension. *European Heart Journal*, **31**, 1898-1907.
- Morani, A, Barros, RPA, Imamov, O, Hultenby, K, Arner, A, Warner, M & Gustafsson, JA. (2006). Lung dysfunction causes systemic hypoxia in estrogen receptor beta knockout (ER beta(-/-)) mice. *Proceedings of the National Academy of Sciences of the United States of America*, **103**, 7165-7169.
- Morecroft, I, Heeley, RP, Prentice, HM, Kirk, A & Maclean, MR. (1999). 5-hydroxytryptamine receptors mediating contraction in human small muscular pulmonary arteries: importance of the 5-HT<sub>1B</sub> receptor. *Br J Pharmacol*, **128**, 730-734.
- Morecroft, I, Dempsie, Y, Bader, M, Walther, DJ, Kotnik, K, Loughlin, L, Nilsen, M & MacLean, MR. (2007). Effect of tryptophan hydroxylase 1 deficiency on the development of hypoxia-induced pulmonary hypertension. *Hypertension*, **49**, 232-236.
- Morecroft, I, Pang, L, Baranowska, M, Nilsen, M, Loughlin, L, Dempsie, Y, Millet, C & MacLean, MR. (2010). In vivo effects of a combined 5-HT<sub>1B</sub> receptor/SERT antagonist in experimental pulmonary hypertension. *Cardiovascular Research*, **85**, 593-603.
- Morecroft, I, White, K, Caruso, P, Nilsen, M, Loughlin, L, Alba, R, Reynolds, PN, Danilov, SM, Baker, AH & MacLean, MR. (2012). Gene therapy by targeted adenovirus-mediated knockdown of pulmonary endothelial Tph1 attenuates hypoxia-induced pulmonary hypertension. *Mol Ther*, **20**, 1516-1528.
- Morrell, NW. (2006). Pulmonary hypertension due to BMPR2 mutation. *Proc Am Thorac Soc*, **3**, 680-686.

- Morse, JH, Horn, EM & Barst, RJ. (1999). Hormone replacement therapy : A possible risk factor in carriers of familial primary pulmonary hypertension. *CHEST Journal*, **116**, 847.
- Mulvany, MJ & Halpern, W. (1977). Contractile properties of small arterial resistance vessels in spontaneously hypertensive and normotensive rats. *Circ Res*, **41**, 19-26.
- Murphy, E. (2011). Estrogen signaling and cardiovascular disease. *Circ Res*, **109**, 687-696.
- Murphy, LC, Seekallu, SV & Watson, PH. (2011). Clinical significance of estrogen receptor phosphorylation. *Endocrine-Related Cancer*, **18**, R1-R14.
- Murray, F, Maclean, MR & Insel, PA (2011). Role of phosphodiesterases in adult-onset pulmonary arterial hypertension. In *Phosphodiesterases as Drug Targets*. ed. Francis, SH, Conti, M & Houslay, MD pp. 279-305. Springer Berlin Heidelberg.
- Murray, F, Patel, HH, Suda, RYS, Zhang, S, Thistlethwaite, PA, Yuan, JXJ & Insel, PA. (2007). Expression and activity of cAMP phosphodiesterase isoforms in pulmonary artery smooth muscle cells from patients with pulmonary hypertension: role for PDE1. *American Journal of Physiology-Lung Cellular and Molecular Physiology*, **292**, L294-L303.
- Murray, GI, Taylor, MC, McFadyen, MCE, McKay, JA, Greenlee, WF, Burke, MD & Melvin, WT. (1997). Tumor-specific expression of cytochrome P450 CYP1B1. *Cancer Research*, **57**, 3026-3031.
- Muti, P, Bradlow, HL, Micheli, A, Krogh, V, Freudenheim, JL, Schunemann, HJ, Stanulla, M, Yang, J, Sepkovic, DW, Trevisan, M & Berrino, F. (2000). Estrogen metabolism and risk of breast cancer: A prospective study of the 2 : 16 alpha-hydroxyestrone ratio in premenopausal and postmenopausal women. *Epidemiology*, **11**, 635-640.
- Myöhänen, TT, Schendzielorz, N & Männistö, PK. (2010). Distribution of catechol-O-methyltransferase (COMT) proteins and enzymatic activities in wild-type and soluble COMT deficient mice. *Journal of Neurochemistry*, **113**, 1632-1643.
- Nasim, M, Ogo, T, Ahmed, M, Randall, R, Chowdhury, HM, Snape, KM, Bradshaw, TY, Southgate, L, Lee, GJ, Jackson, I, Lord, GM, Gibbs, JS, Wilkins, MR, Ohta-Ogo, K, Nakamura, K, Girerd, B, Coulet, F, Soubrier, F, Humbert, M, Morrell, NW, Trembath, RC & Machado, RD. (2011). Molecular genetic characterization of SMAD signaling molecules in pulmonary arterial hypertension. *Hum Mutat*, **32**, 1385-1389.
- Nebert, DW & Dalton, TP. (2006). The role of cytochrome P450 enzymes in endogenous signalling pathways and environmental carcinogenesis. *Nature Reviews Cancer*, **6**, 947-960.
- Newbold, RR, Bullock, BC & Mclachlan, JA. (1990). Uterine adenocarcinoma in mice following developmental treatment with estrogens - A model for hormonal carcinogenesis. *Cancer Research*, **50**, 7677-7681.
- Newman, JH, Wheeler, L, Lane, KB, Loyd, E, Gaddipati, R, Phillips, JA & Loyd, JE. (2001). Mutation in the gene for bone morphogenetic protein receptor II as a cause of primary pulmonary hypertension in a large kindred. *N Engl J Med*, **345**, 319-324.

- Newman, JH, Trembath, RC, Morse, JA, Grunig, E, Loyd, JE, Adnot, S, Coccolo, F, Ventura, C, Phillips, JA, III, Knowles, JA, Janssen, B, Eickelberg, O, Eddahibi, S, Herve, P, Nichols, WC & Elliott, G. (2004). Genetic basis of pulmonary arterial hypertension: Current understanding and future directions. *Journal of the American College of Cardiology*, **43**, 33S-39.
- Nichols, WC, Koller, DL, Slovis, B, Foroud, T, Terry, VH, Arnold, ND, Siemieniak, DR, Wheeler, L, Phillips, JA, Newman, JH, Conneally, PM, Ginsburg, D & Loyd, JE. (1997). Localization of the gene for familial primary pulmonary hypertension to chromosome 2q31-32. *Nature Genetics*, **15**, 277-280.
- Nutter, LM, Ngo, EO & Abulhadj, YJ. (1991). Characterization of DNA damage induced by 3,4-estrone-ortho-quinone in human-cells. *Journal of Biological Chemistry*, **266**, 16380-16386.
- Nutter, LM, Wu, YY, Ngo, EO, Sierra, EE, Gutierrez, PL & Abulhadj, YJ. (1994). An o-quinone form of estrogen produces free-radicals in human breast-cancer cells - Correlation with DNA-damage. *Chemical Research in Toxicology*, **7**, 23-28.
- Ochs, M, Nyengaard, LR, Lung, A, Knudsen, L, Voigt, M, Wahlers, T, Richter, J & Gundersen, HJG. (2004). The number of alveoli in the human lung. *Am J Respir Crit Care Med*, **169**, 120-124.
- Oduwole, OO, Li, Y, Isomaa, VV, Mäntyniemi, A, Pulkka, AE, Soini, Y & Vihko, PT. (2004). 17 $\beta$ -hydroxysteroid dehydrogenase Type 1 is an independent prognostic marker in breast cancer. *Cancer Research*, **64**, 7604-7609.
- Olschewski, A, Li, Y, Tang, B, Hanze, J+, Eul, B, Bohle, RM, Wilhelm, J, Morty, RE, Brau, ME, Weir, EK, Kwapiszewska, G, Klepetko, W, Seeger, W & Olschewski, H. (2006). Impact of TASK-1 in human pulmonary artery smooth muscle cells. *Circ Res*, **98**, 1072-1080.
- Olson, TP, Snyder, EM, Frantz, RP, Turner, ST & Johnson, BD. (2007). Repeat length polymorphism of the serotonin transporter gene influences pulmonary artery pressure in heart failure. *American Heart Journal*, **153**, 426-432.
- Orchard, TJ. (1996). The impact of gender and general risk factors on the occurrence of atherosclerotic vascular disease in non-insulin-dependent diabetes mellitus. *Annals of Medicine*, **28**, 323-333.
- Ortmann, J, Veit, M, Zingg, S, Di Santo, S, Traupe, T, Yang, Z, Völzmann, J, Dubey, RK, Christen, S & Baumgartner, I. (2011). Estrogen receptor- $\alpha$  but not - $\beta$  or GPER inhibits high glucose-induced human VSMC proliferation: Potential role of ROS and ERK. *Journal of Clinical Endocrinology & Metabolism*, **96**, 220-228.
- Oudiz, RJ, Galie, N, Olschewski, H, Torres, F, Frost, A, Ghofrani, HA, Badesch, DB, McGoon, MD, McLaughlin, VV, Roecker, EB, Harrison, BC, Despain, D, Dufton, C & Rubin, LJ. (2009). Long-term ambrisentan therapy for the treatment of pulmonary arterial hypertension. *Journal of the American College of Cardiology*, **54**, 1971-1981.
- Paria, BC, Chakraborty, C & Dey, SK. (1990). Catechol estrogen formation in the mouse uterus and its role in implantation. *Molecular and Cellular Endocrinology*, **69**, 25-32.

Park, H, Aiyar, SE, Fan, P, Wang, JP, Yue, W, Okouneva, T, Cox, C, Jordan, MA, Demers, L, Cho, HJ, Kim, S, Song, RXD & Santen, RJ. (2007). Effects of tetramethoxystilbene on hormone-resistant breast cancer cells: Biological and biochemical mechanisms of action. *Cancer Research*, **67**, 5717-5726.

Parker, CR. (1999). Dehydrosoepiandrosterone and dehydroepiandrosterone sulfate production in the human adrenal during development and aging. *Steroids*, **64**, 640-647.

Pasqualini, JR, Chetrite, G, Blacker, C, Feinstein, MC, Delalonde, L, Talbi, M & Maloche, C. (1996). Concentrations of estrone, estradiol, and estrone sulfate and evaluation of sulfatase and aromatase activities in pre- and postmenopausal breast cancer patients. *Journal of Clinical Endocrinology & Metabolism*, **81**, 1460-1464.

Patrone, C, Cassel, TN, Pettersson, K, Piao, YS, Cheng, GJ, Ciana, P, Maggi, A, Warner, M, Gustafsson, JA & Nord, M. (2003). Regulation of postnatal lung development and homeostasis by estrogen receptor beta. *Molecular and Cellular Biology*, **23**, 8542-8552.

Pedram, A, Razandi, M, Lubahn, D, Liu, J, Vannan, M & Levin, ER. (2008). Estrogen inhibits cardiac hypertrophy: Role of estrogen receptor- $\beta$  to inhibit calcineurin. *Endocrinology*, **149**, 3361-3369.

Peng, J, Xu, X, Mace, BE, Vanderveer, LA, Workman, LR, Slifker, MJ, Sullivan, PM, Veenstra, TD & Clapper, ML. (2013). Estrogen metabolism within the lung and its modulation by tobacco smoke. *Carcinogenesis*, **34**, 909-915.

Pfister, SL. (2011). Role of lipoxygenase metabolites of arachidonic acid in enhanced pulmonary artery contractions of female rabbits. *Hypertension*, **57**, 825-832.

Pietra, GG, Capron, F, Stewart, S, Leone, O, Humbert, M, Robbins, IM, Reid, LM & Tuder, RM. (2004). Pathologic assessment of vasculopathies in pulmonary hypertension. *Journal of the American College of Cardiology*, **43**, 25S-32S.

Pietra, GG, Edwards, WD, Kay, JM, Rich, S, Kernis, J, Schloo, B, Ayres, SM, Bergofsky, EH, Brundage, BH, Detre, KM, Fishman, AP, Goldring, RM, Groves, BM, Levy, PS, Reid, LM, Vreim, CE & Williams, GW. (1989). Histopathology of primary pulmonary-hypertension - A qualitative and quantitative study of pulmonary blood-vessels from 58 patients in the national-heart-lung-and-blood-institute, primary pulmonary-hypertension registry. *Circulation*, **80**, 1198-1206.

Pogoriler, JE, Rich, S, Archer, SL & Husain, AN. (2012). Persistence of complex vascular lesions despite prolonged prostacyclin therapy of pulmonary arterial hypertension. *Histopathology*, **61**, 597-609.

Post, JM, Hume, JR, Archer, SL & Weir, EK. (1992). Direct role for potassium channel inhibition in hypoxic pulmonary vasoconstriction. *American Journal of Physiology*, **262**, C882-C890.

Preston, IR, Sagliani, KD, Warburton, RR, Hill, NS, Fanburg, BL & Jaffe, IZ. (2013). Mineralocorticoid receptor antagonism attenuates experimental pulmonary hypertension. *American Journal of Physiology-Lung Cellular and Molecular Physiology*, **304**, L678-L688.

Price, LC, Wort, SJ, Perros, Fdr, Dorfmueller, P, Huertas, A, Montani, D, Cohen-Kaminsky, S & Humbert, M. (2012). Inflammation in pulmonary arterial hypertension. *CHEST Journal*, **141**, 210-221.

Prossnitz, ER, Arterburn, JB, Smith, HO, Oprea, TI, Sklar, LA & Hathaway, HJ. (2008). Estrogen signaling through the transmembrane G protein-coupled receptor GPR30. *Annu Rev Physiol*, **70**, 165-190.

Rabinovitch, M, Gamble, WJ, Miettinen, OS & Reid, L. (1981). Age and sex influence on pulmonary hypertension of chronic hypoxia and on recovery. *American Journal of Physiology - Heart and Circulatory Physiology*, **240**, H62-H72.

Rabinovitch, M. (2012). Molecular pathogenesis of pulmonary arterial hypertension. *J Clin Invest*, **122**, 4306-4313.

Rajkumar, R, Konishi, K, Richards, TJ, Ishizawa, DC, Wiechert, AC, Kaminski, N & Ahmad, F. (2010). Genomewide RNA expression profiling in lung identifies distinct signatures in idiopathic pulmonary arterial hypertension and secondary pulmonary hypertension. *Am J Physiol Heart Circ Physiol*, **298**, H1235-H1248.

Rakugi, H, Tabuchi, Y, Nakamaru, M, Nagano, M, Higashimori, K, Mikami, H, Ogihara, T & Suzuki, N. (1990). Evidence for endothelin-1 release from resistance vessels of rats in response to hypoxia. *Biochemical and Biophysical Research Communications*, **169**, 973-977.

Ramamoorthy, S, Bauman, AL, Moore, KR, Han, H, Yang-Feng, T, Chang, AS, Ganapathy, V & Blakely, RD. (1993). Antidepressant- and cocaine-sensitive human serotonin transporter: molecular cloning, expression, and chromosomal localization. *Proceedings of the National Academy of Sciences*, **90**, 2542-2546.

Reid, MJ, Lamé, MW, Morin, D, Wilson, DW & Segall, HJ. (1998). Involvement of cytochrome P450 3A in the metabolism and covalent binding of <sup>14</sup>C-monocrotaline in rat liver microsomes. *J Biochem Mol Toxicol*, **12**, 157-166.

Rich, S & Brundage, BH. (1987). High-dose calcium-channel blocking therapy for primary pulmonary-hypertension - evidence for long-term reduction in pulmonary arterial-pressure and regression of right ventricular hypertrophy. *Circulation*, **76**, 135-141.

Rich, S, Dantzker, DR, Ayres, SM, Bergofsky, EH, Brundage, BH, Detre, KM, Fisman, AP, Goldring, RM, Groves, BM & Koerner, SK. (1987). Primary pulmonary hypertension. A national prospective study. *Ann Intern Med*, **107**, 216-223.

Rich, S, Kaufmann, E & Levy, PS. (1992). The effect of high-doses of calcium-channel blockers on survival in primary pulmonary-hypertension. *N Engl J Med*, **327**, 76-81.

Ritchie, M, Waggoner, AD, Dávila-román, VG, Barzilai, B, Trulock, EP & Eisenberg, PR. (1993). Echocardiographic characterization of the improvement in right ventricular function in patients with severe pulmonary hypertension after single-lung transplantation. *Journal of the American College of Cardiology*, **22**, 1170-1174.

Roberts, KE, Fallon, MB, Krowka, MJ, Brown, RS, Trotter, JF, Peter, I, Tighiouart, H, Knowles, JA, Rabinowitz, D, Benza, RL, Badesch, DB, Taichman, DB, Horn, EM, Zacks, S, Kaplowitz, N, Kawut, SM & for the Pulmonary Vascular Complications of

- Liver Disease Study Group. (2009). Genetic risk factors for portopulmonary hypertension in patients with advanced liver disease. *Am J Respir Crit Care Med*, **179**, 835-842.
- Rogan, EG, Badawi, AF, Devanesan, PD, Meza, JL, Edney, JA, West, WW, Higginbotham, SM & Cavalieri, EL. (2003). Relative imbalances in estrogen metabolism and conjugation in breast tissue of women with carcinoma: potential biomarkers of susceptibility to cancer. *Carcinogenesis*, **24**, 697-702.
- Rosenberg, HC & Rabinovitch, M. (1988). Endothelial injury and vascular reactivity in monocrotaline pulmonary-hypertension. *American Journal of Physiology*, **255**, H1484-H1491.
- Rothman, RB, Ayestas, MA, Dersch, CM & Baumann, MH. (1999). Aminorex, fenfluramine, and chlorphentermine are serotonin transporter substrates. Implications for primary pulmonary hypertension. *Circulation*, **100**, 869-875.
- Rowell, KO, Hall, J, Pugh, PJ, Jones, TH, Channer, KS & Jones, RD. (2009). Testosterone acts as an efficacious vasodilator in isolated human pulmonary arteries and veins: Evidence for a biphasic effect at physiological and supra-physiological concentrations. *Journal of Endocrinological Investigation*, **32**, 718-723.
- Sahan-Firat, S, Jennings, BL, Yaghini, FA, Song, CY, Estes, AM, Fang, XR, Farjana, N, Khan, AI & Malik, KU. (2010). 2,3',4,5'-Tetramethoxystilbene prevents deoxycorticosterone-salt-induced hypertension: contribution of cytochrome P-450 1B1. *American Journal of Physiology-Heart and Circulatory Physiology*, **299**, H1891-H1901.
- Samarajeewa, N, Yang, F, Docanto, M, Sakurai, M, McNamara, K, Sasano, H, Fox, S, Simpson, E & Brown, K. (2013). HIF-1alpha stimulates aromatase expression driven by prostaglandin E2 in breast adipose stroma. *Breast Cancer Research*, **15**, R30.
- Sandoval, J, Bauerle, O, Palomar, A, Gómez, A, Martínez-Guerra, ML, Beltrán, M & Guerrero, ML. (1994). Survival in primary pulmonary hypertension. Validation of a prognostic equation. *Circulation*, **89**, 1733-1744.
- Santer, SJ, FEIL, PD & Santen, RJ. (1984). In situ estrogen production via the estrone sulfatase pathway in breast tumors: Relative importance versus the aromatase pathway. *The Journal of Clinical Endocrinology & Metabolism*, **59**, 29-33.
- Savai, R, Pullamsetti, SS, Kolbe, J, Bieniek, E, Voswinckel, R, Fink, L, Scheed, A, Ritter, C, Dahal, BK, Vater, A, Klussmann, S, Ghofrani, HA, Weissmann, N, Klepetko, W, Banat, GA, Seeger, W, Grimminger, F & Schermuly, RT. (2012). Immune and inflammatory cell involvement in the pathology of idiopathic pulmonary arterial hypertension. *Am J Respir Crit Care Med*, **186**, 897-908.
- Schermuly, RT, Ghofrani, HA, Wilkins, MR & Grimminger, F. (2011). Mechanisms of disease: pulmonary arterial hypertension. *Nat Rev Cardiol*, **8**, 443-455.
- Scott, HM, Mason, JI & Sharpe, RM. (2009). Steroidogenesis in the fetal testis and its susceptibility to disruption by exogenous compounds. *Endocrine Reviews*, **30**, 883-925.

- Seeger, H, Wallwiener, D, Kraemer, E & Mueck, AO. (2006). Comparison of possible carcinogenic estradiol metabolites: Effects on proliferation, apoptosis and metastasis of human breast cancer cell. *Maturitas*, **54**, 72-77.
- Seeger, H, Mueck, AO & Lippert, TH. (1999). Effect of estradiol metabolites on prostacyclin synthesis in human endothelial cell cultures. *Life Sciences*, **65**, L167-L170.
- Shapiro, S, Traiger, GL, Turner, M, McGoon, MD, Wason, P & Barst, RJ. (2012). Sex differences in the diagnosis, treatment, and outcome of patients with pulmonary arterial hypertension enrolled in the registry to evaluate early and long-term pulmonary arterial hypertension disease management sex differences in pulmonary arterial hypertension. *CHEST Journal*, **141**, 363-373.
- Sharma, S, Taegtmeyer, H, Adroge, J & Essop, MF. (2004). Dynamic changes of gene expression in hypoxia-induced right ventricular hypertrophy. *Journal of Investigative Medicine*, **52**, S289.
- Shen, S, Spratt, C, Sheward, WJ, Kallo, I, West, K, Morrison, CF, Coen, CW, Marston, HM & Harmar, AJ. (2000). Overexpression of the human VPAC2 receptor in the suprachiasmatic nucleus alters the circadian phenotype of mice. *Proceedings of the National Academy of Sciences*, **97**, 11575-11580.
- Sherman, TS, Chambliss, KL, Gibson, LL, Pace, MC, Mendelsohn, ME, Pfister, SL & Shaul, PW. (2002). Estrogen acutely activates prostacyclin synthesis in ovine fetal pulmonary artery endothelium. *American Journal of Respiratory Cell and Molecular Biology*, **26**, 610-616.
- Simoncini, T, Hafezi-Moghadam, A, Brazil, DP, Ley, K, Chin, WW & Liao, JK. (2000). Interaction of oestrogen receptor with the regulatory subunit of phosphatidylinositol-3-OH kinase. *Nature*, **407**, 538-541.
- Simonneau, G, Gatzoulis, MA, Adatia, I, Celermajer, D, Denton, C, Ghofrani, A, Gomez-Sanchez, MA, Krishna Kumar, R, Landzberg, M, Machado, RF, Olschewski, H, Robbins, IM & Souza, R. (2013). Updated clinical classification of pulmonary hypertension. p. D34-D41.
- Simpson, ER. (2003). Sources of estrogen and their importance. *The Journal of Steroid Biochemistry and Molecular Biology*, **86**, 225-230.
- Simpson, ER, Zhao, Y, Agarwal, VR, Michael, MD, Bulun, SE, Hinshelwood, MM, Graham-Lorence, S, Sun, TJ, Fisher, CR, Qin, KN & Mendelson, CR. (1997). Aromatase expression in health and disease. *Recent Progress in Hormone Research, Proceedings of the 1996 Conference, Vol 52*, **52**, 185-214.
- Sitbon, O, Humbert, M, Jais, X, Ioos, V, Hamid, AM, Provencher, S, Garcia, G, Parent, F, Herve, P & Simonneau, G. (2005). Long-term response to calcium channel blockers in idiopathic pulmonary arterial hypertension. *Circulation*, **111**, 3105-3111.
- Sitbon, O, Lascoux-Combe, C, Delfraissy, JF, Yeni, PG, Raffi, F, De Zuttere, D, Gressin, V, Clerson, P, Sereni, D & Simonneau, G. (2008). Prevalence of HIV-related pulmonary arterial hypertension in the current antiretroviral therapy era. *Am J Respir Crit Care Med*, **177**, 108-113.

- Sitbon, O & Morrell, N. (2012). Pathways in pulmonary arterial hypertension: the future is here. *European Respiratory Review*, **21**, 321-327.
- Sivritas, D, Becher, M, Ebrahimian, T, Arfa, O, Rapp, S, Bohner, A, Mueller, C, Umemura, T, Wassmann, S, Nickenig, G & Wassmann, K. (2011). Antiproliferative effect of estrogen in vascular smooth muscle cells is mediated by Kruppel-like factor-4 and manganese superoxide dismutase. *Basic Res Cardiol*, **106**, 563-575.
- Smith, AM, Bennett, RT, Jones, TH, Cowen, ME, Channer, KS & Jones, RD. (2005). Characterisation of the vasodilatory action of testosterone in the human pulmonary circulation. *Thorax*, **60**, II7.
- Song, YL, Jones, JE, Beppu, H, Keaney, JF, Loscalzo, J & Zhang, YY. (2005). Increased susceptibility to pulmonary hypertension in heterozygous BMPR2-mutant mice. *Circulation*, **112**, 553-562.
- Soon, E, Holmes, AM, Treacy, CM, Doughty, NJ, Southgate, L, Machado, RD, Trembath, RC, Jennings, S, Barker, L, Nicklin, P, Walker, C, Budd, DC, Pepke-Zaba, J & Morrell, NW. (2010). Elevated levels of inflammatory cytokines predict survival in idiopathic and familial pulmonary arterial hypertension. *Circulation*, **122**, 921-U90.
- Spiekerkoetter, E, Tian, X, Cai, J, Hopper, RK, Sudheendra, D, Li, CG, El-Bizri, N, Sawada, H, Haghghat, R, Chan, R, Haghghat, L, de Jesus Perez, V, Wang, L, Reddy, S, Zhao, M, Bernstein, D, Solow-Cordero, DE, Beachy, PA, Wandless, TJ, ten Dijke, P & Rabinovitch, M. (2013). FK506 activates BMPR2, rescues endothelial dysfunction, and reverses pulmonary hypertension. *J Clin Invest*, **123**, 3600-3613.
- Spivack, SD, Hurteau, GJ, Reilly, AA, Aldous, KM, Ding, X & Kaminsky, LS. (2001). CYP1B1 expression in human lung  
111. *Drug Metab Dispos*, **29**, 916-922.
- Stacher, E, Graham, BB, Hunt, JM, Gandjeva, A, Groshong, SD, McLaughlin, VV, Jessup, M, Grizzle, WE, Aldred, MA, Cool, CD & Tuder, RM. (2012). Modern age pathology of pulmonary arterial hypertension. *Am J Respir Crit Care Med*, **186**, 261-272.
- Stanway, SJ, Purohit, A, Woo, LWL, Sufi, S, Vigushin, D, Ward, R, Wilson, RH, Stanczyk, FZ, Dobbs, N, Kulinskaya, E, Elliott, M, Potter, BVL, Reed, MJ & Coombes, RC. (2006). Phase I study of STX 64 (667 Coumate) in breast cancer patients: The first study of a steroid sulfatase inhibitor. *Clinical Cancer Research*, **12**, 1585-1592.
- Steiner, MK, Syrkina, OL, Kolliputi, N, Mark, EJ, Hales, CA & Waxman, AB. (2009). Interleukin-6 overexpression induces pulmonary hypertension. *Circ Res*, **104**, 236-U208.
- Stenmark, KR, Fagan, KA & Frid, MG. (2006). Hypoxia-induced pulmonary vascular remodeling - Cellular and molecular mechanisms. *Circ Res*, **99**, 675-691.
- Stenmark, KR & Mecham, RP. (1997). Cellular and molecular mechanisms of pulmonary vascular remodeling. *Annu Rev Physiol*, **59**, 89-144.
- Stevens, T, Janssen, PL & Tucker, A. (1992). Acute and Long-Term Tnf-Alpha Administration Increases Pulmonary Vascular Reactivity in Isolated Rat Lungs. *Journal of Applied Physiology*, **73**, 708-712.

- Stewart, DJ, Levy, RD, Cernacek, P & Langleben, D. (1991). Increased plasma endothelin-1 in pulmonary-hypertension - marker or mediator of disease. *Annals of Internal Medicine*, **114**, 464-469.
- Stiebellehner, L, Frid, MG, Reeves, JT, Low, RB, Gnanasekharan, M & Stenmark, KR. (2003). Bovine distal pulmonary arterial media is composed of a uniform population of well-differentiated smooth muscle cells with low proliferative capabilities. *American Journal of Physiology-Lung Cellular and Molecular Physiology*, **285**, L819-L828.
- Straub, RH. (2007). The complex role of estrogens in inflammation. *Endocrine Reviews*, **28**, 521-574.
- Suchar, LA, Chang, RL, Rosen, RT, Lech, J & Conney, AH. (1995). High-Performance Liquid-Chromatography Separation of Hydroxylated Estradiol Metabolites - Formation of Estradiol Metabolites by Liver-Microsomes from Male and Female Rats. *Journal of Pharmacology and Experimental Therapeutics*, **272**, 197-206.
- Swaneck, GE & Fishman, J. (1988). Covalent binding of the endogenous estrogen 16- $\alpha$ -hydroxyestrone to estradiol-receptor in human-breast cancer-cells - Characterization and intranuclear localization. *Proceedings of the National Academy of Sciences of the United States of America*, **85**, 7831-7835.
- Sweeney, L & Voelkel, N. (2009). Estrogen exposure, obesity and thyroid disease in women with severe pulmonary hypertension. *European Journal of Medical Research*, **14**, 433-442.
- Taioli, E, Im, A, Xu, X, Veenstra, TD, Ahrendt, G & Garte, S. (2010). Comparison of estrogens and estrogen metabolites in human breast tissue and urine. *Reproductive Biology and Endocrinology*, **8**.
- Teichert-Kuliszewska, K, Kutryk, MJB, Kuliszewski, MA, Karoubi, G, Courtman, DW, Zucco, L, Granton, J & Stewart, DJ. (2006). Bone morphogenetic protein receptor-2 signaling promotes pulmonary arterial endothelial cell survival: Implications for loss-of-function mutations in the pathogenesis of pulmonary hypertension. *Circ Res*, **98**, 209-217.
- Thomson, JR, Machado, RD, Pauciulo, MW, Morgan, NV, Humbert, M, Elliott, GC, Ward, K, Yacoub, M, Mikhail, G, Rogers, P, Newman, J, Wheeler, L, Higenbottam, T, Gibbs, JS, Egan, J, Crozier, A, Peacock, A, Allcock, R, Corris, P, Loyd, JE, Trembath, RC & Nichols, WC. (2000). Sporadic primary pulmonary hypertension is associated with germline mutations of the gene encoding BMPR-II, a receptor member of the TGF- $\beta$  family. *Journal of Medical Genetics*, **37**, 741-745.
- Thum, T & Borlak, J. (2002). Testosterone, cytochrome P450, and cardiac hypertrophy. *Faseb Journal*, **16**, 1537-1549.
- Tofovic, SP, Bilan, V, Mi, Z, Jackson, EK & Schneider, F. (2013). Aromatase inhibition attenuates and ovariectomy and 4-hydroxyestradiol have mixed effects on development of angioproliferative pulmonary hypertension in female rats. *Am J Respir Crit Care Med*, **187**, A6099.

- Tofovic, SP & Rafikova, O. (2009). Preventive and therapeutic effects of 2-methoxyestradiol, but not estradiol, in severe occlusive pulmonary arterial hypertension in female rats. *Am J Respir Crit Care Med*, **179**, A1802.
- Tofovic, SP, Rafikova, O, Champion, H & Schneider, F. (2012). Estrogens exacerbate development of occlusive pulmonary arterial hypertension and formation of plexiform lesions. *Am J Respir Crit Care Med*, **185**, A6803.
- Tofovic, SP, Salah, EM, Mady, HH, Jackson, EK & Melhem, ME. (2005). Estradiol metabolites attenuate monocrotaline-induced pulmonary hypertension in rats. *Journal of Cardiovascular Pharmacology*, **46**, 430-437.
- Tofovic, SP, Zhang X. & Petrusevska G. (2009a). Progesterone inhibits vascular remodeling and attenuates monocrotaline-induced pulmonary hypertension in estrogen-deficient rats. *Prilozi*, **30**, 25-44.
- Tofovic, SP, Zhang, XC, Jackson, EK, Dacic, S & Petrusevska, G. (2006). 2-Methoxyestradiol mediates the protective effects of estradiol in monocrotaline-induced pulmonary hypertension. *Vascular Pharmacology*, **45**, 358-367.
- Tofovic, SP, Zhang, XC, Jackson, EK, Zhu, H & Petrusevska, G. (2009b). 2-methoxyestradiol attenuates bleomycin-induced pulmonary hypertension and fibrosis in estrogen-deficient rats. *Vascular Pharmacology*, **51**, 190-197.
- Torres, GE, Gainetdinov, RR & Caron, MG. (2003). Plasma membrane monoamine transporters: structure, regulation and function. *Nat Rev Neurosci*, **4**, 13-25.
- Toshner, M & Morrell, NW. (2010). Endothelial progenitor cells in pulmonary hypertension - dawn of cell-based therapy? *International Journal of Clinical Practice*, **64**, 7-12.
- Toshner, M, Voswinckel, R, Southwood, M, Al-Lamki, R, Howard, LS, Marchesan, D, Yang, J, Suntharalingam, J, Soon, E, Exley, A, Stewart, S, Hecker, M, Zhu, Z, Gehling, U, Seeger, W, Pepke-Zaba, J & Morrell, NW. (2009). Evidence of dysfunction of endothelial progenitors in pulmonary arterial hypertension. *Am J Respir Crit Care Med*, **180**, 780-787.
- Townsend, EA, Miller, VM & Prakash, YS. (2012). Sex differences and sex steroids in lung health and disease. *Endocrine Reviews*, **33**, 1-47.
- Tsuchiya, Y, Nakajima, M, Kyo, S, Kanaya, T, Inoue, M & Yokoi, T. (2004). Human CYP1B1 is regulated by estradiol via estrogen receptor. *Cancer Research*, **64**, 3119-3125.
- Tsuchiya, Y, Nakajima, M & Yokoi, T. (2005). Cytochrome P450-mediated metabolism of estrogens and its regulation in human. *Cancer Letters*, **227**, 115-124.
- Tucker, A, McMurtry, IF, Reeves, JT, Alexander, AF, Will, DH & Grover, RF. (1975). Lung vascular smooth-muscle as a determinant of pulmonary-hypertension at high-altitude. *American Journal of Physiology*, **228**, 762-767.
- Tuder, RM, Cool, CD, Geraci, MW, Wang, J, Abman, SH, Wright, L, Badesch, D & Voelkel, NF. (1999). Prostacyclin synthase expression is decreased in lungs front patients with severe pulmonary hypertension. *Am J Respir Crit Care Med*, **159**, 1925-1932.

- Tuder, RM, Groves, B, Badesch, DB & Voelkel, NF. (1994). Exuberant endothelial-cell growth and elements of inflammation are present in plexiform lesions of pulmonary-hypertension. *American Journal of Pathology*, **144**, 275-285.
- Umar, S, Iorga, A, Matori, H, Nadadur, RD, Li, J, Maltese, F, van der Laarse, A & Eghbali, M. (2011). Estrogen rescues preexisting severe pulmonary hypertension in rats. *Am J Respir Crit Care Med*, **184**, 715-723.
- Valdimarsdottir, G, Goumans, MJ, Rosendahl, A, Brugman, M, Itoh, S, Lebrin, F, Sideras, P & ten Dijke, P. (2002). Stimulation of Id1 expression by bone morphogenetic protein is sufficient and necessary for bone morphogenetic protein-induced activation of endothelial cells. *Circulation*, **106**, 2263-2270.
- Vanderpool, RR, El-Bizri, N, Rabinovitch, M & Chesler, NC. (2013). Patchy deletion of Bmpr1a potentiates proximal pulmonary artery remodeling in mice exposed to chronic hypoxia. *Biomechanics and Modeling in Mechanobiology*, **12**, 33-42.
- Vasiliou, V & Gonzalez, FJ. (2008). Role of CYP1B1 in glaucoma. *Annual Review of Pharmacology and Toxicology*, **48**, 333-358.
- Ventetuolo, CE, Ouyang, P, Bluemke, DA, Tandri, H, Barr, RG, Bagiella, E, Cappola, AR, Bristow, MR, Johnson, C, Kronmal, RA, Kizer, JR, Lima, JAC & Kawut, SM. (2011). Sex hormones are associated with right ventricular structure and function the MESA-right ventricle study. *Am J Respir Crit Care Med*, **183**, 659-667.
- Ventetuolo, CE, Praestgaard, A, Palevsky, HI, Klinger, JR, Halpern, SD & Kawut, SM. (2014). Sex and haemodynamics in pulmonary arterial hypertension. *European Respiratory Journal*, **43**, 523-530.
- Verma, MK, Miki, Y, Abe, K, Suzuki, T, Niikawa, H, Suzuki, S, Kondo, T & Sasano, H. (2013). Intratumoral localization and activity of 17 beta-hydroxysteroid dehydrogenase type 1 in non-small cell lung cancer: a potent prognostic factor. *Journal of Translational Medicine*, **11**.
- Voelkel, NF, Quaife, RA, Leinwand, LA, Barst, RJ, McGoon, MD, Meldrum, DR, Dupuis, J, Long, CS, Rubin, LJ, Smart, FW, Suzuki, YJ, Gladwin, M, Denholm, EM & Gail, DB. (2006). Right ventricular function and failure: Report of a national heart, lung, and blood institute working group on cellular and molecular mechanisms of right heart failure. *Circulation*, **114**, 1883-1891.
- Wang, ZY, Zhang, XT, Shen, P, Loggie, BW, Chang, YC & Deuel, TF. (2005). Identification, cloning, and expression of human estrogen receptor-alpha 36, a novel variant of human estrogen receptor-alpha 66. *Biochemical and Biophysical Research Communications*, **336**, 1023-1027.
- Wang, Z, Zhang, X, Shen, P, Loggie, BW, Chang, Y & Deuel, TF. (2006). A variant of estrogen receptor- $\alpha$ , hER- $\alpha$ 36: Transduction of estrogen- and antiestrogen-dependent membrane-initiated mitogenic signaling. *Proceedings of the National Academy of Sciences*, **103**, 9063-9068.
- Ward, JPT & Knock, GA (2011). Excitation-contraction coupling and regulation of pulmonary vascular contractility. In *Textbook of pulmonary vascular diseases*. ed. Yuan, JXJ, Garcia, JGN, Hales, CA, Rich, S, Archer, SL & West, JB pp. 147-166. Springer: New York.

Wedgwood, S, Dettman, RW & Black, SM. (2001). ET-1 stimulates pulmonary arterial smooth muscle cell proliferation via induction of reactive oxygen species. *American Journal of Physiology-Lung Cellular and Molecular Physiology*, **281**, L1058-L1067.

Weibel, ER. (1963). *Morphometry of the human lung*. Springer: Berlin.

Weir, EK & Archer, SL. (1995). The mechanism of acute hypoxic pulmonary vasoconstriction: the tale of two channels. *The FASEB Journal*, **9**, 183-189.

Weir, EK & Olschewski, A. (2006). Role of ion channels in acute and chronic responses of the pulmonary vasculature to hypoxia. *Cardiovascular Research*, **71**, 630-641.

Weisz, J, Bui, QD, Roy, D & Liehr, JG. (1992). Elevated 4-hydroxylation of estradiol by hamster-kidney microsomes - A potential pathway of metabolic-activation of estrogens. *Endocrinology*, **131**, 655-661.

Weitzmann, MN & Pacifici, R. (2006). Estrogen deficiency and bone loss: an inflammatory tale. *J Clin Invest*, **116**, 1186-1194.

West, J, Cogan, J, Geraci, M, Robinson, L, Newman, J, Phillips, JA, Lane, K, Meyrick, B & Loyd, J. (2008). Gene expression in BMPR2 mutation carriers with and without evidence of pulmonary arterial hypertension suggests pathways relevant to disease penetrance. *BMC Med Genomics*, **1**, 45.

West, JB & Dollery, CT. (1960). Distribution of blood flow and ventilation-perfusion ratio in the lung, measured with radioactive Co<sup>2</sup>. *Journal of Applied Physiology*, **15**, 405-410.

West, JB, Dollery, CT & Naimark, A. (1964). Distribution of blood flow in isolated lung - Relation to vascular + alveolar pressures. *Journal of Applied Physiology*, **19**, 713-&.

Wharton, J, Davie, N, Upton, PD, Yacoub, MH, Polak, JM & Morrell, NW. (2000). Prostacyclin analogues differentially inhibit growth of distal and proximal human pulmonary artery smooth muscle cells. *Circulation*, **102**, 3130-3136.

Wharton, J, Strange, JW, Moller, GMO, Growcott, EJ, Ren, XH, Franklyn, AP, Phillips, SC & Wilkins, MR. (2005). Antiproliferative effects of phosphodiesterase type 5 inhibition in human pulmonary artery cells. *Am J Respir Crit Care Med*, **172**, 105-113.

White, K, Loughlin, L, Maqbool, Z, Nilsen, M, McClure, J, Dempsie, Y, Baker, AH & Maclean, MR. (2011a). Serotonin transporter, sex, and hypoxia: microarray analysis in the pulmonary arteries of mice identifies genes with relevance to human PAH. *Physiological Genomics*, **43**, 417-437.

White, K, Dempsie, Y, Nilsen, M, Wright, AF, Loughlin, L & MacLean, MR. (2011b). The serotonin transporter, gender, and 17 $\beta$  oestradiol in the development of pulmonary arterial hypertension. *Cardiovascular Research*, **90**, 373-382.

White, K, Johansen, AK, Nilsen, M, Ciucan, L, Wallace, E, Paton, L, Campbell, A, Morecroft, I, Loughlin, L, McClure, JD, Thomas, M, Mair, KM & MacLean, MR. (2012). Activity of the estrogen-metabolizing enzyme cytochrome P450 1B1

- influences the development of pulmonary arterial hypertension / clinical perspective. *Circulation*, **126**, 1087-1098.
- Will, DH, Reeves, JT, Alexander, AF & Grover, RF. (1962). High altitude-induced pulmonary hypertension in normal cattle. *Circ Res*, **10**, 172-&.
- Willers, ED, Newman, JH, Loyd, JE, Robbins, IM, Wheeler, LA, Prince, MA, Stanton, KC, Cogan, JA, Runo, JR & Byrne, D. (2006). Serotonin transporter polymorphisms in familial and idiopathic pulmonary arterial hypertension. *Am J Respir Crit Care Med*, **173**, 798-802.
- Wu, W, Dave, NB, Yu, GY, Stollo, PJ, Kovkarova-Naumovski, E, Ryter, SW, Reeves, SR, Dayyat, E, Wang, Y, Choi, AMK, Gozal, D & Kaminski, N. (2008). Network analysis of temporal effects of intermittent and sustained hypoxia on rat lungs. *Physiological Genomics*, **36**, 24-34.
- Xu, DQ, Luo, Y, Liu, Y, Wang, J, Zhang, B, Xu, M, Wang, YX, Dong, HY, Dong, MQ, Zhao, PT, Niu, W, Liu, ML, Gao, YQ & Li, ZC. (2010). Beta-estradiol attenuates hypoxic pulmonary hypertension by stabilizing the expression of p27kip1 in rats. *Respiratory Research*, **11**, 182.
- Yaghini, FA, Song, CY, Lavrentyev, EN, Ghafoor, HUB, Fang, XR, Estes, AM, Campbell, WB & Malik, KU. (2010). Angiotensin II-induced vascular smooth muscle cell migration and growth are mediated by cytochrome P450 1B1-dependent superoxide generation. *Hypertension*, **55**, 1461-1467.
- Yanagisawa, M, Kurihara, H, Kimura, S, Tomobe, Y, Kobayashi, M, Mitsui, Y, Yazaki, Y, Goto, K & Masaki, T. (1988). A novel potent vasoconstrictor peptide produced by vascular endothelial-cells. *Nature*, **332**, 411-415.
- Yang, X, Long, L, Southwood, M, Rudarakanchana, N, Upton, PD, Jeffery, TK, Atkinson, C, Chen, H, Trembath, RC & Morrell, NW. (2005). Dysfunctional Smad signaling contributes to abnormal smooth muscle cell proliferation in familial pulmonary arterial hypertension. *Circ Res*, **96**, 1053-1063.
- Yasunari, K, Kohno, M, Kano, H, Yokokawa, K, Horio, T & Yoshikawa, J. (1996). Possible involvement of phospholipase D and protein kinase C in vascular growth induced by elevated glucose concentration. *Hypertension*, **28**, 159-168.
- Yuan, P, Wu, WH, Gao, L, Zheng, ZQ, Liu, D, Mei, HY, Zhang, ZL & Jing, ZC. (2013). Oestradiol ameliorates monocrotaline pulmonary hypertension via NO, prostacyclin and endothelin-1 pathways. *European Respiratory Journal*, **41**, 1116-1125.
- Zeng, DX, Xu, GP, Lei, W, Wang, R, Wang, CG & Huang, JA. (2013). Suppression of cyclin D1 by plasmid-based short hairpin RNA ameliorated experimental pulmonary vascular remodeling. *Microvascular Research*, **90**, 144-149.
- Zern, TL & Fernandez, ML. (2005). Cardioprotective effects of dietary polyphenols. *Journal of Nutrition*, **135**, 2291-2294.
- Zhang, XT, Kang, LG, Ding, L, Vranic, S, Gatalica, Z & Wang, ZY. (2011). A positive feedback loop of ER-alpha 36/EGFR promotes malignant growth of ER-negative breast cancer cells. *Oncogene*, **30**, 770-780.

Zhao, Y, Agarwal, VR, Mendelson, CR & Simpson, ER. (1996). Estrogen biosynthesis proximal to a breast tumor is stimulated by PGE(2) via cyclic AMP, leading to activation of promoter II of the CYP19 (aromatase) gene. *Endocrinology*, **137**, 5739-5742.

Zhu, BT & Conney, AH. (1998). Functional role of estrogen metabolism in target cells: review and perspectives. *Carcinogenesis*, **19**, 1-27.

Zhu, BT, Han, GZ, Shim, JY, Wen, Y & Jiang, XR. (2006). Quantitative structure-activity relationship of various endogenous estrogen metabolites for human estrogen receptor  $\alpha$  and  $\beta$  subtypes: insights into the structural determinants favoring a differential subtype binding. *Endocrinology*, **147**, 4132-4150.

Zhu, D & Ran, Y. (2012). Role of 15-lipoxygenase/15-hydroxyeicosatetraenoic acid in hypoxia-induced pulmonary hypertension. *J Physiol Sci*, **62**, 163-172.

Zhu, Y, Bian, Z, Lu, P, Karas, RH, Bao, L, Cox, D, Hodgins, J, Shaul, PW, Thoren, P, Smithies, O, Gustafsson, JA & Mendelsohn, ME. (2002). Abnormal vascular function and hypertension in mice deficient in estrogen receptor beta. *Science*, **295**, 505-508.

## 7.1 Appendices

Supplemental data [Appendix 1]

Mair, KM, Johansen, AKZ, Wright, AF, Wallace, E & Maclean, MR. (2013). Pulmonary arterial hypertension: basis of sex differences in incidence and treatment response. *Br J Pharmacol*, 171, 567-579. [Appendix 2]

Austin, ED, Lahm, T, West, J, Tofovic, SP, Johansen, AK, MacLean, MR, Alzoubi, A & Oka, M. (2013). Gender, sex hormones and pulmonary hypertension. *Pulm Circ*, 3, 294-314. (All authors contributed equally to this article) [Appendix 3]

White, K, Johansen, AK (co-first), Nilsen, M, Ciucan, L, Wallace, E, Paton, L, Campbell, A, Morecroft, I, Loughlin, L, McClure, JD, Thomas, M, Mair, KM & MacLean, MR. (2012). Activity of the estrogen-metabolizing enzyme cytochrome P450 1B1 influences the development of pulmonary arterial hypertension / clinical perspective. *Circulation*, 126, 1087-1098. [Appendix 4]

## 8.1 Supplemental data

### 8.1.1 Western blots corresponding to figure 3-1

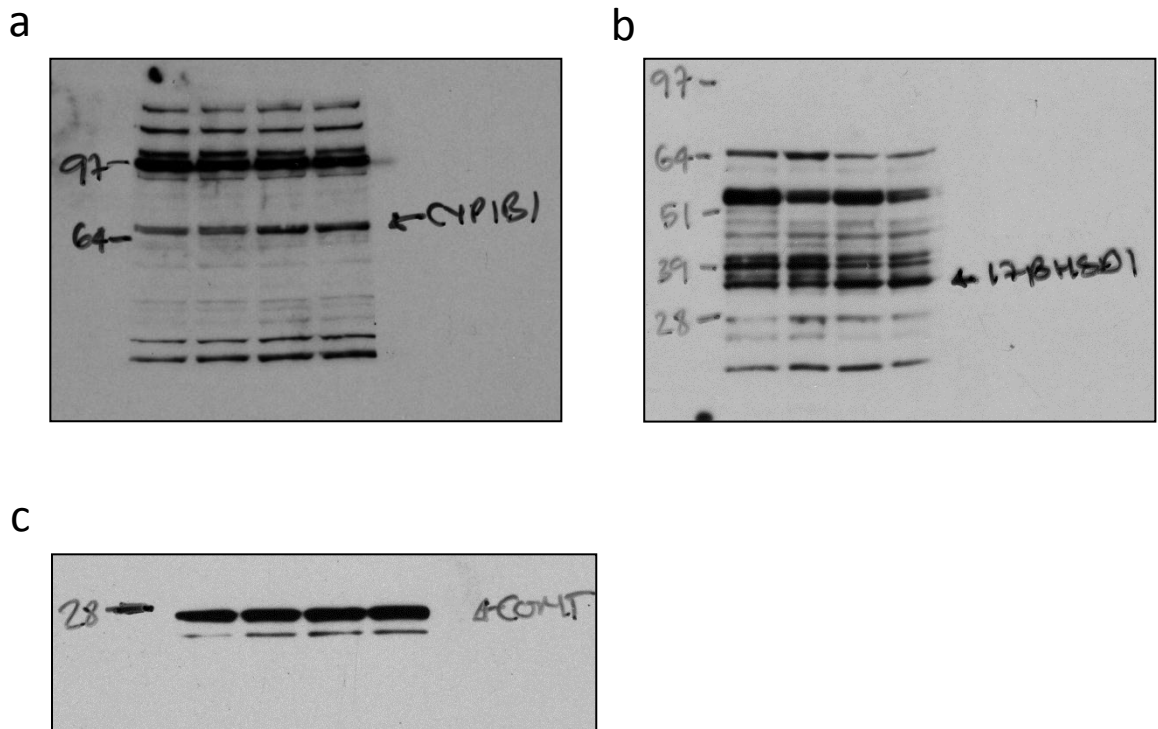
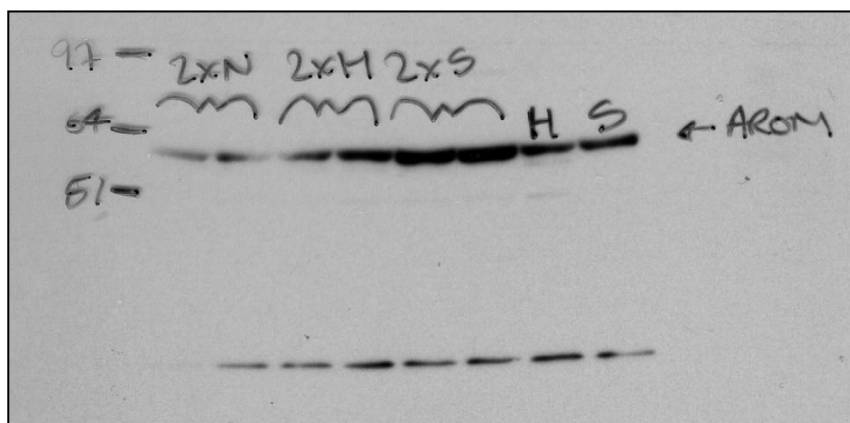


**Figure 8-1 Full western blots for effect of hypoxia on protein expression of CYP1B1, COMT and 17β-HSD1**

Female control human pulmonary arterial smooth muscle cells (hPASMCs) were quiesced for 24 hours and then exposed to either normoxic or hypoxic conditions (1% oxygen) for 24 hours. Cell homogenates were assayed for protein expression by western blotting for CYP1B1, COMT and 17β-HSD1. CYP1B1 (a), 17β-HSD1 (b), COMT (c). The first two samples are normoxic controls and the latter two samples are hypoxic (1% samples).

## 8.1.2 Western blots corresponding to figure 3-22 and 3-23

a



b

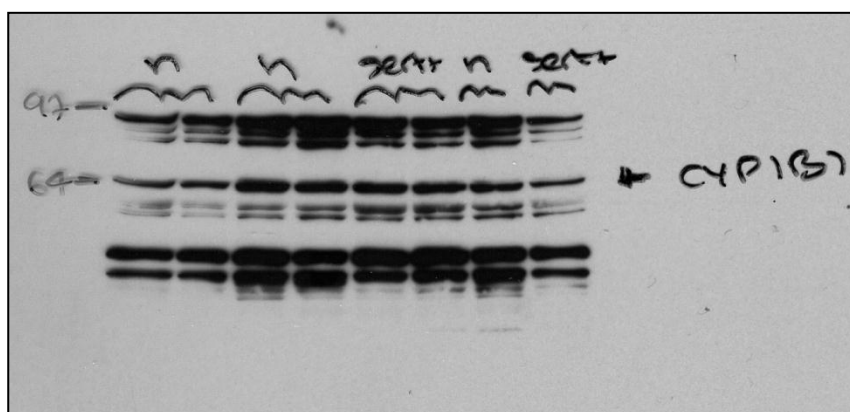


**Figure 8-2 Full western blots of aromatase and CYP1B1 expression in normoxic, hypoxic and SERT+ mice**

5-6 month old female wild-type (C57BL/6 x CBA), hypoxic and SERT+ mice lung homogenates were analyzed for aromatase and CYP1B1 expression by western blotting. Aromatase (a), CYP1B1 (b). Note that in Chapter 3, hypoxic samples were not included to retain focus on SERT+ mice. Samples are run in the following order: 2 x wild-type, 2 x hypoxic, 2 x SERT+, 1 x hypoxic, 1 x SERT+.

### 8.1.3 Effect of tempol and UO126 on cell proliferation to complement figure 4-7

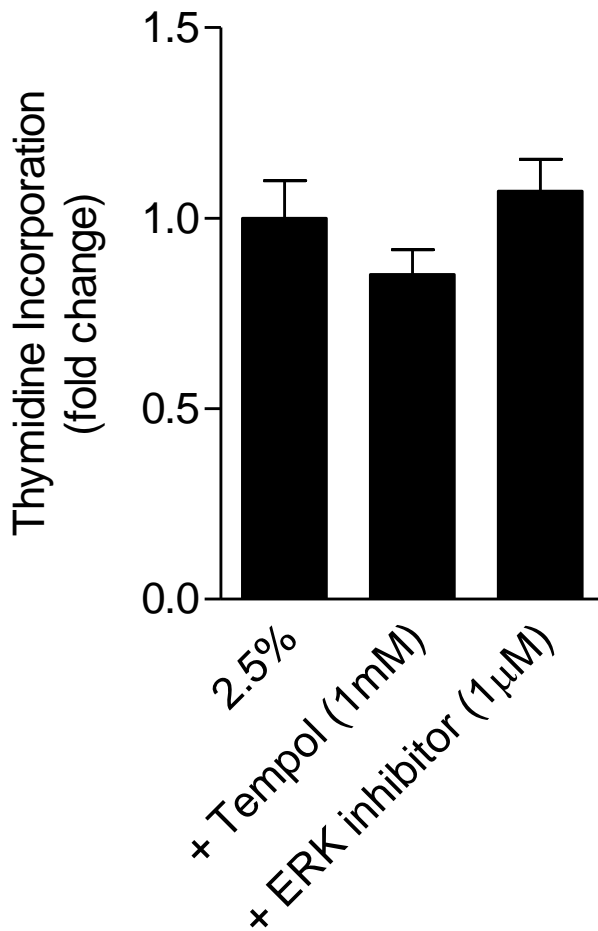


**Figure 8-3 The effect of tempol and UO126 on thymidine incorporation**

Female hPASCs were quiesced for 24 hours in 0.2% charcoal-stripped FBS (estrogen free) phenol red free DMEM. HPASCs were then incubated with either a vehicle (water), an ERK inhibitor (UO126, 1µM) or tempol (ROS scavenger, 1mM) in the presence of 2.5% charcoal-stripped FBS phenol red free DMEM. Thymidine was added for the last 24 hours (0.1µCi) and thymidine incorporation was assessed after 72 hours. n=1, repeated 3 times, One-way ANOVA with a Bonferroni's post-hoc test. Data is expressed as the mean ± SEM.